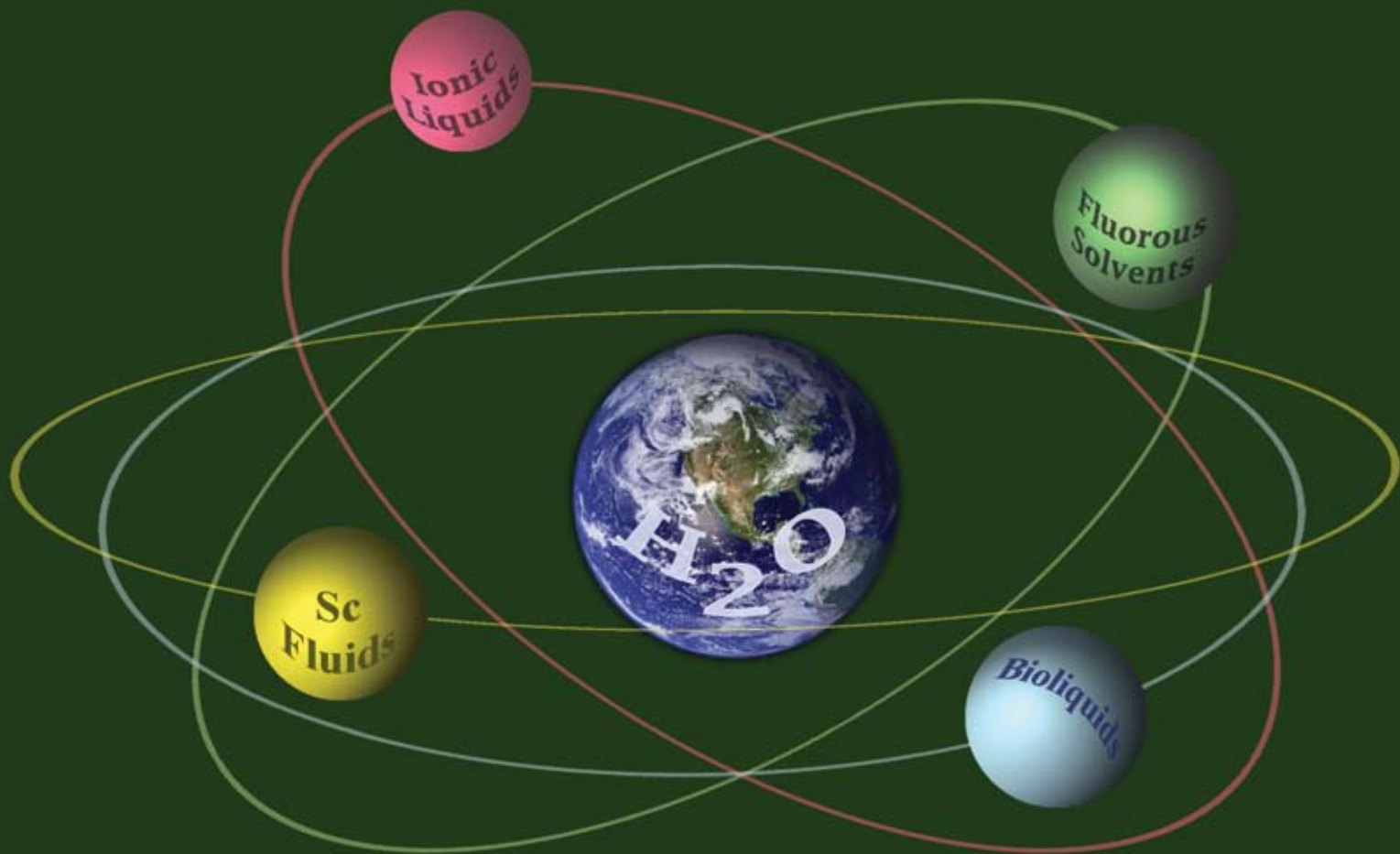


Green Chemistry

Cutting-edge research for a greener sustainable future

www.rsc.org/greenchem

Volume 10 | Number 10 | October 2008 | Pages 1013–1120

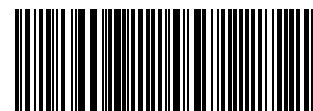


ISSN 1463-9262

RSC Publishing

Horváth
Solvents from nature

Suib *et al.*
Manganese molecular sieve catalysts



1463-9262(2008)10:10;1-E



years of publishing!

Green Chemistry...



- The most highly cited *Green Chemistry* journal, Impact factor = 4.836*
- Fast publication, typically <90 days for full papers
- Full variety of research including reviews, communications, full papers and perspectives.

Celebrating 10 years of publishing, *Green Chemistry* offers the latest research that reduces the environmental impact of the chemical enterprise by developing alternative sustainable technologies, and provides a unique forum for the rapid publication of cutting-edge and innovative research for a greener, sustainable future

...for a sustainable future!

* 2007 Thomson Scientific (ISI) Journal Citation Reports ®

Green Chemistry

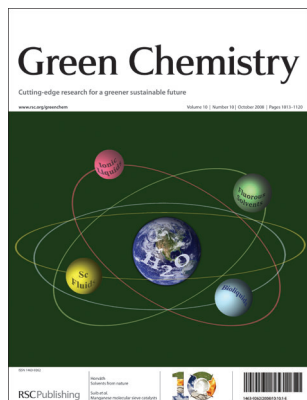
Cutting-edge research for a greener sustainable future

www.rsc.org/greenchem

RSC Publishing is a not-for-profit publisher and a division of the Royal Society of Chemistry. Any surplus made is used to support charitable activities aimed at advancing the chemical sciences. Full details are available from www.rsc.org

IN THIS ISSUE

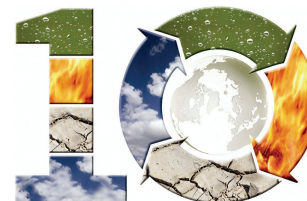
ISSN 1463-9262 CODEN GRCHFJ 10(10) 1013–1120 (2008)



Cover

See Horváth, pp. 1024–1028. The cover shows that solvents are important components of Nature, providing one or more liquid phases to assist chemical reactions and processes. While some solvents, including water, are available from Nature in large quantities, most solvents are man-made. Historically, solvents were developed and/or selected to help the chemical or physical objectives of the users only. With the increasing importance of local and global health and environmental issues, the potential impacts of solvents have become important selection tools.

Image reproduced by permission of László T. Mika, from *Green Chem.*, 2008, **10**, 1024.



CHEMICAL TECHNOLOGY

T73

Drawing together research highlights and news from all RSC publications, *Chemical Technology* provides a 'snapshot' of the latest applications and technological aspects of research across the chemical sciences, showcasing newsworthy articles and significant scientific advances.

Chemical Technology

October 2008/Volume 5/Issue 10

www.rsc.org/chemicaltechnology

EDITORIAL

1023

Inspired by nature: green solvents in science and application

Walter Leitner discusses the 2008 Green Solvents Conference and introduces István Horváth's perspective.



EDITORIAL STAFF

Editor

Sarah Ruthven

Assistant editor

Sarah Dixon

Publishing assistant

Ruth Bircham

Team leader, serials production

Stephen Wilkes

Technical editor

Edward Morgan

Production administration coordinator

Sonya Spring

Administration assistantsClare Davies, Donna Fordham, Kirsty Lunnon,
Julie Thompson**Publisher**

Emma Wilson

Green Chemistry (print: ISSN 1463-9262; electronic: ISSN 1463-9270) is published 12 times a year by the Royal Society of Chemistry, Thomas Graham House, Science Park, Milton Road, Cambridge, UK CB4 0WF.

All orders, with cheques made payable to the Royal Society of Chemistry, should be sent to RSC Distribution Services, c/o Portland Customer Services, Commerce Way, Colchester, Essex, UK CO2 8HP. Tel +44 (0) 1206 226050; E-mail sales@rscdistribution.org

2008 Annual (print + electronic) subscription price: £947; US\$1799. 2008 Annual (electronic) subscription price: £852; US\$1695. Customers in Canada will be subject to a surcharge to cover GST. Customers in the EU subscribing to the electronic version only will be charged VAT.

If you take an institutional subscription to any RSC journal you are entitled to free, site-wide web access to that journal. You can arrange access via Internet Protocol (IP) address at www.rsc.org/ip. Customers should make payments by cheque in sterling payable on a UK clearing bank or in US dollars payable on a US clearing bank. Periodicals postage paid at Rahway, NJ, USA and at additional mailing offices. Airfreight and mailing in the USA by Mercury Airfreight International Ltd., 365 Blair Road, Avenel, NJ 07001, USA.

US Postmaster: send address changes to Green Chemistry, c/o Mercury Airfreight International Ltd., 365 Blair Road, Avenel, NJ 07001. All despatches outside the UK by Consolidated Airfreight.

PRINTED IN THE UK

Advertisement sales: Tel +44 (0) 1223 432246; Fax +44 (0) 1223 426017; E-mail advertising@rsc.org

Green Chemistry

Cutting-edge research for a greener sustainable future

www.rsc.org/greenchem

Green Chemistry focuses on cutting-edge research that attempts to reduce the environmental impact of the chemical enterprise by developing a technology base that is inherently non-toxic to living things and the environment.

EDITORIAL BOARD

Chair

Professor Martyn Poliakoff
Nottingham, UK

Scientific Editor

Professor Walter Leitner
RWTH-Aachen, Germany

Associate Editors

Professor C. J. Li
McGill University, Canada

Members

Professor Paul Anastas
Yale University, USA
Professor Joan Brennecke
University of Notre Dame, USA
Professor Mike Green
Sasol, South Africa
Professor Buxing Han
Chinese Academy of Sciences,
China

Dr Alexei Lapkin
Bath University, UK
Professor Steven Ley
Cambridge, UK
Dr Janet Scott
Unilever, UK
Professor Tom Welton
Imperial College, UK

ADVISORY BOARD

James Clark, York, UK
Avelino Corma, Universidad
Politécnica de Valencia, Spain
Mark Harmer, DuPont Central
R&D, USA
Herbert Hugl, Lanxess Fine
Chemicals, Germany
Roshan Jachuck,
Clarkson University, USA
Makoto Misono, nite,
Japan

Colin Raston,
University of Western Australia,
Australia
Robin D. Rogers, Centre for Green
Manufacturing, USA
Kenneth Seddon, Queen's
University, Belfast, UK
Roger Sheldon, Delft University of
Technology, The Netherlands
Gary Sheldrake, Queen's
University, Belfast, UK

Pietro Tundo, Università ca
Foscari di Venezia, Italy

INFORMATION FOR AUTHORS

Full details of how to submit material for publication in Green Chemistry are given in the Instructions for Authors (available from <http://www.rsc.org/authors>). Submissions should be sent via ReSource: <http://www.rsc.org/resource>.

Authors may reproduce/republish portions of their published contribution without seeking permission from the RSC, provided that any such republication is accompanied by an acknowledgement in the form: (Original citation) – Reproduced by permission of the Royal Society of Chemistry.

© The Royal Society of Chemistry 2008. Apart from fair dealing for the purposes of research or private study for non-commercial purposes, or criticism or review, as permitted under the Copyright, Designs and Patents Act 1988 and the Copyright and Related Rights Regulations 2003, this publication may only be reproduced, stored or transmitted, in any form or by any means, with the prior permission in writing of the Publishers or in the case of reprographic reproduction in accordance with the terms of licences issued by the Copyright Licensing Agency in the UK. US copyright law is applicable to users in the USA.

The Royal Society of Chemistry takes reasonable care in the preparation of this publication but does not accept liability for the consequences of any errors or omissions.

The paper used in this publication meets the requirements of ANSI/NISO Z39.48-1992 (Permanence of Paper).

Royal Society of Chemistry: Registered Charity No. 207890

PERSPECTIVE

1024

Solvents from nature

István T. Horváth*

A personal journey from solvent to solvent is presented to demonstrate how environmentally friendly solvents can be part of the solution of various chemical challenges.



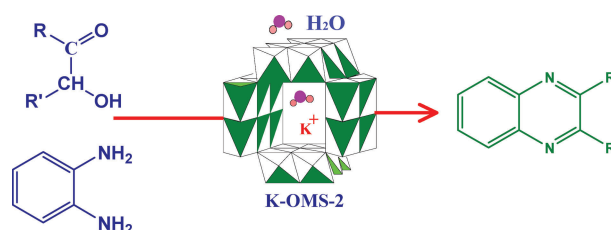
COMMUNICATION

1029

Manganese octahedral molecular sieves catalyzed tandem process for synthesis of quinoxalines

Shanthakumar Sithambaram, Yunshuang Ding, Weina Li, Xiongfei Shen, Faith Gaenzler and Steven L. Suib

An efficient environmentally benign tandem synthetic route to prepare quinoxalines leading to 100% yields using reusable manganese oxide octahedral molecular sieves (OMS-2) is described.



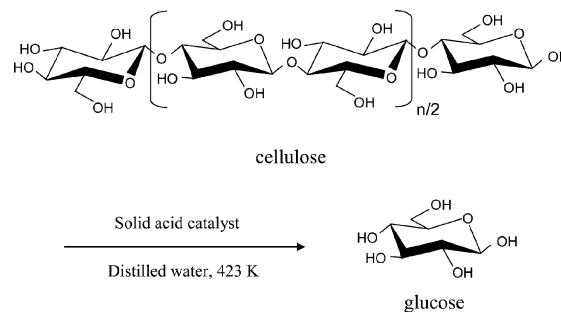
PAPERS

1033

Selective hydrolysis of cellulose into glucose over solid acid catalysts

Ayumu Onda,* Takafumi Ochi and Kazumichi Yanagisawa

Solid acid catalysts with high hydrothermal stability and hydrophobic planes have excellent catalytic properties for selective hydrolysis of cellulose with β -1,4-glycosidic bonds into glucose under hydrothermal conditions.

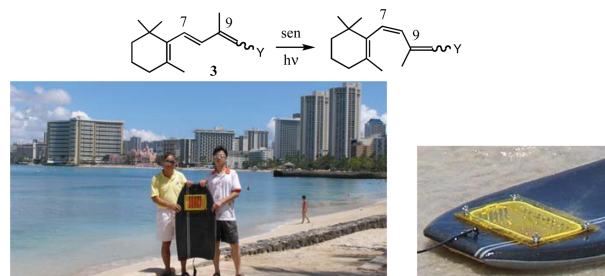


1038

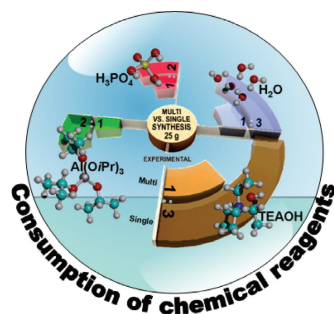
Solar reactions for preparing hindered 7-cis-isomers of dienes and trienes in the vitamin A series

Yao-Peng Zhao, Roger O. Campbell and Robert S. H. Liu*

Floating solar reactors allowed photochemical synthesis of hindered 7-cis isomers of compounds in the vitamin A series. One such reaction was carried out with a boogie-board reactor at Waikiki.



1043

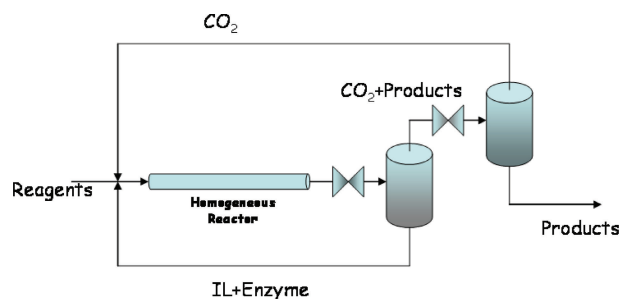


Environmentally benign synthesis of nanosized aluminophosphate enhanced by microwave heating

Eng-Poh Ng, Luc Delmotte and Svetlana Mintova*

The environmentally benign synthesis of microporous aluminophosphate nanocrystals by a multicycle approach under microwave heating resulting in decreasing or almost eliminating the related waste is reported.

1049

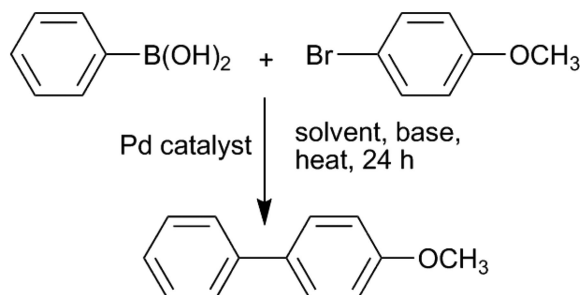


Influence of the enzyme concentration on the phase behaviour for developing a homogeneous enzymatic reaction in ionic liquid–CO₂ media

Maria Dolores Bermejo, Aleksandra J. Kotlewska, Louw J. Florusse, Maria José Cocero, Fred van Rantwijk and Cor J. Peters*

A homogeneous enzymatic reaction in an ionic liquid–CO₂ medium integrated with the separation of the product is proposed. In this work the solubility of CO₂ in solutions of CaL B in HOPMImNO₃ was experimentally determined.

1055

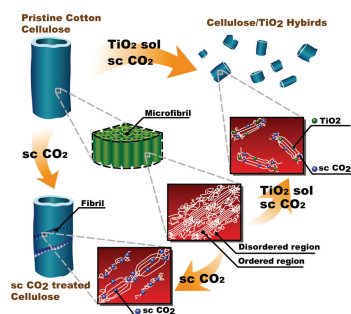


Supported phosphine-free palladium catalysts for the Suzuki–Miyaura reaction in aqueous media

Nam T. S. Phan and Peter Styring*

Complete conversion has been achieved in a Suzuki reaction carried out in a predominantly water environment and without phosphines using a polymer-supported catalyst.

1061



Synthesis of cellulose/titanium dioxide hybrids in supercritical carbon dioxide

Qisi Yu, Peiyi Wu,* Peng Xu,* Lei Li, Tao Liu and Ling Zhao

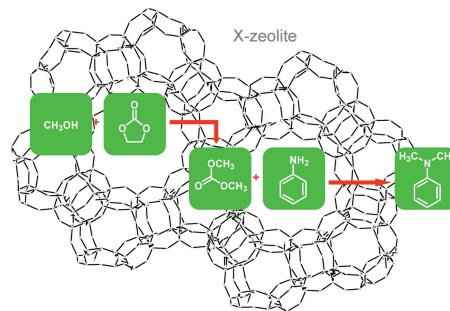
Novel cellulose/titania hybrids were synthesized *via* a supercritical carbon dioxide (scCO₂)-assisted adsorption and impregnation into cellulose fibers with a titania sol which was prepared through a non-hydrolytic sol-gel route.

1068

Sequential coupling of the transesterification of cyclic carbonates with the selective *N*-methylation of anilines catalysed by faujasites

Maurizio Selva,* Alvisse Perosa and Massimo Fabris

Two sequential transformations catalysed by a NaX faujasite, allow the synthesis of the non-toxic dimethyl carbonate and its use *in situ*, as a methylating agent of primary aromatic amines.



1078

Foam-like materials produced from abundant natural resources

Matthew D. Gawryla, Melissa Nezamzadeh and David A. Schiraldi*

Low density polymer/clay aerogel composites, which possess outstanding thermal and mechanical properties, can be produced from bio-based casein and smectite clays using water as solvent and an environmentally-benign freeze drying process.

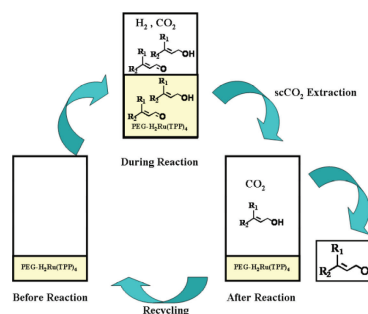


1082

Selective hydrogenation of unsaturated aldehydes in a poly(ethylene glycol)/compressed carbon dioxide biphasic system

Ruixia Liu, Haiyang Cheng, Qiang Wang, Chaoyong Wu, Jun Ming, Chunyu Xi, Yancun Yu, Shuxia Cai, Fengyu Zhao* and Masahiko Arai

Unsaturated alcohols were produced with a selectivity above 97% in the hydrogenation of α,β -unsaturated aldehydes. They were extracted by high pressure CO₂ stream and separated from the PEG phase, dissolving the Ru catalyst, and the catalyst was directly recyclable.

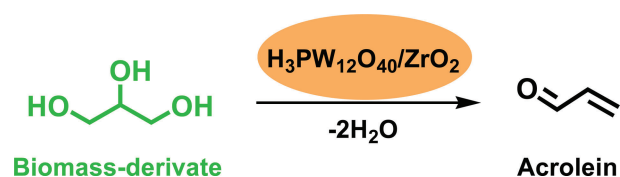


1087

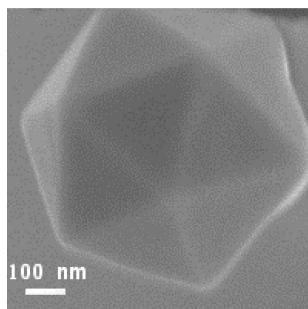
Sustainable production of acrolein: gas-phase dehydration of glycerol over 12-tungstophosphoric acid supported on ZrO₂ and SiO₂

Song-Hai Chai, Hao-Peng Wang, Yu Liang and Bo-Qing Xu*

Keggin 12-tungstophosphoric acid (H₃PW₁₂O₄₀, HPW) catalysts supported on zirconia are found to be much more active, selective and stable than those on silica for acrolein production from glycerol dehydration.



1094

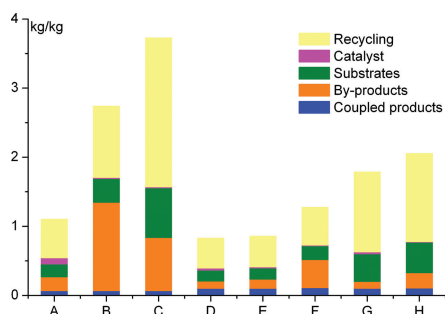


Synthesis of icosahedral gold particles by a simple and mild route

Chaoxing Zhang, Jianling Zhang, Buxing Han,* Yueju Zhao and Wei Li

Icosahedral gold nanoparticles can be prepared using HAuCl_4 as precursor and Pluronic as reductant and directing agent under mild conditions, and the particles size can be tuned from 100 nm to 1 μm .

1099

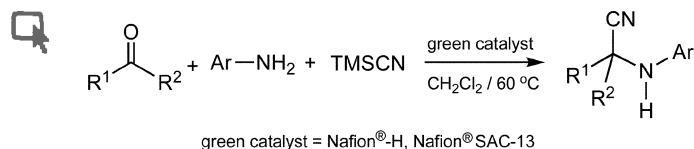


Cross-metathesis of oleyl alcohol with methyl acrylate: optimization of reaction conditions and comparison of their environmental impact

Anastasiya Rybak and Michael A. R. Meier*

The synthesis of α,ω -difunctional monomers from the renewable resource oleyl alcohol *via* the cross-metathesis reaction with methyl acrylate is described and optimized.

1105

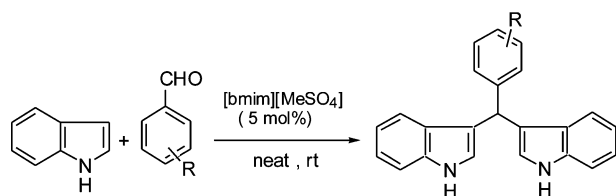


Efficient green synthesis of α -aminonitriles, precursors of α -amino acids

G. K. Surya Prakash,* Tisa Elizabeth Thomas, Inessa Bychinskaya, Arjun G. Prakash, Chiradeep Panja, Habiba Vaghoo and George A. Olah*

The synthesis of α -aminonitriles by a direct three component Strecker reaction has been achieved using environmentally friendly solid acid catalysts, Nafion[®]-H and Nafion[®] SAC-13.

1111



Catalytic application of room temperature ionic liquids: [bmim][MeSO₄] as a recyclable catalyst for synthesis of bis(indolyl)methanes. Ion-fishing by MALDI-TOF-TOF MS and MS/MS studies to probe the proposed mechanistic model of catalysis

Asit K. Chakraborti,* Sudipta Raha Roy, Dinesh Kumar and Pradeep Chopra

[bmim][MeSO₄] has been found to be a highly efficient reusable catalyst for the synthesis of bis(indolyl)methanes by the reaction of indole with alkyl/aryl/heteroaryl aldehydes under neat conditions, at room temperature and in short reaction times.

AUTHOR INDEX

Arai, Masahiko, 1082
 Bermejo, Maria Dolores, 1049
 Bychinskaya, Inessa, 1105
 Cai, Shuxia, 1082
 Campbell, Roger O., 1038
 Chai, Song-Hai, 1087
 Chakraborti, Asit K., 1111
 Cheng, Haiyang, 1082
 Chopra, Pradeep, 1111
 Cocero, Maria José, 1049
 Delmotte, Luc, 1043
 Ding, Yunshuang, 1029
 Fabris, Massimo, 1068
 Florusse, Louw J., 1049
 Gaenzler, Faith, 1029
 Gawryla, Matthew D., 1078
 Han, Buxing, 1094
 Horváth, István T., 1024

Kotlewska, Aleksandra J., 1049
 Kumar, Dinesh, 1111
 Li, Lei, 1061
 Li, Wei, 1094
 Li, Weina, 1029
 Liang, Yu, 1087
 Liu, Robert S. H., 1038
 Liu, Ruixia, 1082
 Liu, Tao, 1061
 Meier, Michael A. R., 1099
 Ming, Jun, 1082
 Mintova, Svetlana, 1043
 Nezamzadeh, Melissa, 1078
 Ng, Eng-Poh, 1043
 Ochi, Takafumi, 1033
 Olah, George A., 1105
 Onda, Ayumu, 1033
 Panja, Chiradeep, 1105

Perosa, Alvise, 1068
 Peters, Cor J., 1049
 Phan, Nam T. S., 1055
 Prakash, Arjun G., 1105
 Prakash, G. K. Surya, 1105
 Roy, Sudipta Raha, 1111
 Rybak, Anastasiya, 1099
 Schiraldi, David A., 1078
 Selva, Maurizio, 1068
 Shen, Xiongfei, 1029
 Sithambaram, Shanthakumar, 1029
 Styring, Peter, 1055
 Suib, Steven L., 1029
 Thomas, Tisa Elizabeth, 1105
 Vaghoo, Habiba, 1105
 van Rantwijk, Fred, 1049
 Wang, Hao-Peng, 1087

Wang, Qiang, 1082
 Wu, Chaoyong, 1082
 Wu, Peiyi, 1061
 Xi, Chunyu, 1082
 Xu, Bo-Qing, 1087
 Xu, Peng, 1061
 Yanagisawa, Kazumichi, 1033
 Yu, Qisi, 1061
 Yu, Yancun, 1082
 Zhang, Chaoxing, 1094
 Zhang, Jianling, 1094
 Zhao, Fengyu, 1082
 Zhao, Ling, 1061
 Zhao, Yao-Peng, 1038
 Zhao, Yueju, 1094

FREE E-MAIL ALERTS AND RSS FEEDS

Contents lists in advance of publication are available on the web *via* www.rsc.org/greenchem – or take advantage of our free e-mail alerting service (www.rsc.org/ej_alert) to receive notification each time a new list becomes available.



Try our RSS feeds for up-to-the-minute news of the latest research. By setting up RSS feeds, preferably using feed reader software, you can be alerted to the latest Advance Articles published on the RSC web site. Visit www.rsc.org/publishing/technology/rss.asp for details.

ADVANCE ARTICLES AND ELECTRONIC JOURNAL

Free site-wide access to Advance Articles and the electronic form of this journal is provided with a full-rate institutional subscription. See www.rsc.org/ejs for more information.

* Indicates the author for correspondence: see article for details.



Electronic supplementary information (ESI) is available *via* the online article (see <http://www.rsc.org/esi> for general information about ESI).

A new journal from RSC Publishing launching in 2009

Metallomics: Integrated biometal science



060877

This timely new journal will cover the research fields related to metals in biological, environmental and clinical systems and is expected to be the core publication for the emerging metallomics community. Professor Joseph A. Caruso of the University of Cincinnati/Agilent Technologies Metallomics Center of the Americas, and a leading player in the field, will chair the Editorial Board.

From launch, the latest issue will be freely available online to all readers. Free institutional access to previous issues throughout 2009 and 2010 will be available following a simple registration process. Email metallomics@rsc.org for further information or visit the website.

Submit your work now!

RSC Publishing

Supporting the **iSM**
 International
 Symposium
 on Metallomics

www.rsc.org/metallomics

Registered Charity Number 207890

Call for Papers

'What the RSC is doing through the publication of this journal is important for progress of science and integration of physical sciences and biology' Dr Mina Bissell

Integrative Biology

Quantitative biosciences from nano to macro

Launching January 2009

Integrative Biology provides a unique venue for elucidating biological processes, mechanisms and phenomena through quantitative enabling technologies at the convergence of biology with physics, chemistry, engineering, imaging and informatics.

The latest issue will be freely available online. Institutional online access to all 2009/10 content will be available following registration at www.rsc.org/ibiology_registration

Contact the Editor, Harp Minhas, at ibiology@rsc.org or visit www.rsc.org/ibiology



International Editorial Board members include:

Distinguished Scientist Dr Mina Bissell, Lawrence Berkeley National Laboratory, USA (*Editorial Board Chair*)

Professor Mary-Helen Barcellos-Hoff, New York University, USA (*Scientific Editor*)

Professor David Beebe, University of Wisconsin, USA (*Scientific Editor*)

Professor Philip Day, University of Manchester, UK

Professor Luke Lee, University of California, Berkeley, USA

Professor John McCarthy, Manchester Interdisciplinary Biocentre, UK

Professor Mehmet Toner, Harvard Medical School, Boston, USA

Submit your work today!

RSC Publishing

www.rsc.org/ibiology

Registered Charity Number 207890

Chemical Technology

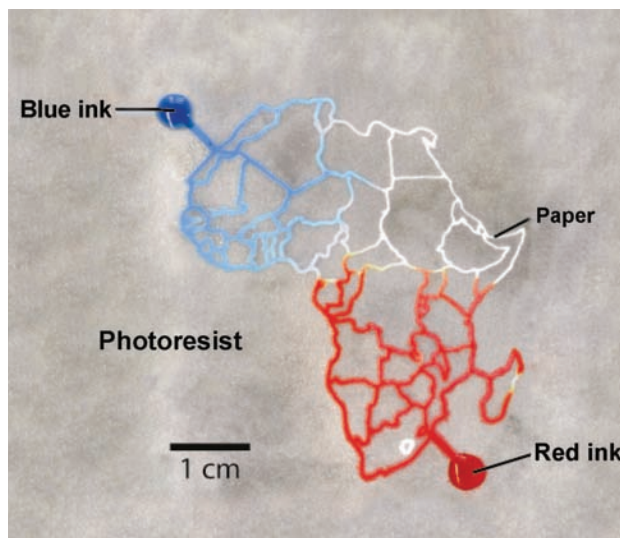
Paper-based devices for diagnostics in the developing world

Microfluidics in a FLASH

US scientists have made microfluidic devices using only paper, a pen and sunlight. The cheap and simple equipment could be used in the developing world for diagnosing disease and monitoring water.

George Whitesides and colleagues from Harvard University, Cambridge, call their new method FLASH (Fast Lithographic Activation of SHEets). Using a special type of paper, they made patterned microfluidic devices using only an ink-jet printer, UV lamp and hot plate. They demonstrated that a pen and sunlight can be used instead if printers, lamps or hot plates are unavailable.

Whitesides says the FLASH paper can be prepared in bulk in advance and stored for more than six months. It is made from a piece of paper impregnated with photoresist (a light-sensitive chemical) and sandwiched between a transparency film and black paper. When a microfluidic device is needed, a pattern is printed on to the transparency film with an



ink-jet printer, photocopier or pen. The paper is then exposed to UV light or sunlight to polymerise the photoresist where it is not covered by ink, before the transparency film and black backing paper are removed. Finally the paper is baked – although this step is not needed if sunlight is used instead

An Africa-shaped microfluidic device patterned using the FLASH method

of UV light – and rinsed to remove the unpolymerised photoresist. Making the device takes less than 30 minutes, says Whitesides.

‘I like the simplicity of the method and the ingenuity to impregnate an entire sheet of paper with photoresist to create barriers,’ says Abraham ‘Abe’ Lee, an expert on microfluidics from the University of California at Irvine, US. ‘It triggers the “why didn’t I think of this?” thought that so many great ideas do,’ he adds.

The Harvard team have shown that a variety of different papers of different sizes can be patterned with channels as small as 200 micrometres wide. They say the patterns can be reproduced quickly using a photocopier and the cost of materials per device is as low as one to three US cents, depending on its size.

Freya Mearns

Reference

A. W. Martinez *et al*, *Lab Chip*, 2008, DOI: 10.1039/b811135a

In this issue

Surf’s up for science

Chemists trade white coats for wetsuits to test lab-on-a-surfboard

Cracking down on counterfeit drugs

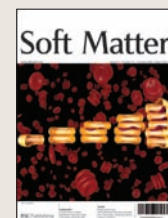
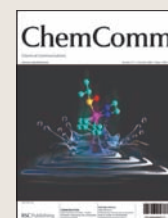
Mass spectrometry screening method offers fast detection of fake bird flu medicines

Interview: Finger on the pulse

Paul Corkum talks to Hilary Crichton about attosecond pulses

Instant insight: Colloids deliver the goods

Unilever’s Krassimir Velikov and Eddie Pelan reveal the design behind innovative, nutritious and tasty foods

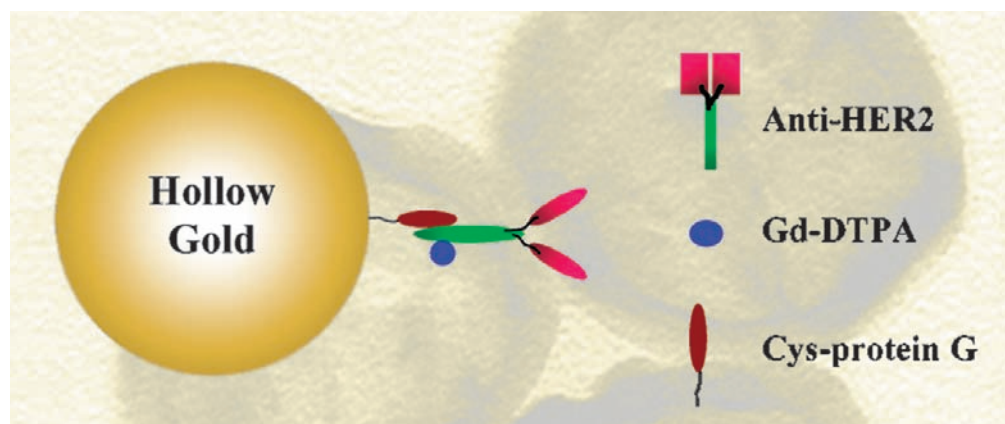


The latest applications and technological aspects of research across the chemical sciences

Application highlights

Therapeutic nanostructures combine gold, gadolinium and antibodies

Nanoparticles hunt down cancer cells



Cancer cells can be detected then destroyed using a nanostructure designed by South Korean researchers.

Bong Hyun Chung and colleagues at the Korea Research Institute of Bioscience and Biotechnology in Daejeon base their structures on hollow gold nanoparticles.

The structures have antibodies on their surface which allow them to bind to cancer cells. They also contain gadolinium, which acts as a molecular resonance imaging (MRI) contrast agent and allows the cells to be seen. When Chung shone an infrared laser on the gold nanoparticles, the heat that formed

The modified nanoparticles seek out and destroy cancer cells

destroyed the surrounding cancer cells.

The gold nanostructures overcome the drawbacks of commonly-used iron oxide MRI contrast agents, suggests Chung. Iron can lead to interference and negative contrast effects, causing errors in diagnosis. The design of the gold nanostructures leads to an enhanced signal and better diagnosis, he says.

Chung's approach is non-invasive and is likely to be effective in the treatment of early-stage cancers because it treats a specific area, unlike chemotherapy which affects the whole body. In the future 'the nanoparticles may be used for the analysis of cancer dissection in surgery', says Chung.

Michael Brown

Reference

Y T Lim *et al*, *Chem. Commun.*, 2008, DOI: 10.1039/b810240f

New portable device enables detection at contamination site

Probing mercury contamination



Detecting mercury pollution could become a lot easier, thanks to a new visual technique developed by scientists in China.

Chunhai Fan and colleagues at the Chinese Academy of Sciences and East China University in Shanghai have designed a new gold nanoprobe that changes colour when it comes into contact with mercury(II) ions.

The mercury(II) ion is the most stable form of inorganic mercury and

is known to have detrimental effects on humans and the environment. Methods to detect mercury usually require lab-based instruments but there is an increasing demand for techniques that allow rapid mercury detection in drinking water, food and soil at the site of contamination.

The new technique, which combines micro- and nano-technologies, allows rapid, selective and portable detection of mercury

Mercury turns the nanoparticles from red to purple

within microfluidic channels at room temperature. When the gold nanoprobe comes into contact with solutions containing mercury, their colour rapidly alters from red to purple. The higher the concentration of mercury, the greater the intensity of the colour change.

'Given its simplicity and low cost, we believe that this device provides a convenient approach for rapid mercury screening in the field detection of water pollution,' says Fan. He adds that the technique could be particularly useful for monitoring mercury contamination in developing countries.

Although the device currently has a mercury detection limit of only five micromolar, Fan expects that 'further design of the nanoprobe and the incorporation of signal amplification will significantly improve the sensitivity to meet more challenging requirements'.

Kathryn Lees

Reference

S He *et al*, *Chem. Commun.*, 2008, DOI: 10.1039/b811528a

Chemists trade white coats for wetsuits to test lab-on-a-surfboard

Surf's up for science

Scientists in Hawaii have developed a green way to make chemicals using a favourite local combination – sun and surfing.

Robert Liu, from the University of Hawaii, Honolulu, and colleagues have designed a solar reactor that floats on the ocean and synthesises organic compounds under the Sun. The reactor uses solar energy to make hindered isomers of vitamin A. While these isomers aren't particularly useful, Liu believes they can use the method to make other, more valuable chemical feedstocks.

Photochemical reactions use a molecule's ability to capture a photon from the Sun. This energy is then used for chemical reactions that cannot usually be done by heating. Liu used a method called triplet sensitisation, where light is



absorbed by a coloured material and the excess energy is passed on to the reactant. 'In this way, we can tap a major portion of the visible light from the Sun,' says Liu.

The floating reactor makes organic compounds using solar energy

The reactor does not require electricity or running water and is small enough to be fitted into a boogie-board (a small surf-board). The reactor uses the Pacific Ocean as an immense heat sink to dissipate excess heat, avoiding the need to circulate cooling water through the device. The reactions can be done within half an hour, the time period of a short surfing session, says Liu.

'An appealing idea,' says Axel Griesbeck, an expert in photochemistry at the University of Cologne, Germany. 'We need to support experiments like these now and not wait for the end of all natural oil, gas and coal.' Sarah Corcoran

Reference

Y-P Zhao, R O Campbell and R S H Liu, *Green Chem.*, 2008, DOI: 10.1039/b809007f

Screening method helps to identify fake Tamiflu

Cracking down on counterfeit drugs

US scientists have developed a method for screening Tamiflu in an attempt to foil counterfeiters.

Counterfeiters have targeted Tamiflu, an antiviral flu drug effective against bird flu, due to its high cost and demand. Scientists have found fake Tamiflu containing vitamin C instead of the active ingredient, oseltamivir.

Facundo Fernández and colleagues at Georgia Institute of Technology and the US Centers for Disease Control and Prevention, Atlanta, used desorption electrospray ionisation mass spectrometry (DESI MS) to help authenticate Tamiflu capsules. They doped the electrospray solvent with crown ethers and studied the competitive complexation of the crown ethers with oseltamivir. They found that by using two different crown ethers with different binding affinities for oseltamivir, they could determine the amount of oseltamivir in the capsules without using an internal standard.

Niklas Lindegardh, head



of the Clinical Pharmacology Laboratory at the Mahidol–Oxford Tropical Medicine Research Unit, Bangkok, Thailand, says he believes this is important research. 'Rapid analytical methods for screening potentially counterfeit Tamiflu capsules are of the

The high cost and demand for Tamiflu makes it a target for counterfeiters

utmost importance. The new reactive DESI method combines rapid throughput with ultimate selectivity and will provide an excellent tool for rapid semi-quantitative screening of large batches of capsules,' he says.

'The new method improves throughput by at least two orders of magnitude,' says Fernández. 'Even with existing instrumentation, this assay could be widely adopted.' He says the next challenge is to couple the ionisation reaction to portable detectors, such as ion mobility spectrometers or portable mass spectrometers. 'This will truly produce a network of point-of-care drug quality screening tools. The challenge is mostly on the engineering side. The basic knowledge is already there and we have proven the basic chemical concepts,' adds Fernández. Edward Morgan

Reference

L Nyadong *et al*, *Analyst*, 2008, DOI: 10.1039/b809471c

Biological assays can be carried out in stabilised water droplets

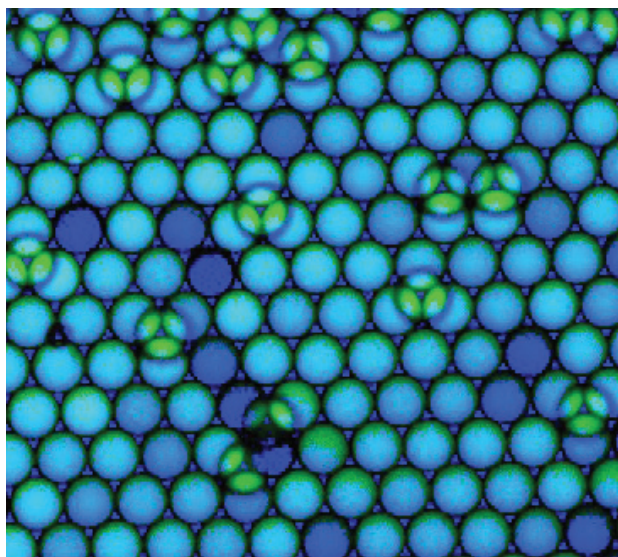
The perfect surfactant

Water droplets can be used as microvessels for bioassays thanks to a new surfactant developed by scientists in Europe and the US.

Fluorocarbon oils are an ideal medium to carry water droplets for biological assays because gases that are needed by biological cells can be dissolved in them, but they prevent cross-contamination of biological material between the droplets. They are also ideal for microfluidic devices, as the oils do not cause the material forming the channels within the device to swell up.

Until now, all commercially available surfactants for water droplets in fluorocarbon oils have either not stabilised the droplets for long enough or have interacted with their contents. Now, researchers from Germany, Italy and the US have come up with a new class of surfactants without these problems.

Christian Holtze at BASF Aktiengesellschaft, Ludwigshafen, Germany, and colleagues made



surfactants with a fluorocarbon tail and a polyethylene glycol head. By testing different variations of these surfactants they created an emulsion that is stable for weeks,

The water droplets remain stable and do not fuse, making them ideal for bioassays

suitable for biological assays which can take hours or days. Holtze also looked at how the emulsion would fare in a microfluidic device. Even when highly compressed, for example, the emulsion stayed stable.

Next Holtze trapped a piece of enzyme-coding DNA in the water droplets together with all the molecules needed to make the enzyme. He found that a fluorescent product formed in the droplets, showing that the new surfactants are biocompatible. Holtze says this could be because they are non-ionic. He also found that his emulsions can be used to contain biological cells.

Holtze says that his surfactants could allow 'unprecedented speed and control of high-throughput analyses ranging from in vitro biochemistry to single cell studies'.
Madeline Chapman

Reference

C Holtze et al, *Lab Chip*, 2008, DOI: 10.1039/b806706f

Organic inks shine in an electric current

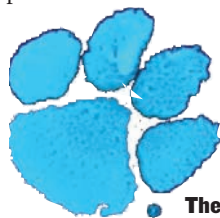
Colloids light the way to printable electronics

Cheap electronic devices can be printed using commercial printing presses thanks to light-emitting colloidal inks developed by US scientists.

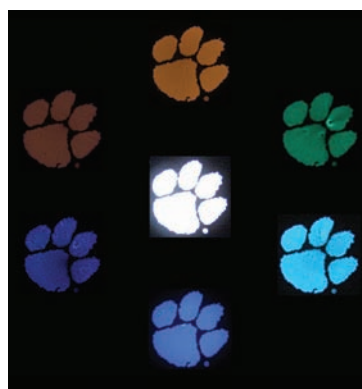
Stephen Foulger and colleagues from Clemson University made colloidal particles from organic molecules that emit red, blue or green light.

They used different ratios of the particles to make organic light emitting devices (OLEDs) in a wide range of colours.

The light emitting molecules are in a water-based colloid so they can be used as ink in commercial high-volume printing techniques, explains Foulger. The team printed the colloidal particles onto a conductive



The printed patterns light up when a voltage is applied



surface and lit up the printed pattern by applying a voltage across the surface.

Foulger says the particles could be used to make coloured electronic displays for car dashboards, for example. He

adds that the combination of low cost starting materials and high volume printing will mean cheaper products.

'The most significant finding is that individual colour has been realised in a colloidal particle and each colloidal particle still emits its original colour even when mixed together in the OLED,' says Hideyuki Murata, an expert in organic electroluminescence at the Advanced Institute of Science and Technology, Ishikawa, Japan.

Foulger says the results will help bring printable electronics to the market quickly. 'We are continuing to improve the luminosity of the devices and reduce defects in printed structures,' he adds. 'The next step is improving yields and transitioning the technology to full-scale printing presses.'

Rachel Cooper



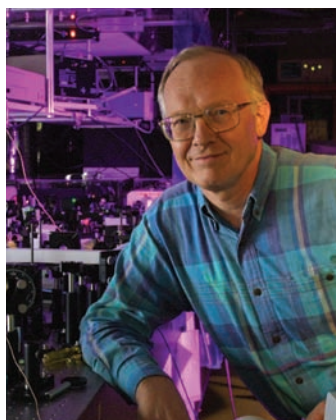
Reference

C F Huebner et al, *J. Mater. Chem.*, 2008, DOI: 10.1039/b809450k

Interview

Finger on the pulse

Paul Corkum talks to Hilary Crichton about attosecond pulses and how developing new ideas is like skiing downhill



Paul Corkum

Paul Corkum OC, FRS, FRSC is director of the Joint University of Ottawa/National Research Council Attosecond Science Laboratory and a professor of physics at the University of Ottawa. He introduced many of the concepts in strong field atomic and molecular science. His many awards include the Canadian Association of Physicists' gold medal for lifetime achievement in physics and the American Physical Society's Arthur L. Schawlow prize for quantum electronics.

Who inspired you to become a scientist?

It was my high school physics teacher. He believed that he should prove any statement. In my very first physics class, he introduced us to the concept that the dimensions of equations must balance. I remember thinking about this a lot and I liked the idea very much. From then on, I loved the simplicity and beauty of physics.

Tell us about your scientific background.

After high school, I attended an excellent small college, Acadia University, in Canada. There were only undergraduates in the physics department, so I was able to get a summer job in the laboratory every year. These summer positions introduced me to research. I published my first paper as an undergraduate.

Then, I headed to the US to attend Lehigh University, Pennsylvania. After Lehigh, I managed to get a postdoctoral fellowship at the National Research Council (NRC) of Canada, where I have worked until this year. About six months ago, the NRC and the University of Ottawa formed a joint laboratory for attosecond science. I am now director of the joint laboratory and I have a faculty position at the university.

Your research paved the way in producing attosecond pulses. What are you currently using them to investigate?

Many things. Attosecond science has implications everywhere. I will single out one very exciting one that has guided a great deal of my research for the past five years. Attosecond technology opens a class of new methods for imaging molecules. The methods are all fully compatible with measuring chemical and electronic dynamics. The image can be of an orbital, the position of the atoms or both simultaneously. That means that it is possible to see the electronic and nuclear structure of a molecule and watch it change. So far, we have concentrated on diatomic or triatomic molecules but I think we can extend the methods to molecules of more chemical or biological interest.

What's going to be the next big thing in your field?

Combining space and time – attosecond and Ångström. What we have really done so far is to introduce a systematic way to sub-divide the laser cycle – currently the shortest laser pulse is

only one-thirtieth of the period of the light that generated it. Equally, it is possible to sub-divide the light wavelength. If we can systematically achieve a spatial resolution of one-thirtieth of a wavelength then we have a powerful tool for nanotechnology. Already, for molecular problems, my group resolves one Ångström features. In other words, our spatial resolution is less than one nanometre. Looking further ahead, the methods that we have developed are only the first of many possible methods. In essence, it is the high nonlinearity that leads to attosecond pulses. Other approaches that do not rely on re-collision will surely arise. They will open even shorter timescales. At this point, the horizon seems limitless.

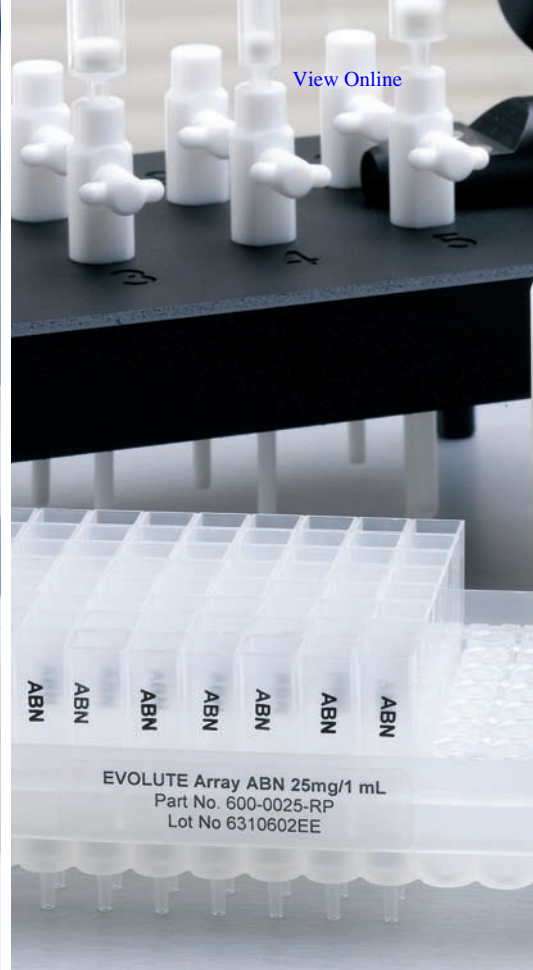
Which piece of research are you most proud of?

The re-collision model [a unique interplay between a coherent electron, coherent atoms or molecules and coherent light] has become the organising concept of a whole sub-field of science. What more can one ask for as a scientist? I am also pleased that I realised its implications almost immediately – for making and measuring attosecond pulses and for imaging molecules.

What is the most rewarding aspect of your work?

I will single out two things. First, there is nothing more rewarding or exciting than to develop a new idea. I think of it as the intellectual equivalent of downhill skiing. When skiing, you slide down a snow-covered hill as fast as you dare. To me, this is the definition of physical fun. In science, you follow a new idea – one that no one has ever thought about before – with total concentration. To me, this is the highest intellectual satisfaction possible.

Second, I like the interplay between the intellectual and social aspects of science. Most people (including me when I started) think of a scientist's life as isolated – always working alone in the laboratory. In fact, science is just the opposite. Scientists almost always work in teams. They discuss ideas openly and continually. Once they make an advance, it is their job to tell others. To do this, they travel the world. I have scientific friends to whom I am as close as to my neighbours. I have met their families and they mine. From them I gain a unique insight into other countries and other cultures. This, to quote physicist and science writer, Jeremy Bernstein, is 'the life it [science] brings'.



IST Sample Preparation • Bioanalysis • Clinical • Environmental • Forensic • Agrochemical • Food • Doping Control

EVOLUTE® CX **NEW!**

Mixed-mode selectivity, generic methodology and efficient extraction

EVOLUTE® CX mixed-mode resin-based SPE sorbent extracts a wide range of **basic drugs** from biological fluid samples. EVOLUTE CX removes matrix components such as proteins, salts, non-ionizable interferences and phospholipids, delivering cleaner extracts with reproducible recoveries for accurate quantitation.

EVOLUTE® ABN

Minimize matrix effects, reduce ion suppression and concentrate analytes of interest

EVOLUTE®ABN (Acid, Base, Neutral) is a water-wettable polymeric sorbent optimized for fast generic reversed phase SPE. Available in 30 μm columns and 96-well plates for bioanalysis and **NEW 50 μm columns** – ideally suited for environmental, food/agrochemical and industrial analysis as well as forensic and doping control applications.

Contact your local Biotage representative or visit www.biotage.com to request a **FREE** sample.

Instant insight

Colloids deliver the goods

Unilever's Krassimir Velikov and Eddie Pelan reveal the design behind innovative, nutritious and tasty foods

Product functionality is a complex product description that covers the formulation, structure, texture, stability, appearance, taste, flavour and bioavailability of food ingredients. To design nutritious foods, we need to introduce the nutrients, known as micronutrients and nutraceuticals, in a proper form to assure the stability, as well as good taste, of the final product. Micronutrients, such as vitamins and minerals, are essential for growth and development whereas nutraceuticals are not essential for life but have a positive effect on health. Unfortunately, they often cause problems when added to food due their physico-chemical properties or interaction with other ingredients. As a result, the food functionality is often compromised.

Incorporating soluble active ingredients into food products can cause a bitter taste, lipid oxidation, colour changes and chemical instability. Use of the insoluble salts can lead to physical instability and insufficient bioavailability. We need a balance between solubility and dispersibility of the active ingredient. We also need control over this balance in order to have flexibility in solving technical issues.

A generic solution for these problems is to use colloidal delivery systems, which are insoluble in the product but dissolve in the gastrointestinal tract when eaten. Colloidal dispersions are small enough not to cause physical instabilities like sedimentation. Unfortunately, there are not readily available natural colloidal delivery systems for most micronutrients and nutraceuticals so custom-made delivery systems are required.

Colloidal dispersions can be used to design and fine tune product structure and enable new product formats. Both nutraceuticals and micronutrients are used in relatively



low concentrations, so their ability to alter product structure can be limited. Nevertheless, particles like rods and platelets can be used as alternatives to biopolymers to increase viscosity or create gels at sufficiently low volumes. Colloidal particles can also stabilise fluid-in-fluid dispersions meaning that emulsions can be formed using little or no surfactant.

Taste and flavour are crucial for the success of any food product. Changes in flavour are often linked to the inherited taste of the ingredients or to unwanted chemical interactions, for example oxidation. Colloidal dispersions offer control on solubility and, as a result, control on taste.

Because a colloid's optical properties vary depending on its size and shape, colloidal dispersions offer great opportunities for fine tuning product appearance – they can deliver translucency, complete transparency or a desired colour.

Bioavailability of functional ingredients is a rapidly growing issue in the area of functional food design. Often ingredients are poorly soluble, crystalline solids at room temperature and are poorly absorbed from the gastrointestinal tract. There are several common approaches to improve their bioavailability:

chemical modification; size reduction; functionalisation of particle surfaces to improve solubility; crystallinity reduction; or polymorph alteration.

The successful application of colloidal delivery systems in foods requires a broad knowledge of molecular, ionic and colloidal interactions in the product, as well as knowledge of the biological function and metabolism of the

Colloids can enhance the flavour, texture, appearance and nutritional benefits of food

micronutrients or nutraceuticals. Since these processes are not independent, successful application into industrial products requires an integrated approach. One where the ingredients are pre-formulated to allow easy incorporation and stabilisation in the product is likely to be most useful. This approach requires linking the in-product and in vivo function of the delivery systems. Also, all aspects of product functionality, like stability, texture, taste, appearance and bioavailability, must be simultaneously considered and addressed to achieve a balanced and consumer acceptable solution.

The strategy is valid not only for food systems but also home and personal care products, drug formulations, agricultural compositions and paints. Importantly, many micronutrients and nutraceuticals are also cosmeceuticals in skin care products. The type of industry determines which aspect of the product functionality will be of highest importance.

Read more in 'Colloidal delivery systems for micronutrients and nutraceuticals' in issue 10 of *Soft Matter*.

Reference
K P Velikov and E Pelan, *Soft Matter*, 2008, 4, 1964 (DOI: 10.1039/b804863k)

Essential elements

Engineering success

CrystEngComm celebrated its tenth year of publication in style on 28 August with a lunch reception held at the XXI Congress and General Assembly of the International Union of Crystallography in Osaka, Japan. As part of the celebrations, the journal also awarded five poster prizes at the meeting.

Since its launch in 1999, *CrystEngComm* has gone from strength to strength, growing in size by more than a factor of ten. The journal now boasts the fastest publication times and highest immediacy index for a crystal engineering journal, plus an impressive impact factor of 3.47. In his welcome speech, *CrystEngComm* editor Jamie Humphrey outlined the successes of the past decade and extended his thanks: 'This success has been possible only through the support that you and other members of the



crystal engineering community have given the journal – your support as authors, referees, readers and in some cases editorial and advisory board members.'

Regular *CrystEngComm* author Pierangelo Metrangolo of Milan, Italy, who attended the lunch reception, cites the journal as one

of his favourites for publication of his research. 'In particular,' he says, 'I appreciate the speed at which papers are processed and the very kind co-operation of the editorial staff. What else to say: Happy Birthday *CrystEngComm*..., and keep up the good work!'

A decade since launch and the future for *CrystEngComm* has never looked so bright. Celebrations will continue later this year with an anniversary theme issue, including articles by editorial and advisory board members, and the journal is also heavily involved in the organisation of a crystal engineering symposium as part of the IUPAC Congress next year in Glasgow.

Visit www.crystengcomm.org for updates on these and other exciting events.

Facebook fans

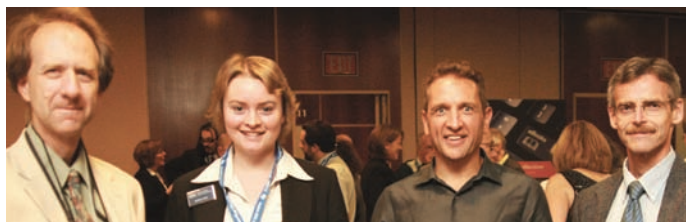
Enjoyed reading the first few issues of RSC Publishing's newest journal, *Energy & Environmental Science (EES)*? Then become a Facebook fan by visiting the *EES* Facebook page and joining in. Fans can see summaries and link to the latest *EES* articles published online, view and share relevant videos, images, events and news. Use the page to find out about upcoming events where you can meet the editors or contribute to a discussion and connect with fellow fans. Fans will see stories in their News Feed when their friends become fans or engage with the *EES* Facebook page in a variety of ways. You can find the *EES* Facebook page by searching for *Energy & Environmental Science* using the Quick Search bar on any Facebook page or by going to the main search page.

Or paste the following URL into your browser: www.facebook.com/pages/Energy-Environmental-Science/24375018213. See you there!

A warm reception in Philadelphia

The atmosphere inside the Philadelphia Marriott mirrored the sunny blue sky outside as guests gathered at the RSC Reception. Held on 17 August, it coincided with the 236th American Chemical Society National Meeting and Exposition taking place at the Pennsylvania Convention Center.

Around 200 people listened to RSC president Dave Garner as he welcomed guests, including Nobel prize winner Bob Grubbs from Caltech,



Left to right: Jonathan Sessler (U Texas at Austin), Kate Sear (deputy editor ChemComm, RSC), Kevin Burgess (Texas A&M), Peter Wipf (Pittsburgh)

a variety of eminent and emerging researchers, plus university librarians and local RSC members. The incoming

president of the ACS, Tom Lane, was also there with a number of his society colleagues, indicating the continuing warm friendship

between the two chemical societies.

Guests enjoyed refreshments while catching up with friends old and new, and RSC staff were on hand to describe the latest RSC initiatives, including the hot topics of *Energy & Environmental Science*, *Integrative Biology* and *Metallomics*, the three newest RSC journals.

At the end of a genial evening, everyone was looking forward to meeting again – so see you all in Salt Lake City in spring 2009!

Chemical Technology (ISSN: 1744-1560) is published monthly by the Royal Society of Chemistry, Thomas Graham House, Science Park, Milton Road, Cambridge UK CB4 0WF. It is distributed free with *Chemical Communications*, *Journal of Materials Chemistry*, *The Analyst*, *Lab on a Chip*, *Journal of Atomic Absorption Spectrometry*, *Green Chemistry*, *CrystEngComm*, *Physical Chemistry Chemical Physics*, *Energy & Environmental Science* and *Analytical Abstracts*. *Chemical Technology* can also be purchased separately. 2008 annual subscription rate: £199; US \$396. All orders accompanied by payment should be sent to Sales and Customer Services, RSC (address above). Tel +44 (0) 1223 432360, Fax +44 (0) 1223 426017. Email: sales@rsc.org

Editor: Joanne Thomson
Deputy editor: Michael Spenceley
Associate editors: Celia Gitterman, Nina Notman
Interviews editor: Elinor Richards
Web editors: Nicola Convine, Michael Townsend, Debora Giovannelli
Essential elements: Sarah Day, Kathryn Lees, and Valerie Simpson

Publishing assistant: Jackie Cockrill
Publisher: Graham McCann

Apart from fair dealing for the purposes of research or private study for non-commercial purposes, or criticism or review, as permitted under the Copyright, Designs and Patents Act 1988 and the copyright and Related Rights Regulations 2003, this publication may only be reproduced, stored or transmitted, in any form or by any means, with the prior permission of the Publisher or in the case of reprographic reproduction in accordance with the terms of licences issued by the Copyright Licensing Agency in the UK. US copyright law is applicable to users in the USA.

The Royal Society of Chemistry takes reasonable care in the preparation of this publication but does not accept liability for the consequences of any errors or omissions.

Royal Society of Chemistry: Registered Charity No. 207890.

RSC Publishing

Inspired by nature: green solvents in science and application

DOI: 10.1039/b815697m

The search for alternative solvents continues to be an important area of green chemistry as reflected over the years by many contributions to this Journal, including the collective issues comprising contributions from the biannual conference series on “Green Solvents”. This year’s conference, which is being held from September 28 to October 2 2008, is devoted to “Progress in Science and Application”, an attempt to take a snapshot of how the state of the art has changed in this area since the conference series started in 2002.

Traditionally, the meeting opens with a Sunday evening lecture that provides a broader perspective on green chemistry issues related to solvents in chemical processes. This lecture is always given by eminent protagonists in the field, who are asked to share with the audience their personal experience and views, their expectations, and their criticisms about recent developments to provoke discussion and to set the scene for the following two and a half days. Previous years have seen Paul Anastas, Roger Sheldon, and Eric Beckman doing an excellent job in this “pole position”.

For the 2008 Green Solvents meeting, the Editorial Board of *Green Chemistry* has decided to declare this particular slot to be one of the “*Green Chemistry Lectures*” initiated on the occasion of the 10th anniversary of the Journal. Immediately and unanimously, István Horváth was nominated as 2008 lecturer, and a condensed version of his presentation can be found in this issue of *Green Chemistry*.¹ Prof. Horváth has pioneered a range of approaches to utilize specifically designed solvent systems in catalytic processes in a very elegant way throughout his career, especially during his period at ExxonMobil in the USA and later at Eötvös Loránd University in Budapest, Hungary. As you follow his personal journey through the chemistry of various solvent systems, it will become evident how the concepts of green chemistry have influenced his research programme and built upon an existing expertise to open up quite new endeavours in the molecular and engineering sciences.

In addition, Prof. Horváth points out nicely in his perspective how nature is still the master of solution phase chemistry.

Understanding the principles that control reactivity through hydrophobic/hydrophilic interactions, phase separation, and compartmentalization found in natural systems and transferring these strategies into advanced solvent systems to achieve multi-step cascade reactions remains a scientific and technical challenge of great potential impact. In this respect, nature can serve as an inspiration for green solvent systems regardless of whether the solvents themselves are of natural origin or not.

We hope that the readers of *Green Chemistry* will enjoy this perspective as much as the participants in Friedrichshafen enjoyed Prof. Horváth’s stimulating lecture and that his continuing enthusiasm for the molecular sciences and green chemistry will be an inspiration to many young chemists and chemical engineers.

Walter Leitner
RWTH-Aachen, Germany

Reference

- 1 I. T. Horváth, *Green Chem.*, 2008, **10**, DOI: 10.1039/b812804a.

Solvents from nature†

István T. Horváth*

Received 24th July 2008, Accepted 22nd August 2008

First published as an Advance Article on the web 9th September 2008

DOI: 10.1039/b812804a

In this perspective, a personal journey from solvent to solvent is presented to demonstrate how environmentally friendly solvents can be part of the solution of various chemical challenges. Solvents are important components of Nature to provide one or more liquid phases for chemical reactions and processes. While some solvents are available from Nature even in large quantities, most of the solvents are man-made. Historically, solvents were developed and/or selected to help the chemical or physical objectives of the user(s) only. With the increasing importance of local and global health and environmental issues, including the introduction of green chemistry and the molecular approach for pollution prevention, the potential impacts of solvents became important selection tools. One of the key principles of green chemistry is the elimination of solvents in chemical processes or the replacement of hazardous solvents with environmentally benign solvents. The development of solvent-free alternative processes is the best solution, especially when either one of the substrates or the product is a liquid and can be used as the solvent of the reaction. However, if solvents are crucial to a process we should select from solvents that will have no or limited impact on health and the environment.

Introduction

Solvents have been used extensively to provide one or more liquid phases for chemical reactions, regulate temperatures, moderate exothermic reactions, clean equipment and clothing, isolate and purify compounds by re-crystallization or extractions, generate azeotropes for separation, assist structural and/or analytical characterization of chemicals, *etc.*¹ While there are solvents that are available in Nature and are environmentally benign, a large number of them are man-made and could result in serious environmental and health problems. For example, the destruction of ozone by chlorofluorocarbons in the upper atmosphere is well established and led to the replacement of refrigerants. The toxicity of some of the chlorinated solvents poses a threat to the workers and, if they enter the environment, to all of us. Solvents frequently cause fires and/or explosions resulting in destruction. One of the key principles of green chemistry is the elimination of solvents in chemical processes or the replacement of hazardous solvents with environmentally benign solvents.² The development of solvent-free alternative processes could be the best solution, especially when either one of the substrates or the product is a liquid and can be used as the solvent of the reaction. However, if a solvent is crucial to a process we should select solvents that will have no or limited impact on health and the environment.

Nature provides only a limited number of molecules that can be used as solvents either directly or after purification. Although water is the most abundant solvent in Earth, its largest portion contains dissolved sodium chloride and some

other salts that make it useless for human consumption. Higher level of salts in water, for example 40% in the Dead Sea, could offer unexpected pleasures to humans, however, *e.g.* floating on the surface of water. Nature uses fresh water, generally containing many less solutes, in our rivers and lakes to assist all form of life on land. Human activities could result in increased levels of dissolved contaminants, including inorganic and organic chemicals. Fortunately, we are releasing less and less contaminated water to the environment because of the increased use of closed waste water systems combined with state-of-the-art waste water treatment technologies. Ethanol has recently become an important molecule as a fuel (*e.g.* bio-ethanol), which is produced by Nature in water; however, mostly along with other chemicals in smaller quantities (in forms of beer, white and red wine) and mostly consumed by mankind before the removal of water. Although vegetable oils could be used as organic solvents from Nature, they have been used rarely. Its recent utilization as a feedstock to produce bio-diesel resulted in a new solvent, glycerol, which therefore can be considered as a solvent from Nature and could replace di- and polyols. Finally, crude oil is not used as a solvent, but most of the conventional organic solvents are made from it in refineries or chemical plants.

I used *n*-hexane as my first solvent to re-crystallize $\text{Co}_2(\text{CO})_8$ to prepare my first cobalt complex in the fall of 1973.³ Subsequently, it was proven that *n*-hexane is one of the most toxic aliphatic hydrocarbons and that *n*-heptane is orders of magnitude less toxic. Over the next 14 years I remained a dedicated user of conventional organic solvents, including alkanes, aromatics, chlorinated, polar aprotic and protic solvents, to assist catalytic reactions and to prepare and characterize cobalt, osmium, iridium, ruthenium, rhodium, platinum and tungsten complexes. I first realized the potential impacts of an alternative solvent such as water during the excellent lectures of Profs Wolfgang A. Herrmann and Boy Cornils at the Königstein Conference in

Institute of Chemistry, Eötvös University, Pázmány Péter sétány 1/A, H-1117, Budapest, Hungary. E-mail: istvan.t.horvath@att.net

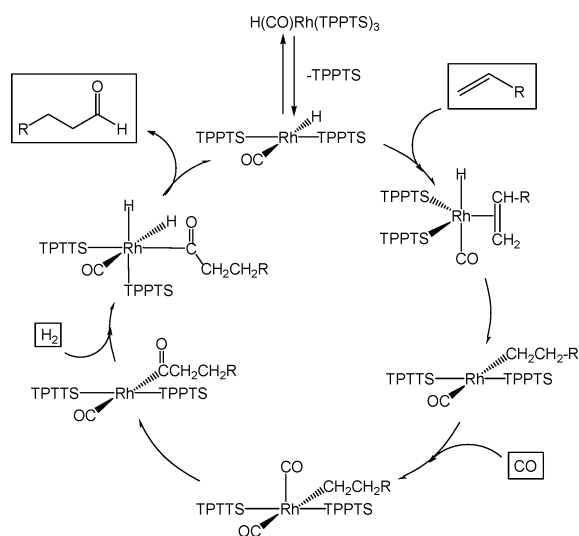
† This perspective is based on the *Green Chemistry* lecture presented at the Green Solvents–Progress in Science and Application meeting at Friedrichshafen, Germany, September 2008

early September 1987.⁴ After that meeting I moved from ETH-Zürich to Exxon Corporate Research (now ExxonMobil) and had the chance to select my first project, which actually was a mechanistic study of the water soluble phosphine modified rhodium hydroformylation catalyst system.⁵ Interestingly, my other project was the use of $\text{BF}_3 \cdot 2\text{H}_2\text{O}$ in the carbonylation of iso-butylene to neopentanoic acid, a good example for a chemical technology performed in an acid and/or in an ionic liquid.⁶ Other applications of acids were the platinum catalyzed hydrogenation of aromatics in supported $\text{BF}_3 \cdot \text{H}_2\text{O}$ (or rather a very strong acid: $\text{H}^+[\text{BF}_3\text{OH}]^-$) phase,⁷ the first observation of the formil cation in solution,⁸ and the carbonylation of methane in superacids.⁹ Methanol served both as a substrate and a solvent in the copper catalyzed oxidative carbonylation of methanol to dimethyl carbonate¹⁰ and in the cobalt catalyzed methoxyhydrocarbonylation of butadiene.¹¹ The frustration with the potential over-oxidation of methanol during the oxidation of methane led to the development of fluorous biphasic systems,¹² including the design of the fluorous soluble phosphine modified rhodium hydroformylation catalyst.¹³ My personal solvent journey continued with the mechanistic study of the Friedel-Crafts reaction¹⁴ and the Beckmann-rearrangement in ionic liquids¹⁵ with my current interest in bio-liquids, in particular in γ -valerolactone, a sustainable liquid for carbon based products, energy, and solvent.¹⁶

Water

Water could be an excellent solvent for chemical reactions, because it is readily available, nonflammable, non toxic, cheap, and could offer the easy separation of reagents or catalysts from many organic products. Water could be a good medium for ionic reactions because it can readily solvate anions and cations. It could serve both as a solvent and as a ligand, which could stabilize coordinatively unsaturated species, a key issue for long term catalyst stability. Water is a good σ -donor with very weak back donation capability. The strong O–H bonds of water do not permit easy reactions with radicals and therefore it could be an attractive medium for radical reactions. Stabilizing structures and effecting reactions by hydrogen bond(s) are important solvent properties of water as solvent, which is indeed supporting life quite well.

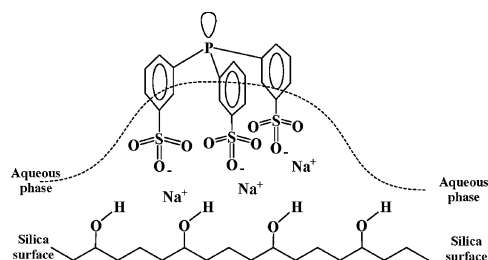
Rhône-Poulenc developed, and Ruhrchemie commercialized, an aqueous biphasic process for the hydroformylation of propylene in the presence of $\text{HRh}(\text{CO})[\text{TPPTS}]_3$ (TPPTS: *m*-trisulfonated-triphenylphosphine).¹⁷ The main product is *n*-butanal and the normal- and iso-butanal ratio is about 25, surprisingly high in comparison to the conventional PPh_3 modified rhodium catalyst under similar conditions. The overall reaction mechanism operating in the aqueous and organic phases is very similar (Scheme 1).⁵ It is believed that the coordination of the olefin to the coordinatively unsaturated $\{\text{HRh}(\text{CO})(\text{TPPTS})_2\}$ or $\{\text{HRh}(\text{CO})_2(\text{TPPTS})\}$ results in high or low normal- to iso-aldehyde ratio, respectively. Indeed, $\text{HRh}(\text{CO})_2(\text{TPPTS})$ was not detectable in water even under high pressure of CO/H_2 , which explains the higher selectivity of the aqueous biphasic system.⁵ The significantly higher activation energy of the dissociation of TPPTS from $\text{HRh}(\text{CO})(\text{TPPTS})_3$, compared with PPh_3 from $\text{HRh}(\text{CO})(\text{PPh}_3)_3$, could be due to



Scheme 1

the intramolecular association of sulfonate substituents of the neighboring TPPTS ligands *via* hydrogen bonding in aqueous media.⁵

One of the limitations of water is the low solubility of some gases (H_2 and CO) and many organic compounds. It was reported that supported aqueous phase (SAP) catalysis could overcome this limitation by immobilizing the aqueous solution of $\text{HRh}(\text{CO})(\text{TPPTS})_3$ on a high surface area silica support.¹⁸ It was later shown that the hydrophilic support holds the water soluble phosphines by hydrogen bonding of the hydrated sodium-sulfonate groups to the surface of silica.¹⁹



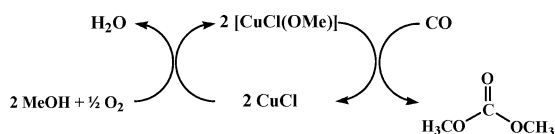
Our most recent work with water focuses on the effective use of aqueous phosphine modified transition metal catalysts by keeping the metal leaching at the lowest possible level. The origin of the metal leaching in the presence of water soluble phosphines is the dissociation or side reactions of the phosphines. The dissociation, of course, primarily depends on the strength of the metal-phosphorous bonds of the metal complexes in solution. The application of basic phosphines will increase the strength of the metal-phosphorous bonds and thus will result in lower metal leaching. The introduction of sulfonate groups as the solubilizing groups in water generally involves sulfonation by oleum and could lead to the formation of phosphine-oxide side-products during work-up. Although several protection/deprotection methods have been introduced to protect the phosphorus atom, these procedures involve two synthetic steps and the production of un-recyclable wastes. We have developed a greener synthetic route for the preparation of alkyldiaryl- and dialkylaryl-phosphanes by controlling the pH

of the reaction mixture during the aqueous/organic separation steps, resulting in oxide free water soluble phosphines.²⁰

Alcohols

A possible approach to overcome of the low solubility of organics in water is the use of alcohols, diols and polyols. They could provide tunable solvent performance by the effects of the alkyl group(s) and the hydrogen bonding of the hydroxyl group(s). The Shell higher olefin process (SHOP) was the first industrial biphasic system in which the separation of the catalyst was successfully achieved.²¹ A Ni-based catalyst is used in 1,4-butanediol to catalyze the oligomerization of ethylene to linear olefins. The catalytic reaction takes place in the diol phase, and the products, the α -olefins have limited solubility in the diol providing facile separation from the catalyst. The olefins are separated from each other by distillation in subsequent distillation towers.

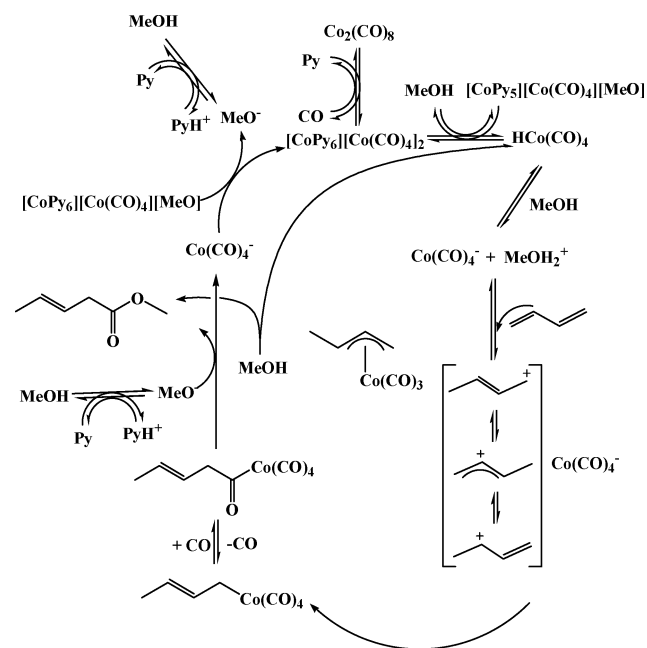
Dimethyl carbonate (DMC) is a safe, non-corrosive, and environmentally friendly alternative to phosgene, methoxycarbonyl chloride, dimethylsulfate and methyl halides and can be used as solvent. The conventional DMC process is based on the reaction of methanol with the highly toxic phosgene using chlorinated solvent. The first alternative process was based on the oxidative carbonylation of methanol in the presence of CuCl at 2–3 MPa and 100–130 °C.²² A major advantage of this approach is that both the substrate methanol and product DMC are used as solvents in the process. Due to the formation of wet HCl by the hydrolysis of chloride containing copper species, the process is extremely corrosive and all commercial equipment, exposed to the CuCl–MeOH–H₂O–HCl mixture, must be glass lined. In addition, the formation of chlorinated organic side-products could be an environmental issue for subsequent applications of DMC.



We have developed a chlorine-free catalyst, prepared *in situ* from Cu(II)acetate and 2,2'-bipyrimidine, which can be used for the oxidative carbonylation of methanol to dimethyl carbonate.¹⁰ *In situ* high pressure spectroscopic studies suggest the formation of [Cu(2,2'-bipyrimidine)(CO)(OMe)] as one of the key intermediates. The catalytic performance of the 2,2'-bipyrimidine-modified Cu-catalyst is similar to the CuCl-based system.

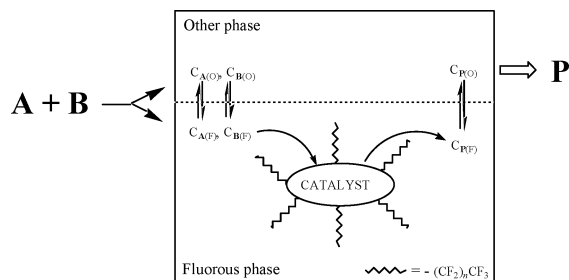
We have been investigating the mechanism of the pyridine modified cobalt-catalyzed hydromethoxycarbonylation of 1,3-butadiene to methyl-3-pentenoate. The initial step of the reaction is the disproportionation of dicobalt-octacarbonyl to [CoPy₆][Co(CO)₄]₂ salt, followed by its reaction with methanol to form HCo(CO)₄. Since the equilibrium between HCo(CO)₄ and [MeOH₂]⁺[Co(CO)₄]⁻ in methanol is shifted to [MeOH₂]⁺[Co(CO)₄]⁻, the reaction of protonated butadiene with [Co(CO)₄]⁻ leads to the formation of the alkyl complex CH₃CH=CHCH₂Co(CO)₄. This species, depending on the conditions, can undergo facile CO-insertion to yield CH₃CH=CHCH₂(C=O)Co(CO)₄ or reversible decarbonylation

to form (η^3 -C₄H₇)Co(CO)₃. The methanolysis of the acyl-cobalt intermediate occurs by the nucleophilic attack of the methoxyanion to yield methyl-3-pentenoate and regenerate the cobalt catalyst. This reaction is five times faster in the presence of pyridine (Py) due to the higher concentration of the methoxyanion.¹¹



Fluorous solvents

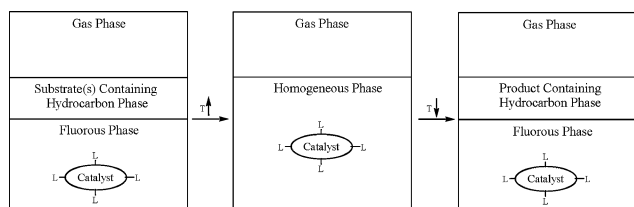
Perfluorinated alkanes, dialkylethers, and trialkylamines are man-made and unusual because of their extremely nonpolar nature and low intermolecular forces. Their miscibility even with common organic solvents is low at room temperature, thus these materials could form fluorous biphasic systems. The term fluorous was introduced, as the analogue to the term aqueous, to emphasize the fact that one of the phases of a biphasic system is richer in fluorocarbons than the other.¹²



Fluorous biphasic systems have been used in stoichiometric and catalytic chemical transformations by immobilizing reagents and catalysts in the fluorous phase. A fluorous system consists of a fluorous phase containing a preferentially fluorous soluble reagent or catalyst and a second product phase, which may be any organic or nonorganic solvent with limited solubility in the fluorous phase. Reagents and catalysts can be made fluorous soluble by attaching fluorocarbon moieties to ligands in appropriate size and number. The most effective fluorocarbon moieties are linear or branched perfluoroalkyl chains with high carbon number that may contain other heteroatoms

(the “fluorous ponytails”). A fluorous biphasic reaction could proceed either in the fluorous phase or at the interface of the two phases, depending on the solubilities of the substrates in the fluorous phase. When the solubilities of the substrates are very low in the fluorous phase, the chemical reaction may still occur at the interface or appropriate phase transfer agents may be added to facilitate the reaction.

It should be emphasized that a fluorous biphasic system might become a one-phase system by increasing the temperature. Thus, a fluorous catalyst could combine the advantages of one phase catalysis with biphasic product separation by running the reaction at higher temperatures and separating the products at lower temperatures.



Alternatively, the temperature-dependent solubilities of solid fluorous catalysts in liquid substrates or in conventional solvents containing the substrates could eliminate the need of fluorous solvents.^{23,24} A large variety of fluorous reagents and catalysts have been prepared by attaching fluorocarbon moieties in appropriate size and number.²⁵ In general, they have similar structures and spectroscopic properties to the parent compounds. The major difference arises from the presence of the fluorous ponytails, which provide a fluorous blanket around the hydrocarbon domain. Because of the well known electron-withdrawing properties of the fluorine atom, the fluorous ponytails could change significantly the electronic properties and consequently the reactivity. Insertion of insulating groups before the fluorous ponytail may be necessary to decrease the strong electron withdrawing effects, an important consideration if reagent or catalyst reactivity is desired to approximate that observed for the unmodified species in hydrocarbon solvents.¹³

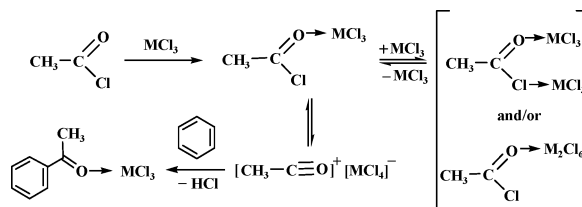
The great potential of the fluorous-liquid/liquid concept for catalyst recovery was first demonstrated for the hydroformylation of olefins.¹³ The fluorous soluble $P[\text{CH}_2\text{CH}_2(\text{CF}_2)_3\text{CF}_3]_3$ modified rhodium catalyst system is an excellent catalyst for the hydroformylation of decene-1 at 100 °C under 11 bar CO/H_2 (1 : 1) in $\text{CF}_3\text{C}_6\text{F}_{11}$ and the aldehydes can be easily separated from the fluorous catalyst. Fluorous chemistry became a well-established area and provides a complementary approach to other biphasic systems.²⁵

Ionic liquids

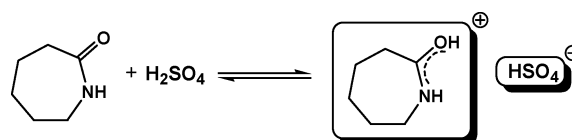
Ionic liquids are molten salts, which are liquids at or close to room temperature.²⁶ While the cations are generally large organic compounds such as *N,N'*-dialkyl-imidazolium, *N*-alkylpyridinium, *N,N*-alkylpyrrolinium, *etc.*, the anions are smaller usually AlCl_4^- , HF_2^- , BF_4^- , PF_6^- , SbF_6^- , CF_3SO_3^- , *etc.* and some of them are commercially available. One of the most attractive properties of ionic liquids is the very low vapor pressure. Furthermore, they are not flammable, easy to handle, have reasonable thermal stability and are liquids at large range

of temperature. They can behave as a Lewis acid and serve as a solvent at the same time or they can be a ligand and solvent simultaneously.

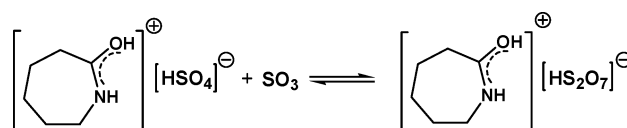
Friedel–Crafts acylation of aromatic compounds has been an important reaction in the production of pharmaceuticals and fine chemicals for more than a century.²⁷ Since most of the conventional industrial processes are performed in volatile and hazardous halogenated solvents, their replacement with ionic liquids can considerably lower the environmental risks involved. We have shown by *in situ* IR studies that the mechanism of the Friedel–Crafts acylation of benzene is exactly the same in ionic liquids as that of in 1,2-dichloroethane.¹⁴ The reaction of acetyl chloride with benzene in the presence of MCl_3 ($\text{M} = \text{Al}$ or Fe) in the ionic liquid 1-butyl-3-methyl-imidazolium chloride, ($[\text{bmim}]\text{Cl}$), leads to the formation of several key intermediates including the MCl_3 adducts of the acetyl chloride, the acylium ion $[\text{CH}_3\text{CO}]^+[\text{MCl}_4]^-$, and the final product, the MCl_3 adduct of acetophenone.



The ultimate success of ionic liquids depends whether they will be used commercially in small or larger scale applications. Of course, a profitable larger scale process will convince others to explore and use the same or similar media for different applications. While ionic liquids have been used in smaller processes,²⁸ the existence of a large scale application was recently realized by investigating the mechanism of the Beckmann rearrangement of cyclohexanone oxim to ϵ -caprolactam in sulfuric acid or oleum.¹⁵ It appears that the rearrangement medium, used by all caprolactam manufacturers, is actually an ionic liquid, the caprolactamium hydrogen sulfate:



We have shown that the vapor pressures of caprolactamium hydrogen sulfate is much lower than that of oleum, which explains why the Beckmann rearrangement could have been used without any serious problems for decades.¹⁵ While the observed low vapor pressure of dissolved SO_3 could be the result of strong interactions between the caprolactamium hydrogen sulfate and sulfur trioxide, the formation of an other anion such as $[\text{HS}_2\text{O}_7]^-$ seems also plausible:



The ecotoxicity of some ionic liquids have been reported,²⁹ which shows that not all of them are green solvents, therefore the measurements of toxicity of solvents must be included in

their evaluations. Furthermore, new ionic liquids have been synthesized using biogenic building blocks.³⁰

γ -Valerolactone

It was recently proposed that γ -valerolactone (GVL), a frequently used food additive, exhibits the most important characteristics of an ideal sustainable liquid, including the possibility to use it for the production of both energy or carbon-based consumer products.¹⁶ It is renewable, has low melting ($-31\text{ }^{\circ}\text{C}$), high boiling ($207\text{ }^{\circ}\text{C}$) and flash ($96\text{ }^{\circ}\text{C}$) points, a definitive but acceptable smell for easy recognition of leaks and spills, low toxicity, and high solubility in water to assist biodegradation. In addition, we have shown that its vapor pressure is 0.65 kPa at $25\text{ }^{\circ}\text{C}$, and it only increases to 3.5 kPa at $80\text{ }^{\circ}\text{C}$. GVL does not hydrolyze under neutral conditions and does not form a measurable amount of peroxides in a glass flask under air in weeks, making it a safe material for large scale use. Comparative evaluation of GVL and ethanol as fuel additives, performed on a mixture of 10 v/v% GVL or EtOH and 90 v/v% 95-octane gasoline, shows very similar properties. Since GVL does not form an azeotrope with water, the latter can be readily removed by distillation, resulting in a less energy demanding process for the production of GVL than that of absolute ethanol. Finally, it is also important to recognize that the use of a single chemical entity, such as GVL, as a sustainable liquid instead of a mixture of compounds could significantly simplify its worldwide monitoring and regulation.

Conclusions

One of the key principles of green chemistry is the elimination of solvents in chemical processes or the replacement of hazardous solvents with environmentally benign solvents. The development of solvent-free alternative processes is the best solution, especially when either one of the substrates or the product is a liquid and can be used as the natural solvent of the reaction. However, if solvents are crucial to a process we can select from solvents that will have no or limited impact on health and the environment, and the selection should be intrinsic part of green innovation.³¹ The main conclusion of my personal journey from solvent to solvent during the last twenty years is that first we should match the solvent properties with the chemical objectives and then identify the best available solvent, or design a new solvent.

Acknowledgements

I would like to thank many of my colleagues, students, and collaborators, whose names are listed in the references, for their

enthusiasm and contributions to our research efforts. Some of the results presented here were funded by the ExxonMobil Research and Engineering (1987–1998), DSM Research (2002–2008), and the Hungarian National Scientific Research Fund (2000–2007).

Notes and references

- 1 C. Reichardt, *Org. Process Res. Dev.*, 2007, **111**, 105.
- 2 P. T. Anastas, J. C. Warner, *Green Chemistry: Theory and Practice*, Oxford University Press, Oxford, 1998.
- 3 I. T. Horváth, G. Pályi, L. Markó and G. Andreetti, *J. Chem. Soc., Chem. Commun.*, 1979, 1054.
- 4 Königstein Conference II, International Workshop on The Chemistry of Heteronuclear Clusters and Multimetallic Catalysts, September 7–11, 1987, Taunus, Germany.
- 5 I. T. Horváth, R. V. Kastrup, A. A. Oswald and E. J. Mozeleski, *Catal. Lett.*, 1989, **2**, 85.
- 6 A. A. Oswald, R. V. Kastrup, M. J. Gula, M. A. Richard, I. T. Horváth, Mechanism of the Koch Reaction, 6th International Symposium on Homogeneous Catalysis, August 21–26, 1988, Vancouver, Canada.
- 7 I. T. Horváth, *Angew. Chem., Int. Ed. Engl.*, 1991, **30**, 1009.
- 8 P. J. F. de Rege, J. A. Gladysz and I. T. Horváth, *Science*, 1997, **276**, 776.
- 9 P. J. F. de Rege, J. A. Gladysz and I. T. Horváth, *Adv. Synth. Catal.*, 2002, **344**, 1059.
- 10 S. Csihony, L. T. Mika, G. Vlád, K. Barta, P. C. Mehnert and I. T. Horváth, *Collect. Czech. Chem. Commun.*, 2007, **72**, 1094.
- 11 R. Tuba, L. T. Mika, A. Bodor, Z. Pusztai, I. Tóth and I. T. Horváth, *Organometallics*, 2003, **22**, 1582.
- 12 I. T. Horváth and J. Rábai, *Science*, 1994, **266**, 72.
- 13 I. T. Horváth, G. Kiss, R. A. Cook, J. E. Bond, P. A. Stevens, J. Rábai and E. J. Mozeleski, *J. Am. Chem. Soc.*, 1998, **120**, 3133.
- 14 S. Csihony, M. Mehdi and I. T. Horváth, *Green Chem*, 2001, **3**, 307.
- 15 V. Fábos, D. Lantos, A. Bodor, A. -M. Bálint, L. T. Mika, L. O. E. Sielcken, A. Cuiper and I. T. Horváth, *ChemSusChem*, 2008, **1**, 189.
- 16 I. T. Horváth, H. Mehdi, V. Fábos, L. Boda and L. T. Mika, *Green Chem*, 2008, **10**, 238.
- 17 B. Cornils and E. G. Kuntz, *J. Organomet. Chem.*, 1995, **502**, 177.
- 18 J. P. Arhancet, M. E. Davis, J. S. Merola and B. E. Hanson, *Nature*, 1989, **339**, 454.
- 19 I. T. Horváth, *Catal. Lett.*, 1990, **6**, 43.
- 20 L. T. Mika, L. Orha, N. Farkas and I. T. Horváth, *Organometallics*, submitted.
- 21 W. Keim, F. H. Kowaldt, R. Goddard and C. Krüger, *Angew. Chem., Int. Ed.*, 1978, **17**, 466.
- 22 U. Romano, R. Tesei, M. M. Mauri and P. Rebora, *Ind. Eng. Chem. Prod. Res. Dev.*, 1980, **19**, 396.
- 23 M. Wende and J. A. Gladysz, *J. Am. Chem. Soc.*, 2001, **123**, 11490.
- 24 K. Ishihara, S. Kondo and H. Yamamoto, *Synlett*, 2001, 1371.
- 25 I. T. Horváth, *Acc. Chem. Res.*, 1998, **31**, 641.
- 26 T. Welton, *Chem. Rev.*, 1999, **99**, 2071.
- 27 C. Friedel and J. M. Crafts, *Bull. Soc. Chim. Fr.*, 1877, **27**, 482.
- 28 P. L. Short, *Chem. Eng. News*, 2004, **84**, 15.
- 29 A. S. Wells and V. T. Coombe, *Org. Process Res Dev*, 2006, **10**, 794.
- 30 Y. Fukaya, Y. Iizuka, K. Sekikawa and H. Ohno, *Green Chem.*, 2007, **9**, 1155.
- 31 I. T. Horváth and P. T. Anastas, *Chem. Rev.*, 2007, **107**, 2169.

Manganese octahedral molecular sieves catalyzed tandem process for synthesis of quinoxalines

Shanthakumar Sithambaram,^a Yunshuang Ding,^b Weina Li,^b Xiongfei Shen,^b Faith Gaenzler^a and Steven L. Suib^{a,b}

Received 26th March 2008, Accepted 4th September 2008

First published as an Advance Article on the web 12th September 2008

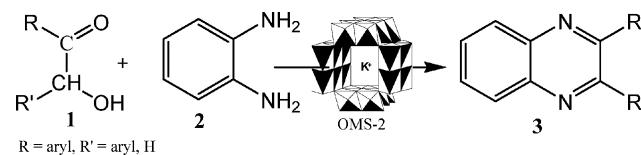
DOI: 10.1039/b805155k

An efficient environmentally benign tandem synthetic route to prepare quinoxalines leading to 100% yields using reusable manganese oxide octahedral molecular sieves (OMS-2) is described.

Single-pot tandem reactions involving catalysis have recently become an important methodology in chemistry.¹ Multi-step organic syntheses are common in the fine chemical industry, and they suffer from several disadvantages. Such reactions are often carried out non-catalytically using relatively large amounts of reagents that produce many kilograms of waste per kilogram of final product. In addition, the separation and purification steps needed after each conversion step produce waste heat. Going from traditional step-by-step methods to a one-pot coupled conversion saves raw materials and energy and reduces waste.²

Quinoxalines are a versatile class of nitrogen containing heterocyclic compounds and they constitute useful intermediates in organic synthesis.³ Quinoxalines have been reported to be biocides,⁴ pharmaceuticals,⁵ and organic semiconductors.⁶ Conventionally, quinoxalines are synthesized by a double condensation reaction involving a dicarbonyl and *ortho*-phenylenediamine.⁷ Due to the highly reactive nature of the dicarbonyls, alternative routes have been proposed recently. Antoniotti and Donach have reported one of these methods to synthesize quinoxalines from epoxides and ene-1,2-diamines.⁸ Active manganese oxide and molecular sieves in combination or manganese oxides in combination with microwaves have also been used in producing quinoxalines.⁹ These processes, however, require excessive amounts of manganese oxide as stoichiometric oxidants and scaling them up for industrial processes can lead to the formation of large amounts of toxic waste leading to environmental issues. In additional studies, Robinson and Taylor reported a homogeneous catalytic process utilizing Pd(OAc)₂, RuCl₂(PPh₃)₂ to synthesize quinoxalines from hydroxy ketones,¹⁰ and recently a copper catalyzed oxidative cyclization process has been reported.¹¹ An improved ruthenium catalyzed direct approach to synthesize quinoxalines from diols and *ortho*-diamines has also been reported.¹² These processes are efficient, but suffer from the major drawback that the catalysts cannot be recovered and reused.

In this communication we report a highly efficient catalytic single pot tandem synthetic route (Scheme 1) to form quinoxalines (3) from hydroxy ketones (1) and diamines (2) using manganese oxide octahedral molecular sieves (K-OMS-2). OMS-2 materials have been used as catalysts for the oxidation and condensation reactions in our laboratory.¹³ K-OMS-2 is a cryptomelane-type manganese oxide with the composition KMn₈O₁₆·*n*H₂O and consists of MnO₆ octahedral units, which are edge and corner shared to form a 2 × 2 tunnel structure.¹⁴ This alternative process to synthesize quinoxalines with K-OMS-2 does not require any additives or promoters as in the processes described above for this transformation and the reaction times are shorter. Moreover, the K-OMS-2 catalysts are relatively inexpensive, easy to prepare and can be reused many times without loss of activity. The reaction proceeds *via* two steps, *i.e.* the oxidation of the hydroxy ketones to their diketones and then the condensation of the diketones with a diamine to form the final product, quinoxaline.



Scheme 1

The synthesis of a quinoxaline with α -pyridoin and 1,2-phenylenediamine was attempted with K-OMS-2 catalysts prepared by different methods (Table 1). K-OMS-2 prepared by solvent free (SF) methods is known as K-OMS-2_{SF}, K-OMS-2 prepared by reflux (R) methods is known as K-OMS-2_R and K-OMS-2 synthesized by high temperature (HT) methods is known as K-OMS-2_{HT}. The main criterion for selecting these catalysts was based on their surface areas. The K-OMS-2_{SF} prepared by the solvent-free method had the highest surface area, while K-OMS-2_{HT} prepared by a high temperature method had the lowest surface area. Interestingly, all the catalysts produced quinoxaline in high to moderate yields. The use of K-OMS-2_R resulted in a 98% quinoxaline yield, while the use of K-OMS-2_{SF} and K-OMS-2_{HT} gave 74% and 49% yield respectively. In all cases, the selectivity for quinoxaline was 100% and no other side products were formed. The difference in the yields of quinoxalines can be related to their intrinsic properties. The surface area and the average oxidation number of the catalysts in combination seem to play a key role in the process. The surface area is related to crystallite size of the catalysts. The average oxidation

^aDepartment of Chemistry, University of Connecticut, U-3060, 55 North Eagleville Rd., Storrs, Connecticut, 06269-3060, USA. E-mail: Steven.Suib@uconn.edu; Fax: (860) 486-2981; Tel: (860) 486-2797

^bDepartment of Chemical, Materials, and Biomolecular Engineering, University of Connecticut, U-3060, 55 North Eagleville Rd., Storrs, Connecticut, 06269-3060, USA

Table 1 Synthesis of quinoxalines with K-OMS-2 catalysts^{a,b}

Entry	Catalyst ^c	AOS ^d	Surface area/m ² g ⁻¹	crystallite size/nm	Yield (%) ^e	TOF ^f /h ⁻¹
1	K-OMS-2 _{SF}	3.72	156	10	74	11.8
2	K-OMS-2 _R	3.90	90	18	98	15.7
3	K-OMS-2 _{HT}	3.85	13	20	49	7.8

^a 1 mmol α -pyridoin, 2 mmol 1,2-phenylenediamine and 50.0 mg catalyst stirred in 10 mL toluene under reflux for 1 h. ^b 50 mg = 0.0625 mmol K-OMS-2. ^c Catalyst preparation methods, SF—solvent free, R—reflux, HT—high temperature. ^d Average oxidation number determined by potentiometric titrations (ref. 15). ^e Determined by GC-MS and NMR (yield = conversion \times selectivity). ^f Turnover frequency = moles of converted substrate/(moles of catalyst \times reaction time in h).

number that represent the ratio of Mn²⁺, Mn³⁺, and Mn⁴⁺ which influences the strength of Lewis acidity of the catalysts may also play a role. However, a detailed investigation to relate the catalytic activity to their properties is still in progress.

This protocol was then extended to a range of substrates using K-OMS-2 as catalysts prepared by reflux methods and the results are listed in Table 2. Quinoxaline synthesis with 2-hydroxyacetophenone (**1a**) and 1,2-phenylenediamine (**2a**) gave 100% yield to the corresponding quinoxaline (**3a**). Benzoin (**1b**) gave a moderate yield to its quinoxaline (**3b**), while heterocyclic substrates pyridoin (**1e**) and furoin (**1d**) showed good yields to their corresponding quinoxalines, 98% (**3e**) and 84% (**3d**) respectively. Hetero-atoms in the cyclic structures also seem to play a role in the formation of the quinoxalines. Anisoin (**1c**) gave the lowest yield of all the hydroxy ketone substrates tried. The presence of the electron donating OCH₃ group in the benzene ring may retard the nucleophilic attack on the *in situ* formed dicarbonyl leading to a lower yield. The effects of electron withdrawing and electron donating substituents in the nucleophile diamine substrate were also studied. The reaction between furoin (**1d**) and 4-methoxy-1,2-phenylenediamine (**2c**) gave an 89% yield for **3g**, indicating that the presence of an electron donating methoxy group in the diamine enhances its nucleophilicity. On the other hand, 4-nitrophenylenediamine (**2b**) with furoin (**1d**) yielded only 20% quinoxaline **3f**. The other product obtained was the intermediate diketone, furil in 22% yield. These results show that electron withdrawing nitro groups in the diamine retard its nucleophilicity. The use of chloro-substituted diamines (**2d**) led to enhanced yields for their quinoxalines (entries 8–12).

Alternative solvent systems such as acetonitrile, THF, toluene, and benzene were evaluated in the formation of quinoxalines at their reflux temperatures. However, toluene gave the highest conversion among the solvents tried. The main reason for this could be that the highest reflux temperature attained with toluene aids in the oxidation step of quinoxaline. In consideration of its abundance, economic, and environmental attractiveness, water was also tried as a solvent for the reaction. The reaction in water afforded only a 9% yield. Additional studies were performed to test the reusability of the catalyst. The reaction with α -pyridoin and 1,2-phenylenediamine was carried

out over four cycles with the same catalyst which was regenerated after each use by simply washing with acetone/methanol and water and heating to 250 °C. Due to the loss of catalysts during the filtration process after each reaction, a reduced amount of catalysts was used in the subsequent cycles. The yields of the “spent” catalysts used in all the cycles were comparable to yields for “fresh” catalysts (Table 3). The X-ray diffraction patterns of the regenerated catalysts indicated that the structure of K-OMS-2 was not altered during the reaction (Fig. 1). In order to prove that the reaction is heterogeneous, a standard leaching experiment was conducted. The catalyst was filtered at the reaction temperature, and the reaction was allowed to proceed without the catalyst. There was no change in yield observed even after 8 h indicating that no homogeneous catalysis was involved. Turnover frequency (TOF) for this catalytic process which is defined as moles of converted substrate per mole of catalyst per hour has been listed in Table 1. TOF of 15 have been achieved for this reaction with K-OMS-2 as catalyst and this value is very high compared to the similar process which requires 10–15 equivalents of active MnO₂ in 20 h (TOF = 1.4 \times 10⁻³).¹⁶

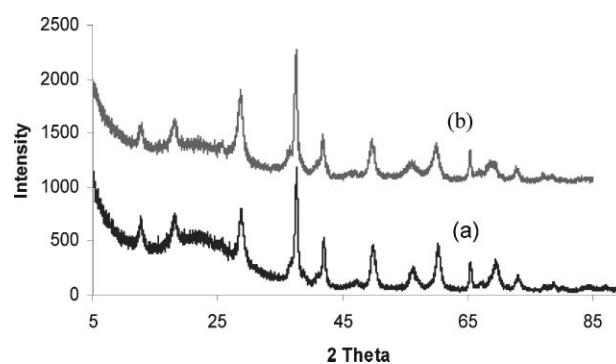
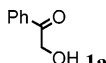
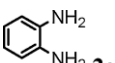
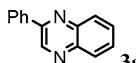
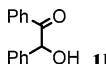
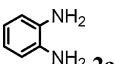
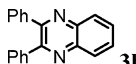
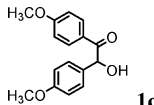
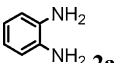
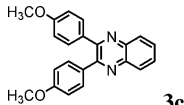
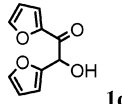
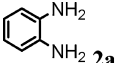
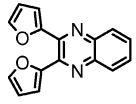
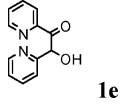
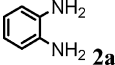
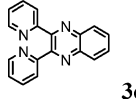
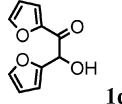
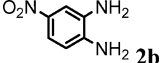
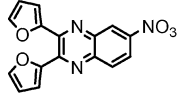
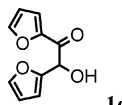
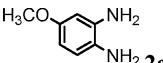
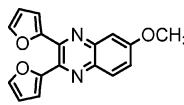
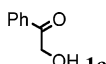
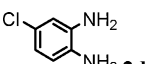
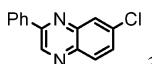
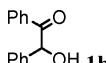
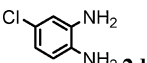
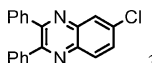
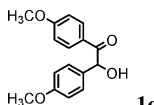
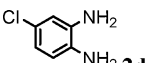
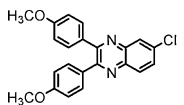
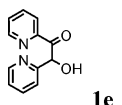
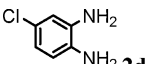
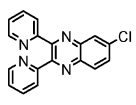
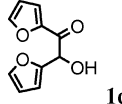
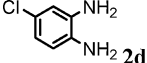
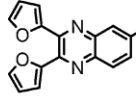


Fig. 1 XRD patterns of K-OMS-2 catalyst in synthesis of quinoxalines: (a) “fresh” catalyst before reaction, (b) “spent” catalyst after 2nd cycle.

Finally, the quinoxaline synthesis was carried out on a gram scale. One gram of pyridoin was reacted with one gram of 1,2-phenylenediamine under the same reaction conditions. The reaction occurred to produce the corresponding quinoxaline in

Table 2 K-OMS-2 catalyzed synthesis of quinoxalines with various substrates^a

Entry	Hydroxy ketone	Diamine	Quinoxaline	Yield (%)
1	 1a	 2a	 3a	100
2	 1b	 2a	 3b	47 (>99) ^b
3	 1c	 2a	 3c	24
4	 1d	 2a	 3d	84
5	 1e	 2a	 3e	98
6	 1d	 2b	 3f	20
7	 1d	 2c	 3g	89 (82) ^c
8	 1a	 2d	 3h	100
9	 1b	 2d	 3i	51
10	 1c	 2d	 3j	37
11	 1e	 2d	 3k	86
12	 1d	 2d	 3l	100

^a 1 mmol hydroxyketone, 2 mmol diamine and 50 mg catalyst were stirred in 10 mL toluene under reflux for 1 h. ^b Yield in 8 h. ^c Isolated yield of product.

81% yield in one hour. This promising result suggests that this catalytic protocol can be extended to larger scale, milligram to gram scale reactions.

In summary, manganese octahedral molecular sieves efficiently catalyze the single-pot synthesis of quinoxalines from

hydroxyl ketones and diamines. The reactions require only a catalytic amount of K-OMS-2 and do not require any additives or promoters for the reaction. The K-OMS-2 catalysts are environmentally benign and after a simple regeneration process can be reused without loss of activity.

Table 3 Catalyst reusability^a

Cycle	Catalyst amount/mg	Yield (%)
1	50.0	96 (98) ^b
2	37.5	85 (84) ^b
3	25.0	62 (64) ^b
4	12.5	39 (43) ^b

^a 1 mmol pyridoin, 2 mmol 1,2-phenylenediamine and K-OMS-2 were stirred in 10 mL toluene under reflux for 1 h. ^b Yield with fresh catalyst.

Experimental section

The catalysts, K-OMS-2_R by a reflux method¹⁷ and K-OMS-2_{SF} by a solvent-free method¹⁸ were prepared according to literature procedures. The high temperature K-OMS-2_{HT}¹⁹ was prepared by a combination of sol-gel and combustion methods with the Mn source as Mn(NO₃)₂, KNO₃ and Mn(NO₃)₂ in a molar ratio of 1 : 5 were dissolved in distilled deionized water (solution A). Glycerol and KNO₃ were mixed in a 1 : 10 ratio (solution B). Solutions A and B were mixed in deionized water with vigorous stirring to form a clear solution and then heated to 120 °C to form a gel (usually 5 h). The gel was then heated to 250 °C for 2 h to complete the combustion reaction. The black powder was then calcined at 600 °C for 3 h to obtain the final product.

The reactions were carried out in batch reactors. A typical reaction procedure as follows: to a round-bottomed flask (50 mL), furoin (1 mmol, 192 mg), toluene (10 mL) as solvent, 4-methoxy-*o*-phenylenediamine (2 mmol, 276 mg), and K-OMS-2 catalyst (50.0 mg) were added. The mixture was stirred under reflux for 1 h at 110 °C in air. After the reaction time, the mixture was cooled; the catalyst was removed by filtration. A gas chromatography-mass spectroscopy (GC-MS) method was used for the identification and quantification of the product mixtures. GC-MS analyses were done using an HP 5890 series II chromatograph with a thermal conductivity detector coupled with an HP 5970 mass selective detector. An HP-1 column (non-polar cross linked siloxane) with dimensions of 12.5 m × 0.2 mm × 0.33 μm was used in the gas chromatograph. The products were also confirmed by ¹H and ¹³C NMR data collected on a Bruker DRX-400 (400.144 MHz ¹H, 100.65 MHz ¹³C). Silica-gel column chromatography after concentration afforded 2,3-bis(2-furyl)-6-methoxy quinoxaline (Table 2, Entry 7). *m/z* = 292, ¹H NMR (400 MHz, CDCl₃): δ = 3.83 (s, 3H), 6.43 (m, 3H), 6.55 (d, 1H, *J* = 4 Hz), 7.26 (dd, 1H, *J* = 4, 8 Hz), 7.51 (m, 2H), 7.87 (d, 1H, *J* = 8 Hz); ¹³C NMR (400 MHz, CDCl₃): δ = 55.9, 106.5, 111.9, 112.0, 113.1, 123.8, 130.1, 136.7, 140.2, 142.4, 142.7, 143.7, 144.3, 149.5, 150.9, 151.1, 161.4.

Acknowledgements

The authors would like to thank the Chemical, Geosciences and Biosciences Division, Office of Basic Energy Sciences, Office of Science, U. S. Department of Energy. The authors would also like to thank Dr Frank Galasso and Dr James Bobbitt for many helpful discussions.

Notes and references

- (a) J. C. Wasilke, S. J. Obrey, R. T. Baker and G. C. Bazan, *Chem. Rev.*, 2005, **105**, 1001–1020; (b) J. L. Notre, D. V. Mele and C. G. Frost, *Adv. Synth. Catal.*, 2007, **349**, 432–440; (c) A. Ajamian and J. L. Gleason, *Angew. Chem., Int. Ed.*, 2004, **43**, 3754–3760.
- (a) T. L. Ho, *Tandem Organic Reactions*, Wiley, New York, 1992; (b) R. Shvoevaart and T. Kieboon, *Chem. Innov.*, 2001, **31**, 33–39.
- D. J. Brown, *The Chemistry of Heterocyclic Compounds, Vol 61, Quinoxalines: Supplement II*, Wiley, New York, 2004.
- R. Sarges, H. R. Howard, R. G. Browne, L. A. Lebel and P. A. Seymour, *J. Med. Chem.*, 1990, **33**, 2240–2254.
- L. E. Seitz, W. J. Suling and R. C. Reynolds, *J. Med. Chem.*, 2002, **45**, 5605–5606.
- S. Dailey, J. W. Feast, R. J. Peace, I. C. Sage, S. Till and E. L. Wood, *J. Mater. Chem.*, 2001, **11**, 2238–2243.
- (a) Z. Zhao, D. D. Wisnoski, S. E. Wolkenberg, W. H. Leister, Y. Wang and C. W. Lindsley, *Tetrahedron Lett.*, 2004, **45**, 4873–4876; (b) S. V. More, M. N. V. Sastry and C. -F. Yao, *Green Chem.*, 2006, **8**, 91–95.
- S. Antoniotti and E. Donach, *Tetrahedron Lett.*, 2002, **43**, 3971–3973.
- (a) S. A. Raw, C. D. Wilfred and R. J. K. Taylor, *Chem. Commun.*, 2003, 2286–2287; (b) S. Y. Kim, K. H. Park and Y. K. Chung, *Chem. Commun.*, 2005, 1321–1323.
- R. S. Robinson and R. J. K. Taylor, *Synlett.*, 2005, **6**, 1003–1005.
- C. S. Cho and S. G. Oh, *J. Mol. Catal. A: Chem.*, 2007, **276**, 205–210.
- C. K. Cho and S. G. Oh, *Tetrahedron Lett.*, 2006, **47**, 5633–5636.
- (a) Y. C. Son, V. D. Makwana, A. R. Howell and S. L. Suib, *Angew. Chem., Int. Ed.*, 2001, **40**, 4280–4283; (b) R. Kumar, L. J. Garces, Y. -C. Son, S. L. Suib and R. E. Malz, *J. Catal.*, 2005, **236**, 387–391; (c) S. Sithambaram, R. Kumar, Y. C. Son and S. L. Suib, *J. Catal.*, 2008, **253**, 269–277.
- (a) Y. F. Shen, R. P. Zerger, R. N. DeGuzman, S. L. Suib, L. McCurdy, D. I. Potter and C. L. O'Young, *Science*, 1993, **260**, 511–515; (b) R. N. DeGuzman, Y. F. Shen, E. J. Neth, S. L. Suib, C. L. O'Young, S. Levine and J. M. Newsam, *Chem. Mater.*, 1994, **6**, 815–821; (c) S. L. Suib, *Curr. Opin. Solid State Mater. Sci.*, 1988, **3**, 63–70; (d) S. L. Brock, N. Duan, Z. R. Tian, O. Giraldo, H. Zhou and S. L. Suib, *Chem. Mater.*, 1998, **10**, 2619–2628.
- G. -G. Xia, W. Tong, E. N. Tolentino, N. -G. Duan, S. L. Brock, J. -Y. Wang, S. L. Suib and T. Ressler, *Chem. Mater.*, 2001, **13**, 1585–1592.
- S. A. Raw, C. D. Wilfred and R. J. K. Taylor, *Org. Biomol. Chem.*, 2004, **2**, 788–796.
- R. N. DeGuzman, Y. -F. Shen, E. J. Neth, S. L. Suib, C. L. O'Young, S. Levine and J. M. Newman, *Chem. Mater.*, 1994, **6**, 815–821.
- Y. -S. Ding, X. F. Shen, S. Sithambaram, S. Gomez, R. Kumar, M. B. Vincent and S. L. Suib, *Chem. Mater.*, 2005, **17**, 5382–5389.
- X. F. Shen, PhD Thesis, University of Connecticut, 2007.

Selective hydrolysis of cellulose into glucose over solid acid catalysts†

Ayumu Onda,* Takafumi Ochi and Kazumichi Yanagisawa

Received 19th May 2008, Accepted 17th June 2008

First published as an Advance Article on the web 11th August 2008

DOI: 10.1039/b808471h

The mildly hydrothermal method using solid acid catalysts for the glucose production from cellulose can be one of the key technologies for a future sustainable society using cellulose biomass. This article is the first to indicate solid acid catalysis for the hydrolysis of cellulose with β -1,4-glycosidic bonds into glucose selectively higher than 90 C-%. Among the solid acid catalysts we tested, such as the H-form zeolite catalysts and the sulfated and sulfonated catalysts, a sulfonated activated-carbon catalyst showed a remarkably high yield of glucose, which was due to the high hydrothermal stability and the excellent catalytic property attributed to the strong acid sites of SO_3H functional groups and the hydrophobic planes.

1. Introduction

Cellulose is the most abundant source of biomass, and it has a potential ability to become an alternative to fossil resources for sustainable production of chemicals and fuels for preventing global warming by decreasing atmospheric CO_2 generated from the consumption of fossil fuels.^{1,2} The utilization of cellulose has been limited to timber, paper, wood fuel, and so on, because of its robust structure composed of β -1,4-glycosidic bonds of D-glucose.³ Glucose is expected as a renewable feedstock molecule, which can be efficiently converted into various chemicals, fuels, foods, and medicines.^{1,2,4-6} Therefore, the cellulose hydrolysis into glucose is a key process for the beneficial use of cellulose.

Thus far, a great deal of effort has been put toward the degradation of cellulose with enzymes,^{3,4} dilute acids,^{3,7} and supercritical water.^{8,9} These processes have significant drawbacks such as separation of products and catalysts, corrosion hazard, and severe controls of enzymes, waste fluids, and reaction conditions. In attempts to solve these problems, recently, Fukuoka *et al.*¹⁰ and Luo *et al.*¹¹ showed heterogeneously catalytic processes for cellulose conversion into sugar alcohols by combination of hydrolysis with instantaneous hydrogenation on supported noble metal catalysts, such as Pt/ Al_2O_3 and Ru/C, in hot water under compressed hydrogen gas. Sugar alcohols are expected as a renewable efficient hydrogen source.¹² The heterogeneously catalytic processes have some advantages over the enzymatic process in the separation of products and catalysts and the severe controls of enzymes but have some disadvantages such as the need for hydrogen gas and noble metals, and limited utilization of produced polyols compared with glucose.

H-form zeolites and sulfonated mesoporous silicas were used as solid acid catalysts for the hydrolysis of soluble

oligosaccharides and starch.^{13,14} Therefore, the H-form zeolite catalysts and the sulfated and sulfonated catalysts, such as sulfated zirconia, ion-exchanging resin, and a sugar acid, are expected to have catalytic activities for the cellulose hydrolysis. The sugar catalyst (*e.g.* $\text{CH}_{0.44}\text{O}_{0.36}(\text{SO}_3)_{0.01}$) was prepared by the carbonization and sulfonation of saccharides.¹⁵⁻¹⁸ The catalysts show the high activity in water media for the hydration of 2,3-dimethyl-2-butene at 343 K,¹⁷ and the esterification of higher fatty acids at 353 K.¹⁶ In this study, an activated carbon is used as a precursor of sulfonated carbon catalysts because its high hydrothermal stability and high surface area are expected to be suited to the selective hydrolysis of cellulose under hydrothermal conditions. A new hydrothermal catalytic process is a challenge for the glucose formation from cellulose over solid acid catalysts.

Cellulose is insoluble in water and a persistent compound. The harsh reaction conditions, such as supercritical water, succeeded in the degradation of cellulose when the reactions are carried out in the extremely short residence time within some seconds to avoid further degradation and dehydration of produced glucose and polysaccharides.^{8,9} However, because of such a short reaction-time, it is difficult to develop a commercial reaction system with an effective heat recovery. Although a mild reaction condition below 453 K is desirable to avoid the sequential reactions of glucose even for not short reaction-times, the mild conditions in cellulose hydrolysis will greatly decrease the reaction rate. It is apparent that the pre-treatment of cellulose to increase its noncrystalline fraction is currently the best method, which accelerates the hydrolysis of cellulose like a digestive system of ruminants. After the ball-milling treatment of microcrystalline cellulose, it was still an insoluble material with β -1,4-glycosidic bonds, but it had large parts of noncrystalline regions which was confirmed by XRD and CP/MAS ^{13}C NMR.¹⁹ The reaction rate of cellulose hydrolysis using the dilute acid at 448 K increased with decreasing cellulose crystallinity.¹⁹ In this study, cellulose powder pre-treated by the ball-milling method is used as a reactant.

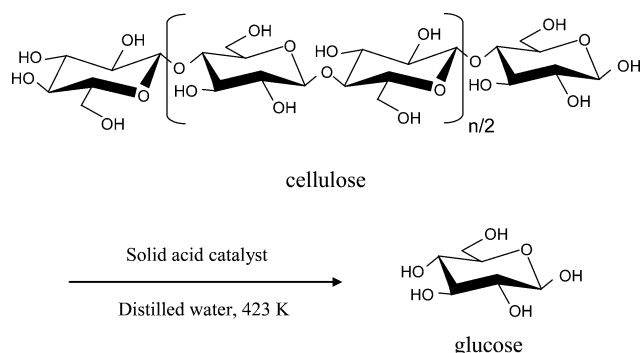
Herein, we report an efficient green process for the selective hydrolysis of cellulose into glucose using solid acid catalysts

Research Laboratory of Hydrothermal Chemistry, Faculty of Science, Kochi University, 2-5-1 Akebono-cho, Kochi, 780-8520, Japan.

E-mail: onda@cc.kochi-u.ac.jp; Fax: +81 88-844-8362

† Electronic supplementary information (ESI) available: SEM images of the tested catalysts (Fig. S1); effect of reaction temperature and reaction time on the starch hydrolysis using the AC- SO_3H catalyst (Fig. S2). See DOI: 10.1039/b808471h

at 423 K as shown in Scheme 1. Water was used as the reaction media, and the separation of products and catalysts was readily carried out by filtration. The glucose production from soluble starch and oligo-saccharides over solid acid catalysts were reported,^{13,14} but no report has shown the highly selective production of glucose from insoluble cellulose over solid acid catalysts without hydrogen gas. H-form zeolites with various structure and Si/Al ratio, a sulfated zirconia, a ion-exchange resin, and a sulfonated activated-carbon are used as solid acid catalysts for the hydrolysis of cellulose under hydrothermal conditions. To clarify the effect of SO_4^{2-} ions eluted in the reaction media on the products, the dilute sulfuric acid is also used as a catalyst.



Scheme 1 Catalytic conversion of cellulose into glucose over solid acid catalysts.

2. Experimental

H-form zeolite materials, as H-beta (12) (Si/Al= 12), H-beta (75) (Si/Al= 75), H-mordenite (10) (Si/Al= 10), and H-ZSM5 (45) (Si/Al= 45), sulfonated zirconia (JRC-SZ-1), and γ -alumina (JRC-ALO-2) were supplied from the Catalysis Society of Japan. Commercial silica (Cariact Q-6, Fuji Silysia) and active carbon (powder, Wako Pure Chemical Industries) were also used as catalysts. The sulfonated activated-carbon (AC- SO_3H) was prepared by the following method based on a previous report.¹⁶ Typically, the activated-carbon (Wako pure chemicals, powder, 1.0 g) was added into concentrated H_2SO_4 (18 mol L^{-1} , 20 mL) and heated under argon flow (40 mL min^{-1}) at 423 K (5 K min^{-1}) for 16 h. The resultant AC- SO_3H was washed repeatedly with hot distilled water (3 L) at 353 K. Furthermore, the black powder was hydrothermally pre-treated at 473 K for 3 h and then washed again with the hot distilled water until sulfate ions are no longer detected in the wash water, to prevent elution of SO_4^{2-} ions under hydrothermal reaction media around 423 K. The S content was determined by a CHNS analyzer (Thermo Finnigan, Flash EA1112). A gas sorption analyzer (Quantachrome, NOVA1000) was used for N_2 physisorption to determine surface areas of solid catalysts kept in glass vials at room temperature. The Brønsted-acid sites in the catalysts were determined by the titration method as follows; a sodium hydroxide aqueous solution (0.01 mol L^{-1} , 20 mL) was added to a catalyst (0.040 g). The mixture was stirred for 2 h at room temperature. After centrifugal separation, the supernatant solution was titrated by a hydrochloric acid (0.01 mol L^{-1}) aqueous solution using phenolphthalein.

Ball-milling experiments were performed using ZrO_2 balls (mass of 1.8 kg and diameter of 2 cm) and 20 g of cellulose (Fluka, Avicel® PH-101, microcrystalline) were loaded into a ZrO_2 bottle (2000 mL). Spinning speed was set at 60 rpm. Typically, the ball-milling was done for 48 h. The X-ray diffraction analysis was carried out on a Rigaku Rotaflex RAD-C using a $\text{Cu-K}\alpha$ source (0.154 nm) to analyze the structure of cellulose. The degree of cellulose crystallinity was calculated as:

$$\text{Crystallinity \%} = I_{\text{cr}} / (I_{\text{cr}} + I_{\text{am}}) \times 100$$

where I_{cr} and I_{am} are the peak intensities from crystalline and amorphous regions of cellulose, respectively.²⁰ The morphology of samples was observed by scanning electron microscopy (SEM) with a Keyence VE-8800 instrument.

A typical catalytic reaction procedure was as follows: cellulose (45 mg) treated by the ball-milling for 48 h, catalyst (50 mg), water (5.0 mL) were introduced in a steel autoclave lined with Teflon (25 mL) under air. The autoclave was heated at 423 K for 24 h with agitation (22 rpm). The hydrolysis of starch was carried out by the same procedure as that of cellulose except for using soluble starch (powder, Wako Pure Chemical Industries) as a reactant. After the reaction, the reaction mixture was filtered and the filtrate solution was analyzed by two HPLC systems (Hitachi L-6200 pump for mobile phase of water, L-7490 RI detector, Shodex Sugar KS-802 column at 353 K; Hitachi L-2130 pump for mobile phase of HClO_4 aqueous solution, Hitachi L-7110 pump for BTB solution, L-2035 UV-vis detector (440 nm), Shodex RSpak KC-811 double columns at 313 K) for saccharides and organic acids. Water soluble organic compounds (WSOCs) in resultant solutions after reactions were determined by TOC analyzer (Shimadzu TOC 5000 A). The dissolved SO_4^{2-} ions in the filtrate solution were determined by ion chromatography (Dionex DX-120, IonPac AS14A column). The yield of glucose was calculated as follows:

$$\text{Glucose yield (\%)} = (\text{mol of glucose} \times 6) / (\text{mol of carbon including charged cellulose determined by CHNS analyzer}) \times 100.$$

The yield of water soluble organic compounds (WSOCs) determined by a TOC analyzer equals to the aqueous solubilization ratio and can be compared with the conversion of cellulose under the reaction conditions in this study.²¹ The yield of WSOCs and by-products and the selectivity of glucose were calculated as follows:

$$\text{WSOCs yield (\%)} = (\text{mol of water soluble organic carbon}) / (\text{mol of carbon including charged cellulose}) \times 100.$$

$$\text{By-products yield (\%)} = (\text{the yield of WSOCs}) - (\text{the yield of glucose}).$$

$$\text{Glucose selectivity (\%)} = (\text{the yield of glucose}) / (\text{the yield of WSOCs}) \times 100.$$

3. Results and discussion

The cellulose of Avicel® was treated by the ball-milling method before the catalytic reaction because the cellulose with robust crystalline structure is less decomposable.¹⁹ The milled cellulose was white and insoluble in water. The XRD patterns of cellulose

before and after the ball-milling for 48 h are shown in Fig. 1. The XRD pattern before the treatment showed diffraction peaks of cellulose crystalline around 16° , 22° , and 34° . From the XRD pattern, the crystallinity of cellulose was calculated to be about 75%.²⁰ In contrast, the crystalline peaks disappeared but the amorphous halo peak appeared around 20° in the XRD pattern of the milled cellulose, which indicated that the crystallinity of cellulose was markedly decreased by the ball-milling treatment. The SEM images of the milled cellulose are shown in Fig. 2. The powder was between 10 and $100\ \mu\text{m}$ in size. The fibrous morphology was not observed.

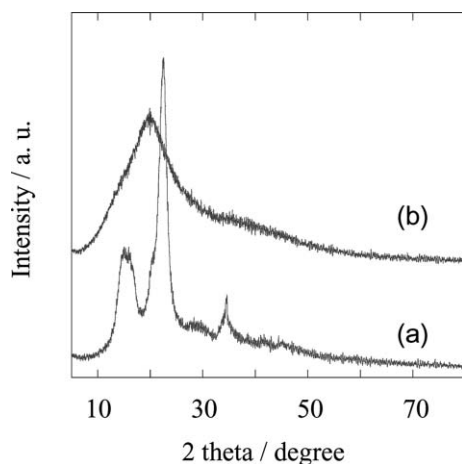


Fig. 1 XRD patterns of cellulose before (a) and after the ball-milling (b).

The characterization data of the catalyst materials are summarized in Table 1, in which the values given in parentheses for the H-form zeolites are the Si/Al ratios. In the case of H-form zeolites, the amounts of Al atoms theoretically correspond to the amounts of Brønsted acid sites. The acid sites were determined by the titration method in aqueous solutions and were inversely proportional to the Si/Al ratios, except for H-mordenite (20). It was difficult to accurately determine the acid sites of H-mordenite (20) because the powder was suspended in the NaOH aqueous solution and some parts of the powder couldn't be separated from the aqueous solution for the titration. The specific surface areas of catalysts were measured without pre-heating treatments (Table 1). The areas of the H-form zeolites were lower than those after the dehydration treatment at about 673 K. In particular, the H-form of zeolites with lower

Table 1 Characterization data

	Si/Al molar ratio	S contents/ mmol g^{-1}	Acid sites ^a / mmol g^{-1}	SA ^b / $\text{m}^2 \text{g}^{-1}$
SiO ₂	nd	nd	0.095	407
γ -Al ₂ O ₃	nd	nd	0.049	140
H-mordenite (10)	10	nd	0.7	15
H-beta (13)	13	nd	1.05	105
H-ZSM5 (45)	45	nd	0.30	124
H-beta (75)	75	nd	0.18	315
Activated-carbon	nd	0.0	1.25	1243
AC-SO ₃ H	nd	0.44	1.63	806
Sulfated zirconia	nd	1.2	1.60	52
Amberlyst 15	nd	1.7	1.8	nd

^a The amounts of acid sites on catalysts were determined by a titration method. ^b The specific surface area was measured without pre-heating treatment of catalysts.

Si/Al ratios, such as H-mordenite (10) and H-beta (13), showed significantly lower specific surface area, because the micropores of such hydrophilic zeolites was filled by water molecules under air.

Activated-carbon had a high surface area of $1243\ \text{m}^2 \text{g}^{-1}$. The activated-carbon was sulfonated and then hydrothermally pre-treated at 473 K to improve its tolerance to the hydrothermal catalytic reactions media around 423 K. Although the sulfonation treatment and the subsequent hydrothermal treatment decreased the surface area, the AC-SO₃H had still high surface area of $806\ \text{m}^2 \text{g}^{-1}$. AC-SO₃H had $1.63\ \text{mmol g}^{-1}$ of acidic sites which is a good agreement with the sum of acidic sites of untreated activated-carbon ($1.25\ \text{mmol g}^{-1}$) and an S content of AC-SO₃H ($0.44\ \text{mmol g}^{-1}$). Hara *et al.* indicated that all S atoms in the sugar catalyst, that is a sulfonated carbon material, are contained in SO₃H groups according to XPS spectra.^{16,17} The same would be true in the case of our AC-SO₃H, and the high catalytic activity would be due to the SO₃H groups. The S contents of the sulfated zirconia and Amberlyst 15 were 1.2 and $1.7\ \text{mmol g}^{-1}$, which were larger than that of the AC-SO₃H. Additional information about the particle sizes of the tested catalysts is provided by SEM images in Fig. S1 (in the ESI†). Both of the AC and AC-SO₃H particles were between 5 and $100\ \mu\text{m}$ in size. Their particle sizes were almost the same as those of the milled cellulose. They were larger than the particles of the H-form zeolites and the sulfated zirconia whose particles were between 0.5 and $20\ \mu\text{m}$ in size.

The catalytic results are summarized in Fig. 3. γ -Alumina and silica catalysts showed almost no activity. The H-form

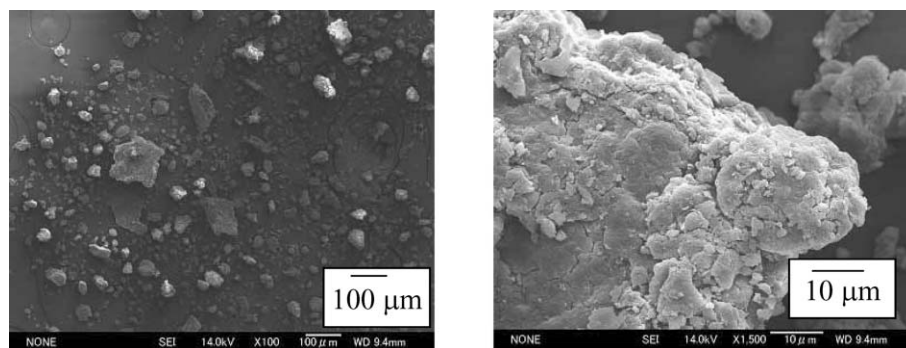


Fig. 2 SEM images of the cellulose after the ball-milling.

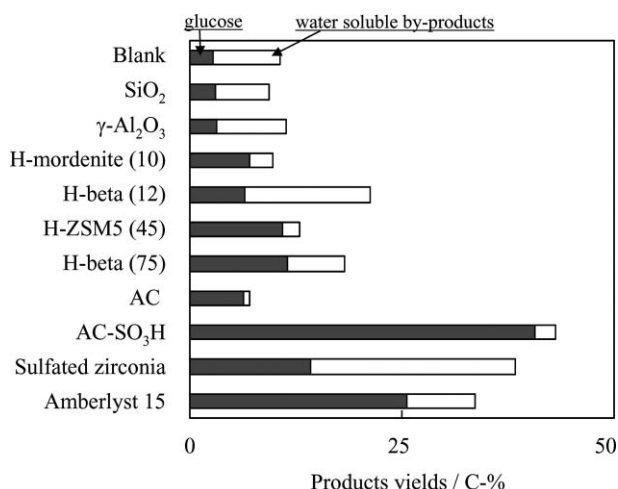


Fig. 3 Cellulose hydrolysis over various solid acid catalysts at 423 K. Reaction conditions: milled cellulose 45 mg, catalyst 50 mg, distilled water 5.0 mL, 24 h.

zeolite catalysts showed significantly higher activity than the blank reaction. The zeolite catalysts with high Si/Al ratio as H-beta (75) and H-ZSM5 (45) showed the higher activity for glucose formation than those of zeolite catalysts with relatively low Si/Al ratio as H-beta (13) and H-mordenite (10). A similar relationship between the Si/Al ratios and the glucose yields was reported in the maltose hydrolysis.¹³ The zeolite catalysts with high Si/Al ratios have relatively highly hydrophobic character, preferring organic compounds to water, which may be a cause of the relatively high glucose yield.

The activated-carbon (AC) and the AC-SO₃H catalysts have higher hydrophobic character than the zeolite catalysts. However, the AC with acidic surface functional groups, such as carboxylic group, showed a low catalytic activity for the cellulose hydrolysis. In contrast, the AC-SO₃H catalyst gave glucose in 40.5% yield, with minor water soluble by-products in about 2% yield including C₁–C₂ acids. The glucose selectivity calculated to be a ratio of the glucose yield to the WSOCs yield was 95%. There was no SO₄²⁻ ions detected in the resultant solution. The AC-SO₃H catalyst showed significantly higher catalytic activity and glucose selectivity than the tested H-form zeolite catalysts, which might be due to the higher hydrophobic graphene planes and strong acidic SO₃H surface functional groups of the AC-SO₃H catalyst.

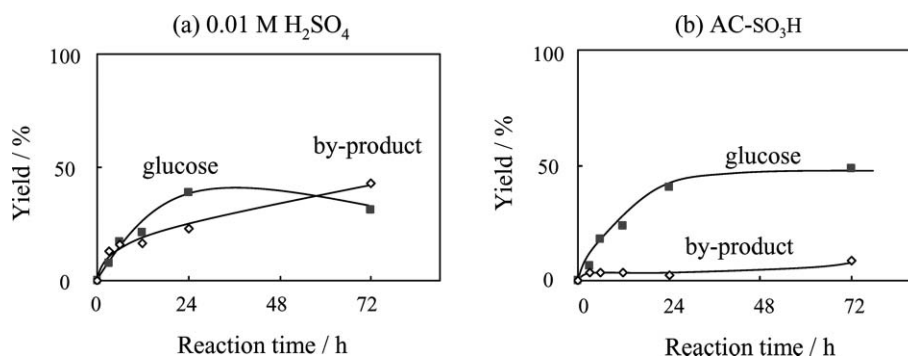


Fig. 4 Changes in product yields during the cellulose hydrolysis using the dilute acid of 0.01 M H₂SO₄ (a) and the AC-SO₃H catalyst (b) at 423 K. Reaction conditions; Catalyst 50 mg, cellulose 45 mg, distilled water (or dilute acid) 5mL, agitation.

Among the solid catalysts we tested, sulfated zirconia and Amberlyst 15 also gave a relatively high yield of glucose. However, the sulfated zirconia catalyst was decomposed during reaction, which resulted in the elution of 14.1 mmol L⁻¹ SO₄²⁻ ions in the resultant solution. And, it gave a significant amount of water soluble by-products, such as carboxylic acids, oligosaccharides, and sugar derivatives. Amberlyst 15 catalyst of an ion-exchange resin with SO₃H groups also showed the not low selectivity into water soluble by-products and the elution of 1.7 mmol L⁻¹ SO₄²⁻ ions. In addition, the ion-exchange resin went a dark brown color after the reaction, which was due to its less hydrothermal stability.

Fig. 4 shows the changes in product yields during the cellulose hydrolysis using the dilute acid of 0.01 mol L⁻¹ H₂SO₄ and AC-SO₃H catalyst at 423 K. The SO₃H functional groups bonded on the AC-SO₃H catalyst (50 mg) in 5 mL corresponded to 0.0044 mmol L⁻¹ which was surely lower than 0.01 mol L⁻¹ of the dilute acid. At the reaction time of 24 h, the dilute acid gave a similar glucose yield to the AC-SO₃H catalyst, but the resultant solution went a brown color and contained large amounts of water soluble by-products including formic, acetic, and glycolic acids. These by-products are known as inhibitors for further chemical and biochemical conversions of glucose into useful chemicals. The solid acid catalysts with SO₄²⁻ elution during reaction, such as sulfated zirconia and Amberlyst 15, showed also relatively high yields of water soluble by-products which would be due to free SO₄²⁻ ions. In the reaction within 24 h, the yields of glucose increased linearly with the increase of the reaction time in both reactions. In such reaction conditions with the low conversion, the AC-SO₃H catalyst always showed a high selectivity of glucose, whereas the dilute acid showed a high selectivity of the by-products. When the reaction time was longer than 24 h, the glucose yield did not increase over the AC-SO₃H and the dilute acid. The insoluble milled cellulose seemed to have a part of its robust structure which is restricted for the hydrolysis over AC-SO₃H. The glucose yield significantly decreased in the dilute acid longer than 24 h of the reaction time. The further reaction of glucose was prevented over the AC-SO₃H, compared with the dilute acid. The results indicated that the AC-SO₃H catalyst without SO₄²⁻ elution showed the excellent catalytic property that was different from that of the dilute acid for the cellulose hydrolysis into glucose.

After the first reaction run using the AC-SO₃H catalyst at 423 K for 24 h, the solid catalyst was filtered with the cellulose

residue. The fresh cellulose was added in the filtrate solution, and then the reaction was carried out at 423 K for 24 h. As shown in Fig. 5, the reaction in the filtrate solution without the solid catalyst resulted in a marked decrease of the glucose yield similar to those in the blank reaction (Fig. 3) and the reactions with dilute formic acid less than 1.0 mmol L^{-1} . On the other hand, after the 1st run, fresh cellulose was added into the resultant solution with the $\text{AC-SO}_3\text{H}$ catalyst, and then the 2nd reaction was carried out. The reaction was repeated once again (3rd reaction). The products in the 2nd and 3rd runs were similar to the 1st run, and the glucose concentration doubled and tripled in the reactor. These results indicated that the cellulose is hydrolyzed into glucose over the solid catalyst and the catalytic performance is not deactivated in the course of the catalytic runs.

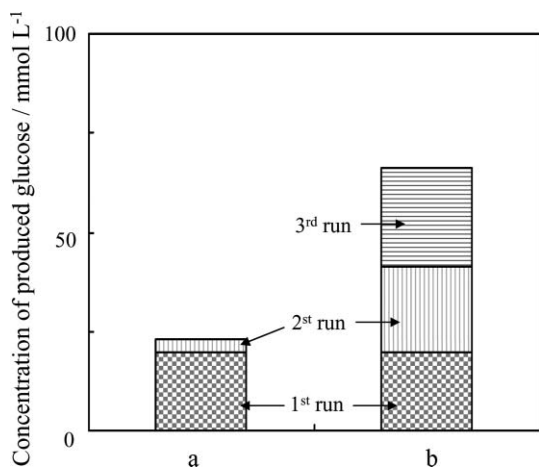


Fig. 5 Recycle catalytic runs. (a) After the 1st run with $\text{AC-SO}_3\text{H}$ catalyst, the catalyst was removed by filtration, and then fresh cellulose was added into the filtrate solution without solid catalyst and the 2nd run occurred. (b) After the 1st run with $\text{AC-SO}_3\text{H}$ catalyst, fresh cellulose was added into the slurry solution including solid catalyst and products. After the 2nd run, fresh cellulose was added again into the solution with the catalyst, and the 3rd run occurred. Reaction conditions were same as those in Fig. 1.

As for the hydrolysis of starch which has α -glycosidic bonds of D-glucose, the $\text{AC-SO}_3\text{H}$ catalyst succeeded in the selective glucose production higher than 90% yield (Fig. S2 in the ESI[†]). We expect that in the near future this mildly hydrothermal catalytic process using $\text{AC-SO}_3\text{H}$ catalyst will succeed in a high glucose yield from cellulose biomass.

4. Conclusions

We have presented for the first time that solid acid catalysts hydrolyze cellulose selectively into glucose by an environmentally friendly chemical process. Among H-form zeolite catalysts, the hydrophobic zeolites with high Si/Al ratios showed the relatively high yield of glucose from cellulose under hydrothermal conditions at 423 K. The sulfated zirconia and Amberlyst 15 catalysts showed higher activity than the H-form zeolite catalysts, however there were large amounts of SO_4^{2-} ions and by-products in the resultant solution. The sulfonated activated-carbon catalyst showed high activity and remarkably high selectivity for the glucose production from cellulose. This hydrothermal process

using the solid acid catalyst with an excellent catalytic property and a high stability opens up new opportunities for the efficient use of the cellulose resource as a chemical feedstock.

Acknowledgements

We thank Prof. M. Ikehara for CHNS analysis, Prof. A. Usui for SEM observations, and the Catalysis Society of Japan for reference catalysts.

Notes and references

- G. W. Huber, S. Iborra and A. Corma, *Chem. Rev.*, 2006, **106**, 4044–4098.
- D. Klemm, B. Heublein, H. Fink and A. Bohn, *Angew. Chem., Int. Ed.*, 2005, **44**, 3358–3393.
- L. T. Fan, M. M. Gharapuray and Y. H. Lee, *Cellulose Hydrolysis*, Springer, Berlin, 1987.
- Y. P. Zhang and L. R. Lynd, *Biotechnol. Bioeng.*, 2004, **88**, 797–824.
- A. J. Ragauskas, C. K. Williams, B. H. Davison, G. Britovsek, J. Cairney, C. A. Eckert, W. J. Frederick, J. P. Hallett, D. J. Leak, C. L. Liotta, J. R. Mielenz, R. Murphy, R. Templer and T. Tschaplinski, *Science*, 2006, **311**, 484–489.
- (a) R. R. Davda and J. A. Dumesic, *Chem. Commun.*, 2004, 36–37; (b) R. R. Davda, J. W. Shabaker, G. W. Huber, R. D. Cortright and J. A. Dumesic, *Appl. Catal., B*, 2005, **56**, 171–186.
- W. S. Mok, M. J. Antal and G. Varhelyi, *Ind. Eng. Chem. Res.*, 1992, **31**, 94–100.
- (a) M. Sasaki, Z. Fang, Y. Fukushima, T. Adschiri and K. Arai, *Ind. Eng. Chem. Res.*, 2000, **39**, 2883–2890; (b) M. Sasaki, T. Adschiri and K. Arai, *AIChE J.*, 2004, **50**, 192–202.
- S. Saka and T. Ueno, *Cellulose*, 1999, **6**, 177–191.
- A. Fukuoka and P. L. Dhepe, *Angew. Chem., Int. Ed.*, 2006, **45**, 5161–5163.
- (a) N. Yan, C. Zhao, C. Luo, P. J. Dyson, H. Liu and Y. Kou, *J. Am. Chem. Soc.*, 2006, **128**, 8714–8715; (b) C. Luo, S. Wang and H. Liu, *Angew. Chem., Int. Ed.*, 2007, **46**, 7636–7639.
- (a) R. D. Cortright, R. R. Davda and J. A. Dumesic, *Nature*, 2002, **418**, 964–967; (b) G. W. Huber, J. W. Shabaker and J. A. Dumesic, *Science*, 2003, **300**, 2075–2077.
- A. Abbadi, K. F. Gotlieb and H. van Bekkum, *Starch*, 1998, **50**, 23–28.
- P. L. Dhepe, M. Ohashi, S. Inagaki, M. Ichikawa and A. Fukuoka, *Catal. Lett.*, 2005, **102**, 163–169.
- M. Hara, T. Yoshida, A. Takagaki, T. Takata, J. N. Kondo, K. Domen and S. Hayashi, *Angew. Chem., Int. Ed.*, 2004, **43**, 2955–2958.
- M. Toda, A. Takagaki, M. Okumura, J. N. Kondo, S. Hayashi, K. Domen and M. Hara, *Nature*, 2005, **438**, 178.
- M. Okumura, A. Takagaki, M. Toda, J. N. Kondo, K. Domen, T. Tatsumi, M. Hara and S. Hayashi, *Chem. Mater.*, 2006, **18**, 3039–3045.
- M. H. Zong, Z. Q. Duan, W. Y. Lou, T. J. Smith and H. Wu, *Green Chem.*, 2007, **9**, 434–437.
- H. Zhao, J. H. Kwak, Y. Wang, J. A. Franz, J. M. White and J. E. Holladay, *Energy Fuels*, 2006, **20**, 807–811.
- F. Rebuzzi and D. V. Evtuguin, *Macromol. Symp.*, 2006, **232**, 121–128.
- In reactions of cellulose using solid catalysts, it is difficult to determine the true conversion of cellulose because it is difficult to completely separate unreacted cellulose residues from solid catalysts and products adsorbing on solid catalysts. In contrast, in the hydrolysis of starch using the $\text{AC-SO}_3\text{H}$ catalyst, the amount of total carbons of water soluble organic compounds was always over 96 C-% of that of charged starch in the reaction-temperature region of 373–423 K for 24 h (Fig. S2 in the ESI[†]). This result suggests that most of the products in the hydrolysis of polysaccharides under such reaction conditions using the $\text{AC-SO}_3\text{H}$ catalyst exist in the aqueous phase. The products would be scarcely in the gas phase and scarcely on solid catalysts. In this study, for the reason discussed above, the conversion of cellulose was estimated to be almost equal to the yield of WSOs.

Solar reactions for preparing hindered 7-*cis*-isomers of dienes and trienes in the vitamin A series

Yao-Peng Zhao, Roger O. Campbell and Robert S. H. Liu*

Received 29th May 2008, Accepted 21st July 2008

First published as an Advance Article on the web 20th August 2008

DOI: 10.1039/b809007f

Selective triplet sensitized isomerizations of dienes and trienes in the vitamin A series were accomplished through solar irradiation. The use of Rose Bengal as a photosensitizer for triene derivatives allowed the tapping of the visible region of the sunlight, thereby making a rapid conversion to the desired hindered 7-*cis* isomers possible. The short exposure time has led to the design of a simple floating solar reactor that eliminated the need of circulating cooling water. That such a very green approach to photochemical reactions could be carried out in a single surfing session, while using the Pacific Ocean as the heat sink, has added an obvious fun component to the photochemical project. Conversion to 7-*cis*- β -ionol was quantitative, albeit at a slower rate because of the need to use a colorless photosensitizer.

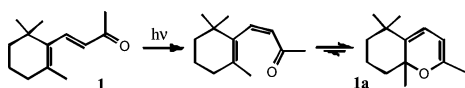
Introduction

A photochemical reaction that can tap the solar energy for production of the photoproduct must have the following desirable features.¹ The reaction should be able to utilize, to the fullest extent, the long wavelength light reaching the surface of the earth. The product(s) should be formed in reasonably high quantum efficiency and the product mixture should be simple and not capable of undergoing destructive secondary photochemical reactions. It appeared to us that the selective *trans* to *cis* triplet photosensitized isomerization reactions² are particularly suited for solar reactions. Some of the photoproducts were in fact key intermediates used previously in synthesis of sterically hindered 7-*cis* isomers of vitamin A.³ In this paper we wish to report preliminary findings from our investigation on solar reactions of this class of compounds.

Results and discussion

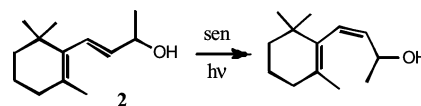
Photoisomerization of dienes in the vitamin A series

The most commonly available truncated compound in the vitamin A series is β -ionone, **1**. However, because of the low-lying n,π state and the ready cyclization of *cis*-ionone to the corresponding α -pyran (**1a**),⁴ the dienone is not suitable as a model compound for triplet sensitized isomerization (see also a recent self-sensitized oxygenation study on β -ionone).⁵



On the other hand, its reduced form, β -ionol, **2**, is an excellent model. In fact, it was the first compound in the vitamin A series successfully converted to its 7-*cis* isomer.² The

triplet excitation of *trans*- β -ionol should be similar to a typical diene (*i.e.* ~ 55 kcal mol⁻¹).⁶ That of the highly twisted *cis*- β -ionol⁷ should be significantly higher (estimated to be >68 kcal mol⁻¹).^{2b} Under selective triplet sensitization conditions, *i.e.*, using sensitizers with triplet energies between those of the *trans* and *cis* isomers,^{2b} one way pumping from the *trans* isomer to the higher energy *cis* isomer became possible, leading to one-way *trans* to *cis* conversion, a rare occurrence in any photoisomerization reaction.⁸



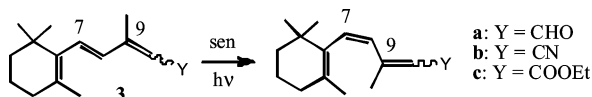
We have now demonstrated that this one-way photoisomerization can readily be achieved through solar radiation. A solar reactor in the form of a modified Liebig condenser, as described in the literature,⁹ without any additional light filtering system other than the Pyrex glassware, was found to be quite satisfactory for this reaction. For a 1.2 g sample of β -ionol with α -acetonephthone as triplet sensitizer in a de-oxygenation ethanol solution,¹⁰ the reaction was found to be complete after 15 h of exposure to late November sunlight in Honolulu. Later, in a separate experiment conducted in the modified solar apparatus described below, we found that reaction of β -ionol in a similar mixture was complete within 7 h upon exposure to the stronger sunlight in early May, consistent with expected seasonal variation of intensity of solar energy.¹¹ In view of the fact that α -acetonephthone ($E_T = 56$ kcal mol⁻¹)¹² is a colorless photosensitizer (*i.e.*, capturing only the weak UV light from the sun),^{1b} the length of the exposure time needed for complete conversion was not surprising. A yellow photosensitizer such as 9-fluorenone ($E_T = 51$ kcal mol⁻¹)¹² is apparently too low in energy and was found to be ineffective to sensitize the *trans* to *cis* conversion. We might also add that the relatively slow triplet sensitization procedure is in fact a tremendous improvement over direct irradiation, which is not possible with dienes that

Department of Chemistry, University of Hawaii, 2545 The Mall, Honolulu, HI, 96822, USA. E-mail: rshl@hawaii.edu; Fax: 1-808-956-5908

absorb in the far UV region. Even for the cinnamates with a more red-shifted UV chromophore, it took more than one month of exposure to sunlight to reach stationary state mixtures of the *cis* and *trans* isomers.¹³

Photosensitized isomerization of trienes in the vitamin A series

Selective triplet photosensitized reactions of trienes in the vitamin A series were the key reactions that led to preparation of the hindered 7-*cis* isomers of vitamin A and eventual completion of preparation of all 16 possible geometric isomers of vitamin A.³ The C₁₅-aldehyde, **3a**, was the key building block in vitamin A synthesis.¹⁴ Because of the low lying n,π state of the aldehyde group, the trienal is a less satisfactory substrate for triplet sensitized reactions. On the other hand, the closely related C₁₅-nitrile (**3b**) and C₁₅-ester (**3c**), having low lying π,π states, were known to be wonderful substrates in selective sensitization reactions for conversion to the corresponding 7-*cis* and 7,9-dicis isomers.¹⁵ The latter can be converted to the corresponding C₁₅-aldehydes by partial reduction *via* established reactions for functional group manipulation,³ thereby satisfying the synthetic need for the key intermediates of 7-*cis* and 7,9-dicis-C₁₅-aldehyde.^{3a,b}



Because of the lengthened conjugation and the associated lower triplet excitation energy, yellow aromatic ketones, such as benzanthrone ($E_T = 46 \text{ kcal mol}^{-1}$),¹² were successfully used as triplet sensitizer for conversion of the 7-*trans* isomers to the hindered 7-*cis* isomers of these trienes.^{3a,b} Subsequently, much to our pleasant surprise, we found that the dye sensitizer Rose Bengal ($E_T = 39.4 \text{ kcal mol}^{-1}$),¹⁶ more popularly used in photosensitized singlet oxygen reactions,¹⁶ is quite satisfactory as a selective triplet sensitizer for these trienes. Thus, we have shown that a mixture of 7-*trans* isomers of **3b** in a deoxygenated solution¹⁰ of ethanol with Rose Bengal as the sensitizer was

readily converted to a mixture containing ~92% of the two hindered 7-*cis* : 7,9-dicis (1.1 : 1.0) isomers after only 30 min exposure to late November sunlight (>380 nm with Corning 3–74 cutoff filter).¹⁷ The reaction time was cut in half when the experiment was carried out in early May.¹¹

7-*cis* versus 7,9-dicis

The progress of the solar reactions of the C₁₅-nitrile (**3b**) and C₁₅-ester (**3c**) are shown respectively in Fig. 1a and 1b. Several interesting points are revealed in these figures. It is clear that the triplet sensitized reaction is dominated by the one-photon-one-bond isomerization process. The initial synthetic mixture of the nitrile and the ester contained mostly the di-*trans* isomer and a smaller amount of the 9-*cis* isomer. Hence, in the initial product mixtures of both compounds, the rise of the 7-*cis* isomer was much faster, while that of the 7,9-dicis trailed. The latter, a one-bond isomerized product from 7-*cis*, became equally or more important, especially in the case of **3c**, after significant accumulation of the 7-*cis* isomer.

The triplet excitation energy of the 7-*trans* isomers of the trienes are likely to be close to 43 kcal mol^{-1} , the reported value for a trienal.¹⁸ That of the more highly twisted 7-*cis* isomer⁷ must be higher. Therefore, with Rose Bengal as a sensitizer, the rate of triplet energy transfer to the 7-*cis* isomers must be more endothermic and slower than that to the 7-*trans*. The conversion to the two 7-*cis* isomers, however, was not complete, suggesting that the rate of the endothermic energy transfer to the 7-*cis* isomers was not negligibly small. The change of relative amounts of the two 7-*cis* isomers during later stages of irradiation offers convenient opportunities to obtain either isomer in larger amounts: up to 66% of the 7-*cis* isomer for **3b** (50% for **3c**) by stopping at early stages of irradiation, or 60% of the 7,9-dicis isomer for **3c** (43% for **3b**) at the eventual photostationary state (pss) (Fig. 1).

It is also worth noting that at pss, the total amount of the two 7-*trans* isomers of **3b** is slightly higher (~8%) than that of **3c** (~6%). We suspect this slight difference is due to a slightly

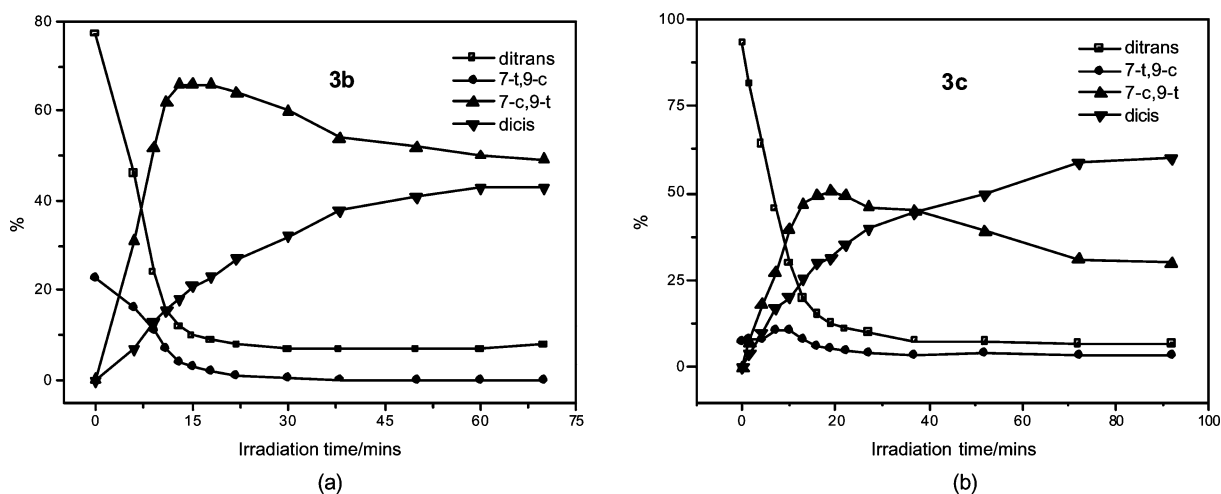


Fig. 1 (a) Changes of isomer composition during exposure of the mixture of the two 7-*trans* isomers of C₁₅-nitrile **3b** (77 to 23 from the synthetic mixture) in ethanol to sunlight with Rose Bengal as a triplet sensitizer using the kick-board reactor shown below. Progress of reaction was followed by ¹H NMR analyses of aliquots in NMR samples tubes exposed in parallel with the main sample tubes. (b) A similar study conducted with **3c** (93 to 7 from the synthetic mixture).

higher triplet excitation energy of the ester than that of the nitrile, making energy transfer to the hindered 7-*cis* isomers slightly less efficient. In agreement, under the same condition, the yellow dinitrile **4** (its triplet state energy likely to be further lowered by the extra cyano group) yielded an even larger amount of the 7-*trans* isomer (18%, Fig. 2). This conclusion suggests the need to search for a photosensitizer with energy slightly less than that of Rose Bengal so that it will lead to an even higher conversion to the hindered 7-*cis* isomers.

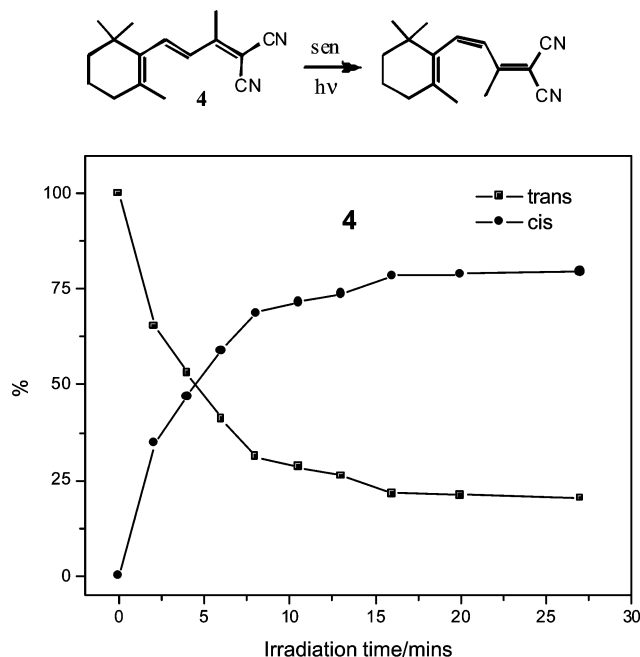


Fig. 2 Conversion of 7-*trans*-**4** to its *cis* isomer. A solution of **4**, similar to that described for **3b** was exposed to sunlight with a yellow Plexiglass with 470 cutoff as a filter. Pss was reached after ~20 min giving 82% of the *cis* isomer. Progress of reaction was followed by changes in ^1H NMR spectra.

A simple solar reactor

The rapid conversion of the trienes under the sun prompted us to design a simple floating solar reactor that does not require circulating cooling water, and would perhaps inject “Sun & Fun” into our photochemical research program. In Fig. 3, such a reactor is shown, with the floating platform being a kick-board. The sample chamber is a plastic box fitted into a hole carved through the middle of the board. The chamber bottom is a wire screen to allow easy flow of water. A UV-cutoff Plexiglass (UVF, 1/8" thick) plate was used as an economical substitute for Corning filter plates to cut off light <400 nm and also to keep the sample tubes in the box. In cases where a longer cutoff filter was needed, a yellow Plexiglass with a cutoff ~470 nm was used. Results conducted with solutions of C_{15} -nitrile (**3b**) or C_{15} -ester (**3c**) are shown above in Fig. 1a and 1b. Subsequently, we have also carried out solar reactions with a larger boogie-board solar reactor (pictures in contents entry) that was suitable for natural water environments, including the Pacific Ocean. The only change we made for the latter was a larger sample cavity for accommodation of a larger number of sample tubes. A total volume of 400 ml could easily be accommodated.



Fig. 3 The kick-board solar reactor in operation in a lily pond at UH (see also Fig. 4). Sample tubes contain Rose Bengal photosensitizer, and the filter is the colorless UVF Plexiglass.

Conclusion

The experiments described above correspond to a simple and very green method for preparative organic photochemical synthesis. A set of hindered isomers in the vitamin A series was conveniently prepared. In the process, we have better defined experimental conditions for preparing precursors to the key 7-*cis* or 7,9-*dicis* isomer of the C_{15} -aldehyde for synthesis of hindered isomers of vitamin A. The assembled solar reactor is a small one that can be conveniently fitted into a kick-board or a boogie-board. The final floating assembly for solar reactions does not require the use of conventional utilities, such as electricity and running water (nor any other coolants). It should be clear that if one wishes to conduct even larger scale experiments, one could simply employ floating platforms that provide much larger usable surface areas, including the possible use of full-size surfboards. This simple boogie-board reactor (and potentially larger surf-board reactors) has allowed us to tap the Pacific Ocean as an immense heat sink for dissipation of the excess thermal energy discharged from the solar reactor, while at the same time it injects “sun & fun” into our photochemical program. The simple setup is not costly.¹⁹ The short exposure time also eliminates the need for any extra features to concentrate solar energy for the type of reactions executed in our solar endeavor. We believe the results described herein are useful addition to the vast collection of synthetic organic photochemical reactions available in the literature.²⁰ At the same time, we do recognize that the use of floating reactors may become cumbersome for other types of solar reactions. However, the simplicity of the current setups for the triplet sensitized reactions makes it a meaningful extension of the foresight on general application of solar reactions as expressed by Ciamician a century ago.²¹

Experimental

Materials

The diene (**2**) and trienes (**3b**, **3c** and **4**) used in this work were prepared from the readily available β -ionone based on established procedures.^{3a,b} The photosensitizers were obtained from Aldrich.

Table 1 Solar reactions under selective triplet sensitization to produce the hindered 7-*cis* isomers of compounds in the vitamin A series

Compound	Sensitizer	Filter	final isomer composition
β -Ionol, 1	α -Acetonaphthone	Pyrex glass ^a	100% <i>cis</i>
C ₁₅ -Nitrile, 3b	Rose Bengal	Clear Plexiglass ^b	49% 7- <i>cis</i> , 43% 7,9- <i>dicis</i> ^d
C ₁₅ -Ester, 3c	Rose Bengal	Clear Plexiglass ^b	30% 7- <i>cis</i> , 60% 7,9- <i>dicis</i> ^d
Triene-dinitrile, 4	Rose Bengal	Yellow Plexiglass ^c	82% <i>cis</i> ^d

^a Pyrex glass, 290 nm cutoff. ^b UVF Plexiglass, 400 cutoff. ^c Yellow Plexiglass, 470 nm cutoff. ^d Remaining amounts being those of di-*trans* and 9-*cis* isomers (*trans* for **4**).

Solar experiments

Two general procedures were followed for preparative solar reactions. The first setup was a modified Liebig condenser reactor⁹ with a 10" condenser. Cooling water was allowed to pass through the inner section of the condenser. In a typical experiment, a 100 ml ethanol solution of β -ionol (1.20 g) along with 30 mg of α -acetonaphthone was placed in the outer jacket of the Liebig condenser (larger surface area). The solution was purged with nitrogen¹⁰ and the two ends of the condenser closed with clamped Tygon tubing. The photo-reactor was placed on the rooftop of our chemistry building.

The second was the kick-board reactor (Fig. 3). Its simple schematics are shown in Fig. 4. The chamber in the middle had a screen bottom to allow free flow of water, thereby ensuring the tubes being half immersed when in operation. In a typical experiment 100 ml of ethanol solution of 1.0 g of **3b** and 10 mg of Rose Bengal was introduced into three 1.6 (d) \times 15.0 (l) cm screw-capped Pyrex test tubes. The solutions were purged with nitrogen

and capped (aluminium foil should be used). A Plexiglass plate (UVF, 1/8") was used to cut off light <400 nm and to hold the tubes in the box. This floating reactor was used either in a wading pool on the roof of the chemistry building or in a lily pond. No additional cooling was required. After 15 min exposure to early May sunlight, the reaction was found to be complete. To follow progress of the solar reaction, a separate set of NMR tube containing a similar solution but with methanol-d₄ as solvent was irradiated in parallel. Samples were withdrawn periodically and the mixture analyzed by their ¹H NMR spectra²² on a 300 MHz spectrometer.

For compound **4**, the yellow Plexiglass with a cutoff at 470 nm was used as filter. In one preparative run, a deoxygenated (by purging with nitrogen) solution of 1.0 g of *trans*-**4** and 15 mg of Rose Bengal in 100 ml of ethanol was placed in three 15 mm screw-capped Pyrex test tubes (tied down with thin copper wire) and exposed to sunlight for 20 min in the boogie-board reactor. The conversion was 82% and the concentrated product mixture was chromatographed over a silica gel column; 0.71 g of the *cis* isomer (a viscous oil, with a shorter retention time than the *trans*) was isolated in 71% yield.

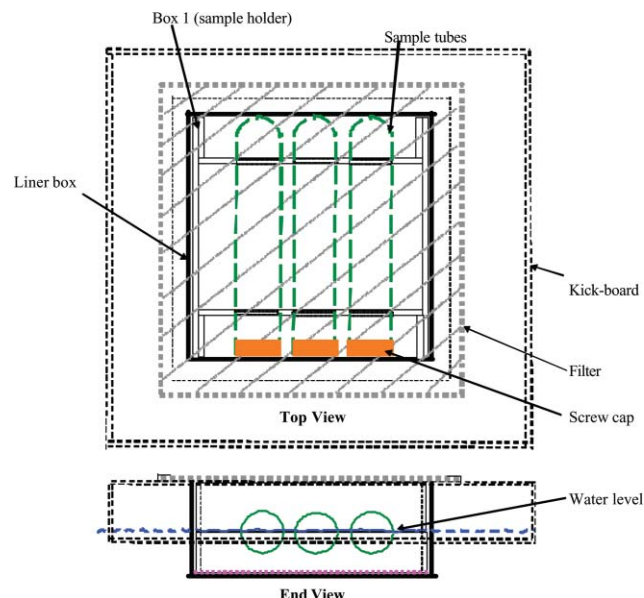


Fig. 4 Schematics for a simple solar reactor. Upper, a top view. The floating platform (a kick-board) with the Plexiglass filter plate on top. The sample box fitted into a hole carved into the kick-board with a wire bottom to permit free flow of water. Three sample Pyrex tubes with screw-caps, 15 (l) \times 1.6 (d) cm. Lower, a side view. Tubes approximately half immersed when the board was placed in water. The dimensions of the box and the size of the filter plate are clearly not critical. In this case, the box was 15.5 \times 13.0 \times 6.2 cm in size, the filter plate 19.8 \times 17.2 cm and 1/8" thick.

Acknowledgements

The work was supported by a grant from the National Science Foundation (CHE-0132250). RSHL thanks Dr M. Oelgemoeller for his continued interest and valuable consultation throughout the course of this work.

References

- (a) See e.g.: P. Esser, B. Pohlmann and H.-D. Scharf, *Angew. Chem., Int. Ed. Engl.*, 1994, **33**, 35; (b) M. Oelgemoeller, C. Jung, J. J. Ortner, J. Matty and E. Zimmerman, *Green Chem.*, 2005, **7**, 35; (c) M. Oelgemoeller, C. Jung and J. Mattay, *Pure Appl. Chem.*, 2007, **79**, 1939 and literature cited therein.
- (a) V. Ramamurthy, Y. Butt, C. Yang, P. Yang and R. S. H. Liu, *J. Org. Chem.*, 1973, **38**, 1247; (b) V. Ramamurthy and R. S. H. Liu, *J. Am. Chem. Soc.*, 1976, **98**, 2935.
- (a) See e.g.: R. S. H. Liu and A. E. Asato, *Methods Enzymol.*, 1982, **88**, 506; (b) R. S. H. Liu and A. E. Asato, *Tetrahedron*, 1984, **40**, 1931; (c) A. Trehan and R. S. H. Liu, *Tetrahedron Lett.*, 1988, **29**, 419.
- E. N. Marvell, G. Caple, T. A. Gosink and G. Zimmer, *J. Am. Chem. Soc.*, 1966, **88**, 619.
- C. D. Borsarelli, M. Mischne, A. La Venia and F. E. M. Vieyra, *Photochem. Photobiol.*, 2007, **83**, 1313.
- R. S. H. Liu, N. J. Turro and G. S. Hammond, *J. Am. Chem. Soc.*, 1965, **87**, 3406.
- V. Ramamurthy, T. T. Bopp and R. S. H. Liu, *Tetrahedron Lett.*, 1972, 3915.
- "Nonvertical excitation" prevents less hindered dienes to undergo one-way *trans* to *cis* isomerization under selective sensitization.

- Typical cases are those of 1,3-pentadiene and stilbene: G. S. Hammond and J. Saltiel, *et al.*, *J. Am. Chem. Soc.*, 1964, **86**, 3197.
- 9 O. Suchard, R. Kane, B. J. Roe, E. Zimmermann, C. Jung, P. A. Waske, J. Mattay and M. Oelgemoeller, *Tetrahedron*, 2006, **62**, 1467.
- 10 This class of compounds is known to undergo ready endo-peroxide formation under conditions of singlet oxygen formation. See, *e.g.*: M. Mousseron, *Adv. Photochem.*, 1966, **4**, 203.
- 11 For seasonal variation of sunlight intensity around different parts of the earth, see: D.-P. Hader, M. Lebert, M. Schuster, L. del Ciampo, E. W. Heilbling and R. M. McKenzie, *Photochem. Photobiol.*, 2007, **83**, 1348.
- 12 See *e.g.*: P. S. Engel and B. M. Monroe, *Adv. Photochem.*, 1971, **8**, 245.
- 13 S. Pattanaatgson, T. Munhapol, P. Hirunsupachot and P. Luangthongaram, *J. Photochem. Photobiol., A*, 2004, **161**, 269.
- 14 See *e.g.*: O. Isler and H. Mayer *Carotenoids*, ed. O. Isler, Birkhauser Verlag, Basel, 1971, p. 325.
- 15 V. Ramamurthy, G. Tustin, C. C. Yau and R. S. H. Liu, *Tetrahedron*, 1975, **31**, 193.
- 16 K. Gollnick, *Adv. Photochem.*, 1968, **6**, 15.
- 17 The dienes and trienes in the vitamin A series undergo ready, but unwanted, sigmatropic 1,5-*H*-migration (and to a lesser extent 6-*e* electrocyclization for the trienes) from the excited singlet state. See, *e.g.*: V. Ramamurthy and R. S. H. Liu, *J. Org. Chem.*, 1976, **41**, 1862.
- 18 D. F. Evans, *J. Chem. Soc.*, 1969, 1735.
- 19 The total cost of materials to construct the boogie-board solar reactor was less than \$50.00.
- 20 See: Synthetic Organic Photochemistry, ed. A. G. Griesbeck and G. Mattay, in *Molecular and Supramolecular Photochemistry*, vol. 12, 2005.
- 21 G. Ciamician, *Science*, 1912, **36**, 385.
- 22 The chemical shifts for the H-10 signals^{3b} for the four isomers of are 5.28, 5.21, 5.33, and 5.20 ppm (all in CD₃OD) for all-*trans*, 7-*cis*, 9-*cis* and 7,9-*dicis*. And, the corresponding numbers for isomers of **3c** are: 5.65, 5.56, 5.75 and 5.56 ppm. The ratio of the two latter two isomers was determined from peaks of H₇: 6.52 (all-*trans*) and 6.54 (9-*cis*) ppm. For characterization purpose, chemical shifts of all other vinyl H's of the four compounds are: **1**, *trans*, 5.94, 5.33 and *cis* 5.76, 5.38 for H₇, H₈; **3b**, all-*trans*, 6.64, 6.12, 9-*cis*, 6.61, 6.57; 7-*cis*, 6.15, 6.00, 7,9-*dicis*, 6.25, 6.45 for H₇, H₈; **3c**, all-*trans*, 6.52, 6.03, 9-*cis*, 6.54, 7.54; 7-*cis*, 6.10, 6.02. 7,9-*dicis*, 6.13, 7.00 for H₇, H₈; and **4**, *trans*, 7.59, 7.15 and *cis* 7.13, 7.03 ppm for H₇, H₈.

Environmentally benign synthesis of nanosized aluminophosphate enhanced by microwave heating

Eng-Poh Ng, Luc Delmotte and Svetlana Mintova*

Received 17th April 2008, Accepted 23rd June 2008

First published as an Advance Article on the web 5th September 2008

DOI: 10.1039/b806525j

The problem addressed with our paper is on the efficient utilization of reacting materials for enhanced syntheses of nanosized aluminophosphate molecular sieve by microwave heating, and decreasing or almost eliminating the related waste. The synthesis procedure deals with the environmental issues concerning the future manufacture re-use and disposal of non-reacted chemicals associated with the production of nanosized aluminophosphate. Nanosized AIPO-18 has been prepared by a multicycle synthesis approach *via* re-using non-reacted compounds from precursor suspensions with minimal requirement of chemical compensation after recovering of crystalline nanoparticles from each step. This approach is implied as environmentally benign and results in almost complete consumption of the organic templates and phosphorous acid without disposing these harmful reagents to the environments. Thus the use of highly expensive and non-desirable chemicals can be reduced and result in reasonable yield while production cost is attained. Also, the use of microwave irradiation leads to the preparation of nanocrystalline material within 5 min, instead of 3 days by using conventional heating, which makes the process economically viable and environmentally benign.

Introduction

The design of greener, more sustainable products and technological processes has become a top priority object for a lot of chemical industries.^{1–5} The green chemistry development is meeting the needs of utilizing raw materials, eliminating waste and avoiding the use of hazardous reagents in the final products. The problem addressed with our paper is on the efficient utilization of reacting materials with decreasing or elimination of the related waste. This technological development is dealing with the environmental issues associated with the future manufacture, re-use and disposal of non-reacted chemicals. By applying more advanced technologies for the preparation of nanosized molecular sieves, the waste problem is expected to be dramatically reduced. The use of organic additives (the commonly used amines or ammonium salts) and solvents for the synthesis of colloidal molecular sieves is a major source of waste, and it is associated with severe health hazards and/or environmental problems. Thus, the need for alternative synthesis procedures for the preparation of nanosized molecular sieves in colloidal form is widely recognized and is becoming a major focus of research mainly in academia and at later stage in the industry.

Nanosized (colloidal) molecular sieves have received considerable attention from both the research and the industrial divisions since they exhibit unusual and important properties in comparison to their micro-sized counterparts.^{6–12} During the last decades, they have been considered for applications different

from catalysis, sorption and ion exchange processes.^{13–17} The recent use of nanosized molecular sieves in the production of high selective sensors,^{18–20} membranes,²¹ optical coatings^{22–23} and medical diagnosing²⁴ is owing to their defined and small crystal size resulting in the presence of large accessible active sites and reduced diffusion path length, which is barely achievable by their micrometre sized counterparts. Due to the remarkable properties of the materials in the nanoscale range, many efforts have been dedicated to the optimization of the synthesis procedures with final goals: (i) increase of crystalline yield, (ii) control of particle size, morphology and structure, (iii) stabilization of nanoparticles in suspensions and powder form, and (iv) decrease of the price.^{10,25–28} In spite of this, no special attention has been paid to the green and environmentally benign chemistry required for the synthesis of microporous nanocrystals.

Typically, the synthesis of nanosized materials starts from clear precursor suspensions with an excess of organic additives and different solvents (water, ethanol, methanol, *etc.*), which are required for directing the crystallization process of crystals with monomodal particle size distribution under hydrothermal conditions. In most of the syntheses, the crystal size has been reduced by increasing the concentration of the organic template tremendously, replacing the water with other solvents, decreasing the synthesis temperature and extending the crystallization process.^{6,16} Unfortunately, these conditions formulate the synthesis of the nanocrystalline material as non-economically visible due to the large consumption of the very expensive organic template (additive) and increased consumption of energy.^{10,29} Besides, the non-reacted chemicals from the precursor solutions are usually discarded after the nanocrystalline materials are separated and thus resulting in

Laboratoire de Matériaux à Porosité Contrôlée, UMR-7016 CNRS, ENSCMu, Université de Haute Alsace, 3 rue Alfred Werner, 68093, Mulhouse, France

the disposal of valuable materials with negative environmental effects. Furthermore, the low product yield (less than 10%) from the reacting synthesis batches makes the scaling up process a very important concern for the chemical industry from the economical and ecological viewpoints.

The preparation of nanocrystals of two types of microporous aluminosilicates (LTA and FAU)^{25,26} and one pure silicate (MFI)²⁶ material with high yield by recycling of the non-reacted chemicals has been reported. The crystallization process was carried out by re-using the non-reacted solutions for the subsequent synthesis steps without additional compensation of the used reactants. Thus, the recycling synthesis process considerably increases the product yield, and at the same time the cost of the material and the waste disposal are reduced. This multi-synthesis crystallization with enhanced consumption of the nutrients without any compensation, however, limits the synthesis to several cycles only.

Recycling of the non-consumed chemical reagents from the reacting synthesis mixtures used for the preparation of microporous aluminophosphate (AIPOs) has not been reported yet. One of the reasons is that the small change in the molar composition of the precursor suspension will have a profound impact on the crystallizing materials, *i.e.* amorphous, new or mixture of two or more phases will be formed instead of the desired single crystalline phase.

One of the significant interests in the environmentally benign synthesis of zeo-type material (AIPO-18) is due to the high demand for new, highly hydrophilic, nanoporous sorbents proper for closed solar cooling systems and heat transformation applications. The required hydrophilic nanoporous materials should release water vapour under heating, thus they will have high storage for "latent" heat, and subsequently under adsorption of moisture they will release the stored heat. Heat transformation applications based on sorption/desorption of water in nanoporous adsorbents appear to be suitable for many processes where improved thermochemical properties, enhanced hydrothermal and mechanical stabilities are required. Most adsorptive chillers and heat pumps built so far are based on commercially available adsorbents originally developed for applications such as gas separation and catalysis. For the next generation of chillers and heat pumps, novel adsorbents, for instance nanosized microporous materials (AIPOs, SAPOs, *etc.*) with properties specifically tailored for these applications, will be of great importance.

In this paper, the environmentally benign synthesis of a nano-product (AIPO-18 with AEI-type topology) by re-using of non-reacted compounds by supplementary compensation of the consumed chemicals is reported. The initial precursor suspension is used in three subsequent cycles and the crystalline yield, morphology, particle size and distribution are kept constant. Also, the crystallization rate of AIPO-18 nanocrystals is increased by using microwave irradiation instead of conventional heating, thus the energy consumption is significantly reduced by decreasing the crystallization time (from 3 days to 5 min).

The environmentally benign process is aiming at the efficient utilization of reacting materials (especially harmful amines) and decreasing or abolishing the related waste (amine/ammonium salt, phosphate) from the synthesis.

Experimental

Environmentally benign multi-step synthesis of AIPO-18 nanocrystals

The initial precursor suspensions for AIPO-18 nanocrystals were prepared with a molar composition of 1 Al₂O₃ : 3.16 P₂O₅ : 3.16 (TEA)₂O : 186 H₂O as described in our previous paper.²⁹ The initial reactants were aluminium isopropoxide, Al(O*i*Pr)₃ (Acros Organic), TEOAH (35 wt.%, Aldrich), phosphoric acid (85 wt.%, Riedel-de-Haän®) and distilled water. For all syntheses, 25 ml of the precursor suspension was added into a Teflon lined autoclave (100 ml) and heated with a microwave oven (Anton Paar Synthos 3000) using the temperature-programmed mode (800 W) for 2.5 min to reach 180 °C and then maintained for 5 min before cooling down immediately to room temperature (RT). The solid product was recovered by high-speed centrifugation (25000 rpm, 30 min), and the non-reacted chemicals in the solutions (water-clear) were saved in a container.

Prior to the second and third syntheses cycles, the chemical composition of the non-reacted solutions was adjusted to the original one by adding the required very small amount of Al(O*i*Pr)₃, TEOAH and phosphoric acid. The last chemical is added slowly until the pH of ~7.5 is reached. The AIPO-18 nanocrystals prepared from the first, second and third synthesis cycles will be denoted as AP-1, AP-2 and AP-3, respectively.

Characterization of AIPO-18 nanocrystals

The chemical composition of the solid samples was determined by X-ray fluorescence (XRF) analysis with a MagiX PHILIPS PW2540, while the initial and re-used suspensions were characterized with inductively coupled plasma atomic emission spectroscopy (Varian, ICP-AES) and confirmed by XRF.

The XRD patterns of the nanocrystalline AIPO-18 samples were recorded on a Stoe STADI-P diffractometer (transmission mode, Cu K_α radiation). The crystal size and morphology of the solids were determined by a Philips XL-30 scanning electron microscopy (SEM) and transmission electron microscopy (TEM) using JEOL JEM 2011 operating at 200 kV. Additionally, dynamic light scattering (DLS) and zeta potential (ξ) of the water suspensions containing AIPO-18 nanocrystals were measured by a Malvern Zetasizer Nano Series. The porosity of the solid samples prepared from the three subsequent cycles was determined by nitrogen sorption using a Micromeritics ASAP 2010, and TG/DTA data were recorded with a SETARAM 16MS thermogravimetric analyzer.

Results and discussion

The multi-step synthesis of nanocrystalline AIPO-18 crystals using non-reacted precursor compounds compensated with the needed chemicals was carried out in three subsequent cycles. Unlike the previous works describing the syntheses of aluminosilicate and pure silica materials,^{25,26} the precursor solutions used for the nanocrystalline AIPO-18 remain clear and no solid (crystalline) products were obtained if no chemical compensation is performed. In addition to the small amount of aluminium source, the pH of the re-used precursor solutions was of significant importance for formulation of the initial

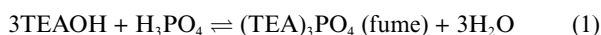
Table 1 Reacting precursor suspensions and crystalline yield of AIPO-18 nanocrystals

AIPO-18 syntheses	1 st Cycle	2 nd Cycle	3 rd Cycle
Non-reacted mixture/g	0	128.15	129.52
Added reagents	1 st cycle	2 nd cycle	3 rd cycle
Al(O <i>i</i> Pr) ₃ /g	11.41	2.62	2.01
H ₃ PO ₄ /g	19.97	4.24	8.10
TEAOH/g	72.75	8.82	6.93
H ₂ O/g	41.48	1.88	2.52
Crystalline yield ^a /wt.%	60	54	55

^aCrystalline yield (%) = $\frac{\text{Weight of solid crystalline product (g)}}{\text{Initial weight of Al}_2\text{O}_3 \text{ and P}_2\text{O}_5 \text{ (g)}} \times 100\%$.

compositions in order to be identical with the original (starting) one.

The chemical composition of the initial and re-used solutions characterized by ICP-AES and XRF are summarized in Table 1. As can be seen, a high amount of P₂O₅ was utilized during the first synthesis cycle of AIPO-18 nanocrystals in comparison to the consumed Al₂O₃. Initially, the phosphoric acid neutralized the basic quaternary ammonium cations in the templated solutions and released a fume of (TEA)₃PO₄ during the mixing procedure (eqn (1)). Subsequently a reaction between the phosphoric acid and aluminium resulted in the formation of an insoluble salt (eqn (2)). The first and second reactions are exothermic and tend to happen especially when the phosphoric acid is introduced very fast into the basic precursor suspensions. Hence, a slow addition of phosphoric acid is required in order to avoid or minimize the formation of any insoluble solid and fume, which further affects the synthesis process of nanosized AIPO-18 crystals. It is important to note that no crystalline solid product was formed in the re-used suspensions. However, another type of microporous aluminophosphate (AIPO-5, AFI-type) has been crystallized as a side or even main product when the phosphate concentration is in excess or the template concentration is insufficient.



The crystalline yield of the nanosized AIPO-18 material for the three subsequent cycles, *i.e.* AP-1, AP-2 and AP-3 is calculated to be 60, 54 and 55 wt.%, respectively. These results suggest that the re-using of the non-reacted precursor solutions from the one-step synthesis is possible as the template has been completely preserved and does not decompose during the microwave heating. Additionally, the crystalline yield remains constant by compensating the consumed reactants prior the next synthesis cycles. On one side, this method is revealed as benign since no harmful non-reacted reagents (TEAOH, H₃PO₄) are disposed to the environment, and on the other side the chemicals are re-used thoroughly and thus high crystalline yield is achieved (the price of the nanoparticles is of important consideration as well).

The crystalline nature of the microporous nanoparticles is confirmed by collecting the XRD patterns of samples AP-1, AP-2 and AP-3 (Fig. 1). All XRD patterns exhibit the typical Bragg

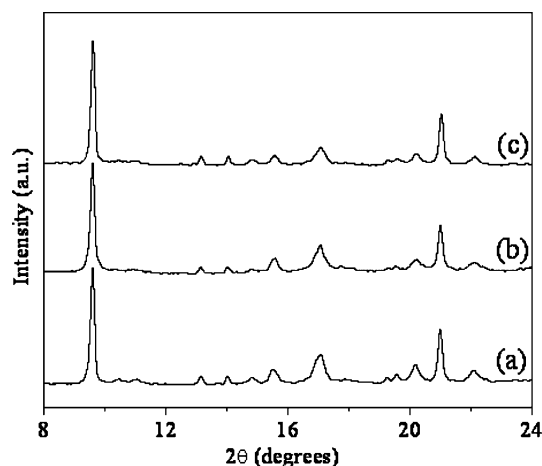


Fig. 1 XRD patterns of AIPO-18 nanocrystals synthesized from the three subsequent cycles (a) AP-1, (b) AP-2 and (c) AP-3.

reflections for AEI-type crystalline structure.³⁰ Neither other crystalline phases (*e.g.* AFI, CHA) nor amorphous products were observed in the diffractograms, showing that only AIPO-18 nanocrystals formed after adjusting the chemical compositions in the three subsequent synthesis cycles. Additionally, the intensity and line widths of the peaks are almost identical for all three samples, revealing that the AIPO-18 nanocrystals have the same degree of crystallinity and size of the individual particles.

The particle size distribution (PSD) of the nanocrystals from the three subsequent cycles (AP-1, AP-2 and AP-3) was investigated by DLS. The average size of crystals in the first batch is 260 nm, and decreased slightly to 190 nm and 250 nm in the second and third cycles, respectively (see Fig. 2a). However, the starting and final points for the three DLS curves are almost the same. Thus, it can be concluded that the AIPO-18 nanocrystals have similar crystal size, and the width of the PSD curves is similar proving the relative stability of the particles at a given concentration in water dispersant. Besides, the stability of the AIPO-18 nanoparticles in the three crystalline suspensions after purification (solid concentration: 6 wt.%, pH = 7) was determined by zeta potential measurements.³¹ The zeta values for the AP-1, AP-2 and AP-3 samples are lower than -30 mV and this explains their long-term stability in the colloidal form (see Fig. 2b). No sedimentation in the crystalline suspensions is observed after several weeks of storage at room temperature.

The morphological features of the AIPO-18 nanoparticles were examined by SEM. As can be seen in Fig. 3, all of the AIPO-18 nanocrystals have an elongated plate-like shape, which is different from the microsized AIPO-18 counterpart synthesized from dense gel (the microsized AIPO-18 crystals have in most of the cases, a tetragonal shape). The differences in the size and crystalline morphology of the particles can be explained by the different synthesis procedure carried out in aluminophosphate gels or clear precursor suspension. In the current case, highly supersaturated suspensions containing excess of organic template³² are subjected to a homogeneous microwave heating.³³ The AIPO-18 nanocrystals from the three subsequent synthesis cycles are well shaped and uniformly developed in comparison to the microsized counterpart, which is due to the spontaneous and controlled nucleation and crystallization processes taking

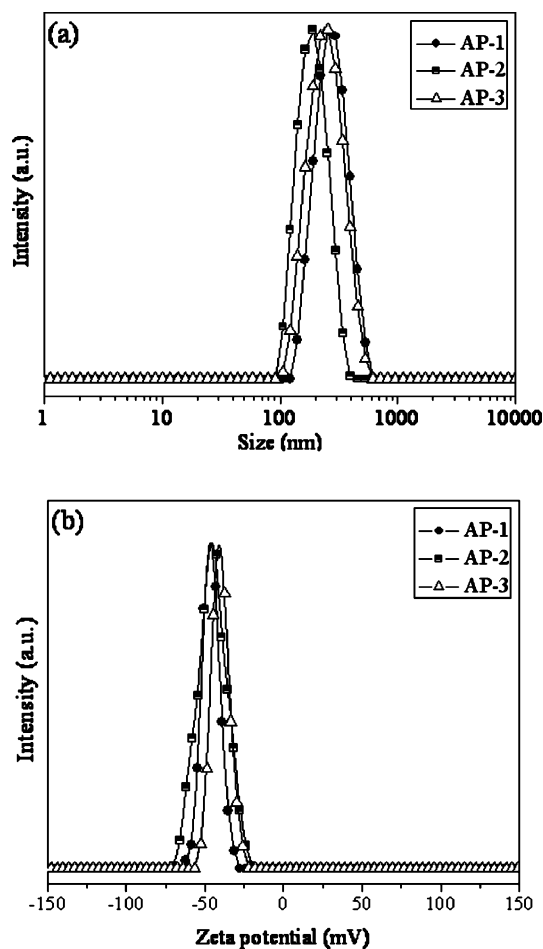


Fig. 2 (a) DLS and (b) zeta potential curves of AlPO-18 nanocrystals prepared from three subsequent synthesis cycles.

place in the clear precursor suspensions. The SEM pictures are in a good agreement with the DLS data, where the sizes of the AP-1 and AP-3 nanocrystals are approximately identical (100–600 nm) and rather smaller crystals are observed in the second synthesis cycle (100–420 nm).

One of the notable features of the aluminophosphate molecular sieves is the constant ratio of Al/P, so that the aluminophosphate framework with an “electrically” neutral framework structure is formed. As expected, the Al/P ratio for all AlPO-18 nanocrystals is almost equal to 1 (see Table 2).

The porosity of the AlPO-18 nanoparticles prepared in the three cycles has been proven by N_2 sorption measurements. It has been confirmed that all samples have a high surface area ($>500 \text{ cm}^2 \text{ g}^{-1}$), which can be explained by their high degree of crystallinity. Among the three samples, the AP-2 has the highest pore volume and the highest total amount of N_2 adsorbed, which

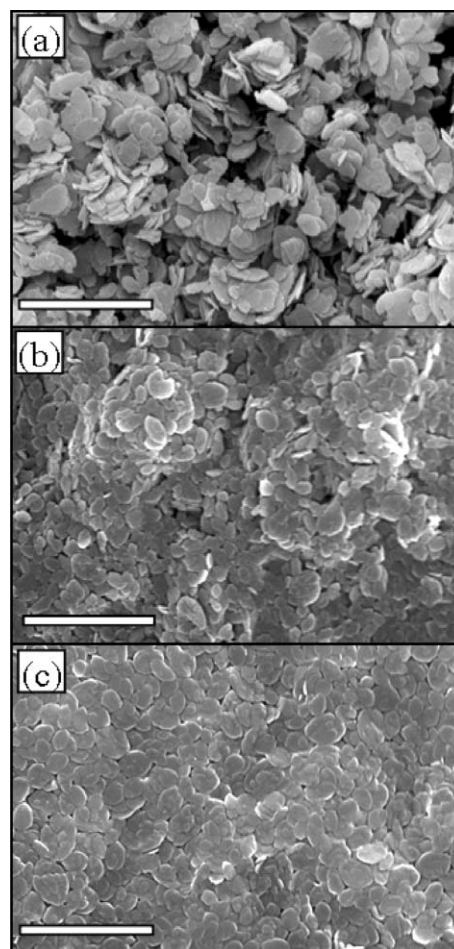


Fig. 3 SEM images of AlPO-18 nanocrystals synthesized from the subsequent cycles (a) AP-1, (b) AP-2 and (c) AP-3. Scale bar: 2 μm .

probably is due to the smaller crystal size of the nanoparticles (see Fig. 2 and 3).

The nitrogen adsorption–desorption curves for the samples AP-1, AP-2 and AP-3 show that the samples possess the typical type IV isotherm with type H1–H3 hybrid loop in accordance with IUPAC classification (see Fig. 4A).³⁴ The three adsorption isotherms exhibit a rapid increase in nitrogen uptake at relative pressure (P/P_0) below 0.1, which corresponds to the filling of the micropores of the materials (see the background of Fig. 4A: TEM picture of AlPO-18 single crystal with the crystalline fringes representing the channels with size of 3.8 Å). A plateau with an abrupt inclination step at high relative pressure ($P/P_0 > 0.8$) was observed, which is associated with multilayer adsorption in the textural mesopores of the nanosized material. The nanocrystals in samples AP-1 and AP-3 have the same

Table 2 Properties of AlPO-18 nanocrystals

Samples	Al/P ratio	Surface area/ $\text{cm}^2 \text{ g}^{-1}$	Pore volume/ $\text{cm}^3 \text{ g}^{-1}$	Zeta potential ^a /mV	Crystal size range/nm
AP-1	1.02	580	0.71	–47	100–600
AP-2	1.04	551	0.74	–47	100–420
AP-3	1.03	512	0.72	–41	100–600

^a Measurements are performed in water solutions with a constant concentration of 6 wt.% at pH = 7 and 25 °C.

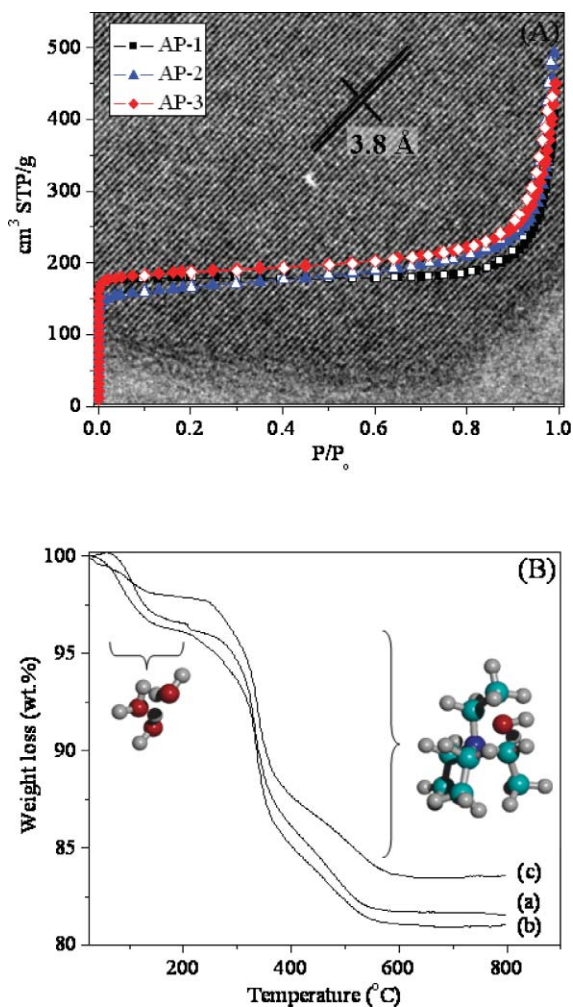


Fig. 4 (A) Nitrogen adsorption–desorption isotherms of AlPO-18 nanocrystals synthesized from the three subsequent cycles. Solid symbols denoted adsorption and open symbol denoted desorption. Background: TEM picture of AlPO-18 single crystal with the crystalline fringes representing the channels with size of 3.8 Å. (B) TG curves of non-calcined AlPO-18 synthesized from the three subsequent cycles: (a) AP-1, (b) AP-2 and (c) AP-3.

initial N_2 uptake, thus suggesting a similar micropore volume and crystal size (see Table 2). In contrast, AP-2 has negligible lower N_2 sorption which is due to the smaller crystal size that has been proven by SEM and DLS analyses (see Fig. 2 and 3). As a consequence, a higher pore volume and textural mesoporosity which results in the enhancement of the total N_2 uptake for the AP-2 sample are measured.

The TG curves of three non-calcined samples have a similar shape (Fig. 4B). The weight loss in the samples occurred in three stages. In the first stage (<200 °C), the weight loss is due to desorption of water. In the second (200 – 350 °C, weight loss $\sim 10\%$) and third (350 – 550 °C, weight loss $\sim 4\%$) stages, the weight losses are due to the thermal decomposition of templates H-bonded to the inorganic framework followed by a sequential Hoffmann degradation reaction. This reaction is followed by β -elimination and oxidation, while the remaining organic components are removed in the third stage.^{35,36} The thermogravimetric analysis is used to verify the amount of organic template incorporated

in the framework, thus the amount of the consumed template is determined (the quantity of template lost during the purification process of the nanocrystals is also taken into account). From the TG data, we can conclude that the AlPO-18 nanocrystals synthesized from the three subsequent cycles contain the same amount of template (total weight loss of ~ 14 wt.% in the range of 240 – 550 °C), thus showing that the consumption of the organic template is constant.

A scheme representing the total utilization of chemical reagents for one- and multi-step syntheses of nanocrystalline AlPO-18 is depicted in Fig. 5. The experiments performed in laboratory-scale are based on 25 g of AlPO-18 solid nanomaterial. In the multi-step synthesis approach (3 cycles are carried out), the consumption of reagents is 50% less for phosphate and alumina sources; special attention has to be given to the very expensive and harmful organic template which is reduced up to 70% (see Fig. 5a). Thus the production cost, which is one of the major concerns in industry, is decreased substantially. The total consumption of reagents at industrial scale based on 1 ton of AlPO-18 nanocrystals is predicted for the single and multi-synthesis methods (Fig. 5b). The low consumption of expensive and also very harmful chemicals is obvious, thus providing large cost saving to industries and environment protection. Furthermore, this approach offers an option for a green synthesis of aluminophosphate molecular sieves, where

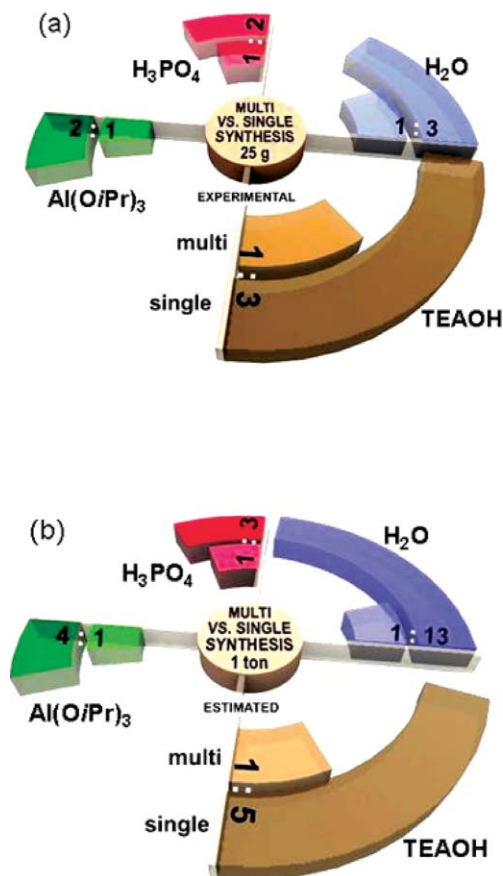


Fig. 5 Total consumption of chemical reagents for the synthesis of nanocrystalline AlPO-18 by single and multi-step synthesis approaches in (a) laboratory (experimental), and (b) industry (calculated) scale production.

the crystalline yield is considerably maintained by re-using the same non-reacted initial chemicals, thus decreasing the risk of waste pollution and making possible the chemical process to be environmentally benign.

Conclusions

An environmentally benign multi-step synthesis of nanocrystalline AlPO-18 is reported by re-using non-reacted initial precursor solution with slight compensation of the needed reactants under microwave irradiation. Unlike in the aluminosilicate and pure silicate systems, no crystalline AlPO-18 product was obtained without minor compensation of the used chemicals in the reacted mixtures. The AlPO-18 nanocrystals synthesized from the three subsequent cycles have the same yield, crystallinity, morphology, particle size and chemical composition. The nanosized AlPO-18 in the water suspensions from the three subsequent syntheses cycles are stable without extra surface modification. All the AlPO-18 samples showed high pore volume and high surface area.

The multi-step synthesis approach presented here is beneficial for both the environment and scaling up through reducing the production cost and disposal of chemical waste after the synthesis of AlPO-18 nanocrystals.

One of the conventional chemical processes for preparation of nanosized microporous molecular sieves, which is using large amounts of toxic reactants (amine/ammonium salt, phosphoric acid) and volatile solvents (ethanol, methanol) is optimized by applying the multi-step synthesis approach. Moreover, a substantial decrease in the amount of the used and waste hazardous reagents in/from the chemical processes, which is one of the main goals of green chemistry, is accomplished.

Moreover, the supply of AlPO-18 nanomaterial with superior water capacity, improved mechanical and hydrothermal stability for the application in heat transformation devices is an ongoing task. The progress in the preparation of composites based on AlPO-18 will enable the development of new products for solar-thermal applications including solar-air-conditioning systems, it will improve conventional heating systems and will reduce CO₂ emissions. The development of new nanoporous materials for heat pumping and cooling applications has been a research priority for many years and by combining the properties of the microporous materials (nanosized AlPO-18) and the porous matrix, it will lead to fast adsorption kinetics at controlled adsorbent temperatures. Therefore, innovative and environmentally benign approaches for synthesis and processing of highly porous adsorbent combined with preparation of coatings with reduced thermal resistances and mechanical long-term stability will be the base for the development of compact heating/cooling devices driven by the heat of solar collectors.

Acknowledgements

The financial support from SOILCY IP and SRIF PNANO-ANR projects is gratefully acknowledged.

References

- 1 S. K. Khetan and T. J. Collins, *Chem. Rev.*, 2007, **107**, 2319.
- 2 R. Llamas, C. J. -Sanchidrián and J. R. Ruiz, *Appl. Catal., B*, 2007, **72**, 18.
- 3 S. J. Haswell and P. Watts, *Green Chem.*, 2003, **5**, 240.
- 4 J. Seayad, A. Tillack, C. G. Hartung and M. Beller, *Adv. Synth. Catal.*, 2002, **344**, 795.
- 5 G. Centi, P. Ciambelli, S. Perathoner and P. Russo, *Catal. Today*, 2002, **75**, 3.
- 6 L. Tosheva and V. P. Valtchev, *Chem. Mater.*, 2005, **17**, 2494.
- 7 S. Mintova, N. Petkov, K. Karaghiosoff and T. Bein, *Mater. Sci. Eng., C*, 2002, **19**, 111.
- 8 S. Mintova, N. Olson, V. Valtchev and T. Bein, *Science*, 1999, **283**, 958.
- 9 S. Mintova, N. Olson and T. Bein, *Angew. Chem., Int. Ed.*, 1999, **38**, 3201.
- 10 B. A. Holmberg, H. Wang, J. M. Norbeck and Y. Yan, *Microporous Mesoporous Mater.*, 2003, **59**, 13.
- 11 G. S. Zhu, S. L. Qiu, J. H. Yu, Y. Sakamoto, F. S. Xiao, R. R. Xu and O. Terasaki, *Chem. Mater.*, 1998, **10**, 1483.
- 12 W. Song, J. F. Woodworth, V. H. Grassian and S. C. Larsen, *Langmuir*, 2005, **21**, 7009.
- 13 G. H. Li, C. A. Jones, V. H. Grassian and S. C. Larsen, *J. Catal.*, 2005, **235**, 431.
- 14 Y.-X. Jiang, D. Si, S.-P. Chen and S.-G. Sun, *Electroanalysis*, 2006, **18**, 1173.
- 15 R. A. Rakoczy and Y. Traa, *Microporous Mesoporous Mater.*, 2003, **60**, 69.
- 16 S. C. Larsen, *J. Phys. Chem. C*, 2007, **111**, 18464.
- 17 S. C. Stout, S. C. Larsen and V. H. Grassian, *Microporous Mesoporous Mater.*, 2007, **100**, 77.
- 18 M. Vilaseca, C. Yagüe, J. Coronas and J. Santamaria, *Sens. Actuators, B*, 2006, **117**, 143.
- 19 S. Mintova and T. Bein, *Microporous Mesoporous Mater.*, 2001, **50**, 159.
- 20 S. Mintova, S. Y. Mo and T. Bein, *Chem. Mater.*, 2001, **13**, 901.
- 21 S. Münzer, J. Caro and P. Behrens, *Microporous Mesoporous Mater.*, 2008, **110**, 3.
- 22 Z. B. Wang, A. P. Mitra, H. T. Wang, L. M. Huang and Y. Yan, *Adv. Mater.*, 2001, **13**, 1463.
- 23 Z. B. Wang, H. T. Wang, A. Mitra, L. M. Huang and Y. Yan, *Adv. Mater.*, 2001, **13**, 746.
- 24 C. P. -Iglesias, L. V. Elst, W. Zhou, R. N. Muller, C. F. G. C. Galdes, T. Maschmeyer and J. A. Peters, *Chem.-Eur. J.*, 2002, **8**, 5121.
- 25 O. Larlus, S. Mintova and T. Bein, *Microporous Mesoporous Mater.*, 2006, **96**, 405.
- 26 W. Song, V. H. Grassian and S. C. Larsen, *Chem. Commun.*, 2005, 295.
- 27 Z. J. Li, C. M. Lew, S. A. Li, D. I. Medina and Y. S. Yan, *J. Phys. Chem. B*, 2005, **109**, 8652.
- 28 Z. J. Li, S. A. Li, H. M. Luo and Y. S. Yan, *Adv. Funct. Mater.*, 2004, **14**, 1019.
- 29 H. V. Heyden, S. Mintova and T. Bein, *J. Mater. Chem.*, 2006, **16**, 514.
- 30 Atlas of zeolite framework types: <http://www.iza-structure.org>.
- 31 T. Maurer and B. Kraushaar-Czarnetzki, *Helv. Chim. Acta*, 2001, **84**, 2550.
- 32 J. Motuzas, A. Julbe, R. D. Noble, C. Guizard, Z. J. Beresnevicius and D. Cot, *Microporous Mesoporous Mater.*, 2005, **80**, 73.
- 33 D. P. Serrano, M. A. Uguina, R. Sanz, E. Castillo, A. Rodríguez and P. Sánchez, *Microporous Mesoporous Mater.*, 2004, **69**, 197.
- 34 F. Rojas, I. Kornhauser, C. Felipe, J. M. Esparza, S. Cordero, A. Domingueza and J. L. Riccardo, *Phys. Chem. Chem. Phys.*, 2002, **4**, 2346.
- 35 E. B. -Lami, F. D. Renzo, F. Fajula, P. H. Mutin and T. D. Courieres, *J. Phys. Chem.*, 1992, **96**, 3807.
- 36 F. Kleitz, W. Schmidt and F. Schüth, *Microporous Mesoporous Mater.*, 2001, **44-45**, 95.

Influence of the enzyme concentration on the phase behaviour for developing a homogeneous enzymatic reaction in ionic liquid–CO₂ media†

Maria Dolores Bermejo,^{a,d} Aleksandra J. Kotlewska,^b Louw J. Florusse,^c Maria José Cocero,^d Fred van Rantwijk^b and Cor J. Peters^{*a}

Received 25th March 2008, Accepted 25th June 2008

First published as an Advance Article on the web 15th August 2008

DOI: 10.1039/b805011b

A homogeneous enzymatic reaction in an ionic liquid (IL)–CO₂ medium integrated with the separation of the product is proposed. It takes advantage of the miscibility switch phenomenon using CO₂, which is able to force two immiscible phases to form one homogeneous phase to perform the reaction. After completion of the reaction the homogeneous fluid phase is split in two or three phases upon pressure decrease in order to facilitate the product recovery. For this purpose the enzyme *Candida antarctica* lipase B (CaL B) and the IL 1-hydroxy-1-propyl-3-methyl imidazolium nitrate (HOPMImNO₃) are used. In this study the solubility of CO₂ in solutions of CaL B in HOPMImNO₃ was experimentally determined using the Cailletet apparatus, which operates according to the synthetic method. Concentrations of the enzyme vary from 3 to 12% by weight, and concentrations of CO₂ from 5 to 20 mol% were investigated in a temperature range from 30 to 75 °C and pressures up to 12 MPa were applied. No precipitation of the enzyme was observed when dissolving CO₂ in the IL. At constant CO₂/IL ratios the pressure of the bubble points remained almost unchanged with the enzyme concentration. Triacetin tests showed that the reduction of the activity of the enzyme after storage for three months in liquid HOPMImNO₃ was only of the order of 20%. Recovery and purification of the IL was possible by precipitation of the enzyme using isopropanol (IPA) as an anti-solvent.

Introduction

Although water is the natural medium for enzymatic reactions, organic solvents are also widely used to improve the solubility of hydrophobic reactants and/or products and to shift the reaction equilibrium from hydrolysis towards synthesis.¹ In the last few years there has been an increasing interest in studying enzymatic reactions in ILs in order to replace volatile halogenated organic solvents by non-volatile ionic liquids as the medium for these kinds of reactions² and the subject has been studied in several reviews.^{1,3,4} In general it holds that ILs as solvents for enzymatic reactions simplify the product separation.

Furthermore, an over-stabilizing effect on biocatalysts compared to traditional organic solvents without affecting the yield of the process has been observed.⁵ Moreover, ILs have been used successfully as additives to protect stabilized enzymes from deactivation when the reaction is performed in organic media.⁶ Most of the enzymatic reactions in ILs have been carried out with immobilized enzymes or free enzymes in suspensions. Recently it has been reported that it is possible to have a homogeneous enzymatic reaction in ILs.^{7–10}

Supercritical carbon dioxide (scCO₂) was found to be able to extract or precipitate substances from an IL without any cross-contamination of the IL itself.¹¹ As an additional feature, CO₂ is able to force two or more immiscible phases to form one homogeneous phase upon pressure increase¹² and, in reverse, to split a homogeneous fluid phase in two or three phases upon pressure decrease. This phenomenon is called miscibility switch,¹³ and can be applied in combined reaction/separation systems for performing monophasic or biphasic reactions. It was applied to the enzymatic processes combining ILs and CO₂.^{14,15} to have a two-phase medium. The enzyme was immobilized in the IL-rich solvent, while substrates and products were introduced and extracted respectively from the system dissolved in the moving phase rich in scCO₂. The protective effect of the IL against the denaturing effect of CO₂ was clearly observed.

In this work, a homogeneous enzymatic reaction is studied in an IL–CO₂ medium, including the separation of the product

^aLaboratory of Process Equipment, Department of Process and Energy, Faculty of Mechanical, Maritime and Materials Engineering, Delft University of Technology, Leeghwaterstraat 44, 2628, CA, Delft, The Netherlands. E-mail: C.J.Peters@tudelft.nl

^bLaboratory of Biocatalysis and Organic Chemistry, Faculty of Applied Sciences (Department of Biotechnology), Delft University of Technology, Julianalaan 136, 2628, BL, Delft, The Netherlands

^cPhysical Chemistry and Molecular Thermodynamics, Faculty of Applied Science (DelftChemTech), Delft University of Technology, Julianalaan 136, 2628, BL, Delft, The Netherlands

^dHigh Pressure Process Group, Dept. Chemical Engineering and Environmental Technology, University of Valladolid, Prado de la Magdalena s/n, 47011, Valladolid, Spain

† Electronic supplementary information (ESI) available: Bubble points of the system CO₂ + HOPMImNO₃ + CaL B for four different concentrations (Tables 1–4). See DOI: 10.1039/b805011b

applying the miscibility switch phenomenon. A simplified scheme of the process is shown in Fig. 1. Pressurizing the system with CO₂ causes the reaction to take place in a homogeneous phase. After completion of the reaction, pressure release causes the homogeneous phase to separate into two phases: a IL rich phase with the enzymes dissolved and a CO₂ rich phase containing the products. After an additional depressurization step, separation of the CO₂ from the products is carried out. In the case that more than one product is obtained or that the reagents are not completely converted, a fractionated separation is possible. For this purpose, the enzyme *Candida antarctica* lipase B (CaL B) and the IL 1-(1-hydroxypropyl)-3-methylimidazolium nitrate (HOPMImNO₃) are used.

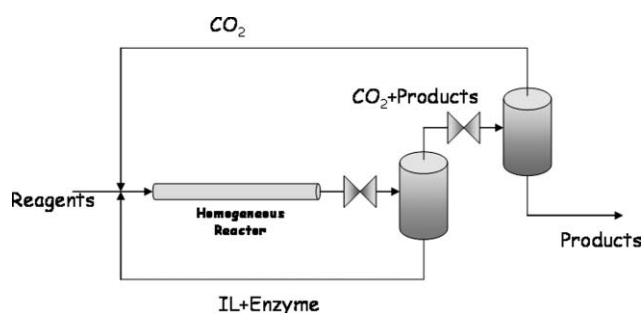


Fig. 1 Scheme of the integrated reaction–separation process in a homogeneous IL–CO₂ medium.

CaL B has been extensively used in enzymatic reactions in IL media.^{8,14,16} Imidazolium type ILs with a nitrate anion have been scarcely studied,^{17,18} but in general it is known that they are highly hygroscopic and solubilise less CO₂ than other ILs. BMImNO₃ was proved to dissolve CaL B. However, besides when its activity was partially recovered by hydration, the enzyme was not active in the IL.^{3,8,19} It was explained that dissolving a protein requires protein–protein interactions to be broken and replaced by stronger ones. Apparently, BMImNO₃ and similar ILs interact too strongly and cause, unlike water, the structure of the protein to be broken. Turner and coworkers²⁰ reported that incorporation of a hydroxyl-functionality in the cation of an imidazolium based IL caused some modifications in the behavior of the ILs that may be advantageous for stabilizing proteins. The potential of the cation HOPMIm for dissolving enzymes without affecting their catalytic activity was demonstrated by Walker and Bruce.⁹ In the Laboratory of Biocatalysis and Organic Chemistry of the TUDelft (The Netherlands) the transesterification activity of enzyme dissolved in HOPMImNO₃ was studied in detail and turned out to work. High enantioselectivity was observed thus the transesterification activity remains and it is even enhanced.²¹

The main objective of this work was studying the solubility of CO₂ in solutions with different concentrations of CaL B in HOPMImNO₃. Experiments related to the stability of the enzyme dissolved in the IL and the recoverability of the IL have also been included. Triacetin tests showed that the reduction of the activity of the enzyme after a long time of storage was considerably small. NMR tests showed the stability of the IL and the enzyme after a long time. Recovery and purification of the IL was possible by precipitation of the enzyme using IPA as an anti-solvent.

Experimental

Synthesis of the ionic liquid 1-(1-hydroxypropyl)-3-methyl-imidazolium nitrate (HOPMImNO₃)

Materials: *N*-methylimidazole 99% purity from Aldrich, 1-chloro-3-propanol 99% purity and Dowex 1 × 8–200 anion-exchange resin from Acros Organics, NaNO₃ sodium nitrate pure from Riedels and NaCl from Baker.

Preparation. *N*-methylimidazole was reacted with an excess (2 : 3) of freshly distilled 1-chloro-3-propanol at 60 °C under a nitrogen atmosphere for 4 days. The excess of 1-chloro-3-propanol was removed by extracting 3 times with ethyl acetate. The remaining ethyl acetate was removed from the desired product with a rotary evaporator yielding a quantitative amount of 1-(1-hydroxypropyl)-3-methyl-imidazolium chloride (HOPMImCl). The next step was the ion exchange of the anion chloride by the anion nitrate using an exchanged column packed with 250 g of Dowex 1 × 8–200 anion-exchange resin. The column was previously flushed thoroughly with a 1 M NaNO₃ solution (1 L), then with Milli-Q water (1 L). HOPMImCl was dissolved in Milli-Q water (1 M; 400 mL), and the resulting solution was slowly run over and eluted with Milli-Q water (1 L). The eluted liquid was collected and concentrated under reduced pressure in a rotary evaporator. The residue was dried extensively under vacuum over phosphorous pentoxide. HOPMImNO₃ was obtained in near-quantitative yield as a colorless viscous liquid that also contained < 30 ppm Cl[−] according to the silver chromate test.

Preparation of the solution of dry enzyme solution in ionic liquid

The aqueous solution of the free enzyme *Candida Antarctica* Lipase B (CaL B) 525 L, provided by CLEA Technologies, was used. It was previously determined that 144 μL of the original solution of the enzyme corresponds to one unit of activity (U). The preparation procedure of the enzyme dissolved in the IL consists of the following steps: (1) Precipitation of a known volume of the commercial aqueous enzyme solution using acetone in a 1.5 mL reaction GC vial; (2) Drying the precipitated enzyme under vacuum in an exsiccator over P₂O₅. Once dried, the amount of enzyme precipitated is determined by weight. (3) Prior to use, the IL, preserved in an exsiccator under vacuum conditions in the presence of P₂O₅, is dried further in an oven at 90 °C and also under vacuum conditions. (4) A known amount of the dry HOPMImNO₃ is added to the dry enzyme. The dissolution of the enzyme is observed after about 30 min under vigorous shaking and heating between 45 and 60 °C. In order to avoid any loss of the activity of the enzyme, the prepared solution was stored in a refrigerator. The day before preparing the sample for the phase behaviour determination, the sample was stored in an exsiccator under vacuum conditions in the presence of P₂O₅. Between 15 and 30 min prior to the preparation of the sample, the solution is dried in the oven at 90 °C under vacuum.

Characterization of the ILs and enzymatic solutions

The water content in the IL and in the enzymatic solutions was determined periodically by Karl–Fisher moisture analysis

(Mettler DL35 Karl Fischer Titrator), and checked gravimetrically. Before preparing the enzymes solution the IL was dried in an oven under vacuum conditions until eliminating all the absorbed water. The last traces of water were eliminated in the Cailletet tube under high vacuum.

The structure of the cationic part of the IL was confirmed using ^1H NMR (300.2 MHz, D_2O , *t*-BuOH) (Batch 1): δ (ppm) 8.708 s1H (N-CH=N), 7.48; 7.42 d2H (CH=CH), 4.68 s1H (D_2O ; OH), 4.304; 4.28; 4.256 t2H ($\text{CH}_2\text{-CH}_2\text{OH}$), 3.88 s3 H ($\text{CH}_3\text{-N}$), 3.623; 3.603; 3.583 t2H (N- $\text{CH}_2\text{-CH}_2\text{-CH}_2\text{OH}$), 2.127; 2.107; 2.2.104; 2.083; 2.062; 2.060; 2.039 m2H ($-\text{CH}_2\text{-CH}_2\text{-CH}_2\text{OH}$); (Batch 2): δ (ppm) 8.69 s1H (N-CH=N), 7.462; 7.405 d2H (CH=CH), 4.666 s1H (D_2O ; OH), 4.286; 4.262; 4.239 t2H ($\text{CH}_2\text{-CH}_2\text{OH}$), 3.891 s3 H ($\text{CH}_3\text{-N}$), 3.618; 3.598; 3.577 t2H (N- $\text{CH}_2\text{-CH}_2\text{-CH}_2\text{OH}$), 2.106; 2.084; 2.062 t2H ($-\text{CH}_2\text{-CH}_2\text{-CH}_2\text{OH}$) and ^{13}C NMR (300.2 MHz, D_2O , *t*-BuOH) Batch 1): δ (ppm) 33.12; 37.16; 48.00; 59.45; 123.80; 125.13; 137.64; (Batch 2): δ (ppm) 31.95; 35.89; 46.73; 58.18; 122.53; 123.87; 136.37 in the Unity Inova 300 s of Varian.

The same technique has been used to determine the structure of the enzyme in the commercial aqueous solution. ^{13}C NMR (300.2 MHz, D_2O , *t*-BuOH): δ (ppm) 62.665; 62.737; 63.045; 69.881; 71.232; 71.353; 72.292; 73.149, and to determine the structure of the enzyme dissolved in the IL.

Proton and carbon NMR of an old and fresh solution of the enzyme in the IL were performed. ^1H NMR (300.2 MHz, D_2O , *t*-BuOH) (fresh solution): δ (ppm) 8.690 s1H (N-CH=N); 7.46; 7.41 d2H (CH=CH); 4.688 s1H (D_2O ; OH); 4.290; 4.266; 4.242 t2H ($\text{CH}_2\text{-CH}_2\text{OH}$); 3.864 s3 H ($\text{CH}_3\text{-N}$); 3.613; 3.593; 3.572 t2H (N- $\text{CH}_2\text{-CH}_2\text{-CH}_2\text{OH}$); 2.095; 2.092; 2.072; 2.048 m2H ($-\text{CH}_2\text{-CH}_2\text{-CH}_2\text{OH}$); (old solution): δ (ppm) 8.700 s1H (N-CH=N); 7.47; 7.42 d2H (CH=CH); 4.683 s1H (D_2O ; OH); 4.298; 4.274; 4.250 t2H ($\text{CH}_2\text{-CH}_2\text{OH}$); 3.874 s3 H ($\text{CH}_3\text{-N}$); 3.619; 3.599; 3.578 t2H; (N- $\text{CH}_2\text{-CH}_2\text{-CH}_2\text{OH}$); 2.102; 2.098; 2.078; 2.057; 2.054 m2H; ($-\text{CH}_2\text{-CH}_2\text{-CH}_2\text{OH}$) and ^{13}C NMR (300.2 MHz, D_2O , *t*-BuOH) (fresh solution): δ (ppm) 37.187; 48.011; 59.459; 64.111; 64.434; 71.238; 72.646; 73.689; 74.555; 123.832; 125.159; 137.65; (old solution): δ (ppm) 37.179; 48.003; 59.459; 64.038; 64.119; 64.442; 71.23; 72.67; 72.791; 73.698; 74.563; 123.816; 125.151; 137.65.

The obtained NMR spectra of the recovered IL by precipitation of the enzyme are the following. ^1H NMR (300.2 MHz, D_2O , *t*-BuOH) (solution 1): δ (ppm) 8.721 s1H (N-CH=N) 7.49; 7.43 d2H (CH=CH), 4.663 s1H (D_2O ; OH), 4.311; 4.287; 4.263 t2H ($\text{CH}_2\text{-CH}_2\text{OH}$), 3.883 s3 H ($\text{CH}_3\text{-N}$), 3.616; 3.596; 3.575 t2H, (N- $\text{CH}_2\text{-CH}_2\text{-CH}_2\text{OH}$), 2.123; 2.103; 2.1; 2.078; 2.058; 2.055 m2H ($-\text{CH}_2\text{-CH}_2\text{-CH}_2\text{OH}$), 1.129; 1.124; 1.108; 1.104 m2H; (solution 2): δ (ppm) 8.735 s1H (N-CH=N) 7.50; 7.45 d2H (CH=CH), 4.665 s1H (D_2O ; OH), 4.304; 4.28; 4.256 t2H ($\text{CH}_2\text{-CH}_2\text{OH}$), 3.862 s3 H ($\text{CH}_3\text{-N}$), 3.606; 3.585; 3.565 t2H (N- $\text{CH}_2\text{-CH}_2\text{-CH}_2\text{OH}$), 2.088; 2.065; 2.043 t2H ($-\text{CH}_2\text{-CH}_2\text{-CH}_2\text{OH}$) 1.126; 1.119; 1.105; 1.099 m2H and ^{13}C NMR (300.2 MHz, D_2O , *t*-BuOH) (solution 1): δ (ppm) 24.139; 32.027; 35.943; 46.784; 58.199; 62.915; 62.915; 63.247; 64.42; 69.962; 71.483; 71.628; 72.478; 73.368; 122.58; 123.915; 136.406; (solution 2): δ (ppm) 24.18; 32.076; 35.951; 46.8; 58.207; 64.388; 122.588; 123.923; 136.438.

Phase equilibrium measurements

For all the equilibrium measurements a Cailletet apparatus was used. A schematic representation of the Cailletet apparatus is given in Fig. 2. It operated according to the synthetic method used, *i.e.*, a sample of known overall composition was confined into the top of the Cailletet tube using mercury as a sealing and pressure transmitting fluid. The tube was placed in a stainless steel autoclave. Within the autoclave, the open end of the tube was always immersed in mercury separating the sample from the hydraulic oil. A hand screw pump outside the autoclave pressurized the system. A small steel ball inside the top of the tube allowed stirring of the sample magnetically. A pressure balance (Budenberg) in combination with a hand screw pump was used to measure pressures and to maintain a constant pressure (range = 0.35–14 MPa, accuracy = 0.005 MPa). The Cailletet tube was jacketed and water was applied as a thermostatic fluid. The thermometer used is a Pt100 with an accuracy of 0.01 K. A detailed description of the experimental facility and the experimental procedures as well can be found elsewhere.²²

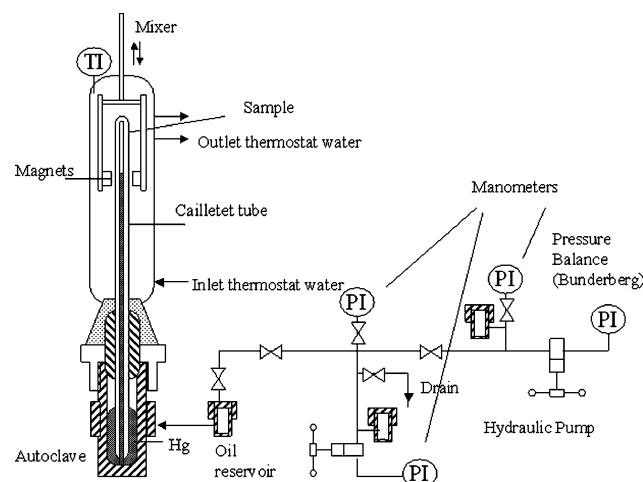


Fig. 2 Schematic representation of a Cailletet apparatus.

The measurements obtained from the Cailletet facility in this work comprise the determination of liquid–vapor two-phase boundaries. Therefore, first the temperature was set at a fixed value and the pressure was brought to a value where two phases, liquid and vapor, existed. Then the pressure was gradually increased until the vapor phase just disappeared. It was essential that after each change in the pressure, equilibrium between the coexisting phases is established. At the pressure where the vapor phase just disappeared a homogeneous liquid phase was obtained and consequently the composition of this liquid was the same as the original overall composition. A two-phase boundary point was obtained when a small change in pressure results in formation of a vapor phase or elimination of the existing vapor phase.

During the sample preparation, the top of the Cailletet tube was filled with a weighted amount of the enzymatic solution weighed (accuracy = 0.0001 g). In addition, it was heated with hot water (70 °C) under high vacuum conditions in order to degasify and eliminate traces of water. This procedure was repeated several times. The next step was addition of a known

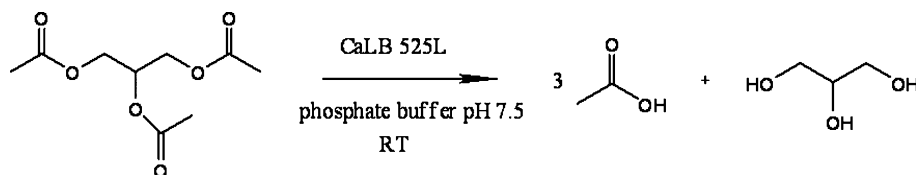


Fig. 3 Schematic representation of the triacetin reaction.

quantity of CO₂ into the top of the Cailletet tube. For that purpose, a known volume of 67.43 cm³ where temperature and pressure are measured was filled with a known quantity of CO₂ (highest dosing error = 0.01 cm Hg, temperature reading error = 0.1 K). Finally the Cailletet tube was removed from the gas-dosing apparatus and then mounted into the stainless steel autoclave.

CO₂ (99.995 vol%) was purchased from Hoek-Loos.

Activity assay for CaL B

Hydrolytic activity of CaL B 525 L towards 0.1 M triacetin (99% Acros Organics) (see reaction in Fig. 3) in sodium phosphate buffer 0.1 M at pH 7.5 was determined by titration of the formed acetic acid with 0.1 M sodium hydroxide as a function of time using DOSIMAT equipment with pH meter. The assay was performed in a volume of 10 mL.

Experimental results

Experimental data of the solubility of CO₂ in HOPMImNO₃-CaL B solutions

Bubble points for the binary systems CO₂ + HOPMImNO₃ + CaL B were determined for several CO₂ concentrations ranging from 5 to 20 mol% in a temperature region from 30 up to 75 °C, and applying pressures up to 12 MPa. Several CaL B concentrations were investigated. The CO₂ concentrations of the samples in the ternary systems were calculated on an enzyme-free basis and represented as compositions (X_i) defined in eqn (1).

$$X_i = \frac{n_{\text{CO}_2}}{n_{\text{CO}_2} + n_{\text{IL}}} \times 100 \quad (1)$$

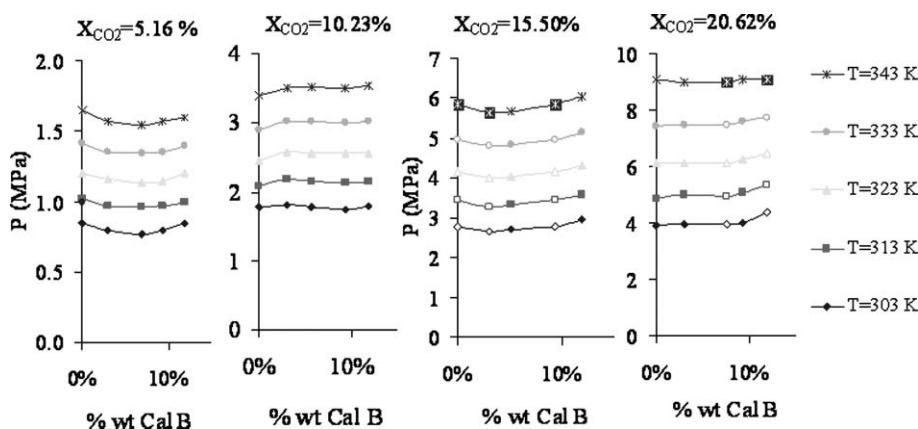


Fig. 4 Equilibrium bubble point pressures *versus* the CaL B concentration. Open symbols are interpolations. Data of the binary system CO₂ + HOPMImNO₃ are taken from Bermejo *et al.*¹⁸

Solutions of 0.5, 1, 1.5 and 2 units (U) enzyme per mL HOPMImNO₃ were studied. These solutions correspond to approximately 3, 6, 9 and 12% by weight of enzyme and approximately 40, 80, 128 and 171 mg mL⁻¹ IL. It should be noted that the solubilized amount of CaL B in the HOPMImNO₃ is higher than the reported solubilities of enzymes in other ILs. Madeira Lau *et al.*⁸ reported a solubility of 3 mg mL⁻¹ of CaL B in [Et₃MeN][MeSO₄]. Nakashima *et al.*¹⁰ reported a solubility of 40 mg mL⁻¹ of poly(ethylene glycol) modified subtilisin Carlsberg in EMImTf₂N (containing 2 mg mL⁻¹ of the enzyme).

The equilibrium data of the systems are summarized in Tables 1 to 4 in the ESI.† As usual in the systems CO₂ + IL, the equilibrium pressure of the bubble points increases with temperature and with CO₂ concentration as well.

In Fig. 4 the equilibrium pressure is plotted *versus* the CaL B concentration for a fixed CO₂ molar fraction in the IL on an enzyme-free basis. The data with a different concentration of CO₂ were interpolated and represented as open symbols. It can be observed that the equilibrium pressure remains almost unchanged with the enzyme concentration. The data of the binary system CO₂ + HOPMImNO₃ have been taken from Bermejo *et al.*¹⁸

Structure and aging of CaL B dissolved in the HOPMImNO₃. Preliminary study

This part of our study has been performed in order to understand the aging effect of both enzyme stored in hydrogen-bonding ionic liquids and the IL itself. The NMR spectra and the activity assay were performed in two solutions of 1.5 U mL⁻¹ HOPMImNO₃: a three months old sample and a freshly prepared equivalent solution. The first solution was three months old and it had

Table 1 Results of the activity assays performed with the original solution of the CaL B, and the two solutions in HOPMImNO₃ (freshly prepared and three months old). The activity is expressed in U mL⁻¹ of the commercial solution

Activity/U mL ⁻¹	50 μL	100 μL	Average	Loss of activity with respect to the free enzyme	Loss of activity with respect to the fresh solution
Free enzyme CaL B	98.4	121.8	110.1		
Fresh solution	71.8	70	70.9	-35.6%	
Old solution (3 months old)	60.4	51.9	56.15	-49.0%	-20.8%

been preserved in an exsiccator at vacuum conditions in the presence of P₂O₅ at room temperature.

Proton and carbon NMR of both solutions were performed and compared to that of the pure IL (see Experimental section). There were no differences in the spectra of the old and freshly prepared solution of the enzyme in the IL. The characteristic peaks of the IL (see Experimental section) were present and the new peaks, characteristic for the enzyme, were the same in both spectra and in the spectra of the commercial aqueous solution of the enzyme as well (see Experimental section). This indicates that aging for the IL does not occur and that the structure of the enzyme is the same for dissolving in HOPMImNO₃ as dissolving in water.

In addition, the enzyme activity in the two solutions was determined. Also the activity of the enzyme in the original commercial aqueous solution was evaluated. Double measurements were performed with each solution, for the equivalent of 50 μL and 100 μL of the original solution. The results are shown in Table 1. The enzyme, freshly dissolved in the HOPMImNO₃, lost 35% of its initial activity. Surprisingly, after three months of storing the solution, the enzyme maintained about 80% of its activity with respect to the fresh solution. This is an excellent result. This indicates that the enzyme stored in HOPMImNO₃ keeps its initial activity up to a very high percentage, which means that hydrogen bonding ILs stabilize the enzymes.

From the equilibrium point of view we assume that this minimal deactivation was the cause of the non-consistency in the equilibrium data. Thus, the new samples were preserved in the fridge to minimize any deactivation and prolonged the reasonable activity of the solution. Using all precautions no more inconsistencies were observed.

Recovery and purification of the IL

It has been shown that 525 L CaL B can remain active for a long period of time when dissolved in HOPMImNO₃. However we assume that the loss of activity will occur within a longer timeframe. Therefore, another interest was to recover both the enzyme and the pure IL. In this study, we would like to present a simple and efficient separation procedure. First the enzyme was precipitated from the HOPMImNO₃ using IPA as an anti-solvent, and this was at least repeated three times. After the precipitation the mixture has to be centrifuged to have a good separation of the enzyme. Remaining IPA in the IL solution was evaporated under reduced pressure. We have applied this procedure to two enzymatic solutions. Solution 1: 1.5 U mL⁻¹ (9.30 wt% CaL B), 41 days old. Solution 2: 0.5 U mL⁻¹ (3.03 wt% CaL B), 25 days old.

The obtained NMR spectra of the recovered IL according to this procedure (see Experimental section) have been compared

to those of pure HOPMImNO₃ and also with that of the starting enzymatic solution. We observed that in solution 2 all the characteristic peaks of the enzyme had disappeared, but in the solution 1 some traces of the enzyme could still be identified. Traces of IPA were still present in both of them. However, IPA can be easily eliminated by further vacuum distillation. In conclusion we observe that the NMR of solutions 1 and 2 are almost identical and this provides us with the information that the IL has been recovered with nearly 100% purity.

Conclusions

Some preliminary aspects for developing an enzymatic reaction/separation process using the IL HOPMImNO₃ have been studied. The phase equilibria of the system CO₂ + HOPMImNO₃ + CaL B have been studied experimentally. It was observed that the equilibrium pressure of the bubble points of the system is essentially unchanged with the concentration of the enzyme.

HOPMImNO₃ is able to solubilize a much larger amount of enzyme than the amount of enzyme solubilised by other ILs in the literature.

¹³C and ¹H NMR tests reveal that the IL does not present degradation when CaL B is dissolved in it. Furthermore, it was found that the structure of the enzyme dissolved in HOPMImNO₃ is the same as the structure of the enzyme dissolved in water.

The activity assays performed in aged solutions of CaL B in HOPMImNO₃ show that the activity of the enzyme dissolved in the IL maintains 80% of its activity compared to a fresh solution after three months of room temperature storage. This reveals that this IL is very appropriate for the preservation of enzymes.

All results presented in this study look very promising for the development of an enzymatic process using the ionic liquid HOPMImNO₃.

Acknowledgements

M.D.B. wants to thank the Secretaría de Estado de Universidades e Investigación, Ministerio de Educación y Ciencia (Spain) for financing her postdoctoral grant.

References

- 1 F. van Rantwijk and R. A. Sheldon, *Chem. Rev.*, 2007, **107**, 2757–2785.
- 2 M. Erbedinger, M. Mesiano and A. J. Russel, *Biotechnol. Prog.*, 2000, **16**, 1129–1131; R. Madeira Lau, F. van Rantwijk, K. R. Seddon and R. A. Sheldon, *Org. Lett.*, 2000, **2**, 4189–4191; S. H. Schofer, N. Kaftzik, P. Wasserscheid and U. Kragl, *Chem. Commun.*, 2001, 425–426; T. Itoh, E. Akasaki, K. Kudo and S. Shirakami, *Chem. Lett.*,

- 2001, 262–263; S. Park and R. J. Kazlauskas, *J. Org. Chem.*, 2001, **66**, 8395–8401; K.-W. Kim, B. Song, M.-Y. Choi and M.-J. Kim, *Org. Lett.*, 2001, **3**, 1507–1509; H. Zhao and S. V. Malhotra, *Biotechnol. Lett.*, 2002, **24**, 1257–1260; R. Bogel-Lukasik, N. M. T. Lourenco, P. Vidinha, M. D. R. Gomes da Silva, C. A. M. Afonso, M. Nunes da Ponte and S. Barreiros, *Green Chem.*, 2008, **10**, 243–248; Y. H. Moon, S. M. Lee, S. H. Ha, Y.-M. Koo and J. Korean, *Chem. Eng.*, 2006, **23**, 247–263.
- 3 R. A. Sheldon, R. Madeira Lau, M. J. Sorgedragger, F. van Rantwijk and K. R. Seddon, *Green Chem.*, 2002, **4**, 147–151.
- 4 C. M. Gordon, *Appl. Catal., A*, 2001, **222**, 101–117; U. Kragl, M. Eckstein and N. Kaftzik, *Curr. Opin. Biotechnol.*, 2002, **13**, 565–571; R. A. Sheldon, R. M. Lau, M. J. Sorgedragger, F. van Rantwijk and K. R. Seddon, *Green Chem.*, 2002, **4**, 147–151; S. Park and R. J. Kazlauskas, *Curr. Opin. Biotechnol.*, 2003, **14**, 432–437; Z. Yang and W. Pan, *Enzyme Microb. Technol.*, 2005, **37**, 19–28; F. Van Rantwijk, R. Madeira Lau and R. A. Sheldon, *Trends Biotechnol.*, 2003, **21**, 131–138; R. Bogel-Lukasik, *Monatsh. Chem.*, 2007, **138**, 1137–1144.
- 5 P. Lozano, T. De Diego, S. Gmouh, M. Vaultier and J. L. Iborra, *Biocatal. Biotransform.*, 2005, **23**, 169–176.
- 6 M. Mori, R. Gomez Garcia, M. P. Belleville, D. Paolucci-Jeanjean, J. Sanchez, P. Lozano, M. Vaultier and G. Rios, *Catal. Today*, 2005, **104**, 313–317; S. H. Lee, T. T. N. Doan, S. H. Ha and Y.-M. Koo, *J. Mol. Catal. B: Enzym.*, 2007, **45**, 57–61; Y. Liu, L. Shi, M. Wang, Z. Li, H. Liu and J. Li, *Green Chem.*, 2005, **7**, 655–658; Y. Liu, M. Wang, J. Li, Z. Li, P. He, H. Liu and J. Li, *Chem. Commun.*, 2005, 1778–1780; P. Lozano, T. De Diego, T. Sauer, M. Vaultier, S. Gmouh and J. L. Iborra, *J. Supercrit. Fluids*, 2007, **40**, 93–100; L. Mantarosie, S. Coman and V. I. Parvulescu, *J. Mol. Catal. A: Chem.*, 2008, **279**, 223–229.
- 7 K. Nakashima, T. Maruyama, N. Kamiya and M. Goto, *Chem. Commun.*, 2005, 4297–4299; K. Nakashima, J. Okada, T. Maruyama, N. Kamiya and M. Goto, *Sci. & Tech Adv.*, 2006, **7**, 3462–3467.
- 8 R. Madeira Lau, M. J. Sorgedragger, G. Carrea, F. van Rantwijk, F. Secundo and R. A. Sheldon, *Green Chem.*, 2004, **6**, 487–487.
- 9 A. J. Walker and N. C. Bruce, *Chem. Commun.*, 2004, 2570–2571; A. J. Walker and N. C. Bruce, *Tetrahedron*, 2004, **60**, 561–568; A. J. Walker and N. C. Bruce, *Chem. Commun.*, 2004, 2570–2571.
- 10 K. Nakashima, T. Maruyama, N. Kamiya and M. Goto, *Org. Biomol. Chem.*, 2006, **4**, 3462–3467.
- 11 L. A. Blanchard, D. Hancu, E. J. Beckman and J. F. Brennecke, *Nature*, 1999, **399**, 28–29; L. A. Blanchard and J. F. Brennecke, *Ind. Eng. Chem. Res.*, 2001, **40**, 287–292; M. C. Kroon, J. van Spronsen, C. J. Peters, R. A. Sheldon and G. Witkamp, *Green Chem.*, 2006, **8**, 246–249; E. M. Saurer, S. N. V. K. Aki and J. F. Brennecke, *Green Chem.*, 2006, **8**, 141–143.
- 12 A. M. Scurto, S. N. V. K. Aki and J. F. Brennecke, *Chem. Commun.*, 2003, 572–573; V. Najdanovic-Visak, A. Serbanovic, J. M. S. S. Esperanca, H. J. R. Guedes, L. P. N. Rebelo and M. N. da Ponte, *ChemPhysChem*, 2003, **4**, 520–522; A. M. Scurto, S. N. V. K. Aki and J. F. Brennecke, *J. Am. Chem. Soc.*, 2002, **124**, 10276–10277.
- 13 C. J. Peters and K. Gauter, *Chem. Rev.*, 1999, **99**, 419–431; K. Gauter, C. J. Peters, A. L. Scheidgen and G. M. Schneider, *Fluid Phase Equilib.*, 2000, **171**, 127–149.
- 14 P. Lozano, T. de Diego, D. Carrié, M. Vaultier and J. L. Iborra, *Chem. Commun.*, 2002, 692–693; P. Lozano, T. De Diego, D. Carrié, M. Vaultier and J. L. Iborra, *Biotechnol. Prog.*, 2003, **19**, 380–382.
- 15 M. T. Reetz, W. Wiesenhöferm, G. Franciò and W. Leitner, *Chem. Commun.*, 2002, 992–993.
- 16 R. Madeira Lau, F. van Rantwijk, K. R. Seddon and R. A. Sheldon, *Org. Lett.*, 2000, **2**, 4189–4191; S. H. Schofer, N. Kaftzik, P. Wasserscheid and U. Kragl, *Chem. Commun.*, 2001, 425–426.
- 17 K. R. Seddon, A. Stark and M. J. Torres, *ACS Symp. Ser.*, 2002, **819**, 34–49; J. S. Wilkes and M. J. Zaworotko, *Chem. Commun.*, 1992, 965–967; K. R. Seddon, A. Stark and M. J. Torres, *Pure Appl. Chem.*, 2000, **72**, 2275–2287; L. Cammarata, S. G. Kazarian, P. A. Salter and T. Welton, *Phys. Chem. Chem. Phys.*, 2001, **3**, 5192–5200; S. N. V. K. Aki, B. R. Mellein, E. M. Saurer and J. F. Brennecke, *J. Phys. Chem. B*, 2004, **108**, 20355–20365; A. Chowdhury and S. T. Thynell, *Thermochim. Acta*, 2006, **443**, 159–172.
- 18 M. D. Bermejo, M. Montero, E. Saez, L. J. Florusse, A. J. Kotlewska, M. J. Cocero, F. van Rantwijk, C. J. Peters, *Proceedings of the V International Symposium on High Pressure Processes Technology and Chemical Engineering*, Segovia, 2007.
- 19 F. van Rantwijk, F. Secundo and R. A. Sheldon, *Green Chem.*, 2006, **8**, 282–286.
- 20 M. B. Turner, J. D. Holbrey, S. K. Spear, M. L. Pusey and R. D. Rogers, *ACS Symp. Ser.*, 2005, **902**, 233–243; J. D. Holbrey, M. B. Turner, W. M. Reichert and R. D. Rogers, *Green Chem.*, 2003, **5**, 731–736.
- 21 F. van Rantwijk, personal communication.
- 22 S. Raeissi and C. J. Peters, *J. Supercrit. Fluids*, 2001, **20**, 221–228; E. Kuhne, C. J. Peters, J. van Spronsen and G. J. Witkamp, *Green Chem.*, 2006, **8**, 287–291.

Supported phosphine-free palladium catalysts for the Suzuki–Miyaura reaction in aqueous media

Nam T. S. Phan and Peter Styring*

Received 28th March 2008, Accepted 7th July 2008

First published as an Advance Article on the web 14th August 2008

DOI: 10.1039/b805290e

The Suzuki–Miyaura reaction has been performed using a non-symmetrical salen-type palladium(II) catalyst that is readily immobilized onto Merrifield resin and functionalized silica. The catalysts combine high activity with the recoverability and reusability offered by a heterogeneous system, without the need for phosphine ligands or additives. The high content of water used in the reaction, which is more than 96% by volume, represents a green process that should have advantages for industrial applications. Leaching of the metal into solution from the supported catalyst proved to be negligible.

Introduction

The importance of biaryl units as components of many kinds of compounds, such as pharmaceuticals, herbicides and natural products; as well as in the field of engineering materials, such as conducting polymers, molecular wires and liquid crystals, has attracted enormous interest from the chemistry community.¹ The Suzuki–Miyaura cross-coupling reaction is proving to be an increasingly popular method for the construction of unsymmetrical biaryl compounds as it represents an attractive alternative over other methods using organometallics because organoboranes are air- and moisture-stable with relatively low toxicity.² Catalysts used in the reaction process are generally based on homogenous palladium-phosphine complexes or nitrogen-containing palladocycles, which are rarely recoverable without elaborate and wasteful procedures, and therefore commercially uneconomic.³ Moreover, phosphine ligands are expensive, toxic and in large-scale applications the phosphines may be a more serious economical burden than even the metal itself.⁴ In recent years there has been an increasing interest in developing greener processes. In this context, heterogeneous catalysis is emerging as an alternative to homogeneous processes so that catalysts can be recovered and reused several times before they deactivate completely. At the same time, the catalyst recovery also decreases the contamination of the desired products with hazardous or unhealthy compounds, and also environmental pollution caused by residual toxic metals can be reduced. However, heterogeneous catalysts normally suffer from limited mass transfer, low specificity and selectivity and leaching of the catalytic species from the surface of the support.⁵

Water, being cheap, readily available, non-toxic and non-flammable has clear advantages over common organic solvents in synthetic chemistry.⁶ However, problems with the use of water, such as solubility of the substrates and stability of the metal catalysts in aqueous solution remains to be improved.

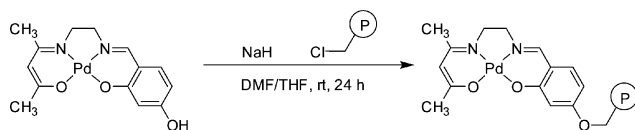
These problems have to some extent been overcome by the use of phase-transfer catalysts. There have been a number of reports of the palladium-mediated Suzuki–Miyaura reaction being performed using water as a solvent, which relate to the coupling of aryl boronic acids with aryl iodides or activated bromides.^{7,8} Microwave heating has also been used to facilitate the Suzuki reaction in pure water above its boiling point in sealed vessels.^{9,10} To date the Suzuki reaction in water has, in most cases, been limited to homogeneous palladium catalysts, with the exception of a few examples of heterogeneous catalysts such as palladium immobilized on carbon and a PEG-PS resin-supported triarylphosphine-palladium complex.^{11,12}

We have previously reported the synthesis and characterization of an unsymmetrical salen-type palladium(II) complex and its immobilization onto Merrifield resin and functionalized silica and its activity in the Heck¹³ and Suzuki–Miyaura¹⁴ reactions in conventional organic solvents. The supported catalyst was air- and moisture-stable, and could be reused several times without a significant degradation in catalytic activity. We herein report for the first time, to our best knowledge, the use of the supported salen-type palladium complex as an effective catalyst for the Suzuki reaction using a 30 : 1 water/toluene mixture as a solvent system without any added phosphine. The high content of water in the procedure, which is more than 96% by volume, and the fact that the catalyst can be easily recovered and reused with minimal palladium leaching into solution, are therefore very effective in terms of practical application and operational safety.

Results and discussion

The Merrifield resin and silica supported salen-type palladium catalysts were prepared according to the procedures reported previously (Scheme 1).^{13–15} Inductively coupled plasma-atomic emission spectroscopy (ICP-AES) measurements showed there to be *ca.* 2% (wt/wt) palladium on the Merrifield beads, corresponding to a catalyst loading of 0.2 mmol palladium per g of resin and *ca.* 1% (wt/wt) palladium on the silica, corresponding to a catalyst loading of 0.1 mmol palladium per g of silica. The intractable nature of the resin and the

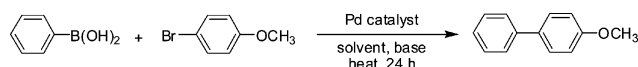
Department of Chemical and Process Engineering, The University of Sheffield, Mappin Street, Sheffield, UK S1 3JD.
E-mail: p.styring@sheffield.ac.uk



Scheme 1 The immobilization of the salen-type palladium(II) complex.

silica, and the low loading of the catalyst made it impossible to obtain meaningful data from infrared analysis. Therefore, proof that the palladium complex is covalently immobilised to the solid supports comes from the ICP-AES analysis of the supported catalysts and the crude reaction solutions, which showed very little, if any, leaching of the metal into solution from the supported catalyst during the course of a reaction.

The palladium resin catalyst was initially assessed for its activity in the Suzuki–Miyaura reaction initially by studying the coupling of 4-bromoanisole with phenylboronic acid to form 4-methoxybiphenyl as the sole product (Scheme 2). The reaction was carried out using 0.5 mol% palladium catalyst relative to 4-bromoanisole, a 20 : 1 water/toluene mixture as the reaction solvent system and K_3PO_4 as a base at 100 °C for 24 h under a nitrogen atmosphere. Precipitation of the product occurred during the course of the reaction because of the high concentration of water in the system. After cooling the mixture, the organic components were extracted into diethyl ether and analyzed by GC and GC-MS. It should be noted that the ether extraction step is only required on the analytical scale for the preparation of diluted samples for GC analysis and that this step is omitted in the preparative syntheses. It was found that the reaction was close to completion with 4-methoxybiphenyl being formed in 98% yield. The absence of phosphines in the system not only reduces process costs but also eliminates side reactions that may occur between the phosphines and phenylboronic acid.¹⁶ Furthermore, it also removes a process step required to separate out the phosphine at the end of the reaction, and also reduces waste. The reaction conditions were then optimized in respect of conversion and the results are shown in Table 1.



Scheme 2 The Suzuki reaction of 4-bromoanisole and phenylboronic acid.

Initial studies addressed the water to toluene ratio in order to increase the amount of water in the system, having studied reactions with various water/toluene ratios from 20 : 1 to pure water. The optimum ratio in the system was found to be 30 : 1 with a 4-methoxybiphenyl yield of 98% by GC, which means only 3.3% (v/v) of the reaction solvent is toluene. Increasing the toluene concentration was unnecessary as the conversion to the principal product, 4-methoxybiphenyl, did not increase any further and decreasing the concentration to below 3.3% resulted in a drop in the conversion. Therefore, it was decided to use a water/toluene ratio of 30 : 1 in further studies. Although the toluene amount used in the solvent mixture was very low compared to the water, it played a crucial role in the system since the reaction using pure water as a solvent was far from complete, resulting in only 10% conversion of 4-bromoanisole to 4-methoxybiphenyl being achieved. The fact that any reaction

Table 1 Study of the Suzuki reaction using 0.5 mol% palladium resin catalyst, 1.5 eq. $PhB(OH)_2$, 3 eq. K_3PO_4 in water/toluene under a nitrogen atmosphere (based on GC data)

Conditions: 100 °C, 24 h

Water/toluene ratio	Conversion (%)
20 : 1	98
30 : 1	98
40 : 1	90
50 : 1	41
60 : 1	14
75 : 1	10
Pure water	10

Conditions: water/toluene of 30 : 1, 24 h

Temperature/°C	Conversion (%)
100	98
90	98
80	90
70	76
60	69

Conditions: water/toluene of 30 : 1, 90 °C

Time/h	Conversion (%)
2	23
4	30
6	55
10.5	83
24	98

Conditions: 90 °C, water/toluene of 30 : 1, 24 h

Run	Conversion (%)
1	98
2	90
3	81
4	80
5	74

at all was achieved in this non-activated system was, however, remarkable in itself. The effect of temperature on the reaction was also taken into account, having studied reaction at temperatures in the range 60–100 °C. It was shown that at 90 °C the most efficient conversion was achieved, although 4-methoxybiphenyl was still formed in a yield of up to 90% at 80 °C. We therefore decided to carry out a kinetic study of the reaction at 90 °C. A plot of $-\ln(1-x)$ against reaction time (Fig. 1), where x is the mole fraction of 4-bromoanisole consumed or 4-methoxybiphenyl produced, indicates the reaction to be pseudo first order overall with an observed rate constant of $5 \times 10^{-5} \text{ s}^{-1}$. This is identical to the results obtained for the same catalyst under the same conditions in organic solvents such as DMF (also $5 \times 10^{-5} \text{ s}^{-1}$).¹⁷ The activation energy for the catalysed reaction was calculated over the range 60–90 °C and found to be 16 kJ mol⁻¹. For the same catalyst in the same reaction but carried out in 1,2-dimethoxyethane-water, the activation energy was calculated as 30 kJ mol⁻¹ and 17 kJ mol⁻¹ in DMF. This compares well with heterogeneous palladium (from $PdCl_2$) on a hydrotalcite catalyst (47 kJ mol⁻¹).¹⁸ For a homogeneous palladium acetate/1,3-pentadieneone catalyst the activation energy was found to

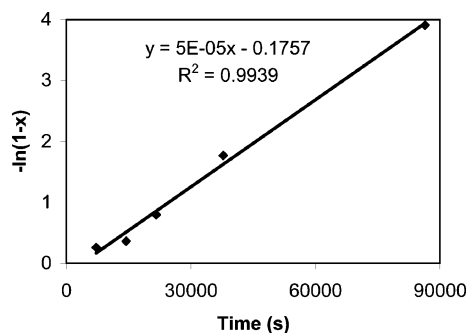


Fig. 1 Kinetic data for the Suzuki reaction of 4-bromoanisole with phenylboronic acid using the palladium resin catalyst at 90 °C over 24 h.

be 4–5 kJ mol⁻¹.¹⁹ The fact that our system falls between the two extremes of totally homogeneous and conventional heterogeneous catalysts supports our theory²⁰ that the properties of the catalyst lies between the two extremes ('androgynous' or 'androgenous') because it is a homogeneous catalyst covalently tethered to a heterogeneous support.

An important point concerning the use of heterogeneous catalysts is its lifetime, particularly for the industrial and pharmaceutical applications of cross-coupling reactions.²¹ The polymer supported catalyst was therefore tested for recoverability and reusability. After each run, the original palladium resin was filtered off, washed several times with THF and water to remove any excess reagents and reused under the same reaction conditions as for the initial run without any regeneration. Results in Table 1 show that the palladium resin catalyst can be recovered and reused in further reactions without a significant degradation in activity. Although the catalytic activity gradually diminished, a conversion of over 70% was still achieved in the fifth run. Subsequent treatment of the catalyst by stirring in boiling water was found to remove organic salts and restore conversion back to around 90%. The leaching of active species from heterogeneous catalysts into solution is also a crucial issue as demonstrated in a review from the Jones group.²² In order to determine the absolute amount of palladium leached into the reaction solution, if any, the catalyst was removed by hot filtration, and the solutions were analyzed using ICP-AES. The amount of palladium in solution was found to be *ca.* 1 ppb indicating low palladium leaching from the catalyst during the course of the reaction. The low level is due to the ligand design which possesses an N₂O₂ donor set which in turn provides two different pincer mechanisms. This makes the catalyst more stable than typical organometallic catalysts where C–M bond fission can result in leaching. This negligible leaching level observed accounts for the recoverability and reusability of the supported catalysts. To demonstrate that a homogeneous reaction through palladium leaching and potential reattachment is not an issue, the reaction was carried out over an initial 2 h period under normal conditions and conversion was monitored by GC. After this period the catalyst particles were removed by hot filtration and the filtrate returned to the reaction vessel. Conversion at this stage was determined to be 8%. Stirring was continued for a further 24 h in the absence of the catalyst but no further increase in conversion was observed. The original catalyst was then reintroduced into the reaction vessel and stirring continued for a further 24 h, monitored by GC analysis. Normal catalytic

behaviour was observed, thereafter, to reach 98% conversion at the end of the process. This clearly demonstrates that the palladium remains on the support and homogeneous catalysis does not occur. Full details of the procedure was initially reported by us for the same catalyst in the Heck reaction.¹³

While the Merrifield resin-supported palladium catalyst exhibited high activity in the Suzuki reaction using the water/toluene (30 : 1) system, the analogous functionalized silica-supported palladium catalyst was found to be less active with only 78% conversion being achieved. It was observed that the silica catalyst was agglomerated during the course of the reaction while it was expected to suspend well in the reaction solvent. We found that using a catalytic amount (5 mol%) of benzyltributylammonium chloride as a phase transfer catalyst (PTC) increased the yield of 4-methoxybiphenyl from 78% to 86% as shown in Table 2. Increasing the PTC concentration was found to improve the reaction close to completion, with the conversion comparable to that of the analogous palladium resin-catalyzed coupling reaction. Interestingly, the presence of the PTC was shown to have no apparent effect on the Suzuki–Miyaura reaction using the palladium resin catalyst in water/toluene (30 : 1), in terms of the yield of 4-methoxybiphenyl being achieved. Indeed, the use of the PTC is essential for the reaction using water-insoluble aryl halides when neat water is used as reaction solvent.⁸ While we did not determine the activation energy in this system, the kinetics were slightly slower than in the case of the resin immobilised catalyst, however, the system was more complex. For the complex tethered to silica, the rate constant was found to be $9.5 \times 10^{-6} \text{ s}^{-1}$ at 90 °C, compared to $5 \times 10^{-5} \text{ s}^{-1}$ for the resin supported complex and $6 \times 10^{-6} \text{ s}^{-1}$ for the complex directly attached to the silica surface without a hydrocarbon tether. One major problem is that any added PTCs need to be removed at the end of the reaction and this adds complexity to the separation process, especially if it needs to be recovered and reused. However, Uozumi *et al.* previously reported the high activity of PEG-PS resin-supported triarylphosphine-palladium complex in the Suzuki–Miyaura reaction of water-insoluble aryl halides in neat water without the use of any PTC.¹²

The function of toluene and PTC in the system still remains unresolved at the present time. It was initially presumed that one key role of toluene in the reaction using the palladium resin catalyst was to swell the Merrifield resin support. Indeed, swelling is an essential feature of gel resins, as it increases the internal flexibility of the polymer backbone which can move to maximize the available functionality as well as permitting

Table 2 Study of the effect of phase transfer catalyst (PTC) loading on the Suzuki reaction using 0.5 mol% palladium catalyst, 1.5 eq. Ph(OH)₂, 3 eq. K₃PO₄ in water/toluene (30 : 1) at 90 °C for 24 h under a nitrogen atmosphere (based on GC data)

PTC loading (mol%)	Palladium resin 4-methoxybiphenyl (%)	Palladium silica 4-methoxybiphenyl (%)
0	98	78
5	98	86
10	98	92
15	98	94
20	99	94
50	96	96

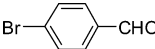
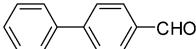
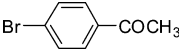


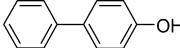
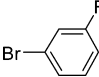
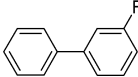
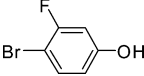
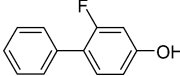
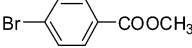
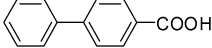
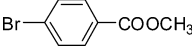
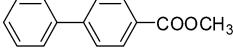

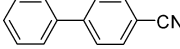
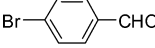
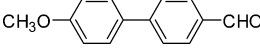
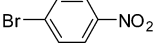
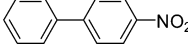
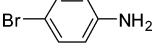
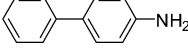
free diffusion of reagents into the bead.²³ It is also important to note that in gelatinous resins, up to 99% of the reactive sites are located inside the bead and only 0.1–1% on the outer surface shell.²⁴ However, we found that it was also necessary to use toluene in the reaction using the non-swelling palladium silica catalyst, as the reaction in pure water with 20 mol% PTC gave only 55% conversion while the analogous reaction in water/toluene (30 : 1) yielded 94% 4-methoxybiphenyl (Table 2). This means that the toluene is also crucial for the solubility of substrates and the phase-transfer mediating process. However, a complete reaction pathway as well as the function of toluene and the PTC in the system still remains to be elucidated.

The study was then extended to several substituted bromobenzenes containing both electron-withdrawing and electron-donating groups using the palladium resin catalyst, in order to test the tolerance of functional groups in aqueous media. Very good to excellent yields of biphenyls were achieved in most cases, as shown in Table 3. It was shown that this coupling reaction was applicable to aryl bromides substituted with various functional groups in aqueous media. The Suzuki–Miyaura reaction of 4-bromobenzaldehyde (entry 1) and 4-bromoacetophenone

(entry 2) proceeded without difficulty, 100% yield being achieved. K_2CO_3 was used instead of K_3PO_4 for base-sensitive groups such as the ester (entry 7) and cyano (entry 8) groups. The coupling of methyl 4-bromobenzoate was accompanied by complete ester hydrolysis in the presence of K_3PO_4 yielding the corresponding carboxylic acid (entry 6), while the ester function survived the reaction when the less basic K_2CO_3 was employed instead. This is a useful feature of the reaction as it can be used to form biaryl derivatives with the option of either retaining the ester protecting group or completely deprotecting to yield the free carboxylic acid in a single step, simply by changing the added base. A favorable effect of electron-withdrawing substituents is normally observed in palladium-catalyzed coupling reactions.²⁵ However, the Suzuki–Miyaura reaction of 4-bromonitrobenzene (entry 10) failed with the coupling product being detected only in trace amounts, despite the fact that the nitro group is strongly electron-withdrawing. All attempts to carry out the reaction of 4-bromoaniline (entry 11) were also unsuccessful. This strange behaviour of the system needs further study as it cannot be explained at present.

We were keen to develop the methodology for the preparation of a larger amount of material using the aqueous

Table 3 The Suzuki reactions of substituted bromobenzenes using 0.5 mol% palladium resin catalyst, 1.5 eq. $PhB(OH)_2$, 3 eq. K_3PO_4 in water/toluene (30 : 1) at 90 °C for 24 h under a nitrogen atmosphere (based on GC-MS data)

Entry	Substrate	Product	Conversion (%)
1			100
2			100
3			91
4			92
5			79
6			100
7			96 ^a
8			100 ^a
9			100 ^b
10			trace
11			0

^a K_2CO_3 was used instead of K_3PO_4 . ^b 4-Methoxybenzeneboronic acid was used instead of benzeneboronic acid.

Suzuki–Miyaura reaction. All studies discussed so far were carried out on a small scale, using a Radley's Carousel Synthesizer, adequate for work-up for GC analysis. As a starting point for the 10 times scale-up of the reaction from 0.25 to 2.5 mmol, the reaction of 4-bromoacetophenone with phenylboronic acid to form 4-acetylbiphenyl was considered. Decreasing the ratio of phenylboronic acid to 4-bromoacetophenone from 1.5 : 1 to 1.1 : 1 could still be tolerated with 100% conversion being achieved, while the equimolar reaction afforded 98% conversion. Therefore, a 1.1 : 1 substrate ratio was used for the scale-up reaction. It was found that the coupling product could be isolated without an extraction step, which always involves the use of an organic solvent. The absence of an organic solvent in the separation step is therefore a major advantage of the process. The product precipitate was separated from the palladium resin using a 125 μm sieve, followed by simple filtration through a 0.45 μm nylon membrane, followed by a number of thorough washes with hot water. The coupling product was isolated in 85% yield. No trace of 4-bromoacetophenone could be detected by GC-MS, however 3% phenylboronic anhydride was produced from the excess phenylboronic acid in the process, giving the product a purity of 97%. It was found that washing the product with an aqueous solution of NaOH removed the excess boronic acid/anhydride to produce the boronate salt. As this was the active species it could then be recycled into subsequent reactions, thereby enhancing the efficiency of the reaction process. No trace of the anhydride was detected by GC-MS in the isolated product. On separation, the product was found to have 100% purity by GC analysis. The structure of the product was then confirmed by its ^1H and ^{13}C NMR spectra and CHN analysis, which were consistent with literature data.²⁶ Furthermore, ICP-AES analysis revealed no palladium in the product and NMR showed there to be no toluene. When the process is considered as a whole to include the aqueous washes, the green credentials are further enhanced with only 1.1% organic solvent by volume being used in total: therefore the process is effectively 98.9% aqueous. The waste water could be recycled a number of times as it contains unreacted boronate salts and minimal amounts of toluene which tend to remain incorporated in the resin matrix. Any toluene remaining in the water can be removed by rotary evaporation.

Experimental

Chemicals were obtained from Aldrich and Fisher and used as received. The unsymmetrical salen-type palladium (II) complex was synthesized and characterized according to the previously published method.^{13,14} NMR spectra were recorded using a Bruker AC250 spectrometer (^1H , 250.1 MHz; ^{13}C , 62.9 MHz). ^1H and ^{13}C chemical shifts were referenced to solvent resonances. Microanalyses were performed by Alan Jones in the Department of Chemistry at the University of Sheffield, ICP-AES analyses were performed on a Spectro Ciros^{CCD} instrument (Spectro Analytical, UK). GC-MS analyses were performed using a Perkin Elmer GC-MS with a 30 m \times 0.25 mm \times 0.25 μm Phenomenex-2B5 column. The temperature program was 60–260 $^\circ\text{C}$ at 10 $^\circ\text{C}$ min⁻¹ with a final temperature isothermal hold for 10 min. The MS mass limit was set between 50 and 450 Da.

Immobilised catalyst preparation

A yellow solution of palladium complex (0.10 g, 0.27 mmol) in dry DMF (20 ml) and THF (10 ml) was added dropwise at room temperature to a dispersion of excess 60% sodium hydride in mineral oil (0.03 g, 0.75 mmol) and the resulting mixture stirred for 10 min. A suspension of Merrifield resin (1 g, 1.7 mmol Cl per g, 1.7 mmol) that had been pre-swelled in DMF (10 ml) for 30 min was then added and the mixture stirred gently at room temperature overnight. The initially white Merrifield resin beads became yellow in color and the solution turned pale yellow. The beads were filtered off, washed several times with water (3 \times 50 ml), soaked in DMF (50 ml) overnight and then triturated for a total of 12 h with DMF (3 \times 50 ml) and THF (3 \times 10 ml) to remove any physically adsorbed palladium complex. The resulting yellow beads were air-dried to yield 1.0 g of the supported complex. The palladium immobilized on silica was prepared using a similar procedure.

ICP analysis of the supported catalysts

ICP-AES was used to determine the palladium concentration on the beads. Calibration against a palladium standard and a blank was linear, using 2% nitric acid solutions containing 0, 1, 5 and 10 ppm palladium made from 1000 ppm stock solution (Aristar). Weighed samples (20.0 mg) of the palladium resin and palladium silica catalyst were placed in glass tubes and digested at 180 $^\circ\text{C}$ in a mixture of concentrated nitric acid (5 cm³, Aristar) and concentrated perchloric acid (0.5 cm³, Aristar). For each catalyst, 3 parallel samples were digested over 2 h, 4 h and 6 h, respectively. The yellow palladium resin and palladium silica catalyst became a white residue after digestion. The digest was then diluted to 50 cm³ with water. Analysis showed that all the metal was removed from the support within 2 h as increasing the digestion time to 4 h and 6 h achieved no increase in the amount of the metal in the digest. The analyses showed there to be *ca.* 2% (wt/wt) palladium on the Merrifield beads, corresponding to a catalyst loading of 0.2 mmol palladium per g of resin and *ca.* 1% (wt/wt) palladium on the silica, corresponding to a catalyst loading of 0.1 mmol palladium per g of silica.

Catalyst testing

Catalytic reactions were performed using a 12-position Radley's Carousel Parallel Synthesiser fitted with a fuzzy logic controller unit giving temperature control to ± 0.1 $^\circ\text{C}$. Unless otherwise stated, a mixture of 4-bromoanisole (47.4 mg, 0.25 mmol), phenylboronic acid (46.2 mg, 0.38 mmol) and K₃PO₄ (0.17 g, 0.75 mmol) in water (3 ml) and the required amount of toluene was added to a Radley's Carousel reaction tube containing the required amount of palladium resin catalyst (6.0 mg, 0.5 mol% palladium) or palladium silica catalyst (12.0 mg, 0.5 mol% palladium). The volume of toluene was measured using a 0.25 ml Hamilton syringe. The mixture was heated at the required temperature for 24 h with magnetic stirring under a nitrogen atmosphere. To work-up the reaction, the mixture was allowed to cool to room temperature and saturated aqueous sodium chloride solution (3 ml) was added. In order to prepare diluted samples for GC analysis, the organic components were extracted into diethyl ether (3 \times 3 ml) which was then dried over

anhydrous MgSO_4 . The resulting solution analyzed by GC and GC-MS with reference to standard solution 4-methoxybiphenyl. The GC data showed conversion of 4-bromoanisole to 4-methoxybiphenyl as the sole product. Note that the diethyl ether extraction was not required to isolate the product on a preparative scale (see Reaction scale-up) as it precipitated from solution on formation.

Reaction scale-up

For the reaction on a 2.5 mmol scale, a mixture of 4-bromoacetophenone (0.504 g, 2.5 mmol), phenylboronic acid (0.338 g, 2.8 mmol) and K_3PO_4 (1.7 g, 7.5 mmol) in water (30 ml) and toluene (1 ml) were added to a 100 ml round-bottomed flask containing the required amount of the palladium resin catalyst (60 mg, 0.5 mol% palladium). The flask was flushed with nitrogen and the mixture was heated at 90 °C for 24 h with magnetic stirring under a nitrogen atmosphere. The toluene was then evaporated at 90 °C and recovered if necessary. However, this step usually proved unnecessary if the catalyst was to be used again. The precipitate formed was separated from the palladium resin using a 125 μm sieve, followed by simple filtration and thorough washing with hot water (3×50 ml) to give the product as a white powder. The powder was then dried under vacuum at room temperature to give 0.42 g (85% isolated yield) of product. GC-MS analysis showed no trace of 4-bromoacetophenone, 97% 4-acetylbiphenyl and 3% phenylboronic anhydride, derived from the excess phenylboronic acid. Washing the product with aqueous NaOH solution (2M, 20 ml) then pure water (2×20 ml) removed the anhydride as the boronate salt, with no trace of the anhydride being detected by GC-MS. Furthermore, ICP-AES analysis of the product revealed there to be no palladium contamination. Microanalysis: found C, 85.28; H, 6.19. $\text{C}_{14}\text{H}_{12}\text{O}$ requires C, 85.68; H, 6.16. δ_{H} (CDCl_3 ; 250.1 MHz) 7.95 (d, 2H), 7.62–7.50 (m, 4H), 7.40–7.25 (m, 3H), 2.55 (s, 3H); δ_{C} (CDCl_3 ; 62.9 MHz) 197.8, 145.8, 139.9, 135.9, 129.0, 128.9, 128.3, 127.3, 127.2, 26.7.

Conclusion

The supported palladium catalysts exhibit a high activity towards the Suzuki–Miyaura cross-coupling reaction without any added phosphine ligands. Using the silica-supported palladium catalyst requires a catalytic amount of PTC but this is not required in the case of the Merrifield resin. The fact that a water/toluene mixture with more than 96% (v/v) water can be used instead of common organic solvents is obviously of great benefit. The product is recovered without the need for organic solvent extraction as it is immediately precipitated from solution on formation through a reactive crystallization. The work-up procedure involves several aqueous base and pure water washes and hence the relative amount of toluene used in the

complete process becomes increasingly small. The catalysts can be easily separated from the reaction mixture by simple filtration and reused after washing without a significant degradation in activity. As little as 1 ppb palladium leaches into solution from the catalyst during the course of the reaction. The water used in the process can be recycled into the reaction and makes use of any unreacted boronate salts remaining in solution. Therefore, this represents a green process that should have advantages for industrial applications.

Acknowledgements

We would like to thank the Vietnamese Government for funding a Studentship for NTSP. Analytical Services at the University of Sheffield, Department of Chemistry are thanked for the provision of spectroscopic facilities.

References

- 1 S. Paul and J. H. Clark, *Green Chem.*, 2003, **5**, 635.
- 2 N. Miyaoura and A. Suzuki, *Chem. Rev.*, 1995, **95**, 2457.
- 3 E. B. Mubofu, J. H. Clark and D. J. Macquarrie, *Green Chem.*, 2001, **3**, 23.
- 4 I. P. Beletskaya and A. V. Cheprakov, *Chem. Rev.*, 2000, **100**, 3009.
- 5 B. Cornils, W. A. Herrmann, P. Panster, and S. Wieland, in *Applied Homogeneous Catalysis with Organometallic Compounds*, ed. B. Cornils and W. A. Herrmann, VCH, Weinheim, 1996, vol. 2, p. 576.
- 6 C. J. Li and T. H. Chan, *Organic Reactions in Aqueous Media*, Wiley, New York, 1997, p. 1.
- 7 J. P. Genêt and M. Savignac, *J. Organomet. Chem.*, 1999, **576**, 305.
- 8 D. Badone, M. Baroni, R. Cardamone, A. Ielmini and U. Guzzi, *J. Org. Chem.*, 1997, **62**, 7170.
- 9 N. E. Leadbeater and M. Marco, *Org. Lett.*, 2002, **4**, 2973.
- 10 N. E. Leadbeater and M. Marco, *J. Org. Chem.*, 2003, **68**, 888.
- 11 H. Sakurai, T. Tsukuda and T. Hirao, *J. Org. Chem.*, 2002, **67**, 2721.
- 12 Y. Uozumi, H. Danjo and T. Hayashi, *J. Org. Chem.*, 1999, **64**, 3384.
- 13 N. T. S. Phan, D. H. Brown, H. Adams, S. E. Spey and P. Styring, *Dalton Trans.*, 2004, 1348.
- 14 N. T. S. Phan, D. H. Brown H. and P. Styring, *Tetrahedron Lett.*, 2004, **45**, 7915.
- 15 P. Styring, C. Grindon and C. M. Fisher, *Catal. Lett.*, 2001, **77**, 219.
- 16 K. C. Kong and C. H. Cheng, *J. Am. Chem. Soc.*, 1991, **113**, 6313.
- 17 N. T. S. Phan, J. Khan and P. Styring, *Tetrahedron*, 2005, **61**, 12065.
- 18 J. R. Ruiz, C. Jimenez-Sanchidrián and M. Mora, *Tetrahedron*, 2006, **62**, 2922.
- 19 B.-Q. Xu, D. Sood, A. V. Iretskii and M. G. White, *J. Catal.*, 1999, **187**, 358.
- 20 N. T. S. Phan, D. H. Brown H. and P. Styring, *Green Chem.*, 2004, **6**, 526.
- 21 L. Djakovitch and K. Koehler, *J. Mol. Catal. A: Chem.*, 1999, **142**, 275.
- 22 N. T. S. Phan, M. Van Der Sluys and C. W. Jones, *Adv. Synth. Catal.*, 2006, **348**, 609.
- 23 N. K. Terrett, in *Combinatorial Chemistry*, ed. R. G. Compton, S. G. Davies and J. Evans, Oxford University Press, 1998, p. 9.
- 24 W. E. Rapp, in *Combinatorial Chemistry*, ed. S. R. Wilson and A. W. Czarnik, John Wiley & Sons, New York, 1997, p. 66.
- 25 V. V. Grushin and H. Alper, *Chem. Rev.*, 1994, **94**, 1047.
- 26 J. P. Wolfe and S. L. Buchwald, *Angew. Chem.*, 1999, **38**, 2413.

Synthesis of cellulose/titanium dioxide hybrids in supercritical carbon dioxide

Qisi Yu,^a Peiyi Wu,^{*a} Peng Xu,^{*a} Lei Li,^b Tao Liu^b and Ling Zhao^b

Received 10th April 2008, Accepted 23rd June 2008

First published as an Advance Article on the web 19th August 2008

DOI: 10.1039/b806094k

The modifications and applications of natural cellulose have attracted more and more interest in recent years, sparked by the progressive shortage of the fossil energy resources and increase in the technological interests in sustainable and renewable raw materials. In this paper, a novel approach for preparation of cellulose/titanium dioxide hybrids was achieved by utilizing supercritical carbon dioxide-assisted impregnation. The hybrids, with a very small scale in length, suggest that the titania particles were not only coating on the external surface but also penetrating into the micro-cavity structure of the cellulose fibers. The penetrating and swelling effect of supercritical carbon dioxide, with a cosolvent of ethanol, on the cellulose was also investigated. It was found that such actions of carbon dioxide in the supercritical state influenced the interactions between the molecular chains of cellulose. The titania particles were facilitated by the effect of supercritical carbon dioxide to access and impregnate into the crystalline structure of cellulose fibers by formation and stabilization of hydrogen bonds with abundant hydroxyl groups of cellulose, resulting in a change of its thermal stability in pyrolysis. This preparative procedure is facile and environmentally friendly, and provides a simple approach for the synthesis of useful materials in various applications.

Introduction

Cellulose, a linear polymer of β -D-glucose, is the most naturally abundant biomass resource on earth. There is about 1.5 trillion tons of cellulose produced yearly, which make it an inexhaustible source of raw material.^{1,2} In a typical structure of cellulose, there are plentiful intra- and inter-molecular hydrogen bond networks, which sustain it with a high crystallinity and excellent hydrophilic and mechanical properties.³ However, this unique crystalline structure also makes the cellulose difficult to melt and insoluble in common solvents¹ and limits its applications. Fortunately, there are many kinds of solvents, and derivative methods have been increasingly developed for cellulose to prepare its derivatives or hybrids, which expand the applications of cellulose in various technical areas, such as textiles, catalysts, pharmaceuticals and films.⁴⁻⁸

Among these derivative methods, supercritical fluids (SCFs) have been widely applied as a media to process biopolymers and synthetic polymers. They provide an alternative technique to modify natural cellulose⁹ by avoiding the process of dissolving and regenerating the cellulose, during which the crystal form of cellulose changes.¹ In addition, supercritical carbon dioxide (scCO₂) with many unique properties, for example, nontoxic,

nonflammable, environmentally benign and inexpensive, has been the most frequently used SCF candidate by far. In particular, the critical pressure and temperature of 7.38 MPa and 31.1 °C, respectively, for CO₂ is relatively low. Furthermore, the properties of CO₂ in the supercritical state, like its relatively high density and low viscosity and dielectric constant, can be easily adjusted by changing the temperature and pressure.^{10,11} In previous work, we have developed an approach to utilize the assistant effect of scCO₂ in grafting of methyl methacrylate onto polypropylene (PP)¹¹ and to disperse the nucleating agents in it.^{12,13} Many other researchers also reported that scCO₂ can remarkably aid the impregnation of low molecular weight additives (such as dyes,¹⁴⁻¹⁶ drugs¹⁷ and organometallic complexes¹⁸) into diverse polymers by means of the zero surface tension and high diffusivity, solubility and plasticizing actions of scCO₂ in polymers.¹⁰

Nowadays, titania (TiO₂) modified cellulose has attracted much attention. Because of the synergistic effects from the physical or chemical interactions between the organic and inorganic components, TiO₂/cellulose hybrids can be utilized as photocatalysts of various environmental pollutants and harmful organic compounds^{19,20} or in the formation of films which have good mechanical and UV-shielding properties,²¹ as well for antibacterial use²² or in the synthesis of transition-metal carbide materials.²³ In terms of the synthetic strategy, a sol-gel route utilizing various biological components or synthetic polymers as templates has been employed by many researchers to prepare the hybrids containing a TiO₂ component.²⁴⁻²⁹ For cellulose hybrids, Huang and Kunitake³⁰ used filter paper as a cellulosic template with a hierarchical structure and further coated it

^aThe Key Laboratory of Molecular Engineering of Polymers (Ministry of Education) and Department of Macromolecular Science, Fudan University, Shanghai, 200433, PR China.

E-mail: peiyiwu@judan.edu.cn; Fax: +86 21 6564 0293

^bUNILAB Research Center of Chemical Reaction Engineering, State Key Laboratory of Chemical Engineering, East China University of Science and Technology, Shanghai, 200237, PR China

with titania with nanoprecision. Zecchina *et al.*¹⁹ prepared the photoactive fibers on which they deposited and grafted of TiO₂ nanoparticles. A supercritical fluid route developed by Liu *et al.*³¹ used the precursor dissolved in scCO₂ to react with the surface active groups and adsorbed surface water on many fabric templates to prepare the composites (without calcination). Some other new approaches have also been developed for preparation of the hybrids. For example, Kemell *et al.*³² used the atomic layer decomposition technique to prepare photocatalytic TiO₂/cellulose composites. Ikushima *et al.*³³ adopted natural fibers as templates and ionic liquids as solvents to synthesise TiO₂/cellulose composite nanowires.

In this study, we report a green and simple approach for synthesis of cellulose/TiO₂ hybrids by combination of scCO₂-assisted adsorption and impregnation into cellulose fibers, with a titania sol which was prepared through a non-hydrolytic sol-gel route reported in our previous work.^{34–36} This method avoids the use of solvents for cellulose regeneration and high temperatures. The structure, morphology and properties of the resulting cellulose/TiO₂ hybrids were characterized by scanning electron microscopy (SEM), energy dispersive spectroscopy (EDS), thermogravimetry (TG) and X-ray diffraction (XRD). Based on which, a possible mechanism of the effect of TiO₂ particles and scCO₂ on the cellulose was proposed finally.

Experimental

Materials

Cotton wool from Shanghai Yinjing Medical Supplies Co., Ltd (Shanghai, China) was used as a cellulose resource. It contains more than 90% α -cellulose. Before use, the fibers were treated with acetone for 4 h in a Soxhlet extractor to remove the impurities, such as wax and fat. CO₂ with a purity of 99.9% was purchased from Shanghai Jifu Gas Co., Ltd (Shanghai, China). Titanium tetrachloride (TiCl₄), tetrahydrofuran (THF) and ethanol (EtOH), all with an analytical reagent grade, were supplied by Shanghai Chemical Reagents Co. Ltd (China National Medicines Group, Shanghai, China) and used without purification. The water used in our experiments was deionized and produced in our laboratory.

Preparation of cellulose/titanium dioxide hybrids

Titanium tetrachloride was used as the precursor of TiO₂. The TiCl₄-EtOH solution was prepared by mixing TiCl₄ with ethanol (TiCl₄/ethanol = 1/4, w/w) and then stirred at room temperature for 12 h. The yellow clear TiO₂ sol formed was uniform and quite stable, containing a large amount of TiO₂ particles with a dimension below 10 nm. In a typical experiment, the cotton wool (0.3 g) immersed in 10 mL of TiO₂ sol was placed in the reactor, a stainless steel autoclave with a capacity of 40 mL. Then, the autoclave was sealed and carbon dioxide was introduced after the air in the reactor was purged twice. In order to reach a higher pressure, the autoclave was firstly placed in the ice water to reach a lower temperature and then transferred into a 60 °C preheated oil bath immediately. Then the pressure of CO₂ in the reactor was increased to reach a supercritical state and kept nearly unchanged. The experimental setup used here was described in our previous work.¹¹ In order to impregnate

the inorganic nanoparticles into the cotton fibers adequately, the experiment was allowed to last for 4 h. Then the autoclave was cooled down and depressurized. The cotton fibers were removed and then washed with deionized water and ethanol repeatedly and dried in the air. In contrast, the same amount of pristine cotton cellulose including 3 mL of ethanol as cosolvent was also treated in scCO₂ without addition of TiO₂ sol under the same experimental conditions.

Characterization

The morphologies of the cotton cellulose samples were investigated using a scanning electron microscope (SEM, Philips XL 30) equipped with an energy dispersive spectroscopic (EDS) micro-analysis system (OXFORD). The samples were also subjected to EDS analysis to verify the elemental composition on the surface of the fibers. Before observation, the fibers were cemented onto the sample stage and sputtered with gold, and then photographed.

Thermogravimetric analysis (TGA) was performed on a Perkin-Elmer Pyris 1 thermal gravimetric analyzer under nitrogen atmosphere from 50 to 700 °C with a heating rate of 10 °C min⁻¹.

The wide X-ray diffraction (WXR) patterns were measured using a PANalytical X'Pert PRO diffractometer with Cu K α radiation ($\lambda = 1.541 \text{ \AA}$) at 40 kV and 40 mA in the range of 2θ from 5 to 40°. The crystallinity was calculated as per the method in ref. 37.

Heat of combustion for pristine cotton cellulose and the cellulose samples treated by scCO₂ were determined using an XRY-1A Digital Display Oxygen Bomb Calorimeter (Shanghai Changji Geological Instrument Co., Ltd, Shanghai, China) according to the method described in ref. 38

Results and discussion

Morphology and EDS analysis of the hybrids

The morphology differences of the treated and untreated cellulose fibers are presented in Fig. 1. It is clear that the structure of the cellulose fibers has changed greatly with introduction of the TiO₂ sol in scCO₂. The characteristic long strip shape of pristine cellulose fibers in a bulky and fluffy state (Fig. 1a) has been broken up in to a powder (Fig. 1c). Furthermore, without addition of the TiO₂ sol, the appearance of the sample only treated by scCO₂ (Fig. 1b) is mostly unchanged.

In order to further investigate the surface morphology of the obtained fibers, the SEM images of comparisons between the treated and untreated samples are shown in Fig. 2. The pristine cotton fibers with a length scale of several centimetres are exhibited in Fig. 2a, and the diameter of the fibers is *ca.* 12–30 μm . The magnified images of the locality around a single fiber with a rough surface, presented in Fig. 2b, show a distinct structure of multi strands of microfibrils with characteristic orientations. The fiber resembles a twisted ribbon,³⁹ on whose surface the folds orientated along the elongation direction of the fiber can be observed clearly. Fig. 2c–e show the scCO₂ treated cellulose fibers. It can be seen that the long strip shape of a typical morphology of cotton fibers does not change, but on the smoother surface of some cotton fibers, it appears



Fig. 1 Photograph of: (a) pristine cotton cellulose, (b) cellulose treated by scCO_2 and (c) cellulose/ TiO_2 hybrids prepared in scCO_2 .

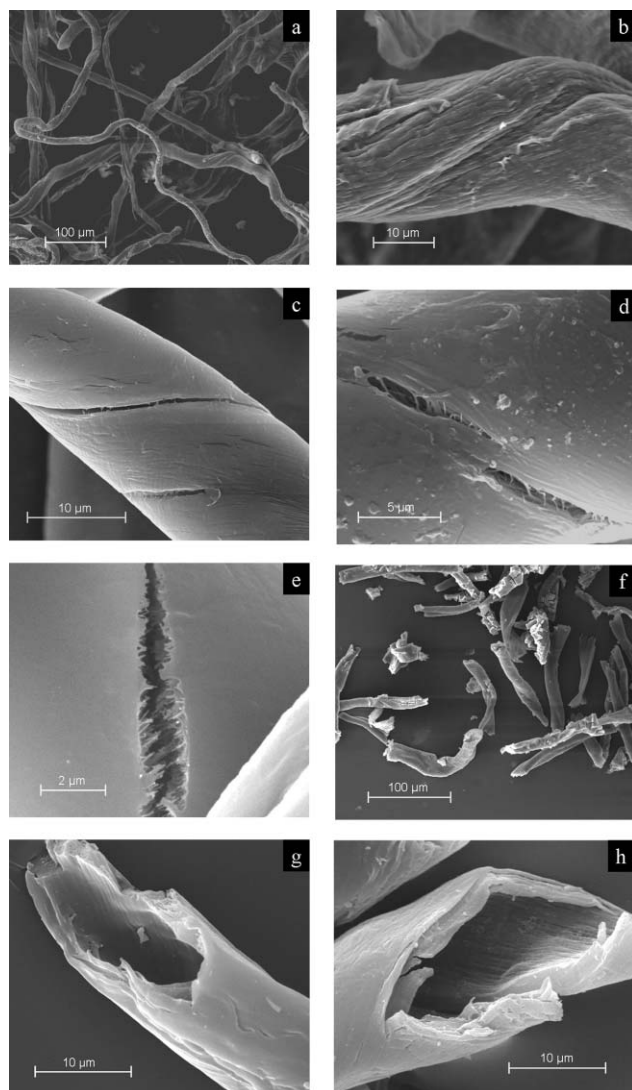


Fig. 2 SEM images of: (a,b) pristine cotton cellulose, (c–e) cellulose treated by scCO_2 and (f–h) cellulose treated by TiO_2 sol in scCO_2 .

that many helical ditches are filled with microfibrils, indicating the characteristic hierarchical structure of the morphology of cellulose fiber. This phenomenon quite resembles the work reported by Shen *et al.*,^{9,40} in which urea (which we did not use here) was added to break the hydrogen bonds of cellulose and prepare cellulose carbamate, resulting in a much more violent bursting of the cotton fibers in scCO_2 than those in our experiment. Herein, the changes in the structure of cellulose fibers in the presence of the ethanol cosolvent might be attributed to the special properties of scCO_2 , especially the high diffusion and outstanding swelling effect on polymers.⁹

Fig. 2f–h clearly shows that the length of the cotton fibers treated by TiO_2 sol and scCO_2 decreases to a magnitude of several hundred micrometres, and their aspect ratios (length vs. diameter) reduce remarkably. In addition, the TiO_2 sol forms a coating covering the surface of the fibers and obscures the folds and convolutions below. Moreover, the fracture surfaces of short fibers are also imaged in Fig. 2g and h, which show a micro-cavity structure of cotton fibers.⁴¹ In order to determine the components on the fibers, EDS analysis of the pristine cellulose fibers and TiO_2 treated fibers are also reported in Fig. 3. It is worth noting that the investigated regions here include both internal and external fracture surfaces of the short fibers treated by TiO_2 sol and scCO_2 . It can be observed that the deposited material is composed of titanium and oxygen, and the sputtered gold element can be also found. This may imply that the TiO_2 has anchored to the external surface of fibers owing to the surface hydroxyl groups on natural cellulose fibers, which can be suitable for immobilizing and stabilizing of metal oxide nanoparticles.³³ In addition, what inspires more interest is that the titanium element is also present on many regions of the internal surface of the fracture short fibers and its content is much lower than that on the external surface of the fibers, showing a decrease in the distribution of TiO_2 from the outer surface to the inner surface of the cellulose fibers. It is important to note that the natural cellulose fibers have a porous structure which is composed of microfibrils of 10–30 nm width that are three-dimensionally connected with each other,⁴² providing many channels for the migration of the TiO_2 particles in scCO_2 . Tang *et al.*⁴³ and Kunitake *et al.*⁴² utilized this unique morphological porous feature of natural cellulose fibers as a template for synthesis of metal nanoparticles with a very small diameter and narrow size distribution. So it is suggested that the TiO_2 sol might penetrate into the cellulose fibers by scCO_2 -assisted impregnation. Such swelling of cellulose fibers, as well as the aided infusion of TiO_2 particles into the fibers by scCO_2 , will be likely to lead to a significant effect on the thermal and crystalline properties of cellulose.

Thermal analysis

Fig. 4 shows the TG and DTG curves of the pristine cotton cellulose and the cellulose treated by scCO_2 , as well as the hybrids containing TiO_2 particles prepared in scCO_2 . The results are listed in Table 1. The curves for untreated and scCO_2 treated cellulose samples both show one major exothermic peak, which represents a typical thermal decomposition behavior of cellulose in an inert atmosphere, as previously reported.^{44,45} It seems that the thermal stability of the cotton cellulose after treatment by

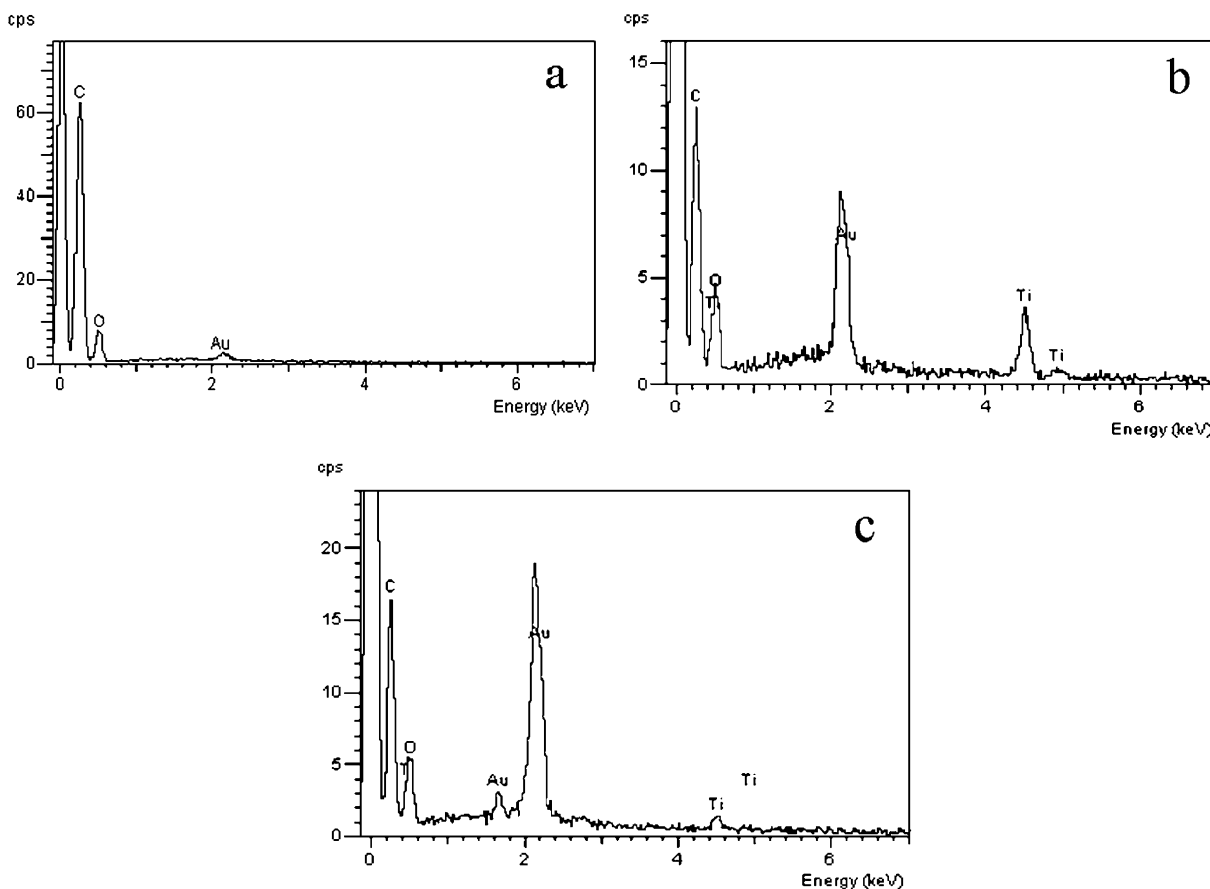


Fig. 3 EDS spectra of: (a) pristine cellulose, shown as a reference; (b) TiO₂ sol treated cellulose at external fracture surface and (c) internal surface.

Table 1 Results of thermal analysis for: (a) pristine cellulose; (b) cellulose treated by scCO₂; (c) cellulose/TiO₂ hybrids prepared in scCO₂

Sample no.	$T_d/^\circ\text{C}^a$	$T_{\max}/^\circ\text{C}^b$	Residue (wt%) ^a	Heat of combustion/ kJ kg ⁻¹
a	324.3	372.3	8.7	16492
b	319.2	369.6	7.8	17901
c	234.4	324.3	45.2	—

^a Temperature at 5 wt% loss in weight of the samples and residual ash determined by the thermal gravimetric analysis (TGA). ^b Peak temperature calculated from derivative thermogravimetric (DTG) curves.

scCO₂ has no appreciable change. In contrast, for the hybrids containing TiO₂ particles, the maximum loss of weight, which was found to be due to the removal of cellulose, shifts to a temperature of ~324 °C, 48 °C lower than that of the pristine cellulose. The smaller loss below 230 °C is probably ascribed to the dehydroxylation and the removal of residual organics from the titania.⁴⁶ One reason for the decrease in thermal stability of the hybrids might be the catalytic character of TiO₂, as reported by Wang *et al.*³⁶ Moreover, the other reason might be due to the CO₂-assisted impregnation of TiO₂ particles which may destroy the intermolecular interactions of the polymer chains of cellulose by the large number of hydroxyl groups in the TiO₂ sol, resulting in the infusion of TiO₂ particles and the loosening of molecular chains in crystalline regions of cellulose. The polymer chains of cellulose may be also destroyed by the TiO₂ sol, since there is a

small amount of HCl in the sol, which may cause the cellulose chains to degrade.

In addition, the crystalline structure of cellulose may be destroyed a little after treatment by scCO₂ with a cosolvent of ethanol. This can be supported by the slight decrease of the decomposition temperature value in TGA results, and further indicated by the results of heat of combustion analysis. Table 1 also shows the heat of combustion of cotton cellulose after treatment by scCO₂, which is higher than that of the pristine cellulose. This means more heat was liberated during the actual combustion process, which facilitates the burning process.⁴⁷ In other words, the heat change of combustion of cellulose might suggest that the proportion of amorphous regions of cellulose is increased after treatment by scCO₂, as Ikumi *et al.*⁴⁸ has reported that the heats of combustion of completely crystallized and completely amorphous cellulose are 664.7 and 676.9 kcal mol⁻¹, respectively. So the increased value of heat of combustion observed for the scCO₂ treated cellulose might imply that the penetrating and swelling effect of the scCO₂ facilitates the movements of the polymer chains, making the burning process easier to occur.

X-Ray diffraction (XRD) analysis

The XRD results in Table 2 show some important information about the change of the crystalline structure of cotton cellulose after treatment by scCO₂ and doped with the TiO₂ particles.

Table 2 Results of X-ray diffraction analysis for: (a) pristine cellulose; (b) cellulose treated by scCO_2 ; (c) cellulose/ TiO_2 hybrids prepared in scCO_2

Sample no.	Peak position			Degree of crystallinity (χ_c)
	(110)	($1\bar{1}0$)	(200)	
a	14.89	16.68	22.87	73.1
b	14.92	16.61	22.84	69.4
c	14.95	16.63	22.79	58.6

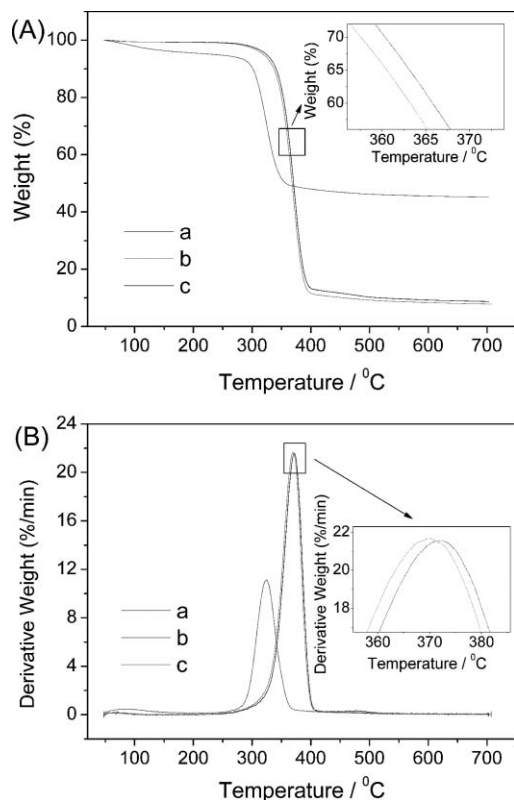


Fig. 4 (A) TG and (B) DTG curves of: (a) pristine cellulose; (b) cellulose treated by scCO_2 and (c) cellulose/ TiO_2 hybrids prepared in scCO_2 (ramp $10\text{ }^\circ\text{C min}^{-1}$, $50\text{--}700\text{ }^\circ\text{C}$, in nitrogen).

The main XRD patterns of the pristine cellulose, the scCO_2 treated cellulose and the hybrids exhibited in Fig. 5 all show a characteristic cellulose I crystalline form. The 2θ diffraction peaks at ~ 14.9 , ~ 16.6 and $\sim 22.8^\circ$ correspond to the (110), ($1\bar{1}0$) and (200) crystal planes, respectively, referring to the previous report.⁴⁹ Since the XRD spectrum (not shown here) of TiO_2 sol treated in the same conditions as those for the hybrids shows an amorphous structure, it is suggested that the difference in the spectra in Fig. 5 is due to the change of the crystalline structure of cellulose. From the slight position shift of the (110) and (200) peaks (in Table 2) and a variation in the ratio of intensities of (110) and ($1\bar{1}0$) peaks (in Fig. 5), it can be speculated that some structural changes of the cellulose might happen during the penetrating process of the scCO_2 , and further become more obvious when the TiO_2 particles are employed as well. Meanwhile, we can also find some new small peaks at $2\theta = 27.1$, 34.6 and 38.3° in Fig. 5c, which shows a possibility of modification of the crystal planes in cellulose. Further investigation of the crystalline properties of

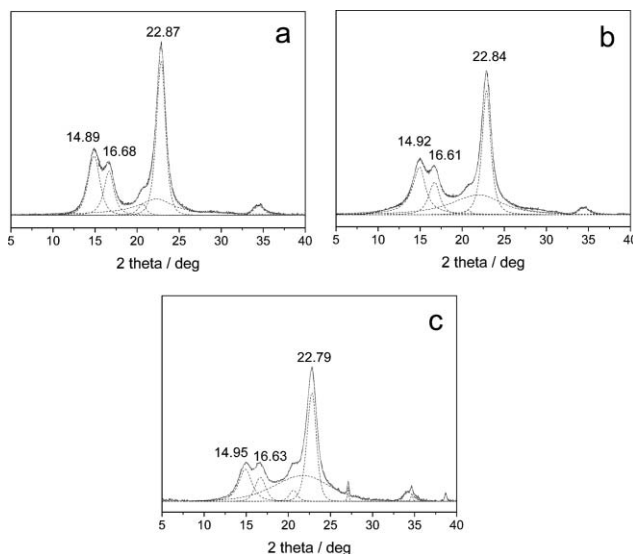


Fig. 5 X-ray diffraction patterns of: (a) pristine cellulose; (b) cellulose treated by scCO_2 ; (c) cellulose/ TiO_2 hybrids prepared in scCO_2 .

the samples reveals a change in the degree of crystallinity (χ_c) of cellulose, which decreases slightly after treatment by scCO_2 and further decreases remarkably after doping with TiO_2 particles in scCO_2 (Table 2). Generally, because of the relatively high crystallinity of natural cellulose, it is not easy for the scCO_2 to impregnate into and damage the crystal regions of cellulose, where the polymer chains are arranged densely and the molecular structure is well-defined by intermolecular interactions. The emergence of a penetration and swelling effect of scCO_2 is more likely to happen in the amorphous and less ordered regions of the cellulose, even though there is a small appearance in crystalline regions, as mentioned in the TGA discussion. So this action of scCO_2 is limited and the crystallinity of cellulose changes little. When the TiO_2 sol is added in scCO_2 , considering that it contains lots of hydroxyl groups which may substitute and form hydrogen bond networks with those of the cotton cellulose, resulting in the reduction of its density of hydrogen bonds, more crystalline regions of cellulose are destroyed by the scCO_2 -assisted infusion of TiO_2 nanoparticles in the presence of the minor effect of HCl and cosolvent of ethanol; therefore, its crystallinity is decreased significantly. Furthermore, the supramolecular structure of cellulose may be partially disintegrated and destroyed by such doping of TiO_2 in scCO_2 , resulting in the change of the cellulose fibers to powders with very small aspect ratios, as observed in the SEM images. Crystalline regions are much more thermally stable than the amorphous regions in cellulose pyrolysis,⁵⁰ and this thermal stability of cellulose and its derivatives have a close relationship to their crystallinities.^{51,52} So, herein, the results of the XRD analysis may explain why the decomposition temperature of cellulose shifts to a much lower value, as the TGA results showed, after introduction of TiO_2 sol in scCO_2 in the respect of crystallinity of the cellulose.

In view of the above information obtained from the morphological and thermal analysis, as well as the results of the X-ray diffraction, we propose a schematic model to describe the mechanism of the effect of scCO_2 and TiO_2 nanoparticles to the natural cotton cellulose, as shown in Fig. 6. By forming large

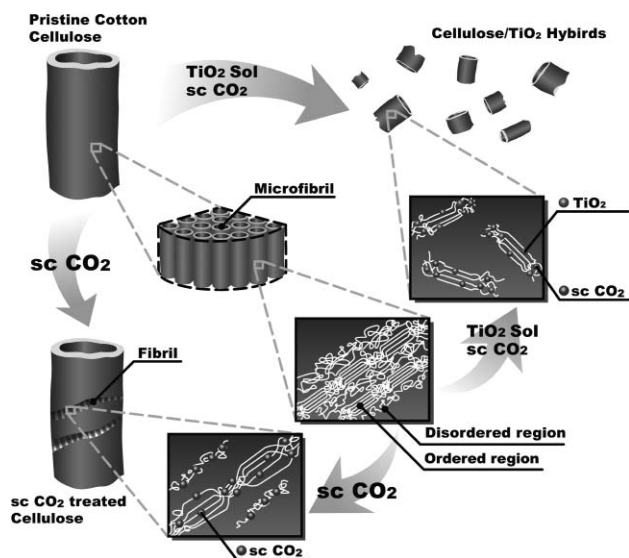


Fig. 6 Schematic model for impregnation of scCO_2 and TiO_2 nanoparticles into cotton cellulose.

scale intra- and intermolecular hydrogen bonds, many parallel and oriented cellulose chains arrange as a crystalline array which constitutes the fundamental structural unit of cellulose, namely microfibril, which contains both crystalline and amorphous domains. The introduction of scCO_2 into the microfibrils of natural cellulose will cause a significant penetrating and swelling effect which is more remarkable in the amorphous regions as compared with the crystalline regions, resulting in a slight decrease of the thermal stability and crystallinity of cellulose. When the TiO_2 sol is added, the weakening of the intermolecular interactions of cellulose by the impregnation of scCO_2 molecules will increase the active and accessible surface for the adsorption of TiO_2 sol and further improve the hierarchical porous structure of the cellulose fibers, which may provide channels for the migration of inorganic nanoparticles. Then, further impregnation of TiO_2 nanoparticles even into the crystal domains of cellulose will cause interactions between the hydroxyl groups of TiO_2 sol and cellulose. The effect of the formed H-bond networks after scCO_2 and TiO_2 sol processing is at least 2-fold. First, the H-bonds of cellulose have been partially substituted and destroyed, especially including those in the crystal domains, resulting in the change of its crystalline structure and physical properties. A second result relates to the impregnated TiO_2 particles which are incorporated and stabilized by such formation of H-bond networks. Therefore, with the penetration into and destruction of cellulose by the TiO_2 sol, an obvious disintegration of the original crystalline arrays of cellulose occurs, leading to some broken fragments with a much smaller aspect ratio. So the thermal and crystalline properties of the hybrids are both decreased to much lower values.

Conclusion

To summarize, we reported a novel approach to a synthesis of a new type of natural cotton cellulose/ TiO_2 hybrids by scCO_2 -assisted impregnation at low temperature. The original long strip shape of the cotton fibers in the hybrids was broken into a powder with a very short aspect ratio. More detailed

study of the hybrids found that the TiO_2 particles are both deposited on the surface of the fibers and impregnated into the micro-cavity structure of cellulose. The effect of only scCO_2 in the presence of a cosolvent of ethanol to the cotton cellulose was also examined, which presented some helical ditches filled with many microfibrils on the surface of the fibers, showing a typical hierarchical structure of natural cellulose. We note that such morphological breakage of the fibers by scCO_2 alone or combined with TiO_2 particles has a close relation with the change of their crystalline structures, including both the changes of their degrees of crystallinity and crystalline allomorph. These changes are found to exhibit some effect on their thermal properties in pyrolysis in turn. The implication of the present results is that the scCO_2 can be actually be used as an effective vehicle to modify natural cellulose with inorganic sols. Such application might be expanded to filter paper, wood cellulose or fabric textiles with other metal oxides, such as silica or zirconia. The preparative approach in our work has provided a green and facile method of synthesis of the cellulose/ TiO_2 hybrids in scCO_2 , which can be used as catalysts, antimicrobial materials, UV-protective agents, and other useful materials.

Acknowledgements

The authors gratefully acknowledge the financial support by the National Science of Foundation of China (NSFC) (Nos. 20774022 20573022, 20425415, 20490220), the "Leading Scientist" Project of Shanghai (No. 07XD14002), the National Basic Research Program of China (2005CB623800) and PHD Program of MOE (20050246010).

References

- 1 D. Klemm, B. Heublein, H. P. Fink and A. Bohn, *Angew. Chem., Int. Ed.*, 2005, **44**, 3358–3393.
- 2 J. Kim, S. Yun and Z. Ounaies, *Macromolecules*, 2006, **39**, 4202–4206.
- 3 J. F. Kennedy, G. O. Phillips, D. J. Wedlock and P. A. Williams, *Cellulose and Its Derivatives: Chemistry, Biochemistry and Applications*, Ellis Horwood Limited, Chichester, 1985.
- 4 P. Sakellariou and R. C. Rowe, *Prog. Polym. Sci.*, 1995, **20**, 889–942.
- 5 A. M. Peiro, G. Doyle, A. Mills and J. R. Durrant, *Adv. Mater.*, 2005, **17**, 2365–2368.
- 6 K. J. Edgar, C. M. Buchanan, J. S. Debenham, P. A. Rundquist, B. D. Seiler, M. C. Shelton and D. Tindall, *Prog. Polym. Sci.*, 2001, **26**, 1605–1688.
- 7 W. K. Son, J. H. Youk, T. S. Lee and W. H. Park, *Macromol. Rapid Commun.*, 2004, **25**, 1632–1637.
- 8 D. Ruan, L. N. Zhang, Z. J. Zhang and X. M. Xia, *J. Polym. Sci., Part B: Polym. Phys.*, 2004, **42**, 367–373.
- 9 C. Y. Yin, J. B. Li, Q. Xu, Q. Peng, Y. B. Liu and X. Y. Shen, *Carbohydr. Polym.*, 2007, **67**, 147–154.
- 10 D. L. Tomasko, H. B. Li, D. H. Liu, X. M. Han, M. J. Wingert, L. J. Lee and K. W. Koelling, *Ind. Eng. Chem. Res.*, 2003, **42**, 6431–6456.
- 11 G. S. Tong, T. Liu, G. H. Hu, L. Zhao and W. K. Yuan, *J. Supercrit. Fluids*, 2007, **43**, 64–73.
- 12 B. Li, G. H. Hu, G. P. Cao, T. Liu, L. Zhao and W. K. Yuan, *J. Appl. Polym. Sci.*, 2006, **102**, 3212–3220.
- 13 B. Li, G. H. Hu, G. P. Cao, T. Liu, L. Zhao and W. K. Yuan, *J. Supercrit. Fluids*, 2008, **44**, 446–456.
- 14 Z. T. Liu, L. L. Zhang, Z. W. Liu, Z. W. Gao, W. S. Dong, H. P. Xiong, Y. D. Peng and S. W. Tang, *Ind. Eng. Chem. Res.*, 2006, **45**, 8932–8938.
- 15 M. van der Kraan, M. V. F. Cid, G. F. Woerlee, W. J. T. Veuglers and G. J. Witkamp, *J. Supercrit. Fluids*, 2007, **40**, 470–476.
- 16 O. S. Fleming, F. Stepanek and S. G. Kazarian, *Macromol. Chem. Phys.*, 2005, **206**, 1077–1083.

- 17 O. Guney and A. Akgerman, *AIChE J.*, 2002, **48**, 856–866.
- 18 E. Said-Galiyev, L. Nikitin, R. Vinokur, M. Gallyamov, M. Kurykin, O. Petrova, B. Lokshin, I. Volkov, A. Khokhlov and K. Schaumburg, *Ind. Eng. Chem. Res.*, 2000, **39**, 4891–4896.
- 19 M. J. Uddin, F. Cesano, F. Bonino, S. Bordiga, G. Spoto, D. Scarano and A. Zecchina, *J. Photochem. Photobiol., A*, 2007, **189**, 286–294.
- 20 G. Goutailler, C. Guillard, S. Daniele and L. G. Hubert-Pfalzgraf, *J. Mater. Chem.*, 2003, **13**, 342–346.
- 21 M. Kusabe, H. Kozuka, S. Abe and H. Suzuki, *J. Sol-Gel Sci. Technol.*, 2007, **44**, 111–118.
- 22 W. A. Daoud, J. H. Xin and Y. H. Zhang, *Surf. Sci.*, 2005, **599**, 69–75.
- 23 Y. S. Shin, X. H. S. Li, C. M. Wang, J. R. Coleman and G. J. Exarhos, *Adv. Mater.*, 2004, **16**, 1212–1215.
- 24 R. A. Caruso, *Angew. Chem., Int. Ed.*, 2004, **43**, 2746–2748.
- 25 R. S. Yuan, X. Z. Fu, X. C. Wang, P. Liu, L. Wu, Y. M. Xu, X. X. Wang and Z. Y. Wang, *Chem. Mater.*, 2006, **18**, 4700–4705.
- 26 S. R. Hall, V. M. Swinerd, F. N. Newby, A. M. Collins and S. Mann, *Chem. Mater.*, 2006, **18**, 598–600.
- 27 Q. Dong, H. L. Su, D. Zhang, Z. T. Liu and Y. J. Lai, *Microporous Mesoporous Mater.*, 2007, **98**, 344–351.
- 28 G. M. An, W. H. Ma, Z. Y. Sun, Z. M. Liu, B. X. Han, S. D. Miao, Z. J. Miao and K. L. Ding, *Carbon*, 2007, **45**, 1795–1801.
- 29 Z. Miao, Z. J. M. Liu, B. X. Han, Y. Wang, Z. Y. Sun and H. L. Zhang, *J. Supercrit. Fluids*, 2007, **42**, 310–315.
- 30 J. G. Huang and T. Kunitake, *J. Am. Chem. Soc.*, 2003, **125**, 11834–11835.
- 31 Y. Wang, Z. M. Liu, B. X. Han, Z. Y. Sun, J. M. Du, J. L. Zhang, T. Jiang, W. Z. Wu and Z. J. Miao, *Chem. Commun.*, 2005, 2948–2950.
- 32 M. Kemell, V. Pore, M. Ritala, M. Leskela and M. Linden, *J. Am. Chem. Soc.*, 2005, **127**, 14178–14179.
- 33 N. S. Venkataramanan, K. Matsui, H. Kawanami and Y. Ikushima, *Green Chem.*, 2007, **9**, 18–19.
- 34 P. Xu, H. T. Wang, R. Lv, Q. G. Du, W. Zhong and Y. L. Yang, *J. Polym. Sci., Part A: Polym. Chem.*, 2006, **44**, 3911–3920.
- 35 H. T. Wang, P. Xu, W. Zhong, L. Shen and Q. G. Du, *Polym. Degrad. Stab.*, 2005, **87**, 319–327.
- 36 H. T. Wang, W. Zhong, P. Xu and Q. G. Do, *Compos. Part A: Appl. Sci. Manufact.*, 2005, **36**, 909–914.
- 37 J. F. Rabek, *Experimental Methods in Polymer Chemistry*, Wiley Interscience, Chichester, 1980.
- 38 D. P. Shoemaker, C. W. Garland and J. W. Nibler, *Experiments in Physical Chemistry*, Hill Book Company, New York, 1989.
- 39 K. Stana-Kleinschek, S. Strnad and V. Ribitsch, *Polym. Eng. Sci.*, 1999, **39**, 1412–1424.
- 40 C. Y. Yin and X. Y. Shen, *Eur. Polym. J.*, 2007, **43**, 2111–2116.
- 41 T. P. Nevell and S. H. Zeronian, *Cellulose chemistry and its applications*, Ellis Horwood Limited, Chichester, 1985.
- 42 J. H. He, T. Kunitake and A. Nakao, *Chem. Mater.*, 2003, **15**, 4401–4406.
- 43 A. G. Dong, Y. J. Wang, Y. Tang, N. Ren, Y. H. Zhang, J. H. Yue and Z. Gao, *Adv. Mater.*, 2002, **14**, 926–929.
- 44 A. A. Farooq, D. Price, G. J. Milnes and A. R. Horrocks, *Polym. Degrad. Stab.*, 1994, **44**, 323–333.
- 45 S. Gaan and G. Sun, *J. Anal. Appl. Pyrolysis*, 2007, **78**, 371–377.
- 46 A. Imhof, *Langmuir*, 2001, **17**, 3579–3585.
- 47 S. Gaan and G. Sun, *Polym. Degrad. Stab.*, 2007, **92**, 968–974.
- 48 K. Ikumi and K. Sukai, *Kogyo Kagaku Zasshi*, 1956, **59**, 797–799.
- 49 A. Isogai and M. Usuda, *Macromolecules*, 1989, **22**, 3168–3172.
- 50 H. Kawamoto and S. Saka, *J. Anal. Appl. Pyrolysis*, 2006, **76**, 280–284.
- 51 A. Basch and M. Lewin, *J. Polym. Sci., Part A: Polym. Chem.*, 1973, **11**, 3071–3093.
- 52 M. E. Calahorra, M. Cortázar, J. I. Eguiazábal and G. M. Guzmán, *J. Appl. Polym. Sci.*, 1989, **37**, 3305–3314.

Sequential coupling of the transesterification of cyclic carbonates with the selective *N*-methylation of anilines catalysed by faujasites

Maurizio Selva,* Alvisè Perosa and Massimo Fabris

Received 1st April 2008, Accepted 27th June 2008

First published as an Advance Article on the web 21st August 2008

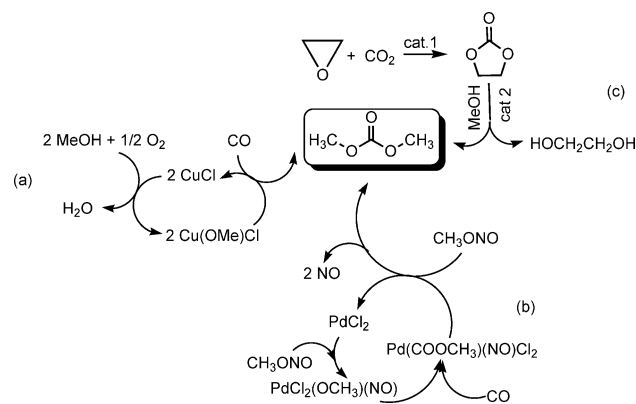
DOI: 10.1039/b805436c

Anilines ($R'C_6H_4NH_2$; $R' = H, p\text{-MeO}, p\text{-Me}; p\text{-Cl}, \text{ and } p\text{-NO}_2$) react with a mixture of ethylene carbonate and methanol at 180 °C in the presence of alkali metal exchanged faujasites—preferably of the X-type—to give the corresponding *N,N*-dimethyl derivatives ($R'C_6H_4NMe_2$) in isolated yields up to 98%. Evidence proves that methanol is not the methylating agent. The reaction instead takes place through two sequential transformations, both catalyzed by faujasites: first transesterification of ethylene carbonate with MeOH to yield dimethyl carbonate, followed by the selective *N*-methylation of anilines by dimethyl carbonate. Propylene carbonate, is less reactive than ethylene carbonate, but it can be used under the same conditions. The overall process is highly chemoselective since the competitive reactions between the anilines and the cyclic carbonates is efficiently ruled out. Ethanol and propanol form the corresponding diethyl- and dipropyl- carbonates in the first step, but these compounds are not successful for the domino alkylation of anilines.

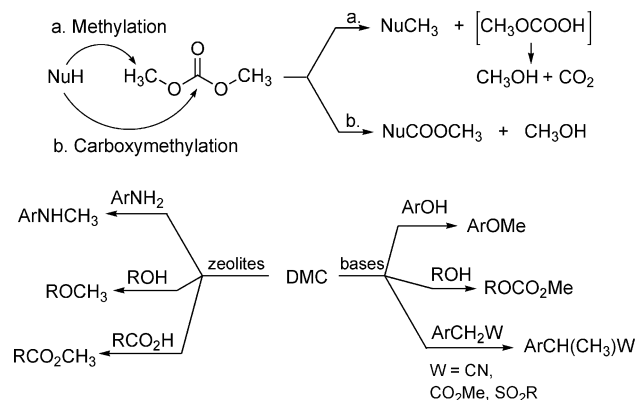
Introduction

The greening of synthetic organic transformations, by the use of eco-friendly reagents has undergone extensive research in the past twenty years.¹ In particular, the alkylation and carbonylation reactions using light organic carbonates in place of the conventional highly noxious alkyl halides, dialkyl sulfates, and phosgene.² This is exemplified by the lightest term of the series, *i.e.* dimethyl carbonate ($MeOCO_2Me$, DMC), whose green features include not only its general reactivity and safety, but also its preparation. In fact, the synthesis of DMC is no longer accomplished using phosgene, instead it is carried out by three greener industrial processes: (a) the oxycarbonylation of methanol,³ (b) the carbonylation of methyl nitrite,⁴ and (c) the two-stage process of insertion of CO_2 into an epoxide, followed by a transesterification reaction with MeOH⁵ (Scheme 1, eqn a–c).

The feedstocks, catalysts, and conditions, for these three processes prevent hazards and pollution at the source, and they produce DMC free from toxic contaminants.⁶ From the reactivity standpoint, both methylation and carboxymethylation reactions of a number of nucleophiles with dimethyl carbonate represent genuine green transformations (Scheme 2, paths a and b) for the following reasons:⁷ (a) a safe reagent (DMC) is used, (b) it often acts simultaneously as a solvent, (c) the transformations are catalytic and do not require the use of additional stoichiometric reagents, (d) the only co-products are MeOH (recyclable to the synthesis of DMC) and CO_2 , and (e) they are slightly, if at all, exothermic.⁸



Scheme 1 Green synthetic routes for dimethyl carbonate.

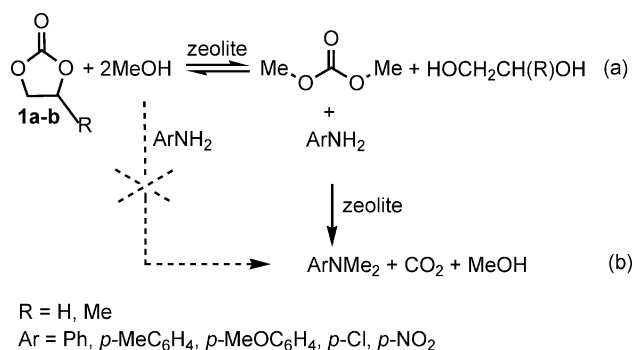


Scheme 2 Methyl and carboxymethyl reactivity of DMC.

Dipartimento di Scienze Ambientali dell'Università Ca' Foscari, Calle Larga S. Maria, 2137, 30123, Venezia, Italy. E-mail: selva@unive.it; Fax: +39 041 234 8584

A more in-depth analysis of the catalytic systems involved in these transformations, shows another potentially valuable aspect: X- and Y-zeolites (alkali metal exchanged faujasites)⁹

not only catalyze methylation and esterification reactions of nucleophiles with DMC (Scheme 2, bottom left), but they also promote the transesterification of ethylene and propylene carbonates with methanol to yield DMC (Scheme 1, eqn c: cat 2).¹⁰ This dual reactivity of the zeolites can, in principle, be exploited for a sequential reaction, *i.e.* in succession: the synthesis of DMC, followed by its reaction with a nucleophile to yield the methylation and esterification products. This concept is named “green domino” in this paper and employs faujasites, preferably of the X-type, to catalyze the reactions illustrated in Scheme 3.



Scheme 3

In particular, when a slurry of a cyclic carbonate (**1a–b**), methanol, a primary aromatic amine (ArNH₂), and a solid zeolite is heated to 180 °C in a batch reactor, two sequential reactions occur: a transesterification process (path a) which generates the active methylating agent dimethyl carbonate, followed by the selective methylation of the amine (path b) which forms the corresponding bis-*N*-methyl derivative (ArNMe₂) in yields up to 98%. Experimental evidence confirms that methanol is not involved in the alkylation step (Scheme 3: dashed path) and that the transformation is unequivocally mediated by DMC.

Interestingly, it is also highly chemoselective: in fact, the competitive reaction of anilines with cyclic carbonates **1** to yield the *N*-(β-hydroxy)ethyl derivatives (ArNHCH₂CH₂OH), is not observed. Overall, the faujasite catalyst significantly intensifies

the process since DMC is formed and its alkylating capability exploited *in situ*.

Under the same conditions, the use of higher alcohols (ethanol and *n*-propanol) is not successful to produce the corresponding *N*-alkylamines. In these cases, both diethyl and dipropyl carbonates form, but anilines preferably react with the starting ethylene carbonate, to give the *N*-(β-hydroxy)ethyl derivatives (ArNHCH₂CH₂OH) as major products.

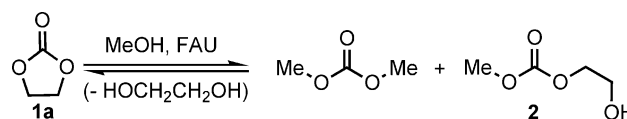
Results

The transesterification of ethylene carbonate with methanol

The initial experiments were carried out to test the activity of faujasites in the transesterification of ethylene carbonate with methanol (Scheme 3, a: R = Me, R' = H). Five different zeolites, namely MX (M = Li, Na, K) and MY (M = H, Na) were used as catalysts. Four of them were either commercially available (NaX and NaY) or synthesized (LiX and KX) by ion exchange using LiCl or KCl.¹¹ HY instead, was obtained by calcination of a commercial NH₄Y solid.¹² The main features of these materials are reported in the Experimental section.

The transesterification reactions were performed at temperatures of 110–150 °C, in a stainless steel autoclave (150 mL) charged with ethylene carbonate (**1a**: 2.2 g, 25 mmol), methanol (8–30 mL), and the faujasite catalyst [the weight ratio *Q* = **1a** : FAU was ranged from 4.8 to 31.4]. After 5 h, the reactor was rapidly cooled to rt and vented, and the reaction mixture was analyzed by GC-MS. Results are reported in Table 1.

In all cases, the major products were dimethyl carbonate and 2-(hydroxy)ethyl methyl carbonate (**2**) (Scheme 4).¹³



Scheme 4

The reaction outcome however, was greatly affected by the nature of the catalysts. At 110 °C (*Q* = 4.8), alkali metal

Table 1 The transesterification of ethylene carbonate with MeOH in presence of different faujasites^a

Entry	FAU/g	MeOH/mL	1a : FA, <i>Q</i> (g : g) ^b	<i>T</i> /°C	Conversion (%) ^c	Products (% GC) ^c		
						DMC	2	Others ^d
1	NaX (0.45)	30	4.8	110	93	73	12	8
2	LiX (0.45)	30	4.8	110	81	50	26	5
3	KX (0.45)	30	4.8	110	96	80	6	10
4	NaY (0.45)	30	4.8	110	79	17	57	5
5	HY (0.45)	30	4.8	110	26	8	14	4
6	NaX (0.45)	30	4.8	130	97	80	7	10
7	NaX (0.45)	30	4.8	150	96	74	7	15
8	NaX (0.28)	30	7.8	110	96	78	10	8
9	NaX (0.14)	30	15.7	110	96	82	10	4
10	NaX (0.07)	30	31.4	110	86	65	20	1
11	NaX (0.14)	15	15.7	110	83	70	12	1
12	NaX (0.14)	8	15.7	110	71	48	23	—

^a All reactions lasted 5 h. ^b *Q* was the weight ratio between ethylene carbonate and faujasite. ^c Both conversion of ethylene carbonate and the product distribution were determined by GC. ^d Others: unidentified products detected by GC/MS analyses.

exchanged faujasites of X-type (MX, M = Li, Na, K) generally afforded both higher conversions (81–97%) and higher yields of dimethyl carbonate (50–80%) with respect to the NaY zeolite (compare entries 1–3 and 4), and to the more acidic HY solid, by far the least effective catalyst (entry 5).

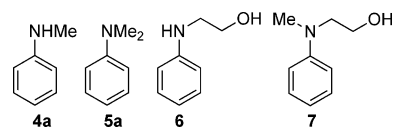
Accordingly, the commercial NaX zeolite was chosen to continue the investigation. Additional experiments were carried out at higher temperatures and with different NaX loadings. At 130 and 150 °C ($Q = 4.8$, entries 6–7), the conversion of ethylene carbonate was substantially quantitative, but the product distribution was not improved. At 110 °C, the zeolite proved to be efficient even at lower loadings: when the Q ratio was increased in the range of 7.8–15.7 (entries 8–9), a conversion of 96% was attained, while the proportion between DMC and compound **2** did not substantially change compared to previous tests. However, a further decrease of the catalyst quantity as well as of the volume of methanol (8–15 mL) resulted in a drop of both conversion and selectivity towards the formation of DMC (entries 10–12).

The *N*-methylation of aniline

The next step of the investigation was to test whether DMC, once prepared through the reaction of Scheme 4, could be used as a methylating agent *in situ*, without isolating it from the mixture. Aniline (**3a**) was chosen as a model nucleophile. Experiments were performed at temperatures of 130–180 °C, in a stainless steel autoclave (150 mL) charged with aniline (**3a**: 0.5 g, 5.4 mmol), ethylene carbonate (**1a**: 2.0–4.0 g, 23–46 mmol), methanol (30–50 mL), and the NaX faujasite catalyst. In particular, four sets of conditions were used:

(i) Molar ratio (W) **1a** : **3a** = 4, methanol 30 mL; (ii) $W = 8.5$, methanol 30 mL; (iii) $W = 4$, methanol 50 mL; (iv) $W = 8.5$, methanol 50 mL. The weight ratio $Q' = \mathbf{3a} : \mathbf{FAU}$ was ranged from 1 to 3. After different time intervals (8–24 h), the reactor was cooled to rt and vented, and the reaction mixture was analyzed by GC-MS. Two additional tests (a–b) were carried out in the absence of (a) ethylene carbonate and of (b) the zeolite.

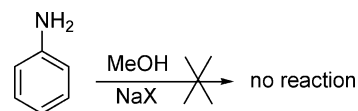
Four main products were identified: their structure was assigned by GC-MS and by comparison to authentic samples (Scheme 5).



Scheme 5

Results are reported in Table 2.

At 150 °C, aniline was recovered unaltered in the absence of faujasite (entry 1). By contrast, in presence of NaX ($Q' = 1$) conversions of 65 and 82% were measured after 8 h, at 150 and 180 °C, respectively (entries 3–4). Under these conditions, a moderate conversion was observed even at 120 °C (entry 2: conv. 43%, 20 h). The formation of both compounds **4a** and **5a** (*N*-methylaniline and *N,N*-dimethylaniline) proved that a methylation process occurred in all cases. By using methanol in the absence of ethylene carbonate at 150–200 °C for the methylation of aniline in the presence of the faujasite, no conversion was observed, thereby confirming that DMC was the active methylating agent (Scheme 6).¹⁴



T = 150–200 °C
MeOH: 30 mL
NaX: $Q = 1$
No ethylene carbonate

Scheme 6

However, under the conditions of entries 2–4, the selectivity was never satisfactory: the presence of sizeable amounts (17–26%) of products **6–7** indicated that competitive methylation and (β -hydroxy) ethylation reactions, mediated by DMC and ethylene carbonate respectively, took place to comparable extents. A higher loading of ethylene carbonate [conditions (ii): $W = 8.5$],

Table 2 The reaction of aniline (**3a**) with ethylene carbonate and methanol, catalyzed by NaX zeolite

Entry	MeOH/mL	3a : FAU, Q' (g : g) ^a	1a : 3a , W (mol : mol) ^b	$T/^\circ\text{C}$	t/h	Conversion (%) ^c	Products (% GC) ^d				
							4a	5a	6	7	Others
1	30	— ^e	4	150	8	—					
2	30	1	4	120	20	43	18	5	16	4	
3	30	1	4	150	8	65	17	22	11	15	
4	30	1	4	180	8	82	26	36	7	10	3
5	30	1	8.5	165	8	88	21	44	7	15	
6	30	1	8.5	180	8	97	8	64	3	19	3
7	30	2	4	180	8	96	5	40	26	20	5
8	30	3	4	180	8	99	9	13	35	30	11
9	50	1	4	150	8	24	20	4			
10	50	1	4	180	8	64	35	29			
11	50	1	4	180	24	88	24	64			
12	50	1	8.5	180	8	82	21	61			
13	50	1	8.5	180	16	99	5	89			5

^a Q' was the weight ratio between aniline and the NaX faujasite. ^b Molar ratio between ethylene carbonate and aniline. ^c Conversion of aniline. ^d The structure of products **4–7** was assigned by GC-MS and by comparison to authentic samples of **4a**, **5a** and **6**. Others were unidentified compounds detected by GC/MS analyses. ^e In the absence of faujasite.

improved aniline conversion (88–97%, entries 5–6), but it did not produce significant changes of the methylation selectivity: the total of methylamines (**4a** + **5a** = 65–72%) remained less than three times the amount of **6** and **7** (22–23%). The formation of the latter compounds was in fact favored by the use of higher catalyst loadings ($Q' = 2-3$, entries 7–8; **6** + **7** = 46–65%).

Although methanol did not take part in the alkylation reaction (Scheme 5) it played a crucial role on the reaction outcome: the increase of its volume (from 30 to 50 mL), had two effects: (a) it decreased the conversion (compare entries 4 and 10, and 6 and 12¹⁵); and (b) it greatly improved the selectivity towards the exclusive formation of methylamines (entries 9–13). Under these conditions, when the molar ratio ethylene carbonate/aniline (W) was augmented from 4 to 8.5, the reaction became faster and the bis-methylation process predominated (entries 9–11 and 12–13). At 180 °C, over a NaX zeolite catalyst, the green domino of Scheme 3, produced dimethylaniline (**5a**) in very high selectivity and yield (89%, 16 h: entry 13). Compound **5a** was purified by FCC (petroleum ether/diethyl ether, 95 : 5 v/v), and it was isolated in a 85% yield.

The *N*-methylation of primary aromatic amines with alkylene carbonates

To extend the scope of the green domino procedure, different anilines ($R'C_6H_4NH_2$; 0.5 g; **3b**: $R' = p\text{-MeO}$; **3c**: $R' = p\text{-Me}$; **3d**: $R' = p\text{-Cl}$; **3e**: $R' = p\text{-NO}_2$) were set to react with both ethylene and propylene carbonates (**1a** and **1b**, respectively). Experiments were run under conditions (iii) and (iv) previously described for aniline ($W = 4-8.5$, $Q' = 1$, $T = 180-200$ °C, MeOH = 50 mL). In all cases, the structures of products were assigned by GC-MS and by comparison to authentic samples.

The reaction of aniline (**3a**) with propylene carbonate was also investigated.

Finally, two further experiments were aimed at improving the overall mass index of the green domino.¹⁶ The reactions of aniline and *p*-anisidine, were performed by decreasing the amounts of both the catalyst and ethylene carbonate: Q' and W ratios were set to 0.1 and 3, respectively. In these cases, the temperature was increased to 190 °C.

Results are reported in Table 3.

Five main features emerged from this investigation:

(a) No competitive formation of *N*-(β-hydroxy)ethyl derivatives due to the reaction of ethylene or propylene carbonates with the amine was observed. The *N*-methylation reaction promoted by DMC was the sole observed process for each of the tested amines.

(b) Different aryl substituents on the anilines affected the final outcome. A reactivity scale was clearly evident: *p*-anisidine > *p*-toluidine ≥ aniline > *p*-chloroaniline >> *p*-nitroaniline. For example, after 8 h at 180 °C ($W = 8.5$), in the presence of ethylene carbonate, the reactions of *p*-anisidine (**3b**) and *p*-toluidine (**3c**) showed comparable conversions (100 and 95%, respectively); though, *N,N*-dimethyl *p*-anisidine **5b** was obtained in a 100% yield (entry 2), while **3c** gave a mixture of mono- and bis-*N*-methyl derivatives (**4c** + **5c**) in 8 and 83%, amounts (entry 5). Under the same conditions, the reaction of *p*-chloroaniline (**3d**) required a considerably longer time: a conversion of 91% was reached after 28 h (entry 7). The corresponding products of mono- and di-methylation (**4c** + **5c**) were observed in 9 and 90% quantities, respectively. Finally, *p*-nitroaniline reacted only at 200 °C: after 24 h, notwithstanding the high temperature, a modest conversion of 16% was attained (entry 9).

Table 3 The reaction of different anilines (**3a–e**) with alkylene (ethylene and propylene) carbonates, and methanol, catalyzed by NaX zeolite^a

$R = \text{H, Me}$
 $R' = \text{a: MeO; b: Me; c: Cl; d: NO}_2$

Entry	Alkyl carbonate	$R'C_6H_4NH_2$, R' :	3 : NaX, Q'	1 : 3 , W (mol: mol) ^b	$T/^\circ\text{C}$	t/h	Conversion (%) ^c	Products (% GC) ^d			Yield (%) ^e
								4	5	Others	
1	1a	3b : <i>p</i> -MeO	1	4	180	16	95	9	86		
2	1a	3b : <i>p</i> -MeO	1	8.5	180	8	100		100		98
3	1b	3b : <i>p</i> -MeO	1	8.5	180	8	96	9	87		
4	1a	3c : <i>p</i> -Me	1	4	180	24	92	12	80		
5	1a	3c : <i>p</i> -Me	1	8.5	180	8	95	8	83	4	78
6	1b	3c : <i>p</i> -Me	1	8.5	180	8	90	12	78		
7	1a	3d : <i>p</i> -Cl	1	8.5	180	28	99	9	90		87
8	1b	3d : <i>p</i> -Cl	1	8.5	180	28	91	23	68		
9	1a	3e : <i>p</i> -NO ₂	1	8.5	200	24	16	16			
10	1b	3a : H	1	8.5	180	24	97	8	86	3	
11	1a	3a : H	0.1	3	190	24	81	25	51	5	
12	1a	3b : <i>p</i> -MeO	0.1	3	190	24	87	18	69		

^a All reactions were carried out using 0.5 g of the substrate (**3a–e**), and 50 mL of MeOH. Q' ratio was in the range of 0.1–1. ^b Molar ratio between alkylene carbonate and aniline. ^c Conversion of the substrate. ^d The structure of products $ArNHMe$ and $ArNMe_2$ was assigned by GC-MS and by comparison to authentic samples. Others were unidentified compounds detected by GC-MS analyses. ^e Isolated yields of compounds **5b**, **5c**, and **5d**.

(c) As in the case of aniline, the increase of the W ratio from 4 to 8.5 improved the methylation rate for both *p*-anisidine and *p*-toluidine (compare entries 1–2, and 4–5).

(d) Both ethylene- and propylene-carbonate (**1a** and **1b**) could be used to produce DMC and to finally methylate amines **3a–e**. However, the use of **1a** allowed faster reactions with respect to **1b**. For example, after 8 h at 180 °C, compound **5b** (*p*-MeOC₆H₄NMe₂) was obtained in 100 and 87% yields using **1a** and **1b**, respectively (entries 2 and 3). Likewise, in the case of *p*-toluidine and *p*-chloroaniline, the amounts of products **5c** and **5d** (*p*-MeC₆H₄NMe₂ and *p*-ClC₆H₄NMe₂) were higher with **1a** than with **1b** (compare entries 5–6 and 7–8). A similar behavior held also for aniline, whose reaction with propylene carbonate (entry 10, Table 3: conv. 97%, 24 h) was slower than that with ethylene carbonate (entry 13, Table 2: conv. 99%, 16 h).

(e) The green domino proceeded even when NaX was used in a catalytic amount ($Q' = 0.1$) and ethylene carbonate was slightly over the stoichiometric quantity ($W = 3$) (entries 11 and 12). Although a temperature of 190 °C was necessary to allow sufficiently rapid conversions of both aniline and *p*-anisidine, these results proved not only the catalytic role of the faujasite, but also that the overall flow of materials involved in the process, could be improved to make the transformation more green and economic. However, further optimization of the conditions/parameters is the object of future studies.

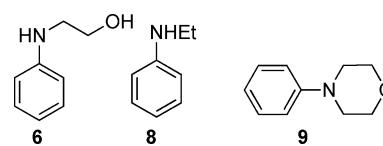
Once reactions of entries 2, 5 and 7 were completed, *N,N*-dimethyl-*p*-anisidine, *p*-toluidine and *p*-chloroaniline were purified by FCC (petroleum ether/diethyl ether, 95 : 5 v/v): they were isolated in 98%, 78%, and 87% yields, respectively.

The reaction of aniline with ethylene carbonate and light alcohols (ethanol and *n*-propanol)

The reaction of aniline and ethylene carbonate (Scheme 3) was carried out also with ethanol and *n*-propanol in place of methanol. Experiments were performed at 180 and 200 °C under the conditions of Table 3 ($W = 8.5$, $Q' = 1$).

Three products were identified by GC-MS and by comparison to authentic samples (Scheme 7).¹⁷ Results are reported in Table 4.

In the presence of ethanol, the conversion was good (89–96% after 15 h), but the selectivity was elusive: mixtures of **6** and **9** (total of 77–81%) were always obtained along with minor amounts of **8** (2–4%) and other unidentified by-products (8–17%) (entries 1–4). A larger volume of ethyl alcohol (from



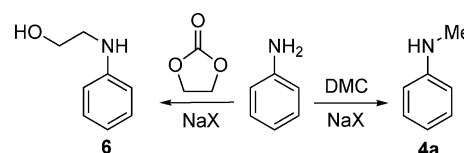
Scheme 7

50 to 110 mL) did not substantially improve the product distribution. Products **6** and **9** were observed also in the presence of *n*-propanol (entry 5): in this case, not even a trace of *N*-propylaniline (PhNHPr) was detected.

The relative reactivity of dialkyl carbonates

The results of Tables 2 and 3 showed that when methanol was present in a relatively large amount, the competition between DMC and ethylene carbonate as methylating and hydroxyethylating agents of primary aromatic amines was suppressed, and the *N*-methylation reaction proceeded with a selectivity up to 100%. By contrast, the corresponding reactions carried out with ethanol and propanol, took place with the exclusive formation of products derived from ethylene carbonate (Table 4). To investigate these aspects, the relative reactivity of DMC and ethylene carbonate was tested in competitive reactions with aniline. Two sets of experiments were performed at 90 °C (refluxing temperature of DMC) and at 140 °C, respectively. In both cases, a mixture of aniline (0.5 g, 5.4 mmol), DMC (10 g, 111 mmol), and NaX (0.5 g, $Q' = 1$), was set to react with different amounts of ethylene carbonate (**1a**). In particular, the molar ratio DMC : **1a** was increased from 1 to 5, 10, 20, and 40, respectively.

GC-MS analyses showed that major products were mono-*N*-methylaniline (**4a**) and mono-*N*-(β-hydroxy)ethylaniline (**6**) (Scheme 8),¹⁸ whose total amount (**4a** + **6**) corresponded to 97–99% of all the observed products.



Scheme 8

Results are reported in Fig. 1, where the ratio of anilines **6** : **4a** (GC amounts) is plotted against the molar ratio DMC : **1a**.

Table 4 The reaction of aniline (**3a**) with ethylene carbonate, in the presence of ethanol or *n*-propanol, and NaX zeolite catalyst^a

Entry	Alcohol/mL	$T/^\circ\text{C}$	t/h	Conversion (%) ^b	Products			
					8	6	9	Others
1	EtOH (50)	180	15	93	2	80	11	
2	EtOH (70)	200	15	96	2	39	38	17
3	EtOH (90)	200	15	94	3	50	11	10
4	EtOH (110)	200	15	89	4	43	34	8
5	<i>n</i> -PrOH (90)	200	15	92		55	32	5

^a All reactions were carried out using 0.5 g of the aniline, 0.5 g of NaX ($Q' = 1$), and 4.0 g of ethylene carbonate ($W = 8.5$). Different volumes of EtOH were used (entries 1–4: 50 to 110 mL). Entry 5: 90 mL of *n*-PrOH. ^b Conversion of aniline. ^c The structure of products **6**, **8** and **9** was assigned by GC-MS and by comparison to authentic samples. Others were unidentified compounds detected by GC-MS analyses.

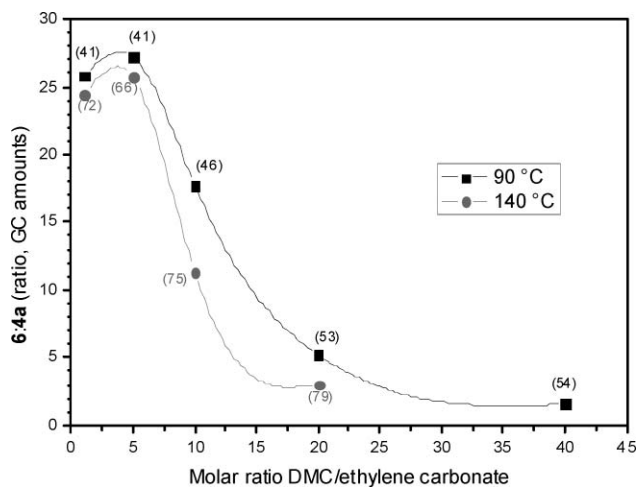


Fig. 1 Ratio of *N*-(β -hydroxy)ethylaniline (**6**)/*N*-methylaniline (**4a**) as a function of the DMC : **1a** molar ratio. Conversions of aniline are shown in parenthesis. ■: reactions at 90 °C; ●: reactions at 140 °C.

For a coherent evaluation, each set of data was calculated at comparable conversions.

At 90 °C, in the range of conversions of 41–54%, *N*-(β -hydroxy)ethylaniline (**6**) was always the main product even though ethylene carbonate (**1a**) was used in a considerably lower amount with respect to DMC (black curve). The ratio **6** : **4a**, decreased smoothly from ~27 to 5 while the molar ratio DMC : **1a** increased from 5 to 20. Remarkably, the quantity of **6** was 1.5 higher than that of *N*-methyl aniline, even when DMC was present in a 40 molar excess over ethylene carbonate: under these conditions, ethylene carbonate was understoichiometric to aniline.

An analogous behavior was observed at 140 °C. In the range of conversions of 66–79%, the ratio **6** : **4a** varied between 3 and 26 (grey curve). Apparently, the reaction temperature had a limited effect on the relative rates of hydroxyethylation and methylation of aniline. Ethylene carbonate was, by far, more reactive than DMC, and the formation of **6** was favored at all times, with respect to **4a**.

Other experiments were run at 140 °C, in the presence of co-solvents of different polarity: cyclohexane, 1,2-dimethoxy ethane, and *N,N*-DMF. A mixture of aniline (0.5 g, 5.4 mmol) dimethylcarbonate (13.11 g, 111 mmol), ethylene carbonate

(0.97 g, 11.1 mmol) (molar ratio DMC : **1a** = 10), and NaX (0.5 g), was set to react in presence of these solvents (20–40 mL).¹⁹

Results are reported in Table 5. For a convenient comparison, the table also includes the reaction carried out without added solvents.

Despite the excess of DMC used in all reactions, β -hydroxyethyl aniline (**6**) was always the preferred product, in particular in the presence of the apolar cyclohexane (40 mL) where **6** was the only observed product (entry 3). In the more polar DME and DMF (20 mL), the ratio **6** : **4a** was ~15 (entries 4–5), comparable to that reported using only DMC as a solvent (11.5, entry 1). A larger volume of DMF (40 mL) resulted in a considerable decrease of the ratio **6** : **4a** to 5.1 (entry 6). Higher dilution also caused longer reaction times for both cyclohexane and DMF: conversions of ~60% were reached after 2 and 3 h, respectively (entries 3 and 6).

Finally, at 140 °C, a mixture of aniline (0.5 g, 5.4 mmol), diethylcarbonate (13.11 g, 111 mmol) and ethylene carbonate (0.48 g, 5.4 mmol) (molar ratio DEC : **1a** = 20), was set to react in the presence of NaX (0.5 g). After 2 h, the conversion was of 60%, and *N*-(β -hydroxy)ethyl aniline (**8**) was the sole product. No competition was observed between ethylene carbonate and diethyl carbonate.

Discussion

The catalytic activity of faujasites

Alkali metal exchanged faujasites are often described as amphoteric solids²⁰ due to the simultaneous presence of Lewis acidic metal cations (Li^+ , Na^+ , K^+ , and Cs^+), and basic oxygen atoms in the zeolite framework. In particular, by following the acid–base scale proposed by Barthomeuf,²¹ Table 1 shows that more basic MX systems (entries 1–3) offer better performances than NaY and HY zeolites (entries 4–5) in the transesterification of ethylene carbonate with methanol. Even more specifically, a comparison among X-type faujasites indicates that KX (entry 3) is more active than NaX and LiX (entries 1 and 2, respectively), thanks to the milder acidic character of K^+ with respect to Na^+ and Li^+ . These results match those observed by other authors¹⁰ in the study of the transesterification of cyclic carbonates over zeolites. In general, this reaction is reported to be rather sensitive to the basic properties of the catalysts involved.^{5,22}

Table 5 The reaction of aniline with ethylene carbonate and DMC, in the presence of NaX and different co-solvents^a

Entry	Solvent/mL	ϵ^b	DMC : 1a (mol : mol) ^c	$T/^\circ\text{C}$	t/h	Conversion (%) ^d	Products			Ratio 6 : 4a
							4a	6	Others	
1	DMC (10)	3.08	10	140	1	75	6	69		11.5
2	CyH (20)	2.02	10	140	1	56	2	54		27
3	CyH (40)		10	140	2	61		61		∞
4	DME (20)	7.2	10	140	1	68	4	61	3	15.3
5	DMF (20)	38.3	10	140	1	60	3	47	10	15.6
6	DMF (40)		10	140	3	59	8	41	10	5.1

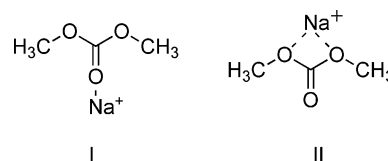
^a All reactions were carried out using aniline (0.5 g, 5.4 mmol), NaX (0.5 g, $Q' = 1$), DMC (10 g, 111 mmol), ethylene carbonate (0.98 g, 10.8 mmol), and the solvent (20 or 40 mL of cyclohexane, of 1,2-dimethoxyethane, and of *N,N*-DMF in entries 2–6, respectively). ^b Dielectric constants were taken from ref. 18. ^c Molar ratio between DMC and ethylene carbonate. ^d Conversion of aniline. ^e The structure of products **4a** and **6** was assigned by GC-MS and by comparison to authentic samples. Others were unidentified compounds detected by GC-MS analyses.

The “green domino”

The results of Table 2 show that in presence of the NaX faujasite catalyst a mixture of aniline, ethylene carbonate, and methanol react to produce mono-*N*- and bis-*N*-methyl anilines (**4a** and **5a**) as major products. In addition, in the absence of ethylene carbonate aniline is recovered fully unreacted (Scheme 5). This is evidence of the fact that methanol does not act itself as the methylating agent of the amine. The most plausible explanation for the occurrence of compounds **4a**–**5a**, is through two sequential processes: the transesterification of ethylene carbonate to yield dimethyl carbonate, which in turn methylates aniline (Scheme 3). This domino reaction may suffer from the competition between the two organic carbonates for the nucleophile (Scheme 8), and the formation of *N*-(β-hydroxy)ethyl anilines (**6** and **7**) is described accordingly.²³ Yet, 100% methylation selectivity can be achieved by increasing the volume of methanol from 30 to 50 mL (Table 2, entries 4 and 11). This beneficial effect is not likely to be due to the shift in the transesterification equilibrium of ethylene carbonate towards the formation of DMC due to MeOH (Scheme 3, path a). In fact, the ratio of the equilibrium concentrations does not vary significantly between the lowest MeOH : **1a** molar ratio (= 27.0) calculated with 50 mL of methanol, and the highest MeOH : **1a** molar ratio (= 34.5) calculated with 30 mL of methanol (Table 6).

Why then the exclusive formation of methyl anilines **4a** and **5a** with respect to hydroxyethyl amines **6** and **7**? A further consequence of the increase of methanol is the reduction of the reaction rate (for instance, compare entries 6 and 13 of Table 2). This result parallels the behavior reported for several liquid-phase processes catalyzed by faujasites:¹⁵ in general, the more polar the solvent is, the more it competes with organic reagents for the adsorption on active sites of the polar surface of zeolites, and consequently, the lower the reaction rates are. In our case however, a strong MeOH/faujasite interaction may also play a further role on the adsorption of dialkyl carbonates over the catalytic surface. In fact, IR and Raman investigations demonstrate that DMC (and likely ethylene carbonate as well) is adsorbed over the zeolites through the formation of acid–base complexes (I and II) with weak Lewis acidic sites (e.g. Na⁺ cations) of the framework of the aluminosilicate (Scheme 9).²⁴

These modes of adsorption of dialkyl carbonates are plausibly altered when methanol is itself co-adsorbed over the catalytic surface. Although the nature (and entity) of such a perturbation is not presently clear, its effect may modify the relative reactivity of DMC and ethylene carbonate, favoring the former (DMC). This behavior becomes unpredictable if the two organic carbonates are compared in the competitive



Scheme 9 Interactions of DMC with Na⁺ of faujasites.

alkylation of aniline catalyzed by NaX (Fig. 1): in the formation of *N*-(β-hydroxy)ethyl anilines (**6** and **7**, Scheme 5), the relief of some ring strain in ethylene carbonate likely accounts for its higher reactivity with respect to DMC.²⁵ Under these conditions however, a moderate, but visible, effect on the reaction selectivity, is observed if co-solvents are used (Table 5). In polar solvating media such as DMF, the methylation of aniline is less disfavored than in apolar cyclohexane, where the reaction may not take place at all. This evidence further corroborates the results above discussed: a large excess of polar MeOH alters the reaction environment to the point that the *N*-methylation of aniline occurs on an exclusive basis.

The outcome of reactions carried out with ethanol and *n*-propanol (Table 4), is also explained through the competitive reactivity of dialkyl carbonates. The alkylation rate of several nucleophiles, drops of 1–2 orders of magnitude by simply substituting DMC with diethyl carbonate (DEC).^{7,26} Accordingly, both diethyl- and dipropyl-carbonates, which form under the conditions of Table 4,²⁷ cannot vie with the more reactive ethylene carbonate.

Different anilines and different cyclic carbonates

Table 3 shows that the green domino is effective for different primary aromatic amines. The reactivity scale of these compounds leaves few doubts about the effect of aryl substituents: the *N*-methylation reaction is accelerated by electron-donating groups, while it becomes difficult with scantily nucleophilic amines such as *p*-chloro- and particularly, *p*-nitro-aniline. This closely follows a result previously described by us, for the alkylation of aromatic amines with DMC catalyzed by faujasites.⁷

Table 3 indicates that also propylene carbonate (**1b**) promotes the selective methylation of different anilines; though, the overall reaction rate drops with respect to the use of ethylene carbonate (**1a**). A plausible explanation comes from the study of the transesterification of cyclic carbonates with methanol: Arai *et al.*,⁵ have reported that when ethylene carbonate is replaced with propylene carbonate, the different steric hindrance of the two carbonates accounts for a sharp decrease of reactivity. For the same reason, the availability of DMC and consequently, the *N*-methylation rates decrease in the green domino promoted by **1b**.

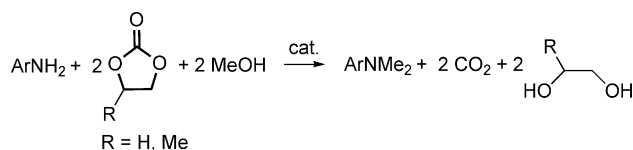
Conclusions

An innovative and selective synthesis of bis-*N*-methyl anilines is described through the reaction of aromatic amines, methanol and a cyclic carbonate. Although in the formal stoichiometry of the process, methanol is the alkylating agent (Scheme 10), the overall transformation proceeds *via* the coupling of two sequential processes, both catalysed by alkali metal exchanged faujasites.

Table 6 The excess of methyl alcohol over ethylene carbonate

Entry	Methanol/mL	1a : 3a (mol : mol) ^a	MeOH : 1a
1	30	4	34.5
2	30	8.5	16.2
3	50	4	57.4
4	50	8.5	27.0

^a Molar ratio between ethylene carbonate (**1a**) and aniline (**3a**). ^b Molar ratio between methanol and ethylene carbonate.



Scheme 10

In particular, ethylene or propylene carbonate react preferably in the presence of a NaX zeolite, with methanol, to produce dimethyl carbonate (DMC) which *in situ*, acts as an efficient methylating agent of anilines. This green domino sequence, offers an original approach from both synthetic and environmental standpoints: in fact, the transesterification of cyclic carbonates with MeOH is the preferred eco-friendly solution for the production of the non-toxic DMC, that itself possesses much better and greener alkylation performances than methanol. *N,N*-dimethylanilines can be isolated in good to excellent yields (78–98%), starting from *p*-substituted amines with both electron-donating and -withdrawing groups; though, the more nucleophilic the substrates (*e.g.* *p*-anisidine and *p*-toluidine), the faster the reaction. In addition, steric reasons likely account for the higher reactivity of ethylene carbonate with respect to propylene carbonate.

The study of competitive reactions of aniline with mixtures of ethylene carbonate and DMC, unequivocally proves that the cyclic carbonate is the better *N*-alkylating agent. Notwithstanding, under the *green domino* conditions, a methylation selectivity up to 99%, is achieved. This intriguing and unpredictable result is explained mainly by the presence of MeOH as a reagent/solvent, whose polar protic features alter the modes of adsorption (and the reactivity) of dialkyl carbonates over the surface of the faujasites catalysts. The effects observed in the presence of other polar and apolar co-solvents (DMF, DME and cyclohexane) further support these considerations.

Experimental

Anilines ($R'C_6H_4NH_2$; **3a**: $R' = H$, **3b**: $R' = p\text{-MeO}$, **3c**: $R' = p\text{-Me}$, **3d**: $R' = p\text{-Cl}$, **3e**: $R' = p\text{-NO}_2$), cyclic carbonates (**1a**: ethylene-; **1b**: propylene-carbonate), and dimethyl carbonate were ACS grade and were employed without further purification. Zeolites NaY and NaX were from Aldrich. The metal content of MX (M = Li, Na, K) and NaY catalysts was determined according to a procedure previously reported by us.¹⁵ Table 7 summarizes the composition of these solids.

Before each reaction, all the faujasites were dried by heating at 65 °C, under vacuum (10 mmHg) overnight.

Table 7 Faujasite catalysts

Starting zeolite (Na, %) ^a	Product	Ionic exchange (%) ^b
NaX (7.5)	LiX	71
NaX (7.5)	KX	92
NaY (8.1)		

^aThe Na content was evaluated through atomic adsorption (AA).

^bPercentage of ionic exchange (from NaX) was evaluated by AA (K) and emission (Li).

MS (EI, 70 eV) analyses were run using HP5/MS capillary columns (30 m), respectively. ¹H NMR spectra were recorded on a 300 MHz spectrometer, using CDCl₃ as solvent.

Reactions carried out in autoclave (Tables 1, 2, 3, 4, and 5).

General

A stainless-steel autoclave (150 mL of internal volume) equipped with a pressure gauge, a thermocouple, and two needle valves, was charged with the mixture of reagents and the catalyst. At room temperature and before each reaction, air was purged with a N₂ stream. The autoclave was then heated by an electric oven, while the reaction mixture was kept under magnetic stirring. After the desired time interval, the autoclave was cooled to rt, vented and opened. The reaction mixture was analysed by GC-MS.

The transesterification of ethylene carbonate with methanol (Table 1). A mixture of ethylene carbonate (**1a**: 2.2 g, 25 mmol), methanol (the volume ranged from 8 to 30 mL), and the catalyst (MX; M = Li, Na, K; NaY, and HY; the weight ratio **1a** : faujasite ranged from 4.8 to 15.7), was set to react at different temperatures (110–150 °C) for 5 h. Major products were dimethyl carbonate and 2-(hydroxy)ethyl methyl carbonate (**2**). Both compounds were not isolated: they were identified by GC-MS. 2-(Hydroxy)ethyl methyl carbonate (**2**): MS (EI), *m/z* (relative int.) 120 (M⁺, 1%), 89 (M⁺ – OCH₃, 14), 59 (M⁺ – O(CH₂)₂OH, 100), 58 (51). The structure of DMC was confirmed also by comparison to an authentic sample.

The methylation of aniline (Table 2). A mixture of aniline (**3a**: 0.5 g, 5.4 mmol), ethylene carbonate (**1a**: the weight amount ranged from 2.0 to 4.0 g; 23–46 mmol), methanol (the volume ranged from 30 to 50 mL), and NaX (the weight ratio **3a** : NaX ranged from 1 to 3), was set to react at temperatures of 130–180 °C, for different time intervals (4–24 h). Two additional tests were carried out in the absence of: (a) ethylene carbonate; (b) the zeolite. Products **4a** (mono-*N*-methyl aniline), **6** [*N*-(2-hydroxyethyl)aniline], and **7** [*N*-(2-hydroxyethyl)-*N*-methylaniline] were not isolated: they were identified by GC-MS and by comparison to authentic samples (only for **4a** and **6**). Product **5a** (bis-*N*-methylaniline) was isolated as reported below.

The methylation of primary aromatic amines (Table 3). A mixture of a primary amine ($R'C_6H_4NH_2$: 0.5 g; **3b**: $R' = p\text{-MeO}$; **3c**: $R' = p\text{-Me}$; **3d**: $R' = p\text{-Cl}$; **3e**: $R' = p\text{-NO}_2$), ethylene carbonate (1.4–3.5 g; the molar ratio **1a** : **3** ranged from 4 to 8.5), methanol (50 mL), and NaX (0.5 g), was set to react at temperatures of 180–200 °C, for different time intervals (8–28 h). Under the same conditions, reactions of *p*-anisidine, *p*-toluidine, *p*-chloroaniline, and aniline were carried out using propylene carbonate (**1b**: 3.5–4.0 g; the molar ratio **1b** : **3** was 8.5) in place of ethylene carbonate.

At 190 °C, the reaction of aniline and *p*-anisidine (0.5 g, 5.4 and 4.1 mmol, respectively) were also performed by decreasing the amounts of both NaX (0.1 g) and ethylene carbonate (1.1–1.4 g; the molar ratio **1a** : **3** was 3).

Isolation and characterization of *N,N*-dimethyl anilines ($R'C_6H_4NMe_2$; $R' = H, p\text{-MeO}, p\text{-Me}, p\text{-Cl}$). Under the

conditions of entry 13 in Table 2, and of entries 2, 5, 7 in Table 3, once reactions were completed (8–28 h), final mixtures were filtered, and methanol was removed by rotary evaporation. The viscous residues were purified by flash-chromatography on silica gel (F60; eluant: petroleum ether/diethyl ether, 95 : 5 v/v). *N,N*-dimethyl- aniline, *p*-anisidine, *p*-toluidine, and *p*-chloroaniline, were obtained in isolated yields of 85% (0.55 g), 98% (0.60 g), 78% (0.49 g), and 87% (0.53 g), respectively.

All *N,N*-dimethyl anilines were known products, whose characterization was carried out by ¹H NMR and GC-MS, and by comparison to commercial authentic samples. The spectroscopic/physical properties were in full agreement to those reported in the literature.²⁸

The reaction of aniline with ethylene carbonate in presence of ethanol or of *n*-propanol (Table 4). A mixture of aniline (**3a**: 0.5 g, 5.4 mmol), ethylene carbonate (4.0 g; 45.5 mmol), ethanol or *n*-propanol (the volume ranged from 50 to 110 mL), and NaX (0.5 g), was set to react at temperatures of 180–200 °C, for 15 h. Products **8** (mono-*N*-ethylaniline), **6** [*N*-(2-hydroxyethyl)aniline], and **9** (*N*-phenylmorpholine) were not isolated: they were identified by GC-MS and by comparison to authentic commercial samples.

The competitive reactions of aniline with ethylene carbonate and dimethyl carbonate (Fig. 1). Two sets of experiments were performed at 90 °C and at 140 °C, respectively. At 90 °C (refluxing temperature of DMC; method A), reactions were carried out using standard laboratory glassware. At 140 °C (method B), reactions were run in an autoclave.

Method A. A two-necked, round-bottomed, 50 mL flask fitted with a reflux condenser, a magnetic stirring bar, and an adapter for the withdrawal of samples, was charged with a mixture of aniline (0.5 g, 5.4 mmol), DMC (10 g, 111 mmol), NaX (0.5 g), and ethylene carbonate (9.7 g, 111 mmol). The mixture was placed under a nitrogen atmosphere at room temperature, and then heated in an oil bath at 90 °C. At intervals, aliquots (0.2 mL) of the mixture were analyzed by GC-MS, and products **4a** (mono-*N*-methylaniline) and **6** [*N*-(2-hydroxyethyl)aniline] were identified accordingly. Four subsequent experiments were carried out with the same procedure: since other conditions were unaltered, the amount of ethylene carbonate was decreased to 1.9, 0.97, 0.48, and 0.24 g (21.6, 11.0, 5.5, and 2.7 mmol), respectively.

Method B. A stainless steel autoclave (45 mL) was charged with a mixture of aniline (0.5 g), DMC (10 g), NaX (0.5 g), and ethylene carbonate (whose amount ranged from 9.7, 1.9, 0.97, and 0.48 g). Before, each reaction, at room temperature, the autoclave was degassed under a moderate vacuum (20 mm), and purged with a N₂ stream. The reactor was electrically heated at 140 °C, while the mixture was kept under a magnetic stirring throughout the reaction. After the desired time interval, the autoclave was cooled to rt and opened. The mixture was analysed by GC-MS.

The competitive reactions of aniline with ethylene carbonate and dimethyl carbonate, in presence of different co-solvents (Table 5). The experiments were performed according to the procedure described for method B. A 45 mL autoclave was charged with

aniline (0.5 g), DMC (10 g), NaX (0.5 g), and ethylene carbonate (0.97 g), in presence of a co-solvent. In particular, cyclohexane (20 and 40 mL), dimethoxyethane (20 mL), and *N,N*-DMF (20 and 40 mL) were used in five subsequent tests carried out at 140 °C.

Acknowledgements

MUR (Italian Ministry of University and Research) is gratefully acknowledged for financial support. Dr E. Militello is also acknowledged for his help in some experiments.

Notes and references

- Green Chemistry and Catalysis*, ed. R. A. Sheldon, I. Arends and U. Hanefeld, Wiley-VCH, Weinheim, Germany 2007.
- M. Selva and P. Tundo, *Acc. Chem. Res.*, 2002, **35**, 706–716.
- M. Massi Mauri, U. Romano, R. Tesei and P. Rebora, *Ind. Eng. Chem. Prod. Res. Dev.*, 1980, **19**, 396–402.
- T. Matsuzaki, A. Nakamura and Catal, *Surv. Jpn.*, 1997, **1**, 77–88.
- B. M. Bhanage, S.-I. Fujita, Y. Ikushina and M. Arai, *Appl. Catal. A: General*, 2001, **219**, 259–266.
- F. Rivetti, U. Romano and D. Delledonne, in *Green Chemistry: Designing Chemistry for the Environment*, ed. P. Anastas and T. C. Williamson, ACS Symposium Series 626, Washington, DC, 1996, pp. 70–80.
- (a) M. Aresta and E. Quaranta, *Tetrahedron*, 1991, **47**, 9489–9502; (b) M. Selva, C. A. Marques and P. Tundo, *J. Chem. Soc., Perkin Trans.*, 1994, **1**, 1323–1328; (c) Y. Ono, *J. Mol. Catal.*, 1994, **91**, 399–405; (d) A. Bomben, C. A. Marques, M. Selva and P. Tundo, *Tetrahedron*, 1995, **51**(42), 11573–11580; (e) M. Selva, A. Bomben and P. Tundo, *J. Chem. Soc., Perkin Trans.*, 1997, **1**, 1041–1045; (f) M. Aresta and E. Quaranta, *Chemtech*, 1997, 32–40; (g) P. Tundo, M. Selva and A. Bomben, *Org. Synth.*, 1999, **76**, 169–177; (h) A. Bomben, M. Selva, P. Tundo and L. Valli, *Ind. Eng. Chem. Res.*, 1999, **38**, 2075–2079; (i) M. Selva, P. Tundo, A. Perosa and S. Memoli, *J. Org. Chem.*, 2002, **67**, 1071–1077; (j) M. Selva, P. Tundo and A. Perosa, *J. Org. Chem.*, 2003, **68**, 7374–7378; (k) M. Selva, P. Tundo and T. Foccardi, *J. Org. Chem.*, 2005, **70**, 2476–2485; (l) M. Selva, P. Tundo, A. Perosa and F. Dall'Acqua, *J. Org. Chem.*, 2005, **70**, 2771–2777; (m) M. Selva and P. Tundo, *J. Org. Chem.*, 2006, **71**, 1464–1470; (n) M. Selva, P. Tundo, A. Perosa and D. Brunelli, *Green Chem.*, 2007, **9**, 463–468.
- By contrast, it should be noted that methylations with methyl halides or dimethyl sulfate, and carbonylations with phosgene always generate stoichiometric amounts of inorganic salts to be disposed of, they usually require additional solvents, and their exothermal outcome often needs a careful control.
- F. Schwochow and L. Puppe, *Angew. Chem., Int. Ed. Engl.*, 1975, **14**, 620.
- (a) T. Kondoh, Y. Okada, F. Tanaka, S. Asaoka, S. Yamamoto and A. Sachio (Chiyoda Corporation), USP 5436362, July 25, 1995; (b) J. F. Knifton and R. G. Duranleau, *J. Mol. Catal.*, 1991, **67**, 389–399.
- M. Onaka and K. Ishikawa, Y. Izumi, *Chem. Lett.*, 1982, 1783.
- Z. Kui, H. Changhua, Z. Huaibin, X. Shouhe, L. Shangyuan, X. Dong and L. Hexuan, *Appl. Catal.*, 1998, **166**, 89–95.
- Other compounds, whose total amount was usually less than 10%, were detected by GC-MS analyses: their structures were not assigned. The co-product ethylene glycol was also observed, but its GC signal showed poor intensity and resolution. It was excluded from the integration. The formation of 2-(hydroxy)ethyl methyl carbonate (**5**) was reported also in the transesterification of ethylene carbonate with MeOH, catalyzed by bases (see ref. 10b).
- (a) In the presence of different heterogeneous catalysts, methanol is often reported as a good *N*-methylating agent of aniline. See for example: N. Nagaraju and G. Kuriakose, *New J. Chem.*, 2003, **27**, 765–768; (b) M. A. Aramendia, V. Borau, C. Jimenez, J. M. Marinas and F. J. Romero, *Appl. Catal. A: General*, 1999, **183**, 73–80; (c) T. Oku, Y. Arita, H. Tsuneki and T. Ikariya, *J. Am. Chem. Soc.*, 2004, **126**, 7368–7377). However, high reaction temperatures of 250–500 °C are usually required.

- 15 Methanol and more generally, polar protic solvents strongly interact with polar surfaces of aluminosilicates (as zeolites are). Consequently, organic reactions catalysed by faujasites, are often inhibited in this media. See, for example: M. Selva, P. Tundo and A. Perosa, *J. Org. Chem.*, 2002, **67**, 9238–9247).
- 16 M. Selva and A. Perosa, *Green Chem.*, 2008, **10**, 457–464.
- 17 (a) Compound **9** (*N*-phenylmorpholine) was plausibly formed by the dehydration of the bis-*N*-alkyl derivative [PhN(CH₂CH₂OH)₂] of aniline. Zeolites are reported to catalyse the dehydration of diols: W. Hoelderich, M. Schwarzmann, *US Pat.*, 4904806, February 27, 1990; (b) C. Moreau, M. Naceur Belgacemb and A. Gandini, *Top. Catal.*, 2004, **27**, 11–30.
- 18 In the presence of faujasites, primary aromatic amines react with dialkyl carbonates to yield selectively the corresponding mono-*N*-alkyl amines (ArNHR). Good examples for both the case of DMC and of ethylene carbonate, are reported in ref. 7c, 7g–h, and by A. B. Shivakar, S. P. Gupte and R. V. Chaudari, *Synlett*, 2006, **9**, 1374–1378.
- 19 The polarity of cyclohexane, 1,2-dimethoxyethane, and *N,N*-dimethylformamide was assessed by the values of the corresponding dielectric constants (ϵ , Table 5) taken from the *Handbook of Chemistry and Physics*, ed. D. R. Lide, 75th edn, 1994, CRC Press.
- 20 B. Su and D. Barthomeuf, *Stud. Surf. Sci. Catal.*, 1995, **94**, 598.
- 21 D. Barthomeuf, *J. Phys. Chem.*, 1984, **88**, 42–45, see also, ref. 7k.
- 22 (a) Y. Watanabe and T. Tasumi, *Microporous Mesoporous Mater.*, 1998, **22**, 399–407; (b) M. S. Han, B. G. Lee, B. S. Ahn, K. Y. Park and S. I. Hong, *React. Kinet. Catal. Lett.*, 2001, **73**, 33–38; (c) H. Cui, T. Wang, F. Wang, C. Gu, P. Wang and Y. Dai, *Ind. Eng. Chem. Res.*, 2003, **42**, 3865–3870.
- 23 The possible reaction of aniline at the carbonyl carbon of both ethylene carbonate and DMC [Scheme 3, path b)], which would produce urethanes, is ruled out by the nature of faujasites. The acid–base features and steric requisites of these catalysts, allow the exclusive *N*-alkylations of aromatic amines (see also ref. 7 and 18).
- 24 (a) T. Beutel, *J. Chem. Soc., Faraday Trans.*, 1998, **94**, 985; (b) F. Bonino, A. Damin, S. Bordiga, M. Selva, P. Tundo and A. Zecchina, *Angew. Chem., Int. Ed.*, 2005, **44**, 4774–4777.
- 25 A similar trend of reactivity has been found also in the reaction of mixtures of ethylene carbonate (dimethyl carbonate with LiPF₆: S. E. Sloop, J. K. Pugh, S. Wang, J. B. Kerr and K. Kinoshita, *Electrochem. Solid-State Lett.*, 2001, **4**, A42–A44.
- 26 A. Perosa, M. Selva, P. Tundo and F. Zordan, *Synlett*, 2000, **2**, 272–274.
- 27 GC-MS analyses of reactions of Table 4 unequivocally prove the formation of both diethyl and dipropyl carbonates. These compounds have been identified by comparison to authentic samples.
- 28 M. Selva, A. Perosa, P. Tundo and D. Brunelli, *J. Org. Chem.*, 2006, **71**, 5770–5773.

Foam-like materials produced from abundant natural resources

Matthew D. Gawryla, Melissa Nezamzadeh and David A. Schiraldi*

Received 2nd May 2008, Accepted 18th July 2008

First published as an Advance Article on the web 22nd August 2008

DOI: 10.1039/b807473a

Low density polymer/clay aerogel composites were prepared using casein and sodium montmorillonite clay (Na⁺-MMT). The use of naturally occurring polymers allows for the creation of environmentally friendly/benign materials. Using a freeze drying process, composites were made that have densities in the range of 0.08–0.15 g cm⁻³ and exhibit properties similar to typical foamed polymers such as expanded polystyrene and rigid polyurethane foams. It was found that a minimum of at least 5wt% casein is required in the initial aqueous mixture in order to create a viable structure. The casein-containing materials created using this freeze drying process are similar to those previously produced with synthetic water soluble polymers such as poly(vinyl alcohol) but exhibit superior mechanical properties when compared to any synthetic polymer/clay aerogel composite tested to date.

Introduction

Low density polymeric materials, such as foams, are typically made from petroleum-based feedstocks, and make use of volatile organic compounds as foaming agents. Typical foaming procedures today use blowing agents such as pentane to expand the polymer structure to achieve the lower densities that are desired for packaging and cushioning applications. While pentane is believed to cause less environmental damage than the chlorofluorocarbons that they replaced, minimizing their use would appear to be sound environmental policy.

Many researchers are looking for ways to produce environmentally friendly low density materials. Several approaches utilize lignin based polyols, a natural byproduct of forestry and agricultural waste, for the synthesis of polyurethane (PU) foams.¹ These lignin type materials are competitive when compared to synthesized petroleum based polyols in price and availability, however they sometimes need to be chemically modified.² These chemical modifications detract from the overall environmental benefit to using natural materials.

We have previously demonstrated a robust, environmentally-benign process in which smectite clays are gelled in water, then freeze dried to produce aerogels with densities typically in the range of 0.05 g cm⁻³.³ These clay aerogels can be combined with a wide range of organic polymers, often in a single step, to produce aerogel/polymer composites with densities in the range 0.05–0.15 g cm⁻³ bearing a striking resemblance to polymer foam products.^{4–6} Preliminary results show these aerogel composites to exhibit thermal insulation properties similar to those of expanded polystyrene and other foamed polymers. Utilization of bio-based polymers in these aerogel composites would seem to be a reasonable next step in producing environmentally-responsible materials. One should note, however, that a full carbon-utilization cycle analysis is required in order to fully

justify the “greenness” of a new material, that the act of replacing a synthetic with a bio-based feedstock does not always ensure that society’s needs are being best served.

Casein is a naturally-occurring protein found in dairy products. There are several variations of casein that are in dairy products but are typically all grouped together under the name casein; the molecular weight of the various forms range from 19 kDa to 24 kDa. The amino acids that make up casein give the polymer significant ability to hydrogen bond; glutamic acid accounts for 20 percent of the chain while aspartic acid is another 6.4 percent. In addition to the strongly hydrogen bonding carboxylic acid groups, every residue in the backbone of the chain contains amides which can participate in hydrogen bonding as well. Recently, casein has been used as a component in PU composites⁷ as well as a component in water-based polymer blends.^{8–10} In the present work casein is combined with clay aerogels, producing useful composite materials in a single freeze drying step from aqueous protein/clay gels.

Experimental

Materials

Casein and sodium hydroxide (NaOH) were purchased from Fisher Scientific and used as received. Sodium montmorillonite, Na⁺-MMT, PGW grade was purchased from Nanocor Inc. and used without further modification. Deionized water was processed using a Barnstead RoPure reverse osmosis system.

Clay aerogel composite preparation

Composite samples were created by dissolving the appropriate amount of casein in 30 mL of a 0.17 M NaOH solution. Higher concentrations (10–15%) required gentle heating in order to fully dissolve the polymer. While the casein was dissolving, 2.75 g of PGW was blended in a Waring model MC2 mini laboratory blender with 27.5 mL of water to create a 10wt% clay gel. The two solutions were slowly mixed together in order to minimize

Department of Macromolecular Science and Engineering, Case Western Reserve University, Cleveland, OH, 44106-7202, USA

generation of trapped air bubbles. Once thoroughly mixed, the solution was poured into 5 dram (18.5 mL) polystyrene vials and frozen in a solid carbon dioxide/ethanol bath.

The frozen samples were dried in a Virtis AdVantage freeze dryer and once dry were removed from the vials for storage/testing. Compression samples approximately two centimeters high were cut from the monoliths using a bandsaw and the height was kept less than the diameter in order to prevent nonuniform deformation under compression. Compression testing was carried out using an Instron Model 5565 universal test machine with a crosshead speed of 1 mm min⁻¹. Density was calculated from dimension measurements using digital calipers and mass measurements to four significant places using a Mettler Toledo AB204-S analytical balance. A total of 6 replicates were tested for each composition whose density and compressive stress-strain properties were evaluated; samples were allowed to equilibrate with laboratory humidity at least 24 hours prior to taking density measurements.

Thermogravimetric analysis was carried out on a Mettler Toledo model TGA-SDTA 851e Thermogravimetric Analyzer, and was used to determine the actual polymer content for the materials. The samples were held at 25 °C for 5 minutes to allow them to equilibrate and then ramped from 25–500 °C at 20 °C min⁻¹ and held at 500 °C for 30 minutes. Samples were run in air in order to allow the entire polymer to be removed for compositional analysis.

A single 10wt% casein/5wt% PGW sample for thermal conductivity testing was made in a six inch square mold. The mold consisted of 1/2" thick, 1" tall polypropylene sides and utilized a 1/4" thick aluminium plate as the bottom to facilitate thermal transfer during freezing on a cold plate held at -70 °C. After freezing and drying, the top of the sample was cut off using a saw blade to create a six inch square panel one half of an inch thick. Thermal conductivity measurements were carried out by the Owens Corning Acoustic and Insulation Product Testing Laboratories, Granville, OH, USA.

Results and discussion

Freeze drying of aqueous clay/casein gels produced stable and sturdy aerogel monoliths in the shapes of the molds used to freeze the gels, Fig. 1. As the concentration of casein in the composite gel was increased, the expected monotonic increase in solution viscosity was observed (qualitatively), and a tendency to trap air bubbles, which translate into imperfections in the frozen water/clay/polymer ice and resultant freeze dried composite, was evident. It was also found that with increasing amounts of casein, the aerogel structure evolved from a highly lamellar morphology, with the layers distinctly separated, to a more continuous structure in which the layers appear to be connected by a web of polymer; the lamellar nature can still be seen but is not nearly as pronounced in the 15wt% as in the 5wt% Fig. 2.

Our previous research has shown that it is typically necessary to make several separate batches of the composites in order to account for structural variations which result from variable freezing conditions. These variations can affect the modulus of the composites, even though bulk densities are largely equivalent. Fig. 3 illustrates the linear dependency of composite



Fig. 1 Casein/clay aerogel composite monoliths, 2 cm diameter.

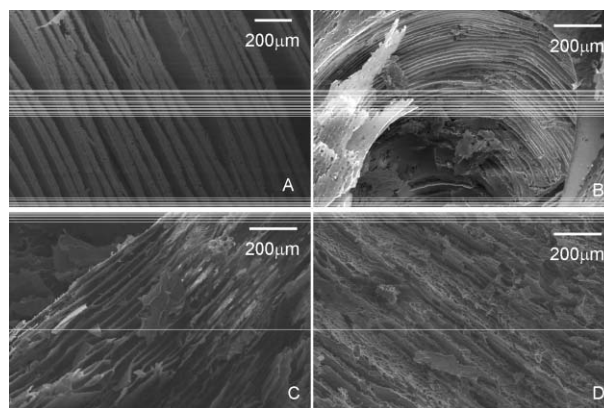


Fig. 2 SEM images of the various compositions (A) no casein (B) 5wt% casein, with an entrapped air bubble (C) 10wt% casein (D) 15wt% casein.

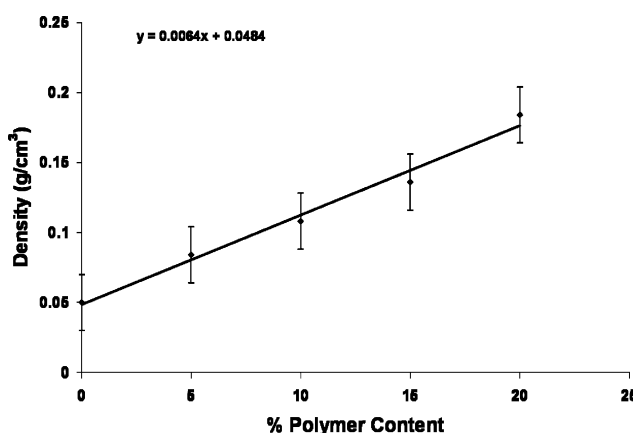


Fig. 3 Density as a function of polymer content.

densities on the polymer content in the composites (given as percentage of polymer in the starting aqueous gels).

One set of composite samples containing 20 wt% polymer was produced to better define the density curve; the high polymer loading of this material made it especially difficult to mix, increasing the potential for significant structural defects.

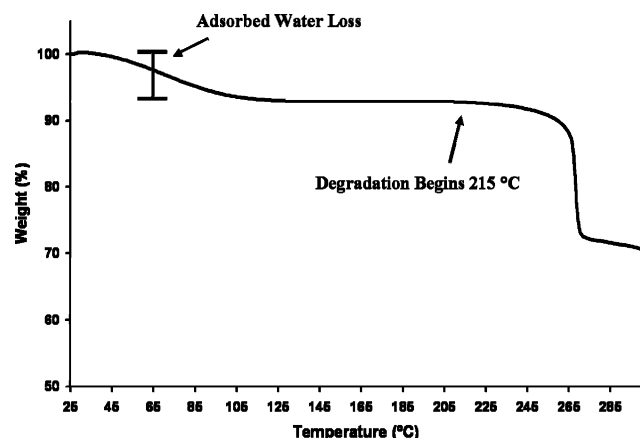
Table 1 Calculated and actual values of casein content in the dried composites

Composition	After freeze drying	
	Theoretical wt.% of casein	Measured wt.% of casein
5 wt%	50	59.4
10 wt%	66	62.4
15 wt%	75	69.5

The 20% polymer composite was not further tested for other properties.

Theoretical and observed values using thermogravimetric analysis for clay content in the composites are given in Table 1. Quantitative transfer of the protein/clay gels is difficult due to the high viscosity and tack of these materials; small losses of both polymer and clay material while transferring between containers used in composite preparation is thought to be responsible for the observed differences.

The initial weight loss routinely seen in our aerogel samples, Fig. 4, is attributed to adsorbed and absorbed water being removed by the dry air flowing over the sample coupled with increasing temperature. The wide temperature range of the moisture loss is likely due to the highly tortuous path created by the layered structure and diffusion out of the polymer. This water is not included in the weight percent calculations (Table 1), samples are normalized to the weight at approximately 150 °C and the difference between that weight and the final weight is determined to be the mass of the polymer.

**Fig. 4** Section of 15% casein composite TGA curve showing the onset of decomposition.

The incorporation of sodium hydroxide in combination with the processing techniques used appears to have no effect on the thermal decomposition of the casein. Thermal degradation of as received casein shows an onset of degradation at 211 °C; a similar water loss is observed in the casein and seems to be due to water uptake by the casein itself. The extent of water loss is increased in the composites and can be attributed to an increased surface area on which water can adsorb.

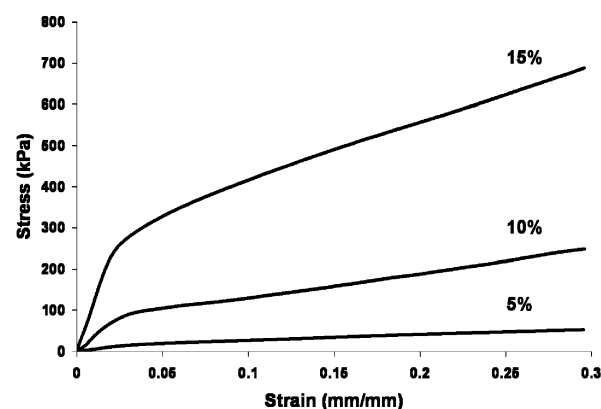
Thermal degradation of these composites is comparable to the thermal degradation of typical PU foam products. During decomposition, some portion of the PU foam returns to the monomers, typically an isocyanate and a polyol; further combustion of the isocyanate can produce hydrogen cyanide, HCN.¹¹

Table 2 Compression and density values

Casein	Modulus/kPa	St.Dev.	Density/g cm ⁻³	St.Dev.
0%	10	—	0.040	0.002
5%	500	200	0.084	0.002
10%	3000	1000	0.108	0.003
15%	12 000	3000	0.136	0.003

Casein is not known to produce hazardous by-products during decomposition, which gives added benefit to the casein/clay aerogel composites.

Density and compressive modulus values for the casein/clay aerogel composites are presented in Table 2. The unmodified clay aerogels are very difficult to handle without significantly damaging them, therefore the 0% polymer data are approximate and are included for order of magnitude comparison purposes. The compression curves exhibit the classical linear stress-strain, stress plateau and densification regions; the compressive yield stress of these materials increases dramatically with increased polymer loading, as can be seen in Fig. 5. A similar compression curve is generally observed with commercial expanded polystyrene foam materials; typical moduli of 3 MPa were measured in our laboratory, for 0.02 g cm⁻³ density foam. “Environmentally friendly” rigid and semi-rigid PU foams reported in the literature^{1,2,12} have compressive moduli in the range of 3–40 MPa and densities ranging from 0.03 g cm⁻³ to 0.16 g cm⁻³.

**Fig. 5** Example stress/strain curves for the various polymer loadings.

The non-linear dependence of compressive modulus on polymer loading within the composites is illustrated in Fig. 6. A minimum amount of casein is needed to form a stable composite structure; it is most likely that at concentrations lower than 5 wt% there is insufficient polymer to form the complete, interpenetrating co-continuous networks⁴ which most effectively transfer applied stress. Increasing the loading of polymer in the composite structures most likely allows for perfection of the foam-like structures, resulting in the vastly improved mechanical properties. When added to water, the 5% composite swells slightly and portions of the material begin to flake off until the entire piece is dispersed in solution. The polymer-free aerogel, being only a kinetically-trapped structure, is rapidly converted into a dispersed hydrogel upon addition of room temperature water. The 15% composite however only sheds a small amount

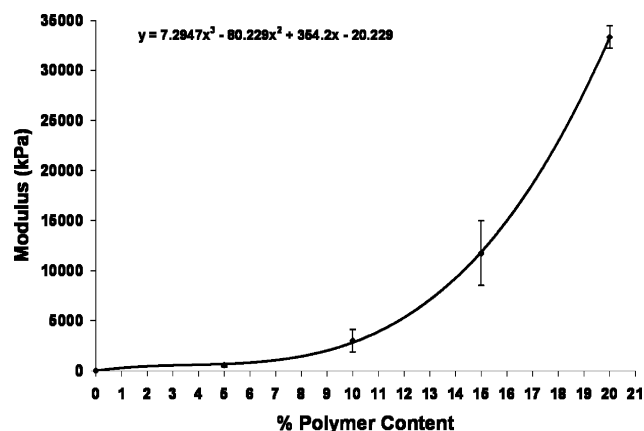


Fig. 6 Modulus as it relates to the initial polymer content. A trinomial fit of the data is shown on the graph.

of material and a dry core can be seen inside of a thin layer of swollen material; such a casein/clay aerogel composite material maintains this dry core/swollen shell state in room temperature water for a period of hours with the amount of dry material remaining shrinking over time as the water is able to penetrate the system.

Casein, a naturally-occurring protein, is known to readily biodegrade when exposed to environmental conditions. Smectite clays, such as montmorillonite, would be expected to simply return to the soil upon biodegradation of any organic components in a polymer/clay aerogel composite. The overall composition then, is a biologically-based, biodegradable organic polymer, combined with clay which can return to the soil from which it is derived. Processing to produce these materials is accomplished using only water as solvent, and commercially-available processing equipment.

Thermal conductivity of clay aerogels has been measured in the same range as that of conventionally foamed polymers. The casein reinforced material was measured to have a thermal conductivity of 0.045 W mK^{-1} which is near that of typical foamed polystyrene (0.03 W mK^{-1}). The low thermal conductivity values obtained when using casein to reinforce the clay aerogels allow these materials to be used as an alternative to conventional insulating foam in applications where environmental friendliness is of importance.

Conclusions

Bio-based, renewable casein can be combined with domestic clay to produce low density, polymer foam-like composite materials, utilizing water as the solvent. Low densities are inherent to these structures and therefore the process does

not need any blowing agents. These materials exhibit mechanical properties similar to those of rigid polyurethane foams specifically designated as being more environmentally friendly. The casein materials show good thermal insulation properties having thermal conductivities in the range of current insulation products. The combination of favorable mechanical and thermal insulation properties, the stability of the composites to elevated temperatures and to moisture, the use of a bio-based polymer (which is readily recovered from agricultural waste streams) and of an environmentally-benign process all suggest that these compositions have significant potential for consumer applications. The low, foam-like densities of the finished polymer/clay aerogel structures also raise the possibility of these being used as structural and/or insulation materials in transportation and other applications, wherein low final densities would translate to lowered energy consumption. Further investigation into other naturally occurring polymers as well as modification of casein should allow the properties to be tailored to fit many applications where low density is of great importance.

References

- 1 M. H. Alma and M. Altay Basturk, New polyurethane-type rigid foams from liquified wood powders, *J. Mater. Sci. Lett.*, 2003, **22**, 1225–1228.
- 2 H. Hatakeyama and T. Hatakeyama, Environmentally compatible hybrid-type polyurethane foams containing saccharide and lignin components, *Macromol. Symp.*, 2005, **224**, 219–226.
- 3 L. S. Somlai, S. A. Bandi, L. J. Mathias and D. A. Schiraldi, Facile processing of clays into organically-modified aerogels, *AIChE J.*, 2006, **52**(3), 1162–1168 March.
- 4 S. Bandi, M. Bell and D. A. Schiraldi, Temperature-responsive clay aerogel polymer composites, *Macromolecules*, 2005, **38**, 9216–20.
- 5 Editors' Choice, *Science*, 2005, 310, p. 407.
- 6 S. Bandi and D. A. Schiraldi, Glass transition behavior of clay/poly(vinyl alcohol) composites, *Macromolecules*, 2006, **39**(19), 6537–6545.
- 7 N. Wang, L. Zhang, Y. Lu and Y. Du, Properties of crosslinked casein/waterborne polyurethane composites, *J. Appl. Polym. Sci.*, 2004, **91**(1), 332–338.
- 8 N. Wang, L. Zhang and Y. Lu, Effect of the particle size in dispersions on the properties of waterborne polyurethane/casein composites, *Ind. Eng. Chem. Res.*, 2004, **43**, 3336–3342.
- 9 A. Bajpai and R. Saini, Preparation and characterization of spongy cryogels of poly(vinyl alcohol)–casein system: water sorption and blood compatibility study, *Polym. Int.*, 2005, **54**, 796–806.
- 10 E. Bulgarelli, F. Forni and M. T. Bernabei, Casein:gelatin beads: I. Cross-linker solution composition effect on cross-linking degree, *Int. J. Pharm.*, 1999, **190**, 175–182.
- 11 S. V. Levchik and E. D. Weil, Thermal decomposition, combustion and fire-retardancy of polyurethanes—a review of the recent literature, *Polym. Int.*, 2004, **53**, 1585–1610.
- 12 S. S. Narine, K. Kong, L. Bouzidi and P. Sporns, Physical properties of polyurethanes produced from polyols from seed oils: II. Foams, *J. Am. Oil Chem. Soc.*, 2007, **84**, 65–72.

Selective hydrogenation of unsaturated aldehydes in a poly(ethylene glycol)/compressed carbon dioxide biphasic system

Ruixia Liu,^{a,b} Haiyang Cheng,^{a,b} Qiang Wang,^{a,b} Chaoyong Wu,^{a,b} Jun Ming,^{a,b} Chunyu Xi,^a Yancun Yu,^a Shuxia Cai,^a Fengyu Zhao^{*a} and Masahiko Arai^c

Received 20th May 2008, Accepted 7th July 2008

First published as an Advance Article on the web 28th August 2008

DOI: 10.1039/b808486f

Hydrogenation of α,β -unsaturated aldehydes (citral, 3-methyl-2-butenal, cinnamaldehyde) has been studied with tetrakis(triphenylphosphine) ruthenium dihydride ($\text{H}_2\text{Ru}(\text{TPP})_4$) catalyst in a poly(ethylene glycol) (PEG)/compressed carbon dioxide biphasic system. The hydrogenation reaction was slow under PEG/ H_2 biphasic conditions at H_2 4 MPa in the absence of CO_2 . When the reaction mixture was pressurized by a non-reactant of CO_2 , however, the reaction was significantly accelerated. As CO_2 pressure was raised from 6 MPa to 12 MPa, the conversion of citral increased from 35% to 98%, and a high selectivity to unsaturated alcohols (geraniol and nerol) of 98% was obtained. The products were able to be extracted by high pressure CO_2 stream and separated from the PEG phase, dissolving the Ru complex catalyst and the catalyst was recyclable without any post-treatment.

Introduction

Selective hydrogenation of unsaturated aldehydes is an important step in producing unsaturated alcohols, which are important intermediates in the synthesis of fine chemicals like flavor, fragrance and pharmaceutical compounds.¹ However, since the C=C bond is more easily hydrogenated than the C=O bond, the selective hydrogenation of C=O in the aldehyde molecules with a conjugated C=C is still a challenging task. Many attempts have been made to develop suitable catalytic systems for improving the selectivity to unsaturated alcohols. Organometallic catalysts² have attracted continuous interest due to their high activity and selectivity and extensive studies have been carried out using Ru, Rh, Ir and other metals with phosphine or phosphate ligands.^{3–5} However, the difficulties in the separation of the noble metals and the ligands, which are often very expensive and/or toxic, have hindered their use in industry.

The immobilization of homogeneous catalysts was proposed to resolve the above problems, and for organometallic complex catalysts, they are usually immobilized in water,^{6–8} ionic liquid,⁹ fluorinated liquid¹⁰ or ethylene glycol¹¹ and the reactants and products are usually contained in organic phase. In the water–organic system, the catalysts must be modified to be sufficiently soluble in water, and the activity and/or selectivity of the water-soluble catalysts are normally lower than those of the organo-soluble parent catalysts. In the case of ionic liquids, the hydrophobic catalysts could be used and recycled easily.^{12,13} However, most of

ionic liquids are expensive and knowledge of their environmental impacts is still limited. Recently, poly(ethylene glycol) (PEG) has attracted increasing interest because it is non-volatile, recyclable and stable to acid and base.^{14–16} In addition, it can dissolve many organometallic complex catalysts without any modification of their structures,¹⁷ and it is inexpensive and non-toxic. In 1995, PEG was firstly used for the immobilization of homogeneous catalysts.¹⁸ It was reported that a water-soluble catalyst of $[\text{HRh}(\text{CO})(\text{TPPTS})_3]$ was dissolved in a PEG film and the mixture was dispersed on a silica gel; this supported liquid phase catalyst (SLPC) was effective for hydroformylation of 1-hexene. Then, the SLPCs were studied in various organic chemical reactions and have been well reviewed in the literature.¹⁹ Recently, PEG and compressed carbon dioxide have been investigated as recyclable and environmentally benign solvents in chemical reactions such as the Heck reaction, hydrogenation, hydroformylation, Suzuki cross-coupling and epoxidation.^{20–28} However, compressed carbon dioxide's low ability to dissolve organometallic complexes prevents its utilization in homogeneous catalytic synthesis. In contrast, PEG can dissolve various metal complexes and it can also dissolve large amount of CO_2 at high pressure, forming an expanded-liquid phase. Such an expansion causes changes in the physical properties of the PEG– CO_2 liquid mixture, lowering melting points and viscosity²⁹ and increasing gas/liquid diffusion rates³⁰ and ability to dissolve H_2 .³¹ Furthermore, PEG has a very limited solubility in compressed carbon dioxide and thus the organometallic catalysts could be immobilized in the PEG phase, useable for chemical reactions, and recyclable. When soluble organometallic complexes are used in the presence of pressurized CO_2 , the catalytic reactions occur in the CO_2 -expanded PEG phase. Heldebrandt and Jessop³² studied the hydrogenation of styrene catalysed with Wilkinson's complex $\text{RhCl}(\text{Ph}_3\text{P})_3$ in compressed CO_2 /PEG system. They pointed out that the catalyst remained stable in the PEG medium and could be recycled four times

^aState Key Laboratory of Electroanalytical Chemistry, Changchun Institute of Applied Chemistry, Chinese Academy of Sciences, Changchun, 130022, P. R. China. E-mail: zhaofy@ciac.jl.cn; Fax: 86 0431 85262410; Tel: 86 0431 85262410

^bGraduate School of the Chinese Academy of Sciences, Beijing, 100049, P. R. China

^cDivision of Chemical Process Engineering, Graduate School of Engineering, Hokkaido University, Sapporo, 060-8628, Japan

without noticeable loss of activity after the product, ethylbenzene, was separated by compressed carbon dioxide extraction. Leitner and co-workers^{33,34} reported that aerobic oxidation of alcohols could be catalysed effectively by PEG-stabilized palladium nanoparticles in compressed CO₂/PEG system. Recently, Wang *et al.*³⁵ also showed that aerobic oxidation of styrene catalysed by PdCl₂/CuCl could occur smoothly in compressed CO₂/PEG system.

Those results indicate that compressed CO₂/PEG biphasic systems are an attractive reaction medium, and so it is interesting and significant to further study their applications to recyclable and green multiphase catalytic systems for various reactions. The present work has hence been undertaken to investigate the features of compressed CO₂/PEG biphasic systems for selective hydrogenations of α,β -unsaturated aldehydes with a catalyst of H₂Ru(TPP)₄. For comparison, the same hydrogenation reactions were conducted in homogeneous systems using either cyclohexane or compressed carbon dioxide as a solvent. The effects of CO₂ pressure and molecular weight of PEG on the selective hydrogenation and the separation and recyclability of the catalyst-containing PEG phase were examined in detail.

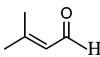
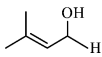
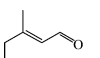
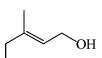
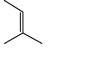
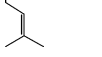
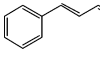
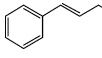
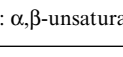
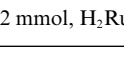
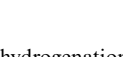

Results and discussion

Three α,β -unsaturated aldehydes were hydrogenated using a biphasic system of gas (H₂, CO₂) and liquid (PEG) including H₂Ru(TPP)₄ complex catalyst. Table 1 shows that for all the alde-

hydes examined, the C=O bonds are selectively hydrogenated, giving the corresponding unsaturated alcohols with selectivity levels >95%. These high selectivity values for unsaturated alcohols are comparable to the best data reported for similar hydrogenation reactions in water–toluene biphasic systems using water-soluble Ru-TPPTS and Ir-TPPTS catalysts.³⁶ The conversion levels with 3-methyl-2-butenal and citral are larger than that with cinnamaldehyde, probably due to differences in the structure of groups attached to the γ -carbon. The phenyl group is less electron-donating and can conjugate with the unsaturated bonds, which would make the C=O bond of cinnamaldehyde less reactive compared with the other two aldehydes.

The influence of solvents and CO₂ pressure has been examined using citral as a model substrate. It is well known that the rate of hydrogenation reactions depends on the solvents used.^{3,37,38} Table 2 shows the results of citral hydrogenation runs with H₂Ru(TPP)₄ catalyst in different solvents. In a conventional non-polar organic solvent of cyclohexane, a total conversion of 75% was observed with a selectivity of 93% to unsaturated alcohols (entry 1). A PEG (PEG-1000) solvent gave a lower conversion of 51% with a comparable high selectivity of 98% (entry 2). This difference in the total conversion between cyclohexane and PEG may be ascribable to differences in the solvent natures, which affect the solubility of a gaseous reactant of H₂ in the liquid phase and the rate of mass transfer between the gas and liquid phases and/or in the liquid phase. The viscosity of liquid PEG is known to drop dramatically (8–10-fold) by dissolution of CO₂.³⁹

Table 1 Results of hydrogenation of α,β -unsaturated aldehydes with H₂Ru(TPP)₄ in compressed CO₂/PEG

Entry	Substrate	Product	Time/h	Conversion (%)	Selectivity (%)
1			0.5	82	98
2			1	100	95
3			1	87	97
4			1.5	>99	99
5			2	43	95
6			8	>99	98

Reaction conditions: α,β -unsaturated aldehydes 2 mmol, H₂Ru(TPP)₄ 0.01 mmol; PEG-1000 2 g, H₂ 4 MPa, CO₂ 10 MPa, 338 K.

Table 2 Results of hydrogenation of citral with H₂Ru(TPP)₄ in different solvents

Entry	Solvent	Conversion (%)	Selectivity (%)	
			Citronellol	Geraniol & nerol
1	Cyclohexane	75	4	93
2	PEG-1000	51	2	98
3	CO ₂	100	1	99
4	CO ₂ /cyclohexane	96	1	99
5	CO ₂ /PEG600	100	1	99
6	CO ₂ /PEG-1000	100	1	99
7	CO ₂ /PEG2000	100	1	99
8	CO ₂ /PEG6000	100	1	99
9	CO ₂ /PEG-10000	79	1	99
10	CO ₂ /PEG-12000	52	1	99

Reaction conditions: citral 2 mmol, H₂Ru(TPP)₄ 0.01 mmol, cyclohexane 2 ml, PEG 2 g, CO₂ 8 MPa, H₂ 4 MPa, 338 K, 2 h.

Probably the solubility of H₂ and the rate of mass transfer should be larger in cyclohexane than in PEG. When neat 8 MPa CO₂ was used, a higher conversion and a similar high selectivity were obtained (entry 3). The reactant of citral used was completely soluble in the solvent, CO₂, and the catalyst was also almost soluble (a minor quantity of the catalyst loaded was not soluble, as seen by visual observation). Under the present conditions, therefore, the hydrogenation should occur in the homogeneous CO₂ gas phase, in which gas–liquid mass transfer boundary is absent and H₂ can be completely miscible, resulting in the high conversion as compared with those obtained in cyclohexane and PEG-1000. The specific nature of the complex catalyst to the selective hydrogenation of carbonyl bond does appear in the compressed CO₂ gas phase as well.

It is interesting that, when the biphasic reaction mixtures using cyclohexane and PEG were pressurized by 8 MPa CO₂, the conversion was enhanced to levels > 95% and the selectivity to unsaturated alcohols was almost perfect (99%) (entries 4, 5). The pressurization with CO₂ promotes the dissolution of H₂ into the liquid phases and the mass transfer in the liquid reaction phases, which may explain the rate enhancement observed. The liquid phases dissolving CO₂ molecules are also effective media for the H₂Ru(TPP)₄ complex catalyst to show its specific activity for selective hydrogenation of the C=O bond. A slight increase in the selectivity was observed with cyclohexane (entries 1, 4) and this could indicate the significance of molecular interactions between the carbonyl bond and the dissolved CO₂ molecules for the selectivity enhancement.^{40–42}

In addition, PEG solvents with different molecular weights have been tested for citral hydrogenation under biphasic conditions with 8 MPa CO₂. Table 2 indicates that the PEG solvents of 600–6000 in molecular weight show no differences in the conversion and in the selectivity (entries 5–8). However, when the molecular weight is increased to 10000 and 12000, the conversion decreases to 79% and 52%, respectively, but the selectivity to unsaturated alcohols remains unchanged (entries 9, 10). Their more viscous natures may have negative effects on the dissolution of H₂ and the mass transfer in the liquid reaction phase.

Table 3 gives the results of citral hydrogenation runs at different CO₂ pressures with a solvent of PEG-1000. The reaction mixture was biphasic at pressures up to 16 MPa, as confirmed by visual observations. The solvent was observed to expand by dissolution of CO₂ with increasing pressure but to a

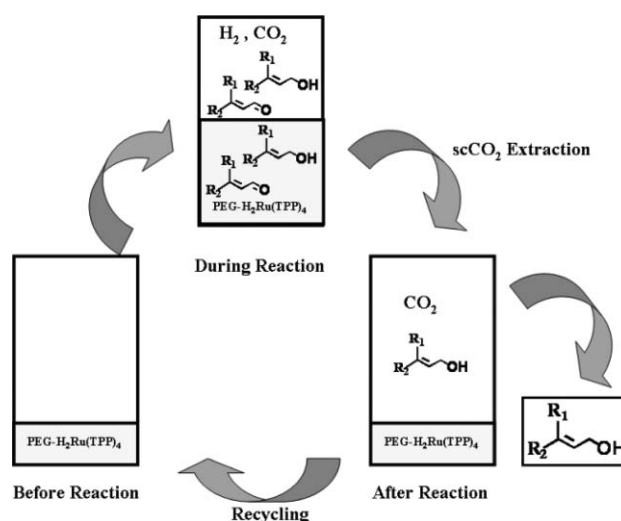
Table 3 Influence of CO₂ pressure on hydrogenation of citral with H₂Ru(TPP)₄ in compressed CO₂/PEG

Entry	CO ₂ /MPa	Conversion (%)	Selectivity (%)	
			Citronellol	Geraniol & nerol
1	0	13	3	97
2	6	35	3	97
3	8	53	2	98
4	10	87	3	97
5	12	98	2	98
6	14	100	2	98
7	16	100	1	99

Reaction conditions: citral 2 mmol, H₂Ru(TPP)₄ 0.01 mmol, PEG-1000 2 g, H₂ 4 MPa, 338 K, 1 h.

less extent <10%, in contrast to a conventional organic solvent like cyclohexane.¹⁶ In the absence of CO₂, a low conversion of 13% was obtained under the conditions used but the selectivity to unsaturated alcohol was as high as 97%, owing to the specific catalytic feature of the H₂Ru(TPP)₄ complex. It should be noted that the conversion can significantly be enhanced when high CO₂ pressure is used. At 12 MPa or higher, the hydrogenation is completed in 1 h. It is reported in the literature that in aerobic oxidation of styrene with PdCl₂/CuCl catalyst in the scCO₂/PEG biphasic system, CO₂ pressure has a small effect on the rate of oxidation but a larger effect on the product selectivity.³⁵

The recyclability of H₂Ru(TPP)₄ complex catalyst has been examined for citral hydrogenation under CO₂ gas-PEG liquid biphasic conditions. Scheme 1 illustrates the processes of catalytic reaction and catalyst–product separation. The products were extracted and separated from the PEG phase with compressed carbon dioxide. After reaction, the reaction mixture was kept in contact with a stream of 10 MPa CO₂ at a flow rate of 5 cm³ min⁻¹ and at 323 K until no products were detected in the effusion from the reactor and collected in *n*-hexane. Then, the separated PEG phase containing the complex catalyst was used for next reaction run without further purification or activation. Fig. 1 shows the results of four runs (three recycling runs), indicating that the conversion decreases but the high selectivity to unsaturated alcohols (geraniol and nerol) remains unchanged. A possible factor responsible for the decrease in the catalytic activity observed is the structural change of H₂Ru(TPP)₄ complex catalyst. We observed a change of the PEG liquid phase from yellow to olive in color after recycling runs.^{43,44} This suggests the dissociation and/or partial oxidation of the phosphine ligands, causing some change of the catalyst complex molecules and resulting in the decrease in the catalytic activity. From the point of industrial utilization, a more air-stable catalyst should be desired and investigated in further work. Another possibility for the loss of activity is the leaching of Ru species. As described above, the products were extracted by scCO₂ and collected in *n*-hexane. The concentration



Scheme 1 Reaction, separation, and recycling processes in hydrogenation of α,β -unsaturated aldehydes with Ru complex catalyst under gas (H₂, CO₂)–liquid (PEG) biphasic conditions.

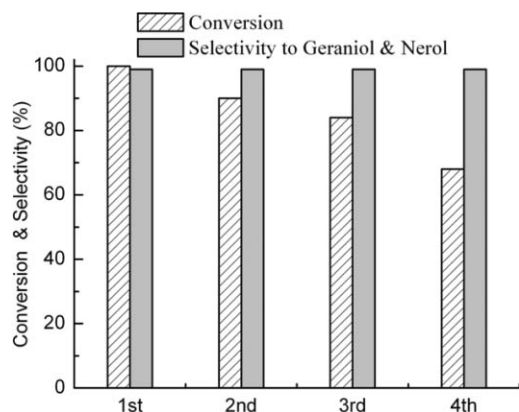


Fig. 1 Results of catalyst recycling test in hydrogenation of citral with $\text{H}_2\text{Ru}(\text{TPP})_4$ in compressed CO_2 /PEG. Reaction conditions: citral 2 mmol, $\text{H}_2\text{Ru}(\text{TPP})_4$ 0.01 mmol, PEG-1000 2 g, H_2 4 MPa, CO_2 8 MPa, 338 K, 2 h.

of Ru species collected in the *n*-hexane was measured by atomic absorption spectroscopy, which was 0.0065 ppm. This indicates that the leaching of Ru species is less than 0.001% of the initial amount of Ru loaded in PEG phase; namely, $\text{H}_2\text{Ru}(\text{TPP})_4$ catalyst could be successfully immobilized in PEG phase and separated from the products easily by CO_2 extraction. The authors did not measure the quantity of the phosphorous species in the effluent and do not deny the possibility of the leaching and loss of the ligand components as a factor causing the catalyst deactivation observed (Fig. 1). By contrast, the metal leaching was claimed to be responsible for the loss of catalytic activity in the hydrogenation of scCO_2 in the presence of dimethylamine with $\text{H}_2\text{Ru}(\text{TPP})_4$ catalyst attached to the terminus of polymer chains.⁴³

Conclusions

The present results demonstrate that the biphasic system of PEG and compressed carbon dioxide is effective for selective hydrogenation of α,β -unsaturated aldehydes using PEG-soluble $\text{H}_2\text{Ru}(\text{TPP})_4$ catalyst and H_2 as a reductant. The reactions can proceed smoothly in this CO_2 -dissolved expanded liquid PEG phase, in which the solubility of H_2 is larger and the mass transfer rate is also larger as compared with the viscous neat PEG phase. The organic products are separable from the PEG phase by extraction with high pressure CO_2 stream and this CO_2 extraction causes no leaching of Ru species from the PEG phase. The catalyst-containing PEG phase is recyclable without any post-treatment but the activity of the catalyst gradually decreases during the repeated reaction runs, probably due to its structural alteration as indicated by the color change. The high selectivity to unsaturated alcohols can remain unchanged during recycling, which is characteristic of the active form of $\text{H}_2\text{Ru}(\text{TPP})_4$.

Experimental

Chemicals

All experiments were carried out under nitrogen atmosphere. Unsaturated aldehydes, $\text{RuCl}_3 \cdot 3\text{H}_2\text{O}$, and triphenylphosphine

(TPP) were purchased from Aldrich and PEGs from Beijing Chemical Reagent Company, and they were used without further purification. Gases of CO_2 (99.995%) and H_2 (99.999%) (Changchun Xinxing Gas Company) were used as delivered. Benzene and methanol were used in catalyst preparation and cyclohexane in hydrogenation, which were dried and distilled under nitrogen atmosphere before use.

Catalyst synthesis and characterization

$\text{RuCl}_2(\text{TPP})_3$ and $(\text{H})_2\text{Ru}(\text{TPP})_4$ were prepared according to the literature.^{45,44} $\text{RuCl}_3 \cdot 3\text{H}_2\text{O}$ (0.8 g, 3.8 mmol) was dissolved in methanol (250 ml) and the solution was refluxed under nitrogen atmosphere at 338 K for 5 min. After cooling, TPP (6.0 g, 22.9 mmol) was added in a TPP/Ru mole ratio of 6, and the solution was refluxed again under nitrogen for 5 h. The complex precipitated from the hot solution and, after cooling, it formed a shiny black crystal. The crystals formed were filtered and washed several times with degassed methanol. Finally, the crystal samples were dried under vacuum. Those crystals were subjected to FTIR measurement with a Bruker Vertex 70 model and absorption bands were observed at 1480, 1433, 1087 cm^{-1} , as shown in Fig. 2, indicating the formation of $\text{RuCl}_2(\text{TPP})_3$. Then, $(\text{H})_2\text{Ru}(\text{TPP})_4$ was synthesized from this prepared complex.⁴⁴ $\text{Ru}(\text{Cl})_2(\text{TPP})_3$ (1.0 g) was dissolved in a hydrogen-saturated solution of benzene (60 ml)–methanol (100 ml) mixture containing TPP (6.0 g), and then NaBH_4 was added until the color of the solution changed from deep red to light orange. The solution was stirred for 1 h at room temperature; initially white $(\text{H})_4\text{Ru}(\text{TPP})_3$ precipitated and changed to yellow $(\text{H})_2\text{Ru}(\text{TPP})_4$. The complex formed was filtrated and washed several times with degassed methanol, and then dried at 313 K in vacuum for 12 h. The complex samples prepared were stored under argon before use. The formation of $(\text{H})_2\text{Ru}(\text{TPP})_4$ complex was confirmed by FTIR (Fig. 2b).

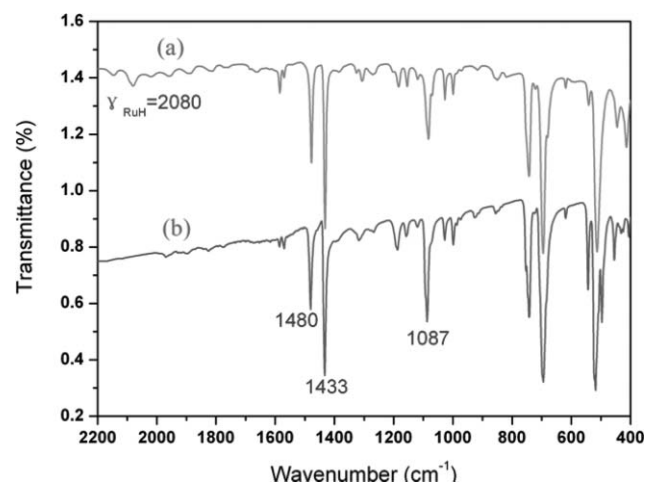


Fig. 2 FTIR spectra of Ru complex samples prepared: (a) $\text{H}_2\text{Ru}(\text{TPP})_4$ and (b) $\text{RuCl}_2(\text{TPP})_3$.

Hydrogenation reaction

The hydrogenations were carried out in a stainless steel batch reactor (50 ml). $(\text{H})_2\text{Ru}(\text{TPP})_4$ (0.01 mmol), PEG (2 g) and

reactant (2 mmol) were loaded into the reactor quickly and then the reactor was sealed and flushed with 2 MPa CO₂ more than three times. After the reactor was heated up to a reaction temperature of 338 K, first H₂ and then CO₂ were introduced into the reactor up to the desired pressures with a high-pressure liquid pump. The reaction time was recorded after the stirring was started. After reaction, the reactor was cooled down to room temperature and depressurized carefully by a backpressure regulator. Then, the products were extracted with *n*-hexane or compressed carbon dioxide and analysed with gas chromatography (GC-Shimadza-14C, FID, Capillary column Rtx-Wax 30 m, 0.53 mm, 0.25 mm) and gas chromatography/mass spectrometry (GC/MS, Agilent 5890). The extraction with compressed carbon dioxide was made by passing 10 MPa CO₂ through the reactor at a flow rate of 5 ml min⁻¹ and at 323 K until no products were detected in effusion.

Phase behavior studies

Since the phase behavior plays a very important role for the chemical reactions in compressed carbon dioxide, it is crucial to observe the state of the reaction system. An 80 ml high-pressure sapphire-windowed reactor was used to examine the phase behavior. Appropriate amounts of reactants, PEG and (H)₂Ru(TPP)₄ were added into the reactor in order to create the same conditions as used in the 50 ml reactor for hydrogenation runs, and then the system was flushed with 2 MPa CO₂ more than three times. The reactor was heated up to 338 K (reaction temperature) and H₂ (4.0 MPa) was introduced into the reactor and then CO₂ was added gradually up to the desired total pressure ranging from 4 to 21.0 MPa. The mixture was maintained at a certain pressure for several minutes while stirring. Then the stirring was stopped and the state of mixture was observed by the naked eye from the window, as described previously.⁴⁶

Acknowledgements

The authors gratefully acknowledge to the financial support from the NSFC 20573104 and the One Hundred Talent Program of CAS.

References

- K. Bauer and D. Garbe, *Common Fragrance and Flavor Materials*, VCH, New York, 1985.
- B. Cornils and W. A. Herrmann, *Applied Homogeneous Catalysis with Organometallic Compounds*, VCH, Weinheim, 2000.
- E. Fache, C. Santini, F. Senocq and J. M. Basset, *J. Mol. Catal. A: Chem.*, 1992, **72**, 337–350.
- K. Nuithitikul and M. Winterbottom, *Chem. Eng. Sci.*, 2004, **59**, 5439–5447.
- F. Lopez-Linares, M. G. Gonzalez and D. E. Paez, *J. Mol. Catal. A: Chem.*, 1999, **145**, 61–68.
- R. A. Sanchez-Delgado, M. Medina, F. Lopez-Linares and A. Fuentes, *J. Mol. Catal. A: Chem.*, 1997, **116**, 167–177.
- F. Joo, J. Kovacs, A. C. Benyei and A. Katho, *Angew. Chem., Int. Ed.*, 1998, **37**, 969–970.
- K. Nomura, *J. Mol. Catal. A: Chem.*, 1998, **130**, 1–28.
- A. L. Monteiro, F. K. Zinn, R. F. DeSouza and J. Dupont, *Tetrahedron: Asymmetry*, 1997, **8**, 177–179.
- I. T. Horva'th and J. Ra'bai, *Science*, 1994, **266**, 72–72.
- S. Fujita, Y. Sano, B. M. Bhanage and M. Arai, *Appl. Catal., B*, 2006, **314**, 89–93.
- R. A. Brown, P. Pollet, E. McKoon, C. A. Eckert, C. L. Liotta and P. G. Jessop, *J. Am. Chem. Soc.*, 2001, **123**, 1254–1255.
- F. C. Liu, M. B. Abrams, R. T. Baker and W. Tumas, *Chem. Commun.*, 2001, 433–434.
- J. Chen, S. K. Spear, J. G. Huddleston and R. D. Rogers, *Green Chem.*, 2005, **7**, 64–82.
- H. F. Zhou, Q. H. Fan, W. J. Tang, L. J. Xu, Y. M. He, G. J. Deng, L. W. Zhao, L. Q. Gu and A. S. C. Chanc, *Adv. Synth. Catal.*, 2006, **348**, 2172–2182.
- D. J. He ldebrant, H. N. Witt, S. M. Walsh, T. Ellis, J. Rauscherb and P. G. Jessop, *Green Chem.*, 2006, **8**, 807–815.
- W. Leitner, *Nature*, 2003, **423**, 930–931.
- M. J. Naughton and R. S. Drago, *J. Catal.*, 1995, **155**, 383–389.
- F. Zhao, S.-I. Fujita and M. Arai, *Curr. Org. Chem.*, 2006, **10**, 1681–1695.
- C. C. Luo, Y. H. Zhang and Y. G. Wang, *J. Mol. Catal. A: Chem.*, 2005, **229**, 7–12.
- S. Chandrasekhar, T. Shyamsunder, G. Chandrashekar and C. Narsihmulu, *Synlett*, 2004, **3**, 522–524.
- S. Chandrasekhar, S. J. Prakash and C. L. Rao, *J. Org. Chem.*, 2006, **71**, 2196–2199.
- Y. C. Yang, J. Y. Jiang, Y. H. Wang, C. Liu and Z. L. Jin, *J. Mol. Catal. A: Chem.*, 2007, **261**, 288–292.
- L. Bai and J. X. Wang, *Curr. Org. Chem.*, 2005, **9**, 535–553.
- Y. Du, J. Q. Wang, J. Y. Chen, F. Cai, J. S. Tian, D. L. Kong and L. N. He, *Tetrahedron Lett.*, 2006, **47**, 1271–1275.
- A. Baiker, *Chem. Rev.*, 1999, **99**, 453–473.
- P. G. Jessop, *Chem. Rev.*, 1999, **99**, 475–493.
- W. Leitner, *Acc. Chem. Res.*, 2002, **35**, 746–756.
- M. A. McHugh and T. J. Yogan, *J. Chem. Eng. Data*, 1984, **29**, 112–115.
- C. Dariva, L. A. F. Coelho and J. V. Oliveira, *Fluid Phase Equilib.*, 1999, **160**, 1045–1054.
- N. P. Freitag and D. B. Robinson, *Fluid Phase Equilib.*, 1986, **31**, 183–201.
- D. J. Heldebrant and P. G. Jessop, *J. Am. Chem. Soc.*, 2003, **125**, 5600–5601.
- Z. S. Hou, N. Theyssena and W. Leitner, *Green Chem.*, 2007, **9**, 127–132.
- Z. S. Hou, N. Theyssena, A. Brinkmann and W. Leitner, *Angew. Chem., Int. Ed.*, 2005, **44**, 1346–1349.
- J. Q. Wang, F. Cai, E. Wang and L. N. He, *Green Chem.*, 2007, **9**, 882–887.
- J. M. Grosselin, C. Mercier, G. Allmang and F. Grass, *Organometallics*, 1991, **10**, 2126–2133.
- S. Mukherjee and M. A. Vannice, *J. Catal.*, 2006, **243**, 108–130.
- S. Mukherjee and M. A. Vannice, *J. Catal.*, 2006, **243**, 131–148.
- D. Gourgouillon, H. Avelino, J. Fareleira and M. N. Da Ponte, *J. Supercrit. Fluids*, 1998, **13**, 177–185.
- F. Zhao, S. Fujita, S. Akihara and M. Arai, *J. Phys. Chem. A*, 2005, **109**, 4419–4424.
- S. Fujita, S. Akihara, F. Zhao, M. Hasegawa, R. Liu and M. Arai, *J. Catal.*, 2005, **236**, 101–121.
- R. Liu, F. Zhao, S. Fujita and M. Arai, *Appl. Catal., A*, 2007, **361**, 127–133.
- Y. Kayaki, Y. Shimokawatoko and T. Ikariya, *Adv. Synth. Catal.*, 2003, **345**, 175–179.
- R. O. Harris, N. K. Hotal, L. Sadavoy and J. M. C. Yuen, *J. Organomet. Chem.*, 1973, **54**, 253–264.
- T. A. Stephenson and G. Wilkinson, *J. Inorg. Nucl. Chem.*, 1966, **28**, 945–956.
- F. Y. Zhao, Y. Ikushima, M. Chatterjee, O. Sato and M. Arai, *J. Supercrit. Fluids*, 2003, **27**, 65–72.

Sustainable production of acrolein: gas-phase dehydration of glycerol over 12-tungstophosphoric acid supported on ZrO₂ and SiO₂

Song-Hai Chai, Hao-Peng Wang, Yu Liang and Bo-Qing Xu*

Received 31st March 2008, Accepted 7th July 2008

First published as an Advance Article on the web 29th August 2008

DOI: 10.1039/b805373a

Catalytic gas-phase dehydration of glycerol to produce acrolein was investigated at 315 °C over ZrO₂- and SiO₂-supported 12-tungstophosphoric acid (H₃PW₁₂O₄₀, HPW) catalysts with different treatment temperatures. Characterizations with XRD and Raman spectroscopy of the prepared HPW/SiO₂, HPW/ZrO₂ catalysts showed that the nature of support materials had a significant effect on the thermal stability of HPW; after thermal treatment at 650 °C, the Keggin structure of HPW remained intact on the surface of ZrO₂ but was completely destroyed on SiO₂. HPW on ZrO₂ also showed higher dispersion than on SiO₂. In comparison to HPW/SiO₂, HPW/ZrO₂ catalysts exhibited significantly higher activity and selectivity for the formation of acrolein, as well as a slower deactivation rate during the dehydration reaction. The selectivity and yield for acrolein over the better HPW/ZrO₂ catalysts can be as high as 70 mol% and 54%, respectively, even after 10 h reaction.

1. Introduction

Renewable biomass and its derivatives show potential to serve as alternatives for sustainable production of fuels, chemicals and materials, because the processing of biomass is CO₂ neutral.^{1,2} Being a biomass-derivative, glycerol is currently produced in a large amount as a by-product in manufacturing biodiesel by transesterification of vegetable oils with methanol or ethanol.^{3,4} Over the last decade, the growing production of biodiesel led to a surplus production and price decline of glycerol, which made glycerol a promising low-cost feedstock for producing value-added chemicals or materials.^{5,6} Much work has been devoted to the transformation of glycerol by various catalytic processes involving reforming, oxidation, hydrogenolysis, etherification, esterification and so on.^{7,8} Catalytic conversion of glycerol to acrolein by a double-dehydration reaction could offer a potential route for sustainable production of acrolein, which is an important intermediate in the chemical industry and currently manufactured by gas-phase oxidation of petroleum-based propylene.

Various acid catalysts, including liquid and solid acids, have been investigated for glycerol dehydration in the gaseous phase, liquid phase, or sub- and super-critical water.^{9–18} Solid acids would be more desirable for practical application because liquid acids would lead to the known technical and environmental problems, such as reactor corrosion, poor catalyst reusability and additional waste management. In our earlier work, we tested a wide variety of typical solid acid–base catalysts for the synthesis of acrolein by gas-phase dehydration of glycerol.^{19,20} It was shown that the most effective acid strength by Hammett

acidity function (H_0) for the selective formation of acrolein is $-8.2 \leq H_0 \leq -3.0$, with which acrolein can be produced at a selectivity up to 60–70 mol%. One of the very selective solid acids was Keggin-structure 12-tungstophosphoric acid (H₃W₁₂O₄₀, HPW) supported on alpha-alumina but this H₃W₁₂O₄₀/α-Al₂O₃ catalyst deactivated rapidly, probably because of its low surface area (*ca.* 4 m² g⁻¹).¹⁹ Acidic or neutral solids with large surface area, such as silica gel (SiO₂), Kieselguhr, and active carbon are documented as suitable supports for HPW,^{21,22} the most frequently used support being SiO₂. However, HPW supported on SiO₂ could have poor thermal stability, due to weak interaction between HPW and SiO₂.²³ Thermal decomposition of Keggin HPW over the support material would cause a significant loss of acidity, and therefore decrease the catalytic activity.

When used as a catalyst support, zirconia (ZrO₂) often produces better catalysis than other conventional oxide supports for a number of reactions.^{24–27} Supporting HPW on ZrO₂ was reported to enhance the thermal stability of HPW.^{28,29} The HPW/ZrO₂ catalyst was also shown to be efficient for various acid-catalyzed reactions including alkylation, esterification, isomerization and dehydration.^{30–34} A simple and effective procedure for the preparation of ZrO₂ (denoted as ZrO₂-AN) by thermal processing of an alcogel-derived ZrO(OH)₂ at elevated temperature has been developed in this laboratory.^{35–38} For thermal treatment up to at least 800 °C, ZrO₂-AN shows always a higher surface area and narrower particle size distribution in comparison to its counterpart prepared from conventional hydrogel-derived ZrO(OH)₂. Our earlier use of ZrO₂-AN as catalyst support has resulted in superior Ni/ZrO₂ catalysts for methane reforming,^{35–39} WO₃/ZrO₂ for *n*-heptane isomerization,⁴⁰ and Au/ZrO₂ for CO oxidation reactions.⁴¹ In the present study, we have compared the catalytic behavior of HPW supported on SiO₂ and ZrO₂-AN for the gas-phase dehydration of glycerol. HPW/ZrO₂-AN catalysts show not

Innovative Catalysis Program, Key Lab of Organic Optoelectronics & Molecular Engineering, Department of Chemistry, Tsinghua University, Beijing, 100084, China. E-mail: bqxu@mail.tsinghua.edu.cn; Fax: +86-10-62792122; Tel: +86-10-62792122

only a significantly higher activity and selectivity for acrolein formation, but also a much better catalytic stability than their HPW/SiO₂ counterparts, which seems to be associated with a higher dispersion and thermal stability of HPW on the surface of ZrO₂-AN. This finding could be important, since a high selectivity combined with higher catalyst stability would always be crucial in green chemistry. Also, the high thermal stability of HPW on ZrO₂-AN catalyst could easily enhance the catalyst survival during repeated regeneration.

2. Experimental

2.1 Catalyst preparation

HPW/ZrO₂-AN catalysts of different HPW loadings were prepared by impregnation of an alcogel-derived ZrO(OH)₂ with an ethanol solution containing the desired amount of HPW. The excess ethanol was removed using a rotary evaporator at 35–45 °C. The resultant powders were dried (110 °C) overnight and then thermally treated up to 350 or 650 °C in an N₂ flow (4 h). According to HPW loading (*x* in wt%) and thermal treatment temperature (*T* in °C), the final catalysts were denoted as *x*PWZ-AN-*T* (*x* = 15 and 30, *T* = 650). A commercial silica gel (Beijing Chemical Reagent Co.), after being calcined at 700 °C (BET surface area: 260 m² g⁻¹), was used to prepare HPW/SiO₂ samples with similar impregnation of HPW in ethanol; these samples were denoted as *x*PWS-*T* (*x* = 15 and 30, *T* = 350 and 650). The preparation procedure of alcogel-derived ZrO(OH)₂ was described in earlier publications.^{35,36,38} The catalyst powders were pressed, crushed, and sieved to 20–40 mesh before use.

2.2 Catalyst characterization

BET surface areas of the catalyst samples were measured by nitrogen physisorption isotherms at -196 °C on a Micromeritics ASAP 2010C instrument. The samples were dehydrated under vacuum at 200 °C for 5 h prior to the measurement. X-Ray diffraction (XRD) patterns were measured on a Bruker D8 Advance X-ray diffractometer with a Ni-filtered Cu K_α (λ = 0.15406 nm) radiation source at 40 kV and 40 mA. Raman spectra were recorded in the range of 200–1100 cm⁻¹ on a RM2000 (Renishaw) microscopic confocal laser (514 nm) Raman spectrometer.

2.3 Catalytic reaction

The gas-phase dehydration reaction of glycerol was carried out at 315 °C (a “standard” reaction temperature for our study of glycerol dehydrogenation^{19,20}) under atmospheric pressure in a vertical fixed-bed tubular quartz reactor (i.d. 9 mm, length 50 cm), which was heated by a tubular furnace with a height of 40 cm. A constant catalyst volume (0.63 ml) was sandwiched in the middle of the reactor with quartz wool. 2 ml quartz sand (2 cm in height) was placed above the catalyst bed. Prior to the reaction, the catalyst was pretreated at 315 °C for 1.5 h in flowing dry nitrogen (30 ml min⁻¹). The reaction feed, an aqueous solution containing 36.2 wt% glycerol (molar glycerol/water = 1/9), was fed continuously into the reactor inlet (at the top of the reactor) by a micro-pump. Our setup of the reactor and furnace provided a long preheating zone (*ca.* 13 cm) in the reactor to heat

and vaporize the reaction feed, and the quartz sand bed above the catalyst ensured complete evaporation of the glycerol/water mixture for the reaction. The catalytic performance of the solid catalysts was evaluated at a gas hourly space velocity (GHSV) of 400 h⁻¹ by glycerol. Our previous work has disclosed that the use of low glycerol GHSV (*i.e.* 80 h⁻¹) for the reaction would produce complete glycerol conversion (100%) for longer than 10 h, during which an induction period up to 8 h would be observed for obtaining a stable acrolein selectivity.¹⁹ Increasing the GHSV to 400 h⁻¹ helped to shorten the induction period for the further study of the catalyst stability.¹⁹ Therefore, the dehydration reaction of this study was conducted with glycerol GHSV = 400 h⁻¹, which is 6–20 times higher than those glycerol GHSVs (20–60 h⁻¹) documented for the same reaction in open patents.^{15–17}

The reaction products were condensed in an ice-water trap and collected hourly for analysis on a HP6890 GC equipped with a HiCap CBP20-S25-050 (Shimadzu) capillary column (i.d.0.32 mm × 25 m) and an FID detector.^{19,20}

3. Results and discussion

3.1 Catalyst characterization

The BET surface area and Keggin-anion density of the PWZ and PWS samples are presented in Table 1. The density of Keggin-anion (HPW nm⁻²) expressed as the number of Keggin anions per square nanometre was calculated according to the actual HPW loading and catalyst surface area. The surface area of PWZ-AN-650 samples (99–133 m² g⁻¹) was much higher than that of ZrO₂-AN-650 (55 m² g⁻¹) without HPW, indicating that impregnation of ZrO(OH)₂-AN with HPW helped to reduce the sintering of ZrO₂ during the thermal treatment. At the same level of HPW loading (15 wt% or 30 wt%), PWS samples showed a higher surface area and consequently a lower Keggin-anion density than PWZ samples.

Fig. 1 shows the XRD patterns of “pure” HPW and PWS samples thermally treated at 350 °C and 650 °C. The samples treated at 350 °C (Fig. 1A) exhibited clear diffractions at 2θ = 10.2°, 20.6°, 25.3°, 29.4°, and 34.6° that were associated with the Keggin structure of HPW,^{29,42} suggesting that Keggin HPW

Table 1 BET surface area and Keggin-anion density of ZrO₂- and SiO₂-supported H₃PW₁₂O₄₀ catalysts

Catalyst	HPW loading (wt%)	BET surface area/m ² g ⁻¹	Keggin-anion density ^a /HPW nm ⁻²
SiO ₂	0	260	0
15PWS-350	15	188	0.17
30PWS-350	30	141	0.46
15PWS-650	15	191	0.17
30PWS-650	30	162	0.40
ZrO ₂ -AN-650	0	55	0
15PWZ-AN-650	15	133	0.19
30PWZ-AN-650	30	99	0.66

^a Keggin-anion density (HPW nm⁻²)

$$= \frac{[\text{HPW loading (wt\%)} \div 100] \times 6.02 \times 10^5}{\text{BET surface area of catalyst (m}^2 \text{ g}^{-1}) \times 2880.2}$$

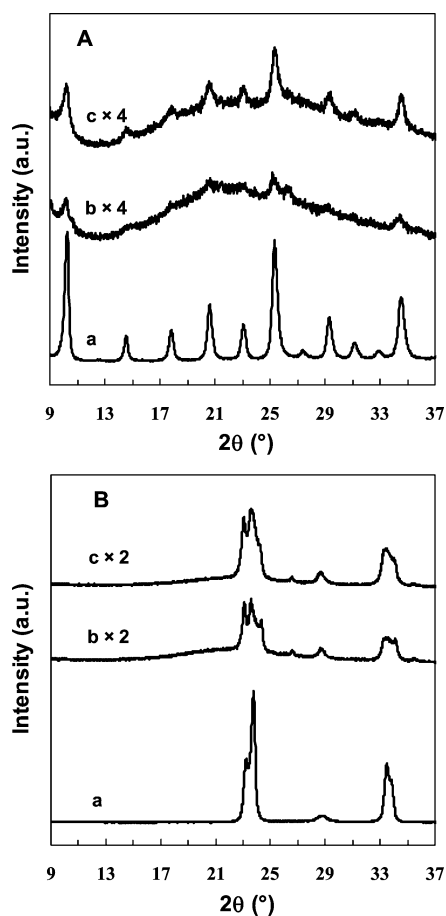


Fig. 1 XRD patterns of (a) $\text{H}_3\text{PW}_{12}\text{O}_{40}$, (b) 15PWS, and (c) 30PWS samples thermally treated at (A) 350 °C and (B) 650 °C.

remained after the treatment at 350 °C. The samples treated at 650 °C (Fig. 1B) showed no diffractions of the HPW Keggin structure but those characteristic of tungsten oxide (WO_3) at $2\theta = 23.2^\circ$, 23.8° , and 33.5° ,²⁸ which indicated a complete decomposition of HPW to WO_3 -based crystallites during the catalyst treatment. These observations are consistent with earlier documentation^{23,43,44} that the stability of HPW on SiO_2 was comparable to or slightly lower than that of pure HPW, and it underwent decomposition at around 500 °C to WO_3 and phosphorous oxide.

Fig. 2 shows the XRD patterns of PWZ-AN-650 as well as “pure” ZrO_2 -AN-650 samples. ZrO_2 -AN-650 without HPW was composed of monoclinic crystallites characterized by the diffractions at $2\theta = 28.5^\circ$ and 31.7° .³⁶ The XRD pattern of 15PWZ-AN-650 sample, which contains 15 wt% HPW, was characterized by a much stronger diffraction at $2\theta = 30.4^\circ$ for tetragonal ZrO_2 crystallites; the diffractions for monoclinic crystallites ($2\theta = 28.5^\circ$ and 31.7°) were weak. The 30PWZ-AN-650 sample with 30 wt% HPW showed no diffractions for monoclinic crystallites but only those for tetragonal ZrO_2 crystallites. These results demonstrate that the interaction between HPW and $\text{ZrO}(\text{OH})_2/\text{ZrO}_2$ during the catalyst preparation inhibited the formation of the monoclinic ZrO_2 phase and such an inhibition effect was dependent on the HPW loading.²⁸ On the other hand, the XRD patterns of PWZ-AN samples showed,

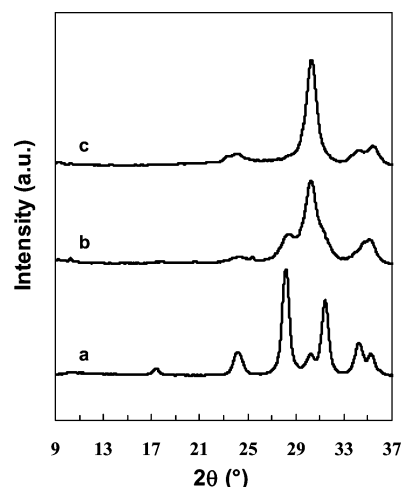


Fig. 2 XRD patterns of (a) ZrO_2 -AN-650, (b) 15PWZ-AN-650 and (c) 30PWZ-AN-650 samples.

in contrast with those of PWS-650 samples shown in Fig. 1, no information about the Keggin structure or its decomposition product WO_3 , which indicates that HPW or its decomposed species (possibly mixed oxides containing WO_3 - P_2O_5 or WO_3 - P_2O_5 - ZrO_2) exist as highly dispersed species in the PWZ samples. The PWZ and PWS samples were further characterized with Raman scattering spectroscopy to gain information about the structure and interaction of HPW in the catalysts.

As shown in Fig. 3, the 15PWS-350 sample showed two overlapping bands at *ca.* 1007 cm^{-1} and 990 cm^{-1} , which can be attributed to the symmetric and asymmetric stretching modes of the terminal $\text{W}=\text{O}$ bond of HPW Keggin anions, respectively.⁴⁵ Whereas, 15PWS-650 showed two bands at around 808 cm^{-1} and 720 cm^{-1} , corresponding to the stretching and bending modes of $\text{W}-\text{O}-\text{W}$ of WO_3 (or WO_3 -based species) produced from the decomposition of HPW, respectively.⁴⁶ These Raman results were in support of the XRD results shown in Fig. 1 on the thermal stability of HPW in PWS samples.

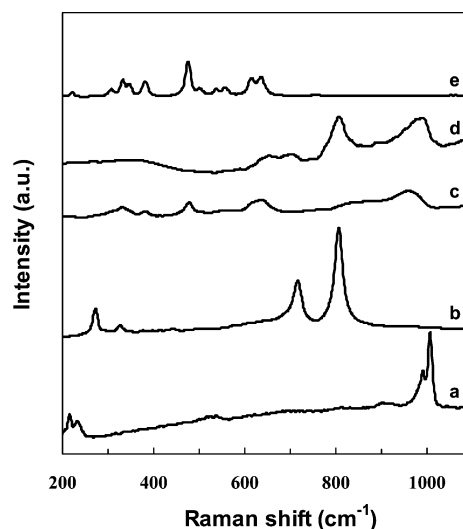


Fig. 3 Raman spectra of (a) 15PWS-350, (b) 15PWS-650, (c) 15PWZ-AN-650, (d) 30PWZ-AN-650 and (e) ZrO_2 -AN-650 samples.

For PWZ samples, Raman bands above 700 cm^{-1} were used to characterize the structure of supported tungsten-containing species (*i.e.* Keggin HPW or WO_3) because any signal for these species below 700 cm^{-1} would be relatively weak and easily overlap with Raman bands associated with the ZrO_2 support. According to Fig. 3c, 15PWZ-AN-650 showed a broad band at *ca.* 960 cm^{-1} with a weak shoulder around 850 cm^{-1} . The band at 960 cm^{-1} can be related to the stretching modes of terminal $\text{W}=\text{O}$ of Keggin HPW. However, the band exhibited a red-shift by about 50 cm^{-1} in comparison to those (1007 cm^{-1} and 990 cm^{-1}) of Keggin HPW, possibly due to the weakening of the terminal $\text{W}=\text{O}$ bond of Keggin HPW by interaction with the ZrO_2 surface. The shoulder at around 850 cm^{-1} could be attributed to the stretching mode of $\text{W}-\text{O}-\text{W}$ in Keggin HPW.⁴⁵ Unlike in the case of PWS-650, no Raman bands corresponding to WO_3 were observed. Thus, the Keggin structure of HPW in 15PWZ-AN-650 appeared to be preserved. For 30PWZ-AN-650, with a higher HPW loading, Raman bands for the Keggin structure were observed at $950\text{--}990\text{ cm}^{-1}$ but a band characteristic of WO_3 was also seen at 807 cm^{-1} ; the presence of WO_3 would indicate a partial decomposition of HPW Keggin structure.

The above results disclose that the nature of the support material has a significant effect on the thermal stability of HPW during the thermal treatment up to $650\text{ }^\circ\text{C}$; the Keggin structure of HPW remained intact on the surface of ZrO_2 but was completely destroyed on SiO_2 . Furthermore, no obvious XRD peaks corresponding to either Keggin HPW or WO_3 in PWZ-AN-650 samples reflected better dispersion of HPW on the surface of ZrO_2 than SiO_2 . The enhanced thermal stability and dispersion of HPW on ZrO_2 would suggest stronger interaction of HPW with the ZrO_2 than with the SiO_2 support. However, partial decomposition of HPW was observed in 30PWZ-AN-650, probably because the Keggin-anion density (0.66 HPW nm^{-2} , Table 1) of this catalyst was slightly above the monolayer coverage (*ca.* 0.60 HPW nm^{-2}) of HPW on the ZrO_2 surface.²⁸ The excessive HPW would have weak or no direct interaction with the ZrO_2 support and thus exhibit a lower thermal stability. Halligudi *et al.*²⁸ studied the thermal stability of HPW supported on ZrO_2 by measuring the state of phosphorous in HPW with a ^{31}P MAS NMR technique. They observed that the Keggin structure of HPW remained thermally stable up to $750\text{ }^\circ\text{C}$ when the loading of HPW was kept below the monolayer coverage of HPW on ZrO_2 surface (*ca.* 7.2 (W) nm^{-2} , equivalent to 0.60 HPW nm^{-2}); the excess HPW above the monolayer coverage easily underwent decomposition, resulting in co-existence of Keggin HPW and WO_3 . On the other hand, HPW can not be well dispersed on SiO_2 due to weak HPW- SiO_2 interaction, although PWS samples had a lower Keggin-anion surface density when compared with PWZ. Even in the 15PWS-350 sample, HPW on SiO_2 agglomerated to form HPW crystallites that can be easily detected by XRD and Raman (Fig. 1 and 3). The HPW crystallites in PWS-350 samples appeared to show thermal stability that was no better than pure HPW.²³

3.2 Catalytic reaction

Fig. 4 shows the time courses of glycerol conversion and acrolein selectivity over PWS catalysts thermally treated at $350\text{ }^\circ\text{C}$ and

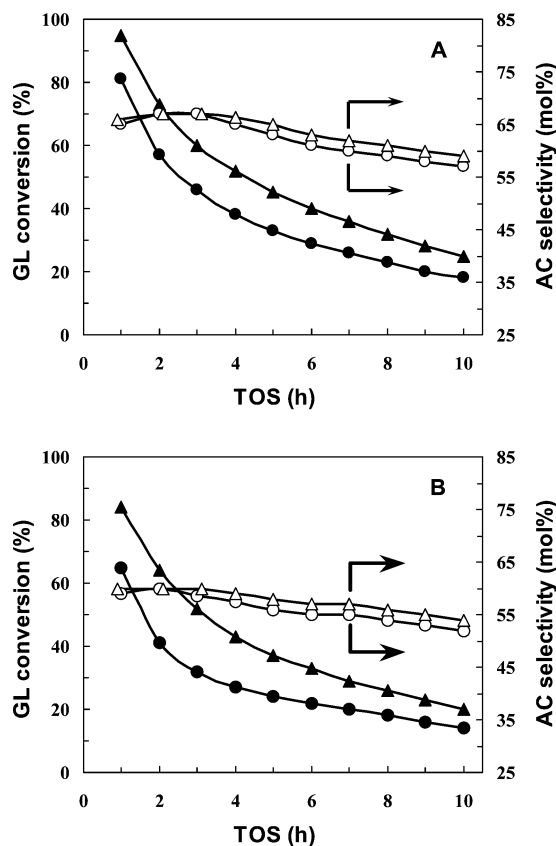


Fig. 4 Time courses of glycerol conversion (solid symbol) and acrolein selectivity (open symbol) over (●,○) 15PWS and (▲,△) 30PWS catalysts thermally treated at (A) $350\text{ }^\circ\text{C}$ and (B) $650\text{ }^\circ\text{C}$.

$650\text{ }^\circ\text{C}$. Glycerol conversion over 30PWS-350 decreased from 95% to 25% in 10 h TOS but was always higher than that (from 81% to 18%) over 15PWS-350 catalyst (Fig. 4A). The selectivity for acrolein over both catalysts was as high as 68 mol% at TOS of 1–4 h, followed by a gradual drop to 59 mol% for 30PWS-350 and 57 mol% for 15PWS-350 at TOS = 10 h. Increasing the treatment temperature from $350\text{ }^\circ\text{C}$ to $650\text{ }^\circ\text{C}$ led to a decrease in both glycerol conversion and acrolein selectivity. For example, the glycerol conversion over 30PWS-650 declined from 84% to 20% after 10 h TOS; the acrolein selectivity dropped from 60 mol% to 54 mol% during the same reaction period (Fig. 4B). The inferior catalytic performance of both PWS-650 catalysts in comparison to their PWS-350 counterparts could be a consequence of the decomposition of Keggin HPW, as shown by the XRD results in Fig. 1. Therefore, it is essential to maintain the Keggin structure in the supported HPW catalyst to benefit acrolein production from glycerol.

Unlike in the PWS-650 catalysts, the Keggin structure of HPW in PWZ-AN-650 catalysts was well preserved. Also, the supported HPW in both PWZ-AN-650 showed much enhanced dispersion (see Fig. 2 and 3) in comparison even to PWS-350, and thus would be expected to show a better catalytic performance for the selective formation of acrolein from glycerol dehydration. Fig. 5 presents the time courses of glycerol conversion and acrolein selectivity over both PWZ-AN-650 catalysts. The reaction data over ZrO_2 -AN-650, to which no HPW was loaded, are also included in Fig. 5 as reference

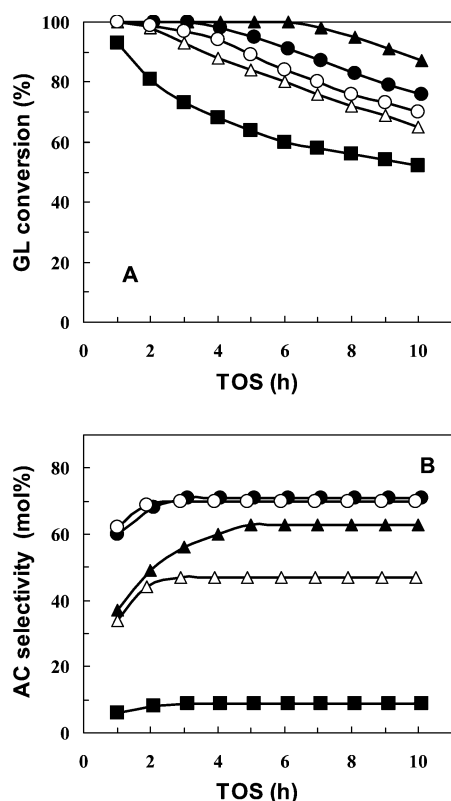


Fig. 5 Time courses of (A) glycerol conversion and (B) acrolein selectivity over (■) ZrO₂-AN-650, (△) 15PWZ-AN-350, (▲) 30PWZ-AN-350, (●) 15PWZ-AN-650, and (○) 30PWZ-AN-650 catalysts.

to show the importance of HPW for increasing the selectivity for acrolein. ZrO₂-AN-650 alone produced significantly lower glycerol conversion, a higher deactivation rate, and very poor acrolein selectivity (less than 10 mol%), showing that ZrO₂ without HPW was not effective for acrolein formation from glycerol. The loading of HPW on ZrO₂ led to a remarkable increase in glycerol conversion, and the acrolein selectivity was enhanced by 7–8 times. The glycerol conversion over 15PWZ-AN-650 was 100% during the initial 3 h and then decreased to 76% at TOS = 9–10 h, however, the selectivity for acrolein remained steady at the level of 71 mol%. In comparison to 15PWZ-AN-650, 30PWZ-AN-650 showed a decreased glycerol conversion from 76% to 70% (TOS = 9–10 h) in spite of acrolein selectivity being almost unchanged. Compared with PWS-350

catalysts (Fig. 4), PWZ-650 at 15 wt% as well as 30 wt% HPW loading (Fig. 5) showed a better catalytic stability, characterized by their lower deactivation rate with TOS.

In response to a referee, who was wondering why PWZ-350 samples had not been included in our catalytic study, we then prepared two samples, 15PWZ- and 30PWZ-AN-350, during our revision of this work. These two catalysts, which were obtained by thermal treatment at 350 °C after the impregnation of ZrO(OH)₂ with HPW in ethanol, showed much higher surface areas (265 m² g⁻¹ for 15PWZ-350, and 215 m² g⁻¹ for 30PWZ-350), and were completely amorphous since only quite diffuse signals featuring neither HPW nor ZrO₂ were detected in XRD as well as Raman measurements (not shown). The time courses of glycerol dehydration over these two catalysts are incorporated into Fig. 5, showing much poorer catalytic performance by acrolein selectivity when compared with PWZ-AN-650 (see also Table 3). In view of applications, the PWZ-AN-350 catalysts would not meet the requirement for regeneration of the coked catalyst, which usually requires an operation temperature higher than 500 °C. The amorphous feature of ZrO₂ in these PWZ-AN-350 catalysts could mean a much stronger interaction between HPW and ZrO₂ and weaker acidity of the supported HPW (some HPW could even be buried in the amorphous support), which would be responsible for their poor catalytic performance.

When similar levels of glycerol conversion (*e.g.* 60–80%) were taken to rank the catalysts by their selectivity for acrolein formation, the following order was obtained: PWZ-AN-650 (70 mol%) > PWS-350 (68 mol%) > PWS-650 (60 mol%) ≥ PWZ-350 (50–60 mol%).

Since catalyst stability is the most important concern in applications, we compare in Table 2 the catalytic data at TOS = 9–10 h of PWS and PWZ catalysts. PWZ catalysts exhibited much better catalytic performance from the viewpoint of glycerol conversion, acrolein selectivity and acrolein yield. The most effective catalyst was 15PWZ-AN-650, with which an acrolein yield as high as 54% could be obtained even after 10 h of reaction. The reaction conversion and selectivity data were based on constant catalyst volume (0.63 ml) used in our experimental reaction study. Given in the last two columns of Table 2 are the mass-specific catalytic rates of HPW (mmol h⁻¹ g-HPW⁻¹) at TOS = 9–10 h, which are obtained by normalizing the reaction data according to the actual mass of HPW in each catalyst, for glycerol consumption and acrolein formation. For the catalysts having either 15 wt% or 30 wt% HPW loading, the mass-specific

Table 2 Catalytic performance of ZrO₂- and SiO₂-supported H₃PW₁₂O₄₀ catalysts for the gas-phase dehydration of glycerol at 315 °C, glycerol GHSV = 400 h⁻¹, and TOS = 9–10 h

Catalyst (0.63 ml)	Catalyst amount/g	Reaction data at TOS = 9–10 h			Mass-specific rate (mmol h ⁻¹ g-HPW ⁻¹)	
		X ^a (%)	S ^b (mol%)	Y ^c (%)	Glycerol consumption	Acrolein formation
15PWS-350	0.30	18	57	10	47	27
30PWS-350	0.37	25	59	15	27	16
15PWS-650	0.30	14	52	7	36	19
30PWS-650	0.37	20	54	11	21	11
ZrO ₂ -AN-650	0.72	52	9	5	—	—
15PWZ-AN-650	0.63	76	71	54	95	67
30PWZ-AN-650	0.71	70	70	49	39	27

^a Conversion of glycerol. ^b Selectivity for acrolein. ^c Yield of acrolein.

Table 3 Product distribution over ZrO₂- and SiO₂-supported H₃PW₁₂O₄₀ catalysts for the gas-phase dehydration of glycerol at 315 °C, glycerol GHSV = 400 h⁻¹, and TOS = 9–10 h

Catalyst (0.63 ml)	X ^a (%)	Product selectivity at TOS = 9–10 h (mol%)				
		Acrolein	Acetaldehyde	Allyl alcohol	1-Hydroxyacetone	Unknowns ^b
15PWS-350	18	57	1	1	7	34
30PWS-350	25	59	1	1	7	32
15PWS-650	14	52	1	2	8	37
30PWS-650	20	54	1	2	9	34
ZrO ₂ -AN-650 ^c	52	9	3	1	28	59
15PWZ-AN-350	69	47	10	4	17	22
30PWZ-AN-350	87	63	6	2	15	14
15PWZ-AN-650	76	71	3	1	12	13
30PWZ-AN-650	70	70	3	1	11	15

^a Conversion of glycerol. ^b Selectivity for unknowns (mol%) = 100 – ∑ selectivity of the listed identified products. ^c Methanol (3 mol%) and 1,2-propanediol (11 mol%) were also present in the product over this catalyst.

catalytic rate decreased in the order of PWZ-AN-650 > PWS-350 > PWS-650 for both glycerol consumption and acrolein formation. On the other hand, the catalytic rates declined with increasing HPW loading in both PWZ and PWS catalysts; furthermore, the rates over PWZ catalysts appeared to decrease more rapidly than those over PWS catalysts.

The preservation of Keggin HPW in PWZ-AN-650 and PWS-350 catalysts could be responsible for their higher acrolein formation rates in comparison to PWS-650. The higher acrolein formation rates over PWZ-AN-650 compared to PWS-350 should be related to the presence of highly dispersed Keggin HPW, due to the relatively strong interaction of HPW with the surface of ZrO₂, but too strong interactions in PWZ-AN-350 samples could lead to weakening of the acidity of the supported HPW or even burying of HPW in amorphous ZrO₂. The increased dispersion would enhance the accessibility of active Keggin HPW in the reaction. Whereas, the decreased mass-specific rates with increasing HPW loading could be caused by a decrease in HPW dispersion at the surfaces of the support materials. The partial decomposition of Keggin HPW in 30PWZ-AN-650 would contribute to its more rapid decrease in the glycerol consumption rate, and, interestingly, the resultant highly dispersed WO₃ species showed no negative effect on acrolein selectivity (Fig. 5B).

In addition to acrolein, a number of other products were also detected (some of them remained unidentified).^{19,20} Table 3 shows the product distribution at TOS = 9–10 h over ZrO₂, PWZ and PWS catalysts. Except during the very initial hours (TOS < 3 h) of the reaction, the product distribution over every catalyst was seen to change little during the reaction up to TOS = 9–10 h. Over all the tested catalysts, except ZrO₂-AN-650, 1-hydroxyacetone from mono-dehydration at either terminal carbon of glycerol¹⁹ appeared as the main byproduct in the reaction; other identified byproducts included acetaldehyde and allyl alcohol. 1-Hydroxyacetone was formed over PWZ catalysts with a selectivity of 11–12 mol%, slightly higher than 7–9 mol% over PWS. The predominant products identified over ZrO₂-AN-650 were 1-hydroxyacetone (28 mol% by selectivity) and 1,2-propanediol (11 mol% by selectivity). The selectivity for acetaldehyde and allyl alcohol over all the catalysts was below 3 mol%, respectively. Besides those listed as identified products in Table 3, propionaldehyde, acetone, acetic acid,

propionic acid, and phenol were also observed but they were all added in the unknowns; the selectivity for each of them was always less than 1 mol%. A number of complicated by-products remained unknown since they were difficult to identify unambiguously by GC-MS analysis; most of them were too small in quantity and sometimes were not well separated by the GC column used. Possible reactions leading to these detected products can be found in our previous work.¹⁹ As we showed earlier,^{19,20} catalysts that produced higher amounts of complicated unknown products also coked more heavily and deactivated more rapidly in this study. Elemental analysis combined with TPO and XRD measurements of the deposited coke^{19,20} uncovered the nature of carbon deposits on PWS and PWZ catalyst; the coke was amorphous and had a molar C/H ratio of 0.50–0.53, and can be removed completely by oxidation in flowing air up to ca. 430 °C.

4. Conclusions

This work demonstrates that Keggin 12-tungstophosphoric acid (HPW) catalysts supported on zirconia polycrystals are much more active, selective and stable than those on silica for the dehydration of glycerol to form acrolein. The desirable acrolein over HPW/ZrO₂ can be produced with high selectivity (70–71 mol%) and yield up to 54% even after its service to the reaction for 10 h. Preservation of the HPW Keggin structure in highly dispersed states in HPW/ZrO₂ catalyst appears to be responsible for their higher acrolein selectivity and acrolein formation rates in comparison to HPW/SiO₂ catalysts. These findings could be important for acrolein production from glycerol, in view of searching for more effective catalysts with improved thermal stability to survive repeated regenerations.

Acknowledgements

This work is partly supported by NSF of China (grant: 20590362).

References

- 1 D. L. Klass, *Biomass for Renewable Energy, Fuels and Chemicals*, Academic Press, San Diego, 1998, pp. 1.

- 2 B. Kamm, M. Kamm, P. R. Gruber and S. Kromus, in *Biorefineries – Industrial Processes and Products: Status quo and Future Directions*, ed. B. Kamm, P. R. Gruber and M. Kamm, Wiley-VCH, Weinheim, 2006, vol. 1, pp. 3–40.
- 3 H. S. Kesling, L. J. Karas and F. J. Liotta, *US Pat* 5 308 365, 1994.
- 4 D. S. Bradin, *US Pat.* 5 578 090, 1996.
- 5 T. Werpy and G. Petersen, *Top Value Added Chemicals from Biomass*, US Department of Energy, Office of Scientific and Technical Information, 2004, No. DOE/GO-102004–1992, (www.osti.gov/bridge).
- 6 P. Gallezot, *Green Chem.*, 2007, **9**, 295–302.
- 7 M. Pagliaro, R. Ciriminna, H. Kimura, M. Rossi and C. D. Pina, *Angew. Chem., Int. Ed.*, 2007, **46**, 4434–4440.
- 8 C.-H. Zhou, J. N. Beltramini, Y.-X. Fana and G. Q. Lu, *Chem. Soc. Rev.*, 2008, **37**, 527–549.
- 9 H. P. A. Groll, Okaland and G. Hearne, *US Pat.* 2 042 224, 1936.
- 10 S. Ramayya, A. Brittain, C. DeAlmeida, W. Mok and M. J. Antal, *Fuel*, 1987, **66**, 1364–1371.
- 11 M. J. Antal Jr., W. S. L. Mok and G. N. Richards, *Carbohydr. Res.*, 1990, **199**, 111–115.
- 12 M. Watanabe, T. Iida, Y. Aizawa, T. M. Aida and H. Inomata, *Bioresour. Technol.*, 2007, **98**, 1285–1290.
- 13 L. Ott, M. Bicker and H. Vogel, *Green Chem.*, 2006, **8**, 214–220.
- 14 H. Adkins and W. H. Hartung, *Org. Synth., Coll. Vol. 1*, 1941, 15–18.
- 15 A. Neher, T. Haas, D. Arntz, H. Klenk and W. Girke, *US Pat.* 5 387 720, 1995.
- 16 A. G. Scheering-Kahlbaum, *Fr. Pat.* 695 931, 1930.
- 17 U. -L. Dubois, C. Duquenne and W. Holderlich, *WO Pat.* 2006/087083 A2, 2006.
- 18 E. Tsukuda, S. Sato, R. Takahashi and T. Sodesawa, *Catal. Commun.*, 2007, **8**, 1349–1353.
- 19 S.-H. Chai, H.-P. Wang, Y. Liang and B.-Q. Xu, *Green Chem.*, 2007, **9**, 1130–1136.
- 20 S.-H. Chai, H.-P. Wang, Y. Liang and B.-Q. Xu, *J. Catal.*, 2007, **250**, 342–349.
- 21 T. Okuhara, N. Mizuno and M. Misono, *Adv. Catal.*, 1996, **41**, 113–252.
- 22 K. Tanabe, M. Misono, Y. Ono and H. Hattori, *New Solid Acids and Bases: Their Catalytic Properties*, Kodansha, Tokyo and Elsevier, Amsterdam, 1989, pp. 163–173.
- 23 I. V. Kozhevnikov, *Chem. Rev.*, 1998, **98**, 171–198.
- 24 T. Yamaguchi, *Catal. Today*, 1994, **20**, 199–217.
- 25 M. Hino and K. Arata, *J. Chem. Soc., Chem. Commun.*, 1988, 1259–1260.
- 26 B.-Q. Xu, S.-B. Cheng, S. Jiang and Q.-M. Zhu, *Appl. Catal., A*, 1999, **188**, 361–368.
- 27 D. He, H. Shi, Y. Wu and B.-Q. Xu, *Green Chem.*, 2007, **9**, 849–851.
- 28 B. M. Devassy, F. Lefebvre and S. B. Halligudi, *J. Catal.*, 2005, **231**, 1–10.
- 29 E. López-Salinas, J. G. Hernández-Cortéz, I. Schifter, E. Torres-García, J. Navarrete, A. Gutiérrez-Carrillo, T. López, P. P. Lottici and D. Bersani, *Appl. Catal., A*, 2000, **193**, 215–225.
- 30 B. M. Devassy, S. B. Halligudi, S. G. Hegde, A. B. Halgeri and F. Lefebvre, *Chem. Commun.*, 2002, 1074–1075.
- 31 E. López-Salinas, J. G. Hernández-Cortéz, Ma. A. Cortés-Jácome, J. Navarrete, Ma. E. Llanos, A. Vázquez, H. Armendáriz and T. López, *Appl. Catal., A*, 1998, **175**, 43–53.
- 32 S. Patel, N. Purohit and A. Patel, *J. Mol. Catal. A*, 2003, **192**, 195–202.
- 33 D. P. Sawant, A. Vinu, N. E. Jacob, F. Lefebvre and S. B. Halligudi, *J. Catal.*, 2005, **235**, 341–352.
- 34 D. P. Sawant, A. Vinu, F. Lefebvre and S. B. Halligudi, *J. Mol. Catal., A*, 2007, **262**, 98–108.
- 35 B.-Q. Xu, J.-M. Wei, Y.-T. Yu, J.-L. Li and Q.-M. Zhu, *Top. Catal.*, 2003, **22**, 77–85.
- 36 B.-Q. Xu, J.-M. Wei, Y.-T. Yu, Y. Li, J.-L. Li and Q.-M. Zhu, *J. Phys. Chem. B*, 2003, **107**, 5203–5207.
- 37 Q.-H. Zhang, Y. Li and B.-Q. Xu, *Catal. Today*, 2004, **98**, 601–605.
- 38 Y. Li, Q. Ye, J. M. Wei and B.-Q. Xu, *Chin. J. Catal.*, 2004, **25**, 326–330.
- 39 H. M. Liu, Q. Ye and B.-Q. Xu, *Stud. Surf. Sci. Catal.*, 2007, **172**, 473–476.
- 40 J. Song, H. Wang and B.-Q. Xu, *Chin. J. Catal.*, 2004, **25**, 599–601.
- 41 X. Zhang, H. Wang and B.-Q. Xu, *J. Phys. Chem. B*, 2005, **109**, 9678–9683.
- 42 Y. Izumi, K. Urabe and M. Onaka, *Zeolite, Clay and Heteropoly Acid in Organic Reactions*, Kodansha/VCH, Tokyo, 1992, pp. 99–161.
- 43 H. Hayashi and J. B. Moffat, *J. Catal.*, 1982, **77**, 473–484.
- 44 L. R. Pizzio, C. V. Caceres and M. N. Blanco, *Appl. Catal., A*, 1998, **167**, 283–294.
- 45 R. Thouvenot, M. Fournier, R. Franck and C. Rocchiccioli-Deltcheff, *Inorg. Chem.*, 1984, **23**, 598–605.
- 46 D. G. Barton, M. Shtein, R. D. Wilson, S. L. Soled and E. Iglesia, *J. Phys. Chem. B*, 1999, **103**, 630–640.

Synthesis of icosahedral gold particles by a simple and mild route

Chaoxing Zhang, Jianling Zhang, Buxing Han,* Yueju Zhao and Wei Li

Received 31st March 2008, Accepted 14th July 2008

First published as an Advance Article on the web 9th September 2008

DOI: 10.1039/b805392h

In this work we prepared icosahedral gold particles using hydrogen tetrachloroaurate(III) hydrate ($\text{HAuCl}_4 \cdot 3\text{H}_2\text{O}$) as precursor and poly(ethylene oxide)–poly(propylene oxide)–poly(ethylene oxide) (PEO-PPO-PEO) triblock copolymers as both reductant and directing agent. The products were characterized by scanning electron microscopy (SEM), transmission electron microscopy (TEM), X-ray diffraction (XRD) analysis, and UV–Vis spectroscopy. The effects of temperature, reaction time, concentration of the precursor, and structure and concentration of the copolymers on the morphology and size of the gold particles were investigated. It was demonstrated that icosahedral gold nanoparticles can be formed under a wide range of experimental conditions and the size of the obtained icosahedral particles can be tuned from 100 nm to 1 μm by varying experimental conditions. This method has some obvious advantages, such as being simple and green, and the particle size can be easily controlled.

1. Introduction

In recent years, synthesis of gold nanoparticles has received much attention because of their characteristic plasmon absorption,¹ effective biolabeling and drug delivery properties,² and their high activity for many chemical reactions.³ Different methods, such as seed mediated growth processes,⁴ template-directed patterning,^{5,6} biomineralization,⁷ two phase reactions⁸ and inverse micelles,⁹ have been used to synthesize nanostructures including rods,^{10,11} plates,⁷ spheres⁵ and cages.¹² There have been some reports on the fabrication of gold crystals with octahedral, decahedral, and cuboctahedral morphologies,^{13–17} which are highly faceted, with sharp corners and edges, and multiply twinned gold crystals. These kinds of gold particles may have some different physical and chemical properties to those of untwinned nanoparticles without sharp corners because of their intrinsic structural characteristics concerning surface energy and lattice symmetry. Up to now, the reported gold crystals with the most number of corners and edges are icosahedrons and three papers have been published on this. Yang and the co-workers successfully prepared icosahedral gold particles in ethylene glycol solution at 280 °C and N_2 atmosphere in the presence of poly(vinyl pyrrolidone) (PVP), and the particle size was about 230 nm.¹⁵ Xu *et al.* synthesized icosahedral gold particles of about 400 nm at 120 °C with ethylene glycol (EG) in the presence of poly(vinyl pyrrolidone) (PVP) under hydrothermal conditions.¹⁸ Zhou *et al.* fabricated icosahedral gold particles of about 220 nm at 100 °C in the presence of PVP with a thermal process strategy.¹⁹

Triblock copolymers of poly(ethylene oxide)–poly(propylene oxide)–poly(ethylene oxide) (PEO-PPO-PEO) are very useful

surfactants with the commercial name of Pluronic. Their properties can be tuned by varying the PO/EO ratio and/or molecular weights of the surfactants, and can meet some specific requirements for different processes. As environmentally more acceptable materials, the Pluronic have been used widely in detergency, dispersion, stabilization, solubilization, emulsification, lubrication, pharmaceuticals and bioprocessing.^{20–22} These kind of surfactants have also been used to synthesize spherical gold nanoparticles with size less than 100 nm in aqueous solution.^{23–25}

Development of versatile, simple and greener methods to prepare gold nanostructures with sharp corners and edges is still an interesting topic. In this work we prepared icosahedral gold nanoparticles (30 sharp edges and 12 corners), by a method in which water, Pluronic, and hydrogen tetrachloroaurate ($\text{HAuCl}_4 \cdot 3\text{H}_2\text{O}$) were used and Pluronic acted as both reducing reagent and directing agent. This method is advantageous in that it is simple, operates at ambient temperature and uses nontoxic materials, which are all in line with a green synthetic strategy.²⁶ With our proposed method, the size of the obtained icosahedral gold nanoparticles can be tuned from 100 nm to 1 μm by varying the experimental conditions, including temperature, reaction time, concentration of the precursor and structure and concentration of Pluronic.

2. Experimental

Materials

The Pluronic PEO-PPO-PEO block copolymers, P85 ($\text{EO}_{26}\text{PO}_{40}\text{PEO}_{26}$), P104 ($\text{EO}_{27}\text{PO}_{61}\text{EO}_{27}$), P105 ($\text{EO}_{37}\text{PO}_{56}\text{EO}_{37}$) and F88 ($\text{EO}_{103}\text{PO}_{39}\text{EO}_{103}$) were provided by BASF Corporation. Hydrogen tetrachloroaurate ($\text{HAuCl}_4 \cdot 3\text{H}_2\text{O}$) was purchased from Shenyang Jinke Reagent Company. All the chemicals were used as received. Double-distilled water and absolute ethanol were used.

Beijing National Laboratory for Molecular Sciences, Institute of Chemistry, Chinese Academy of Sciences, Beijing, 100080, China.
E-mail: Hanbx@iccas.ac.cn; Fax: +86-10-62559373;
Tel: +86-10-62562821

Preparation of gold nanoparticles

HAuCl₄·3H₂O aqueous solutions (0.3 M) were firstly prepared by dissolving solid HAuCl₄·3H₂O in water. In a typical synthesis of the gold particles, a vial containing 4 mL aqueous solution of Pluronic PEO-PPO-PEO block copolymer (F88, P85, P104 or P105) was thermostatted in a constant-temperature water bath. A suitable amount of HAuCl₄·3H₂O aqueous solution was added dropwise into the vial under agitation. After the reaction proceeded for a desired time, the sample was centrifuged and collected, and washed by ethanol several times. In this work, we studied the effect of reaction time, the concentration of the precursor (HAuCl₄·3H₂O) and structure and concentration of the surfactants. The Au particles were characterized by different methods, as described below.

Characterization

The morphology and size of the obtained particles were characterized by scanning electron microscopy (SEM, S-4300, 15 kV) and transmission electron microscopy (TEM, JEOL-1010, 100 kV). X-Ray diffraction analysis of the samples was performed on an X-ray diffractometer (XRD, Model D/MAX2500, Rigaku) with Cu K α radiation at a scanning rate of 2° min⁻¹. The UV-Vis absorption spectra of the product dispersed in water were recorded on a TU-1901 Model spectrophotometer with a resolution of 0.5 nm (Beijing General Instrument Company).

3. Results and discussion

Gold icosahedrons prepared using F88 at different conditions

Fig. 1 shows the typical SEM and TEM images of the product prepared at 40 °C with a reaction time of one day in the presence of F88 (0.84 mM), and the concentration of HAuCl₄ in the solution was 5.8 mM. In this work, the concentrations of the polymers and HAuCl₄ in the solution are the concentrations of the chemicals before reaction. Fig. 1a shows that particles with a uniform size of 600 ± 100 nm were formed. The higher magnification SEM image (Fig. 1b) clearly reveals that the particles have an icosahedron structure with 12 corners and 30 edges. Fig. 1c and 1d show the icosahedral gold particles

observed from different angles of view. The lengths of edges are the same. As a result, there are three types of rotational axes: twofold, threefold, and fivefold.²⁷ A geometrical model of the icosahedral particles is shown in Fig. 1e. Fig. 1f is a representative TEM image of the as-prepared gold icosahedrons, which shows a hexagonal shape under TEM. Because lying on a flat surface is more stable than on a corner or an edge, the icosahedrons under TEM prefer to show the orientation with a threefold axis parallel to the electron beam, which is consistent with the TEM result of gold icosahedrons prepared by Yang and co-workers.¹⁵

Gold can be easily obtained by a reduction method. Except for the usual reducing reagents, such as H₂ and NaBH₄, some other reagents, such as *N,N*-dimethylformamide (DMF)¹⁷ and ethylene glycol (EG),¹⁵ can also achieve this goal. The reducing function of the triblock copolymer Pluronic has been used before to synthesize gold particles.^{23–25} When this kind of surfactant was used to synthesize gold particles from reducing AuCl₄⁻, the formation process comprises three main steps:^{23,28} (1) reduction of metal ions facilitated by block copolymers in solution, (2) absorption of block copolymers on gold clusters and reduction of metal ions on the surface of these gold clusters, and (3) growth of gold particles and stabilization by block copolymers. Therefore, in the presence of Pluronic in our work the AuCl₄⁻ can be reduced to gold, and the gold particles formed.

The phase purity and high crystallinity of the gold icosahedrons are supported by powder X-ray diffraction (XRD, Fig. 2a). Apparently, only two sharp peaks and one minor peak can be observed, and the peaks are assigned to the diffraction from the {111}, {200} and {220} planes of face-centered cubic (fcc) gold, respectively. No diffraction peaks due to possible impurities were observed. The intensity ratio of {200} and {111}, {220} and {111} is 0.11 and 0.023, respectively, which is much lower than the conventional values (0.53 and 0.33) of face-centered cubic (fcc) gold, indicating that for the as-prepared icosahedron gold particles, the {111} family of planes is dominant. Because the {111} facet of fcc metal has the lowest surface energy compared to the other facets ({110} > {100} > {111}), the fcc metal confers its tendency to nucleate and grows into nanoparticles with their surfaces bounded by {111} facets.¹⁸

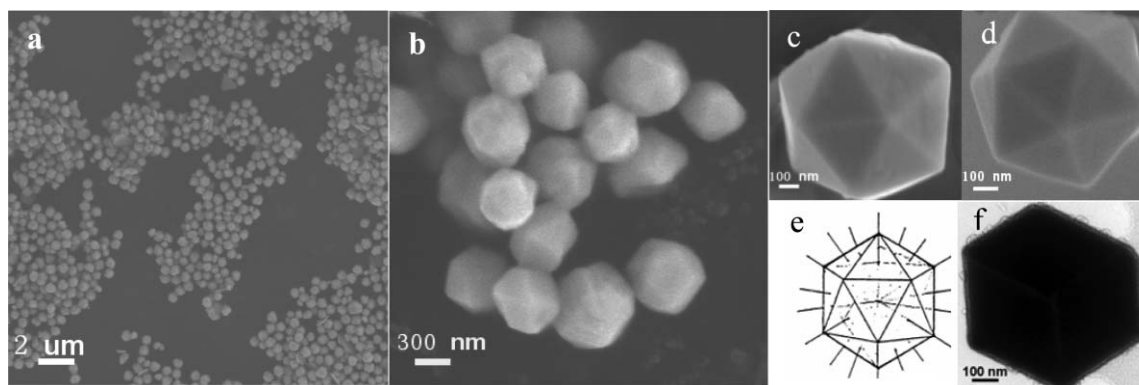


Fig. 1 Characterization of gold icosahedrons synthesized at 40 °C with a reaction time of one day, and the concentrations of F88 and HAuCl₄ are 0.84 mM and 5.8 mM, respectively: (a) SEM image; (b) higher magnification SEM image; (c) and (d) SEM image of a single gold particle observed from different angles of view; (e) geometrical model of the obtained icosahedron particles; (f) representative TEM image.

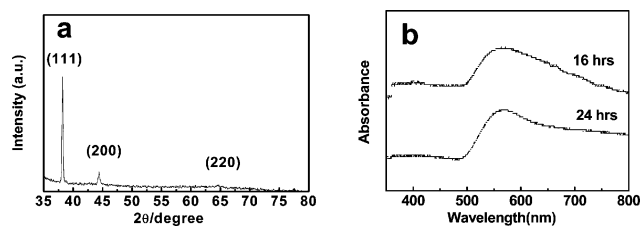


Fig. 2 (a) XRD pattern of the obtained icosahedral gold particles supported by a glass slide; (b) UV-vis spectrum of the gold icosahedron aqueous solution, the reaction times are 16 h and 24 h, respectively. Other experimental conditions are the same as in Fig. 1.

Thus, the XRD spectra (Fig. 2a) show that the {111} family of planes is dominant.

It is known that the optical properties of metal nanoparticles are highly dependent on the size and shape of the particles.^{15,17,29} Fig. 2b shows the UV-vis spectra of obtained icosahedral gold particles dispersed in water. An absorption peak was observed at 568 nm, corresponding to the surface plasmon resonance of icosahedral gold particles. The spectral feature is consistent with that of icosahedral gold particles reported in literature.¹⁵ The sharp absorption peak again indicates that the prepared icosahedral gold nanoparticles are uniform in shape and size.

The effect of concentration of F88 in the solution on the morphology of gold particles was also investigated in this work. Fig. 3a and 3b show the SEM images of the icosahedral gold particles prepared at F88 concentrations of 8.4 mM and 16.8 mM, respectively. The sizes of the particles prepared at the two concentrations were ~400–500 nm (Fig. 3a) and ~300–400 nm (Fig. 3b), respectively. By comparison with the gold icosahedral particles fabricated at the F88 concentration of 0.84 mM, it is clear that the size of the gold icosahedral particles decreases with the increasing of F88 concentration. When the concentration of F88 was increased, more surfactant molecules attached to the gold facets, which inhibited their further growth and resulted in the smaller particle size.

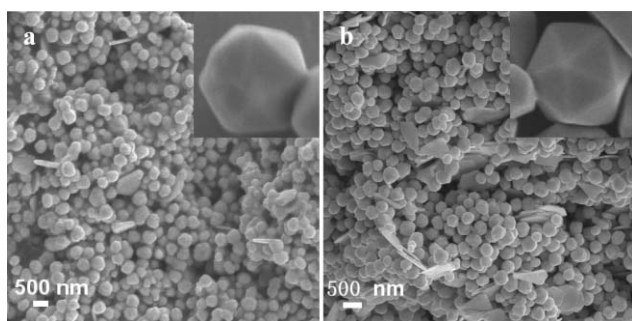


Fig. 3 SEM images of the icosahedral gold particles prepared at F88 concentrations of (a) 8.4 mM and (b) 16.8 mM. The other experimental conditions were the same as that in Fig. 1. The insets of (a) and (b) show the magnified SEM images of representative icosahedrons.

The effects of other experimental conditions, such as the reaction time, temperature and concentration of HAuCl_4 , on the morphology and size of the gold particles were also investigated. Fig. 4a and 4b show the SEM images of the as-prepared gold nanoparticles under the same synthetic conditions as those in Fig. 1, except that the reaction time was different. When the reaction time was 16 h, icosahedral gold particles with an average

size of ~100–150 nm were obtained (Fig. 4a). When the reaction time was increased to 24 h and 6 days, the icosahedrons with a larger size of about 600 nm (Fig. 1) and about 1 μm (Fig. 4b) were obtained, respectively. This suggests that the icosahedrons were formed in the early stage, in accordance with the formation process of Pd icosahedrons.³⁰ The gold particles became larger as the reaction time was prolonged.

Reaction temperature also affected the size of icosahedral gold products. As the reaction temperature was decreased to 17 °C, icosahedral gold nanoparticles with size of about 150 nm were formed (shown in Fig. 4c). When the reaction temperature was increased to a higher temperature of 35 °C, the size of the obtained icosahedral gold particles was increased to 500 nm (shown in Fig. 4d), smaller than that formed at 40 °C (Fig. 1), but larger than that prepared at 17 °C. These results indicate that the size of particles increases with the increasing temperature. The main reason may be that the reaction rate increases with increasing temperature and bigger particles were formed. This is consistent with the argument that the icosahedrons were formed in the early stage, as discussed above.

We further studied the effect of concentration of HAuCl_4 on the morphology and size of product. By increasing the concentration of HAuCl_4 to 17.4 mM, while other experimental conditions were the same as those in Fig. 1, icosahedral gold nanoparticles with size of about 800 nm (shown in Fig. 4e) were obtained, which is larger than those obtained when the concentration of the gold precursor concentration was 5.8 mM (about 600 nm, see Fig. 1). The main reason is that the reaction rate at the higher HAuCl_4 concentration was larger, which is favorable to form larger gold particles.

We also determined the UV-vis spectrum of the icosahedral gold particles, as shown in Fig. 4a (dispersed in water), which have an average size of ~100–150 nm and are the smallest particles prepared in this work, and the result is also presented in Fig. 2b. It can be seen from the figure that the absorption peak of the particles of ~100–150 nm is similar to that of particles of about 600 ± 100 nm.

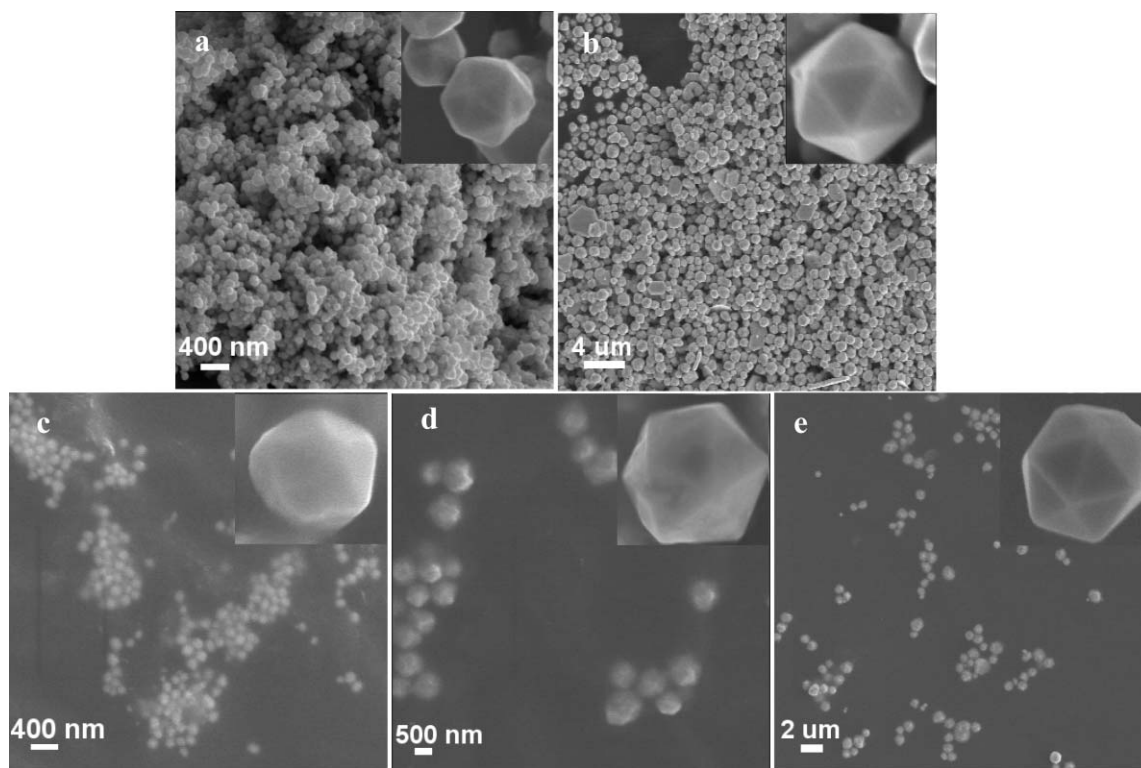
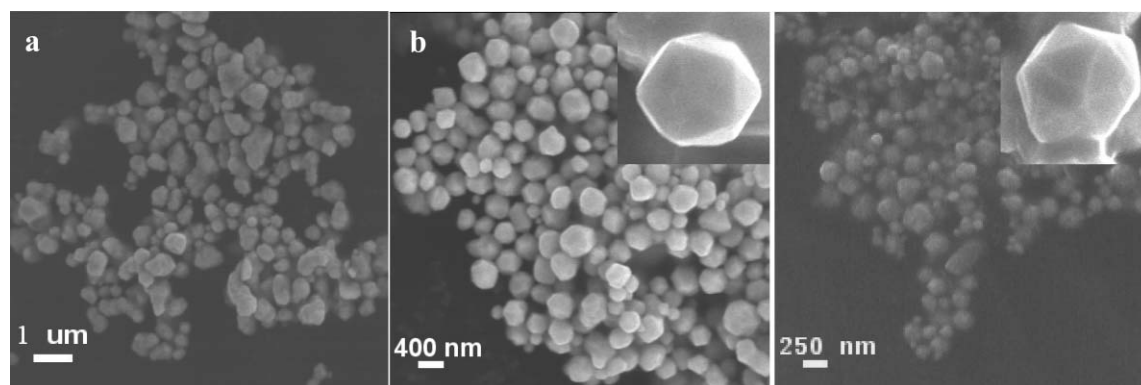
Effect of copolymers

The above results indicate that F88 plays an important role for the formation of the gold nanostructures. We also investigated the synthesis of gold particles with other three Pluronic copolymers, P85, P104, P105, and the structure parameters of the polymers are listed in Table 1. Fig. 5a is the SEM image of gold particles prepared using P85. As we can see, most of the obtained particles had irregular shapes. We further studied the synthesis of gold particles using P104, which has a similar PEO block length to P85 and a larger PPO block length than P85. Fig. 5b shows the SEM image of gold products obtained by using P104, in which icosahedral gold particles with size of about 300 ± 100 nm can be observed. P105 has medium PEO and PPO block lengths among the polymers used. Icosahedral gold nanoparticles with sizes of about ~100–250 nm were formed in the presence of P105, as can be seen in Fig. 5c. The shape and size of the Au particles are also presented in Table 1.

The above results indicate that the structure parameters of the Pluronic affect the size and shape of the Au particles considerably. It can be seen from Fig. 1 and 5 that the more

Table 1 The structure parameters of the Pluronics used in this study,³¹ and the corresponding morphology and size Au particles obtained

Polymer	MW	PPO _{segm wt}	PO _{units}	EO _{units}	Morphology	Size/nm
F88	11400	2280	39	2*103	Icosahedron	600 ± 100
P85	4600	2300	40	2*26	Irregular	250 ± 100
P104	5900	3540	61	2*27	Icosahedron	300 ± 100
P105	6500	3250	56	2*37	Icosahedron	~100–250

**Fig. 4** SEM images of the as-prepared gold nanoparticles in the presence of 0.84 mM F88; (a) 40 °C, 16 h, 5.8 mM HAuCl₄; (b) 40 °C, 6 days, 5.8 mM HAuCl₄; (c) 17 °C, 1 day, 5.8 mM HAuCl₄; (d) 35 °C, 1 day, 5.8 mM HAuCl₄; (e) 40 °C, 1 day, 17.4 mM HAuCl₄. The insets of (a), (b), (c), (d), (e) show the magnified SEM images of representative gold icosahedrons.**Fig. 5** SEM images of the as-synthesized particles when using different Pluronic copolymers at 40 °C, the concentrations of HAuCl₄ and copolymers were 0.84 mM and 5.8 mM, respectively. (a) P85; (b) P104; (c) P105. The concentration of the Pluronics was 8.4 mM. The other experimental conditions are the same as in Fig. 1. The insets of (b) and (c) show the magnified SEM images of the icosahedrons.

regular icosahedral gold nanoparticles are formed when a high molecular weight copolymer is used. This may result from the fact that a copolymer with a larger molecular weight is more flexible and can be absorbed on the surface of gold clusters more efficiently, which is favorable for forming regular icosahedral gold nanoparticles.

Possible mechanism

The above results show that icosahedral gold particles can be obtained under a wide range of experimental conditions. It is challenging to provide a convincing formation mechanism for the icosahedral gold particles at present. Surfactants are often

used to control the morphology of the particles by absorbing on to the surfaces.^{15,19} Many researchers have pointed out that adsorption and desorption of surfactants affect the growth speed of different crystalline faces.^{17,19} The Pluronics adsorbed on specific crystalline surfaces of gold could significantly decrease their growth rates and lead to a high anisotropic growth and results in the final nanoparticles with icosahedral shape. The results discussed above indicate that the size of the icosahedral particles prepared in this work can be controlled in the range of 100 nm to 1 μm , suggesting that the icosahedral gold particles were formed at an early stage in the reaction.

4. Conclusion

The above results show that icosahedral gold particles can be obtained under a wide range of experimental conditions. Icosahedral gold nanoparticles can be prepared using HAuCl_4 as precursor and Pluronics as reductant and directing agent. The route is simple and green, and the particle size can be tuned from 100 nm to 1 μm by varying the experimental conditions, including temperature, reaction time, concentration of the precursor and structure and concentration of the Pluronics. These icosahedral gold particles have potential applications in different fields.

Acknowledgements

This work was supported by National Natural Science Foundation of China (20633080).

References

- N. R. Jana, L. Gearheart and C. J. Murphy, *Adv. Mater.*, 2001, **13**, 1389–1393.
- M. D. Senarath-Yapa, S. Phimphivong, J. W. Coym, M. J. Wirth, C. A. Aspinwall and S. S. Saavedra, *Langmuir*, 2007, **23**, 12624–12633.
- C. Mohr, H. Hofmeister, J. Radnik and P. Claus, *J. Am. Chem. Soc.*, 2003, **125**, 1905–1911.
- M. Iqbal, Y. I. Chung and G. Tae, *J. Mater. Chem.*, 2007, **17**, 335–342.
- H. P. Liang, L. J. Wan, C. L. Bai and L. Jiang, *J. Phys. Chem. B*, 2005, **109**, 7795–7800.
- C. J. Johnson, E. Dujardin, S. A. Davis, C. J. Murphy and S. Mann, *J. Mater. Chem.*, 2002, **12**, 1765–1770.
- J. P. Xie, J. Y. Lee and D. I. C. Wang, *J. Phys. Chem. C*, 2007, **111**, 10226–10232.
- M. C. Daniel and D. Astruc, *Chem. Rev.*, 2004, **104**, 293–346.
- M. P. Pileni, *Nat. Mater.*, 2003, **2**, 145–150.
- H. A. Keul, M. Moller and M. R. Bockstaller, *Langmuir*, 2007, **23**, 10307–10315.
- Y. Niidome, K. Honda, K. Higashimoto, H. Kawazumi, S. Yamada, N. Nakashima, Y. Sasaki, Y. Ishida and J. Kikuchi, *Chem. Commun.*, 2007, **36**, 3777–3779.
- J. Y. Chen, B. Wiley, Z. Y. Li, D. Campbell, F. Saeki, H. Cang, L. Au, J. Lee, X. D. Li and Y. N. Xia, *Adv. Mater.*, 2005, **17**, 2255–2261.
- D. Seo, J. C. Park and H. Song, *J. Am. Chem. Soc.*, 2006, **128**, 14863–14870.
- Y. G. Sun and Y. N. Xia, *Science*, 2002, **298**, 2176–2179.
- F. Kim, S. Connor, H. Song, T. Kuykendall and P. D. Yang, *Angew. Chem., Int. Ed.*, 2004, **43**, 3673–3677.
- F. Fievet, J. P. Lagier and M. Figlarz, *Mater. Res. Soc. Bull.*, 1989, **14**, 29–32.
- Y. Chen, X. Gu, C. G. Nie, Z. Y. Jiang, Z. X. Xie and C. J. Lin, *Chem. Commun.*, 2005, **33**, 4181–4183.
- J. Xu, S. Li, J. Weng, X. Wang, Z. Zhou, K. Yang, M. Liu, X. Chen, Q. Cui, M. Cao and Q. Zhang, *Adv. Funct. Mater.*, 2008, **18**, 277–284.
- M. Zhou, S. Chen and S. Zhao, *J. Phys. Chem. B*, 2006, **110**, 4510–4513.
- P. Alexandridis and L. Yang, *Macromolecules*, 2000, **33**, 3382–3391.
- M. Y. Kozlov, N. S. Melik-Nubarov, E. V. Batrakova and A. V. Kabanov, *Macromolecules*, 2000, **33**, 3305–3313.
- I. F. Paterson, B. Z. Chowdhry and S. A. Leharne, *Langmuir*, 1999, **15**, 6187–6194.
- T. Sakai and P. Alexandridis, *J. Phys. Chem. B*, 2005, **109**, 7766–7777.
- T. Sakai and P. Alexandridis, *Langmuir*, 2004, **20**, 8426–8430.
- S. Chen, C. Guo, G. H. Hu, J. Wang, J. H. Ma, X. F. Liang, L. Zheng and H. Z. Liu, *Langmuir*, 2006, **22**, 9704–9711.
- P. Raveendran, J. Fu and S. L. Wallen, *J. Am. Chem. Soc.*, 2003, **125**, 13940–13941.
- S. A. Harfenist, Z. L. Wang, R. L. Whetten, I. Vezmar and M. M. Alvarez, *Adv. Mater.*, 1997, **9**, 817–822.
- S. Chen, C. Guo, G. H. Hu, J. Wang, J. H. Ma, X. F. Liang, L. Zheng and H. Z. Liu, *Langmuir*, 2006, **22**, 9704–9711.
- I. O. Sosa, C. Noguez and R. G. Barrera, *J. Phys. Chem. B*, 2003, **107**, 6269–6275.
- Y. Xiong, J. M. McLellan, Y. Yin and Y. Xia, *Angew. Chem., Int. Ed.*, 2007, **46**, 790–794.
- P. Alexandridis, J. Holzwarth and T. A. Hatton, *Macromolecules*, 1994, **27**, 2414–2425.

Cross-metathesis of oleyl alcohol with methyl acrylate: optimization of reaction conditions and comparison of their environmental impact

Anastasiya Rybak and Michael A. R. Meier*

Received 29th May 2008, Accepted 23rd July 2008

First published as an Advance Article on the web 12th September 2008

DOI: 10.1039/b808930b

The synthesis of α,ω -difunctional monomers from the renewable resource oleyl alcohol *via* a cross-metathesis reaction with methyl acrylate is described. The reaction conditions were optimized for high conversions in combination with high cross-metathesis selectivity. The introduction of a protecting group for the alcohol functionality of oleyl alcohol was found to be a necessary step in order to significantly reduce the amount of metathesis catalyst required to obtain full conversions and good selectivities. All reaction conditions were compared to each other in a quantitative fashion with the program EATOS (environmental assessment tool for organic syntheses) revealing the environmentally most benign approach for the synthesis of the desired α,ω -difunctional monomers. These calculations also clearly revealed that the introduction of the protecting group was a necessary step in order to minimize the amount of the produced waste and to use the raw materials more efficiently.

Introduction

Olefin metathesis with oleochemicals is a very versatile approach to obtain value added chemical intermediates from renewable raw materials.¹ Especially cross-metathesis reactions with fatty acid derivatives allow for the synthesis of a variety of monomers for many different kinds of polymers, including, *e.g.* polyesters, polyamides, polyethers as well as polyolefins. So far, cross-metathesis reactions with these renewable raw materials were almost exclusively investigated with ethylene as the cross-metathesis reaction partner in order to obtain ω -olefin functional fatty acid derivatives.^{1,2} These have then to be converted to the desired α,ω -difunctional derivatives for polyester and polyamide applications in a second reaction step.³ Recently, we were able to show that the cross-metathesis of different fatty acid methyl esters with methyl acrylate (MA) can be performed with very low catalyst loadings of 0.5 mol% or less applying the second generation Hoveyda–Grubbs catalyst.⁴ Conversions were quantitative under bulk conditions and the self-metathesis reactions could be efficiently suppressed by using excess amounts of MA thus allowing for an efficient synthesis of α,ω -diesters with different chain-lengths from plant oils as renewable raw materials.⁴ Oleyl alcohol **1** would be a perfect substrate for the cross-metathesis with MA since an α -ester, ω -hydroxy-difunctional monomer could thus be obtained in a single reaction step. Until today, only very few metathesis reactions of **1** are known.^{5,6} In the first case, unfortunately only the reaction scheme was given without providing any experimental details.⁵ In the second case the self-metathesis of oleyl oleate was investigated in an attempt to prepare macrocyclic esters.⁶ Other long chain alcohols, such as 10-undecenol that can be derived

from castor oil, were also investigated in metathesis reactions. Warwel *et al.* could show that protecting groups have a large influence on the reactivity of these chemicals in cross-metathesis reactions with ethene or 4-octene⁷ and that it is possible to use silylated fatty alcohol derivatives to yield chain shortened fatty alcohols upon metathesis with hexenes.⁸ In both cases heterogeneous rhenium catalysts were applied. Moreover, even if generally very functional group tolerant ruthenium based metathesis catalysts were used for the self-metathesis of 10-undecenol only moderate yields and reduced conversions were observed.⁹

Within this article we describe the cross-metathesis of oleyl alcohol **1** with MA under different reaction conditions and compare these conditions to each other in terms of conversion, cross-metathesis selectivity, catalyst consumption, as well as environmental impact.

Results and discussion

Within this article we investigated the possibility of preparing an α,ω -difunctional monomer from oleyl alcohol **1** *via* a cross-metathesis procedure. As shown in Fig. 1 the cross-metathesis of **1** with MA yields 11-hydroxy-2-undecenoic acid methyl ester **2** and 2-undecenoic acid methyl ester **3**. Whereas **2** is a valuable monomer for polymers from plant oil renewable resources,¹⁰ **3** has the appropriate chain length for detergent applications.¹¹ Moreover, both chemicals are valuable intermediates for fine chemical synthesis from renewable resources.¹² Therefore, the reaction depicted in Fig. 1 potentially offers an efficient access to value added chemicals from renewable resources since it is almost 100% atom economic.^{13–15} However, since atom economy does not take conversions or product yields into account this reaction can only be considered as a green chemistry approach if high conversion in combination with little or no formation of side-products can be obtained. During this cross-metathesis

University of Applied Sciences Oldenburg/Ostfriesland/Wilhelmshaven, Constantiaplatz 4, 26723, Emden, Germany.
E-mail: michael.meier@fh-oow.de; Web: www.meier-michael.com

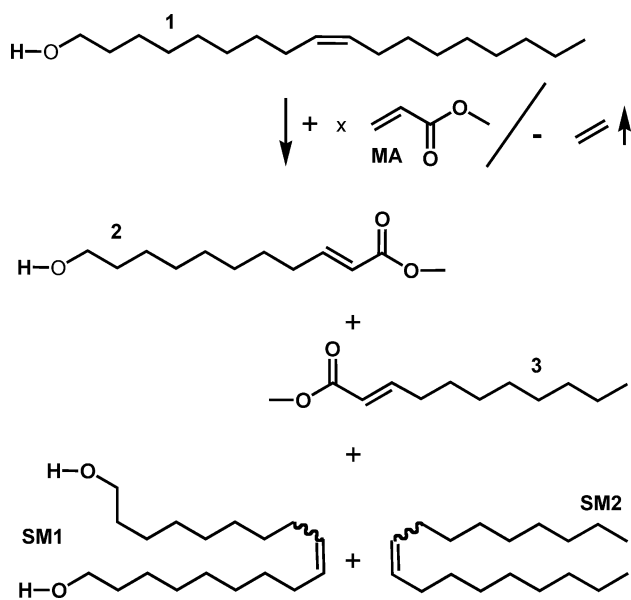


Fig. 1 Cross-metathesis of oleyl alcohol **1** with methyl acrylate (**SM1** and **SM2** are self-metathesis products).

reaction self-metathesis of **1** can also occur to give the self-metathesis products **SM1** and **SM2**. Even if these products would not be considered as waste in an industrial setting, because they would find applications as monomer, lubricant or biodiesel component, we tried to minimize their formation in the course of these investigations for ease of purification and because **2** is considered the most valuable product of this reaction. We started our investigations by performing self-metathesis reactions of **1** in order to understand the behaviour of **1** with different metathesis catalysts and to obtain reference substances for further GC and GC-MS investigations of the subsequently performed cross-metathesis reactions. The first generation Grubbs catalyst was not suited for these reactions and the second generation catalyst from Grubbs gave somewhat poorer results than the Hoveyda–Grubbs second generation metathesis catalyst. Similar observations were made for the cross-metathesis reactions of **1**. Therefore, we performed all further reactions under bulk conditions with the Hoveyda–Grubbs second generation metathesis catalyst. The results of these investigations are summarized in Table 1 and clearly show that the reaction only proceeds well with high catalyst loadings.

The results presented in Table 1 stem from GC analysis with tetradecane as internal standard. Generally, the GC traces were easy to interpret, but up to 10% of unknown side-products were observed in the GC traces, especially if high catalyst amounts were used. Additional analysis of the reaction mixtures by GC-MS unambiguously identified **2** in the reaction mixture and revealed identical (within experimental error) quantitative results as for the GC analysis presented in Table 1. Moreover, the expected and yet unknown products **2** and **SM1** of these cross-metathesis reactions were easily identified by ESI-MS experiments. Reducing the catalyst amount favoured the self-metathesis reaction in all cases and increasing the excess of MA in order to suppress the self-metathesis reaction had only a relatively small effect. This behaviour is in sharp contrast to our experience of the cross-metathesis reactions of fatty acid

Table 1 Cross-metathesis results of **1** with MA ($T = 50\text{ }^\circ\text{C}$, $t = 21\text{ h}$, reactions performed with 0.4 g **1** in bulk)

	Catalyst (mol%) ^a	C% ^b	SM% ^c	CM% ^d	x^e
1	5	93.3	9.7	90.3	5
2	1	89.9	16.4	83.6	5
3	0.5	79.6	46.6	53.4	5
4	0.2	76.1	53.0	47.0	5
5	0.1	48.5	71.6	28.4	5
6	5	97.6	2.8	97.2	10
7	1	88.0	13.2	86.8	10
8	0.5	80.5	27.8	72.2	10
9	0.2	70.4	47.6	52.4	10
10	0.1	66.5	53.9	46.1	10

^a Amount of catalyst in mol% relative to **1**. ^b Conversion of **1** in % (by GC). ^c % Self-metathesis products of all products (GC estimate). ^d % Cross-metathesis products of all products (GC estimate). ^e Ratio: MA : **1** (see Fig. 1).

methyl esters with MA, where the self-metathesis could be very efficiently suppressed and catalyst loadings of 0.5 mol% or less were sufficient to obtain full conversions.⁴ It is known from the literature that the electron deficient substrate MA requires up to 20 mol% of second generation metathesis catalysts in cross-metathesis reactions if the reactions are performed in solvents.^{16–19} Moreover, alcohols have been frequently reported to produce side products and/or lead to a degradation of the catalyst during metathesis reactions.^{20–22} Therefore, the combination of electron withdrawing substrate and the presence of –OH functional groups in large excess to the catalyst might lead to the observed low conversions and the requirement of high catalyst loadings for good cross-metathesis selectivity. In order to circumvent this behaviour the alcohol functionality of **1** was protected with acetic acid to form oleyl acetate **4** (see Fig. 2).

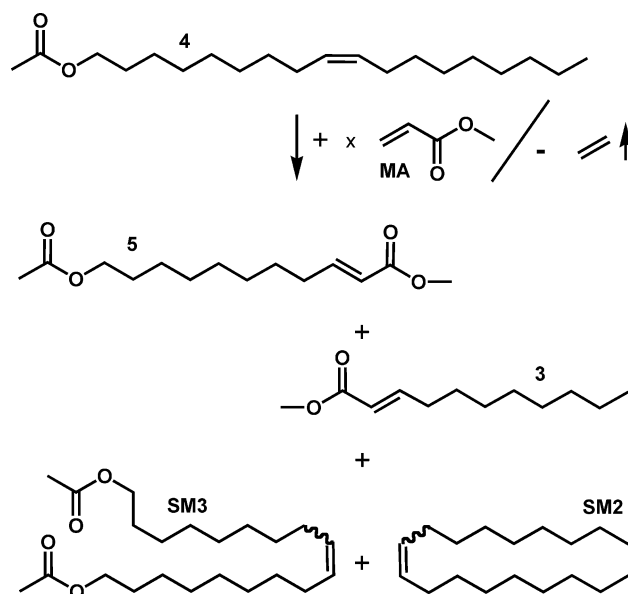


Fig. 2 Cross-metathesis of oleyl acetate **4** with methyl acrylate (**SM2** and **SM3** are self-metathesis products).

Indeed, if cross-metathesis reactions were performed with **4** and MA (see Fig. 2) the situation changed completely and much

Table 2 Cross-metathesis results of **4** with MA ($T = 50\text{ }^{\circ}\text{C}$, $t = 21\text{h}$, reactions performed with 1.0 g **4** in bulk)

	Catalyst (mol%) ^a	C% ^b	SM% ^c	CM% ^d	λ ^e
1 ^f	2	99.1	1.2	98.8	5
2	1	99.5	3.8	96.2	5
3	0.5	92.8	16.1	83.9	5
4	0.2	87.8	29.6	70.4	5
5	0.1	55.8	63.1	36.9	5
6 ^f	2	99.0	0.6	99.3	10
7	1	98.0	1.4	98.6	10
8	0.5	94.7	6.0	94.0	10
9	0.2	85.9	27.2	72.8	10
10	0.1	64.0	51.1	48.9	10

^a Amount of catalyst in mol% relative to **4**. ^b Conversion of **4** in % (by GC). ^c % Self-metathesis products of all products (GC estimate). ^d % Cross-metathesis products of all products (GC estimate). ^e Ratio: MA : **4** (see Fig. 2). ^f Results after 5 h reaction time.

smaller amounts of catalyst were required in order to obtain full conversions and good selectivities as summarized in Table 2. Also here, the unknown compounds **5** as well as **SM3** were easily identified by GC-MS and ESI-MS experiments and the data provided in Table 2 could be confirmed independently by GC-MS measurements. It is obvious from the data presented in Table 2 that the protection of the alcohol group was well worth the efforts since the protected alcohol **4** can be fully converted to the cross-metathesis products with only 1% of the Hoveyda–Grubbs second generation catalyst. Comparing the results directly to results obtained with the unprotected alcohol, the entries of, e.g. Table 1 entry 6 and Table 2 entry 7 reveal that the protected alcohol substrate allows the reduction of the catalyst amount of at least five fold, while the conversion remains the same and the selectivity is slightly improved. Also for the cross-metathesis of **4** the reduction of the amount of catalyst led to decreased selectivity for the cross-metathesis products **5** and **3** and to a decrease of the observed conversion of **4**. In summary, the catalytic results of the cross-metathesis of **4** are, in contrast to those of **1**, in good agreement with the results obtained for fatty acid methyl esters leading us to the conclusion that the –OH functionality in the substrate **1** leads to decreased catalyst activity and selectivity, probably due to degradation of the catalyst.

Additionally to the presented catalytic results we performed a larger scale synthesis of **3** and **5** in order to be able to separate the new compounds and analyze them by NMR spectroscopy. Indeed, if the synthesis as depicted in Fig. 2 was performed on a 5 g scale according to the general experimental procedure provided below we were able to obtain both **3** and **5** by column chromatography in approximately 75% isolated yield, respectively. The protecting group of **5** was then removed by transesterification with excess methanol to obtain **2** in a reaction showing complete conversion. The NMR spectra as well as GC and GC-MS data of all isolated compounds were as expected thus further proving their correct structure as well as chromatographic assignments.

In order to better understand and be able to compare these results to each other, also in terms of environmental impact, we used EATOS (environmental assessment tool for organic syntheses).²³ We thus calculated the mass index S^{-1} (mass of all

raw materials used for the synthesis per mass unit of the purified product) and the environmental factor E (waste per mass unit of the product) for different synthetic pathways towards the desired products **2** or **5** allowing the evaluation and comparison of different reaction routes in a quantitative fashion.²⁴ In an ideal situation both factors should be minimal indicating an efficient use of the raw materials and a minimal production of waste, respectively. The different synthetic approaches compared and discussed are Table 1, entries 1, 3 and 8 as well as Table 2, entries 1, 2, 3, 6 and 8. For the data from Table 2 the necessary esterification step of oleyl alcohol was also included in the calculations and the data discussed here are overall data of the two reaction steps in the sequence (Fig. 3).

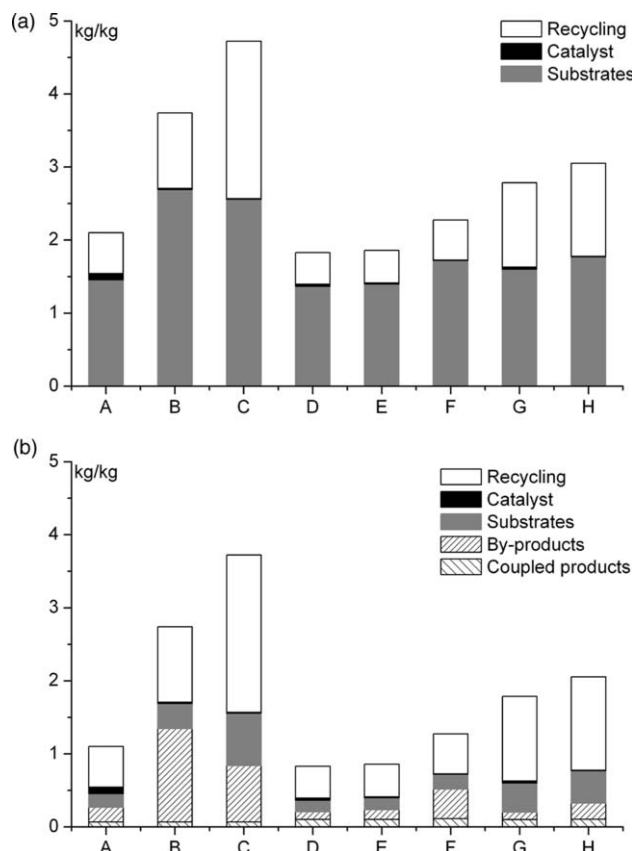


Fig. 3 Mass index (top) and environmental factor (bottom) for the following reactions: A: Table 1, entry 1; B: Table 1, entry 3; C: Table 1, entry 8; D: Table 2, entry 1; E: Table 2, entry 2; F: Table 2, entry 3; G: Table 2, entry 6; H: Table 2, entry 8.

The height of the columns in Fig. 3(a) represents the mass index S^{-1} and indicates the amounts of raw materials necessary to produce 1 kg of **2** or **5**, respectively. The columns of Fig. 3(b) show the environmental factor E indicating the amount of waste formed. The E columns are normalized to the desired products (**2** and **3** or **5** and **3**, respectively) and these products are not shown as output of the synthesis. This is also the reason why the E column of a particular synthesis is lower than the corresponding S^{-1} column. The remaining coupled product indicated in Fig. 3(b) is the produced ethene, which is regarded as waste in this comparison but could be recovered in an industrial application further optimizing the environmental impact of this

procedure. The grey parts of both S^{-1} and E show the substrates that are used for the synthesis (S^{-1}) or that are left unreacted after the reaction (E). The same counts for the black part that belongs to the catalyst. The white parts of the columns in Fig. 3 indicate the amount of unused MA possibly being recyclable. For this estimation an unambiguous recovery of 75% of the unreacted MA was taken into account. This means that all columns of Fig. 3 can be cut by the white parts just by recycling unused substrates. Columns B, C, and F–G of Fig. 3 clearly show that the corresponding procedures need more raw material and/or produce more waste to obtain the same amounts of products. Comparing the remaining three options (A, D, and E) it is obvious that A produces the highest amount of waste and uses the raw materials least efficiently. The remaining two options D and E show only a very small advantage of 2% more efficient raw materials use for the synthetic pathway D. Therefore, D might be considered as the environmentally most benign approach of the herein studied approaches to produce an α,ω -difunctional monomer from oleyl alcohol, if the catalyst amount is not taken into account. If compared to procedure E, procedure D requires 1.95 times the amount of catalyst to produce the same amount of products. This is not only relevant in terms of costs, but might finally also influence the environmental impact if the toxicity of the catalyst was taken into account. Unfortunately, this is not possible at this moment since such data is unavailable. It is also interesting to note that procedure H uses the smallest and procedure A the highest amount of catalyst to produce the desired products of all compared procedures. Moreover, procedure A is by far the most expensive approach being on average 5 times more expensive than all other procedures due to the high amount of catalyst used. The low amount of catalyst used is also the reason why in terms of economics the procedures F and H are the cheapest to produce the same amounts of products. Also these calculations were performed with EATOS.

Conclusions

In conclusion, we have shown that oleyl alcohol is a valuable renewable raw material to produce desired α,ω -difunctional monomers for polyesters and a shorter chain fatty acid methyl ester for detergent applications at the same time. The reaction conditions were optimized and compared to each other and a protecting group for the hydroxyl functionality was found to be necessary to reduce the amounts of precious catalyst to lower levels. Quantitative comparison of the different synthetic approaches with EATOS revealed that the introduction of a protecting group is a necessary second reaction step in order to minimize the overall production of waste and use the raw materials more efficiently. Moreover, it was shown that the recycling of unreacted starting materials has a large influence on the overall environmental impact of these reactions and that no unnecessary waste was produced since all reactions were performed under bulk conditions.

Experimental

Experimental procedures and details

Materials. Oleyl alcohol **1** (90–95%) was kindly provided by Cognis. Acetic acid (Fluka, $\geq 99\%$), ethyl vinyl ether (Aldrich,

99%), tetradecane (Fluka, $\geq 99\%$) and (1,3-bis-(2,4,6-trimethylphenyl)-2-imidazolidinylidene)dichloro(*o*-isopropoxyphenylmethylene)ruthenium (Hoveyda–Grubbs Catalyst 2nd Generation, Aldrich) were used as received. MA (Aldrich, 99%) was purified by filtration over silica gel.

Analytical equipment and methods. Thin layer chromatography (TLC) was performed on silica gel TLC-cards (layer thickness 0.20 mm, Fluka). Compounds were visualized by permanganate reagent. For column chromatography silica gel 60 (0.035–0.070 mm, Fluka) was used.

Infrared (IR) spectra were obtained using a Bruker EQUINOX 55 FTIR spectrometer fitted with an ATR cell. Data are presented as the frequency of absorption (cm^{-1}).

$^1\text{H-NMR}$ (^{13}C NMR) spectra were recorded in CDCl_3 on a Bruker AVANCE DPX spectrometer operating at 300 (75.5) MHz. Chemical shifts (δ) are reported in parts per million relative to the internal standard tetramethylsilane (TMS, $\delta = 0.00$ ppm).

Analytical GC characterization of mixtures was carried out with a Shimadzu GC-2010 equipped with a fused silica capillary column (Stabilwax[®], 30 m \times 0.25 mm \times 0.25 μm , Restek), using flame ionization detection. The oven temperature program was: initial temperature 200 $^\circ\text{C}$, ramp at 8 $^\circ\text{C min}^{-1}$ to 250 $^\circ\text{C}$, hold for 4 min. Measurements were performed in the split-split mode (split ratio 45 : 1) using hydrogen as the carrier gas (linear velocity of 31.4 cm s^{-1} at 220 $^\circ\text{C}$).

GC-MS (EI) chromatograms were recorded using a VARIAN 3900 GC instrument with a capillary column FactorFour[™] VF-5ms (30 m \times 0.25 mm \times 0.25 μm , Varian) and a Saturn 2100T ion trap mass detector. Scans were performed from 40 to 650 m/z at rate of 1.0 scans s^{-1} . The oven temperature program was: initial temperature 95 $^\circ\text{C}$, hold for 1 min, ramp at 15 $^\circ\text{C min}^{-1}$ to 220 $^\circ\text{C}$, hold for 4 min, ramp at 15 $^\circ\text{C min}^{-1}$ to 300 $^\circ\text{C}$, hold for 2 min. The injector transfer line temperature was set to 250 $^\circ\text{C}$. Measurements were performed in the splitless and split-split mode (split ratio 50 : 1) using helium as carrier gas (flow rate 1.0 ml min^{-1}).

Mass spectra (ESI) were recorded on a VARIAN 500-MS ion trap mass spectrometer with the TurboDDST[™] option installed.

Synthesis of octadec-9-enyl acetate (4). A mixture of oleyl alcohol **1** (100.0 g, 0.39 mol) and acetic acid (118.0 g, 1.96 mol) was stirred magnetically and refluxed overnight at 120 $^\circ\text{C}$. At the end of reaction the mixture was cooled to ambient temperature and an excess of acetic acid was removed *in vacuo*. The residue was washed with water several times, dried with anhydrous sodium sulfate and then purified by column chromatography with hexane–diethyl ether (8 : 2) as eluent. The liquid product was obtained with a yield of 91.8 g (75%). IR: $\nu = 2923, 2853, 1741, 1462, 1365, 1234, 1036, 968$ cm^{-1} . $^1\text{H-NMR}$ (300 MHz, CDCl_3 , δ): 5.39–5.32 (m, 2H, $-\text{CH}=\text{CH}-$), 4.07–4.03 (t, $J = 6.9$ Hz, 2H, $\text{CH}_2\text{COOCH}_2-$), 2.03–1.98 (m, 7H, $\text{CH}_2\text{COO}-$ and $=\text{CH}-\text{CH}_2-$), 1.64–1.59 (m, $J = 6.9$ Hz, 2H, CH_2), 1.29 (br. s., 22H, 11 CH_2), 0.90–0.86 (t, $J = 6.9$ Hz, 3H, CH_3). $^{13}\text{C-NMR}$ (75.5 MHz, CDCl_3 , δ): 172.9 (s, $-\text{COO}-$), 132.1 (s, $\text{CH}=\text{CH}$), 66.4 (s, $\text{CH}_2\text{COOCH}_2-$), 34.4 (s, CH_2), 33.8 (s, CH_2), 33.7 (s, CH_2), 31.6 (s, CH_2), 31.5 (s, CH_2), 31.4 (s, CH_2), 31.3 (s, CH_2), 31.2 (s, CH_2), 31.1 (s, CH_2), 30.9 (s, CH_2), 30.5 (s, CH_2), 29.1 (s, CH_2), 27.8 (s, CH_2), 23.1 (s, CH_2), 22.8 (s, $\text{CH}_2\text{COO}-$), 15.9

(s, CH₃). GC-MS (EI, *m/z* %): 311.0 (15) (M⁺, calc. 310.5), 250.1 (43), 194.1 (8), 136.2 (18), 123.2 (25), 109.2 (35), 95.3 (60), 81.3 (100). MS (ESI-positive, CH₃OH, *m/z*): 333.4 (MNa⁺, calc. 333.5).

Solvent-free cross-metathesis reaction (general procedure). In a typical experiment, 0.5 ml (0.4 g, 1.57 mmol) of **1** or 1.0 g of **4** (3.22 mmol) and an excess of MA (5 to 10 equivalents according to **1** or **4**, respectively) were used. Tetradecane (olefin free, 10% of the volume of starting fatty acid derivate) was used as an internal standard for GC analysis. The reaction mixture was stirred with a magnetical stirrer and heated at 50 °C. The solid catalyst was then added to the solution, in the range of 0.1–5 mol%. No additional solvents were added. All reactions were carried out without a nitrogen atmosphere. Samples were taken periodically and quenched with an excess of ethyl vinyl ether in order to stop the metathesis reaction. After this procedure a conversion analysis was performed by GC.

For isolation of the products **3** and **5** this procedure was performed with 5 g (16.10 mmol) of **4**, 14.5 ml (161.02 mmol) of MA and 0.101 g (0.16 mmol) of catalyst. The reaction mixture was stirred magnetically at 50 °C. After 20 h reaction time, the excess of MA was evaporated *in vacuo* and the residue was separated by column chromatography with a mixture of hexane and diethyl ether (19 : 1) as eluate. The isolated yield of compounds **3** and **5** was 2.44 g (76.4%) and 3.09 g (74.7%), respectively.

Methyl-11-hydroxy-undec-9-enoate (2). GC-MS retention time of **2**: 9.33 min. GC-MS (EI, *m/z* %): 214.9 (M⁺, 17), 183.0 (7), 163.9 (21), 135.8 (23), 121.9 (24), 112.8 (40), 93.8 (48), 86.8 (62), 80.9 (100), 67.0 (85). MS (ESI-positive, CH₃OH, *m/z*): 237.3 (MNa⁺, calc. 237.31). IR: $\nu = 3357$ (br.), 2927, 2855, 1721, 1655, 1435, 1268, 1179, 1038, 978 cm⁻¹.

Methyl-undec-2-enoate (3). GC-MS retention time of **3**: 7.08 min. GC-MS (EI, *m/z* %): 199.0 (M⁺, 100), 166.9 (40), 148.0 (30), 137.0 (25), 123.0 (25), 113.0 (35), 98.0 (20), 96.0 (40), 81.0 (70), 68.0 (45), 54.9 (95). MS (ESI-positive, CH₃OH, *m/z*): 221.1 (MNa⁺, calc. 221.31). IR: $\nu = 2925, 2855, 1725, 1657, 1435, 1268, 1196, 1171, 1127, 1039, 980$ cm⁻¹. ¹H-NMR (300 MHz, CDCl₃): $\delta = 7.0$ – 6.92 (m, 1H, $-\text{CH}=\text{CH}-\text{COOCH}_3$), 5.84 – 5.79 (d, $J = 15.7$ Hz, 1H, $-\text{CH}=\text{CH}-\text{COOCH}_3$), 3.72 (s, 3H, $-\text{CH}=\text{CH}-\text{COOCH}_3$), 2.23 – 2.15 (dt, $J = 7.2$ and 14.2 Hz, 2H, $-\text{CH}_2-\text{CH}=\text{CH}-\text{COOCH}_3$), 1.48 – 1.41 (m, 2H, CH₂), 1.27 (br. s, 10H, 5CH₂), 0.88 (t, $J = 7.1$, 3H, CH₃) ppm. ¹³C-NMR (75.5 MHz, CDCl₃): $\delta = 167.2$ (s, $-\text{COOCH}_3$), 149.8 (s, $-\text{CH}=\text{CH}-\text{COOCH}_3$), 120.8 (s, $-\text{CH}=\text{CH}-\text{COOCH}_3$), 51.4 (s, $-\text{COOCH}_3$), 32.2 (s, CH₂), 31.6 (s, CH₂), 29.4 (s, CH₂), 29.2 (s, CH₂), 28.0 (s, CH₂), 22.7 (s, CH₂), 14.1 (s, CH₃) ppm.

Methyl-11-acetoxy-undec-9-enoate (5). GC-MS retention time of **5**: 10.39 min. GC-MS (EI, *m/z* %): 256.8 (M⁺, 6), 224.1 (6), 182.0 (15), 163.9 (26), 135.8 (78), 120.9 (55), 107.0 (38), 93.8 (43), 80.9 (75), 67.0 (55), 43.0 (100). MS (ESI-positive, CH₃OH, *m/z*): 279.2 (MNa⁺, calc. 279.34). IR: $\nu = 2928, 2856, 1723, 1656, 1436, 1366, 1235, 1035, 980$ cm⁻¹. ¹H-NMR (300 MHz, CDCl₃): $\delta = 7.02$ – 6.92 (m, 1H, $-\text{CH}=\text{CH}-\text{COOCH}_3$), 5.84 – 5.79 (d, $J = 15.6$ Hz, 1H, $-\text{CH}=\text{CH}-\text{COOCH}_3$), 4.07 – 4.03 (t, $J = 6.9$ Hz, 2H, $-\text{CH}_2\text{OCOCH}_3$), 3.72 (s, 3H, $-\text{COOCH}_3$), 2.23 – 2.16 (dt, $J = 7.2$ and 14.2 Hz, 2H, $-\text{CH}_2-\text{CH}=\text{CH}-\text{COOCH}_3$),

2.04 (s, 3H, $-\text{OCOCH}_3$), 1.64 – 1.57 (m, 2H, CH₂), 1.48 – 1.43 (m, 2H, CH₂), 1.31 (br. s, 8H, 4CH₂) ppm. ¹³C-NMR (75.5 MHz, CDCl₃): $\delta = 171.5$ (s, $-\text{OCOCH}_3$), 167.2 (s, $-\text{COOCH}_3$), 149.9 (s, $-\text{CH}=\text{CH}-\text{COOCH}_3$), 121.3 (s, $-\text{CH}=\text{CH}-\text{COOCH}_3$), 64.9 (s, $-\text{CH}_2\text{OCOCH}_3$), 51.7 (s, $-\text{COOCH}_3$), 32.5 (s, CH₂), 29.7 (s, CH₂), 29.6 (s, CH₂), 29.5 (s, CH₂), 29.0 (s, CH₂), 28.3 (s, CH₂), 26.2 (s, CH₂) ppm.

Octadec-9-ene-1,18-diol (SM1). This compound was not detected by GC-MS. MS (ESI-positive, CH₃OH, *m/z*): 307.3 (MNa⁺, calc. 307.49).

Octadec-9-ene (SM2). GC-MS retention time of **SM2**: 9.47 min. GC-MS (EI, *m/z* %): 252.0 (M⁺, 3), 208.0 (2), 193.9 (2), 180.0 (3), 166.0 (4), 152.0 (3), 138.0 (5), 124.9 (20), 110.9 (40), 97.0 (100), 82.8 (87), 57.0 (56), 55.1 (90).

18-Acetoxy-octadec-9-enyl acetate (SM3). GC-MS retention time of **SM3**: 18.02 min. GC-MS (EI, *m/z* %): 369.2 (M⁺, 2), 327.2 (3), 308.2 (4), 248.1 (5), 191.9 (3), 177.0 (3), 163.0 (5), 149.0 (10), 135.1 (22), 120.9 (33), 109.0 (30), 107.0 (8), 95.1 (55), 80.9 (90), 67.0 (100), 55.1 (40). MS (ESI-positive, CH₃OH, *m/z*): 391.3 (MNa⁺, calc. 391.56).

Acknowledgements

We kindly acknowledge financial support from the German Federal Ministry of Food, Agriculture and Consumer Protection (represented by the Fachagentur Nachwachsende Rohstoffe; FKZ 22026905). We thank Marco Eissen for help with the EATOS program. The authors are grateful for the access to NMR facilities at the University of Oldenburg, Germany. M. A. R. Meier kindly acknowledges support from Prof. Dr J. O. Metzger as well as financial support from BASF.

Notes and references

- 1 A. Rybak, P. A. Fokou and M. A. R. Meier, *Eur. J. Lipid Sci. Technol.*, 2008, DOI: 10.1002/ejlt.200800027.
- 2 S. Warwel, F. Bruse and M. Kunz, *Fresenius' Environ. Bull.*, 2003, **12**, 534–539.
- 3 S. Warwel, F. Brüse, C. Demes and M. Kunz, *Ind. Crops Prod.*, 2004, **20**, 301–309.
- 4 A. Rybak and M. A. R. Meier, *Green Chem.*, 2007, **9**, 1356–1361.
- 5 C. Brändli and T. R. Ward, *Helv. Chim. Acta*, 1998, **81**, 1616–1621.
- 6 J. Tsuji and S. Hashiguchi, *Tetrahedron Lett.*, 1980, **21**, 2955–2958.
- 7 S. Warwel, N. Döring and F. J. Biermanns, *Fett Wiss. Technol.*, 1987, **89**, 335–339.
- 8 S. Warwel, N. Döring and A. Deckers, *Fett Wiss. Technol.*, 1988, **90**, 125–129.
- 9 H. E. Blackwell, D. J. O'Leary, A. K. Chatterjee, R. A. Washenfelder, D. A. Bussmann and R. H. Grubbs, *J. Am. Chem. Soc.*, 2000, **122**, 58–71.
- 10 M. A. R. Meier, J. O. Metzger and U. S. Schubert, *Chem. Soc. Rev.*, 2007, **36**, 1788–1802.
- 11 A. Behr and A. Westfechtel, *Chem.-Ing.-Tech.*, 2007, **79**, 621–636.
- 12 U. Biermann, W. Friedt, S. Lang, W. Lühs, G. Machmüller, J. O. Metzger, M. Rüschen, Klaas, H. J. Schäfer and M. P. Schneider, *Angew. Chem., Int. Ed.*, 2000, **39**, 2206–2224.
- 13 Note: for the reaction of 1 mole of **1** with 2 moles of MA, 1 mole of **2**, 1 mole of **3**, and 1 mole of ethene are produced; therefore, if ethene is considered as a waste product the atom economy is 93.6%; if ethene is considered a useful product and would be recovered on an industrial scale the atom economy would be 100%.
- 14 B. M. Trost, *Science*, 1991, **254**, 1471–1477.
- 15 M. Eissen, R. Mazur, H.-G. Quebbemann and K.-H. Pennemann, *Helv. Chim. Acta*, 2004, **87**, 524–535.

- 16 A. K. Chatterjee, T.-L. Choi, D. P. Sanders and R. H. Grubbs, *J. Am. Chem. Soc.*, 2003, **125**, 11360–11370.
- 17 L. Ferrié, D. Amans, S. Reymond, V. Bellosta, P. Capdevielle and J. Cossy, *J. Organomet. Chem.*, 2006, **692**, 5456–5465.
- 18 S. Fustero, M. Sánchez-Roselló, J. F. Sanz-Cervera, J. L. Aceña, C. del Pozo, B. Fernández, A. Bartolomé and A. Asensio, *Org. Lett.*, 2006, **8**, 4633–4636.
- 19 S. J. Langford, M. J. Latter and C. P. Woodward, *Org. Lett.*, 2006, **8**, 2595–2598.
- 20 B. Schmidt and L. Staude, *J. Organomet. Chem.*, 2006, **691**, 5218–5221.
- 21 B. Schmidt, *Eur. J. Org. Chem.*, 2004, **9**, 1865–1880.
- 22 D. Banti and J. C. Mol, *J. Organomet. Chem.*, 2004, **689**, 3113–3116.
- 23 M. Eissen and J. O. Metzger, *Chem.–Eur. J.*, 2002, **8**, 3580–3585.
- 24 Note: **2** and **5** are considered as equally useful products for a direct polyester synthesis; in the first case methanol would be the condensation by-product; in the second case methyl acetate would be formed; both would be recycled on an industrial scale.

Efficient green synthesis of α -aminonitriles, precursors of α -amino acids†

G. K. Surya Prakash,^{*a} Tisa Elizabeth Thomas,^{a,b} Inessa Bychinskaya,^a Arjun G. Prakash,^{a,c} Chiradeep Panja,^a Habiba Vaghoo^a and George A. Olah^{*a}

Received 25th February 2008, Accepted 1st August 2008

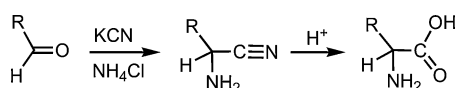
First published as an Advance Article on the web 12th September 2008

DOI: 10.1039/b803152e

The synthesis of α -aminonitriles by a direct three component Strecker reaction has been achieved using environmentally friendly solid acid catalysts, Nafion[®]-H and Nafion[®] SAC-13.

Introduction

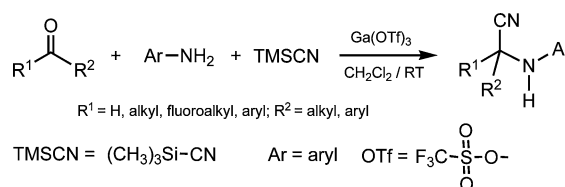
One of the major aims of sustainable development is the protection of the natural environment. Chemistry and chemical processes are essential for the development of life and life processes. The Strecker reaction is one of the most important and well known chemical reactions, which has significant biological applications¹ (Scheme 1). It is the most used method towards the synthesis of α -amino acids *via* the formation of α -aminonitriles. This approach involves a direct multi-component (three component) reaction using an aldehyde or ketone, an amine or its equivalent and a cyanide reagent to form α -aminonitriles, which can be subsequently converted to α -amino acids. Amino acids are the basic building units of proteins in all living organisms. Miller's experiment to mimic prebiotic synthesis of amino acids from a mixture of CH₄, NH₃, H₂, and H₂O reveals the probable key role of the Strecker reaction in the origin of life under primitive Earth conditions.² Environmentally friendly "green" catalysts have profound influence and greatly contribute towards sustainable development in a faster pace. Therefore it is worthwhile to investigate the potential of such catalyst systems for the Strecker reaction.



Scheme 1 Strecker reaction (A. Strecker, 1850).

Fluorinated amino acids are important building blocks in pharmaceuticals and other biological applications³ in the development of anticancer drugs for the control of tumor growth, drugs for the control of blood pressure and allergies.⁴ They have been shown as irreversible inhibitors of pyridoxal phosphate dependent enzymes.⁵ Fluorinated amino acids are also valuable tools for the screening of protein dynamics by nuclear magnetic resonance (NMR) studies.⁶ Consequently, fluorinated

amino acids have also become the object of intense synthetic activity in recent years. The Strecker reaction with aldehydes has been studied extensively with a variety of heterogeneous and homogeneous catalysts.^{7,8} However, the reactions were not feasible for ketones until the development of a mild and efficient method using catalysts such as gallium triflate (or the related metal triflates) (Scheme 2), trimethylsilyl triflate and Fe(Cp)₂PF₆.⁹ Prior to our studies, an efficient, clean and direct three component Strecker reaction using aromatic ketones and aromatic amines was considered a challenge.^{7,8,10}



Scheme 2 Ga(OTf)₃ catalyzed Strecker reaction using aldehydes, ketones or fluorinated ketones and amines.

During our ongoing efforts to search for environmentally friendly and reusable acidic catalysts, we have found that Nafion[®]-H (perfluoroalkanesulfonic acid polymer)¹¹ and Nafion[®] SAC-13 (10–20% Nafion[®]-H polymer on amorphous silica, porous nanocomposite)¹² are effective heterogeneous catalysts for the direct three component Strecker reaction of not only aldehydes but ketones and most importantly fluorinated ketones. They display the characteristic properties of a desired heterogeneous catalyst. They are easily accessible, non-toxic, highly catalytic, environmentally benign, stable and easily recoverable. Most importantly, their reusability makes them ideal catalysts. Easy work-up and product isolation, simplicity and mildness of the reaction, and high purity of the products in most cases are the added advantages of using these heterogeneous catalysts. Further, during these investigations it was found that silica gel and fumed silica (without any functionalization), also have potential as inexpensive heterogeneous catalysts for the Strecker reaction.

Experimental

¹H, ¹³C and ¹⁹F NMR spectra were recorded on Varian NMR spectrometers at 400 MHz. Structures of all products were confirmed by comparison with those of the authentic samples.⁹ ¹H NMR chemical shifts were determined relative

^aLoker Hydrocarbon Research Institute and Department of Chemistry, University of Southern California, Los Angeles, CA, 90089-1661, USA. E-mail: gprakash@usc.edu; Fax: +1 213-7405087; Tel: +1 213-7405984

^bSiemens Competition Regional Finalist, Troy High School, 2200 E. Dorothy Lane, Fullerton, CA, 92831, USA

^cHigh School Sophomore Research Fellow, Glen A. Wilson High School, 16455 E. Wedgeworth Drive, Hacienda Heights, CA, 91745, USA

† Electronic supplementary information (ESI) available: Experimental details and characterization data. See DOI: 10.1039/b803152e

to tetramethylsilane (internal standard) at δ 0.0. ^{13}C NMR chemical shifts were determined relative to tetramethylsilane (internal standard) at δ 0.0 or to the ^{13}C signal of CDCl_3 at δ 77.0. ^{19}F NMR chemical shifts were determined relative to internal CFCl_3 at δ 0.0.

Materials and methods

The aldehydes, ketones, amines, Nafion[®]-K, and Nafion[®] SAC-13 were purchased from commercial sources. Nafion[®]-H was prepared from Nafion[®]-K (potassium salt) following a literature procedure.^{11a} The fluorinated ketones, trimethylsilyl cyanide (TMSCN), silica gel and fumed silica were purchased from other commercial sources. The solvent used in all the reactions was dichloromethane (CH_2Cl_2). For comparison, control experiments were conducted using the previously studied $\text{Ga}(\text{OTf})_3$ as the catalyst.¹³

Preparation of Nafion[®]-H from Nafion[®]-K^{11a}

Nafion[®]-K (50 g) was stirred in boiling deionized water (150 mL) for 2 h and filtered. The resin was then stirred with 20% nitric acid (200 mL) for 5 h at room temperature and filtered. This step was repeated four times for maximum exchange of K^+ with H^+ . The polymer was washed many times with deionized water till the filtrate became neutral, when tested with pH paper. It was then dried under vacuum at 105 °C for 24 h. The dry Nafion[®]-H polymer was finely ground in a grinder (by cooling the material in liquid nitrogen to make it brittle) and sieved in a testing sieve (VWR, USA standard testing sieve, No. 60 with 250 μm opening). This was further dried under vacuum and used for the reactions.

General procedure for the Strecker reaction of aldehydes and ketones

Aldehyde or ketone (2 mmol)/fluorinated ketone (3 mmol), amine (2 mmol), TMSCN (3 mmol) and catalyst (200 mg) were taken in CH_2Cl_2 (5 mL) in a sealed pressure tube (15 mL) and the reaction mixture was stirred at the required temperature for several hours as indicated (Schemes and Tables). Completion of the reaction was monitored by ^1H or ^{19}F NMR. After completion of the reaction, the mixture was then filtered and the residue was washed with CH_2Cl_2 (3×15 mL) and ethyl acetate (3×15 mL). The filtrate was collected and the solvent was removed under reduced pressure to obtain the crude product. Further purification can be carried out by trituration of the residue with excess hexane followed by evaporation of the hexane. Products were characterized by spectral analysis (^1H NMR, ^{13}C NMR, ^{19}F NMR and GC/MS) and by comparison with those of the authentic samples.⁹ All the yields reported pertain to isolated yields.

Results and discussion

Environmentally benign catalyst systems and their importance

It has been found that for many acid catalyzed reactions the classical acid catalysts were used in amounts much larger than the stoichiometric ratio. Many of the acid catalysts such as sulfuric acid are liquids, often corrosive, sensitive to moisture

and difficult to handle. Many strong solid Lewis acids such as AlCl_3 also have similar drawbacks. Quite often, the overall reaction becomes quite complex and the work-up remains tedious due to secondary reactions. On the other hand, the catalysts used in the present project are very efficient in their catalytic activity, recovery, and stability making them very prominent as environmentally friendly catalysts. The heterogeneous catalysts (sparingly soluble in CH_2Cl_2) used in the current investigations were $\text{Ga}(\text{OTf})_3$, Nafion[®]-H (perfluoroalkanesulfonic acid polymer), Nafion[®] SAC-13 (Nafion[®]-H polymer on amorphous silica, 10–20%, porous nanocomposite), dry silica gel, and fumed silica.

Nafion[®]-H (Fig. 1) is thermally stable (up to 200 °C), more convenient and environmentally benign in comparison with corrosive acid catalysts (liquid acids) generally used in reactions involving strong acids. These unique properties have led to the application of Nafion[®]-H as a multi-purpose heterogeneous catalyst to a wide variety of organic reactions such as Friedel–Crafts type electrophilic reactions, synthesis of esters and ethers, various rearrangements, *etc.*¹¹ Mechanistic studies of various transformations show that the acidity of Nafion[®]-H under different reaction conditions can reach up to that of 100% sulfuric acid ($-\text{H}_0 \approx 12$),¹⁴ yet keeping the reaction mild and much safer. After the reactions with Nafion[®]-H, the catalyst can be easily recovered and recycled.

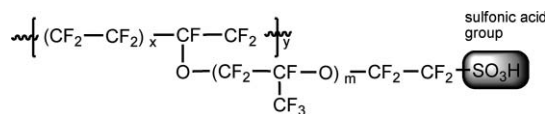


Fig. 1 Nafion[®]-H (solid resin).

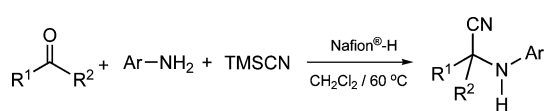
Nafion[®] SAC-13 is a porous nanocomposite which contains 10–20% Nafion[®]-H polymer on amorphous silica (SiO_2).¹² The surface area of Nafion[®] SAC-13 nanoparticles is higher than that of Nafion[®]-H particles and the reagents will have more contact with the solid acid catalyst and sulfonic acid group. Therefore in many reactions, the catalytic activity of Nafion[®] SAC-13 is higher than Nafion[®]-H due to the enhancement in bulk acidity.

The search for an effective “green” catalyst suitable for the direct Strecker reaction of both aldehydes and ketones led us to the present investigation. As a result it is found that Nafion[®]-H and Nafion[®] SAC-13 (and even silica gel and fumed silica) can catalyze the Strecker reactions. Not only aldehydes, but ketones and fluorinated ketones also react effectively. This observation is very significant due to the fact that these heterogeneous catalysts are stable, non-toxic, recoverable and easily available. By simple filtration and evaporation of the solvent (CH_2Cl_2) products are separated in pure form in most of the cases. Further purification by column chromatography which requires large amounts of solvent or mixture of solvents can be avoided.

The role and efficacy of Nafion[®]-H as a catalyst towards the Strecker reaction of aldehydes and ketones with various amines under similar conditions were explored (Scheme 3). With proper modification of the reaction conditions, the developed method was found to be simple and clean giving the nitrile products in high yields (Table 1).

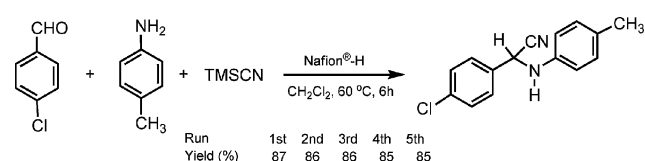
Table 1 Nafion[®]-H catalyzed Strecker reactions of various aldehydes/ketones and amines

Entry	Ketone/aldehyde	Amine	Product	Time/h	Yield (%)
1				6	80
2				6	85
3		H ₂ N-C ₄ H ₉		6	92
4				6	84
5				6	80
6				6	75
7				10	97
8				6	85
9				6	85
10				6	75

**Scheme 3** Nafion[®]-H catalyzed Strecker reaction.

As discovered recently,⁹ one of the key factors for the success of this reaction is the introduction of CH₂Cl₂ as the solvent. Acetonitrile, THF and toluene were used as solvents in earlier studies,⁸ which are, however, not suitable for the direct Strecker reaction of ketones. These solvents are more basic and they interact with the acidic catalysts thus reducing the catalytic activity.¹⁵ Use of CH₂Cl₂ minimizes such interaction resulting in enhanced catalytic activity of the catalyst providing a suitable environment for the reaction.

Nafion[®]-H is not only a stable solid acid but also can be recycled. After the reaction, the solid acid was washed several times with CH₂Cl₂ followed by acetone and dried. This sample was reused for five consecutive reactions (washed and dried after each reaction) and it was found that the catalytic efficiency remains almost unchanged as displayed from the yields (Fig. 2).

**Fig. 2** Recyclability of Nafion[®]-H for the Strecker reaction of *p*-chlorobenzaldehyde with *p*-toluidine and TMSCN.

Commercially available Nafion[®]-silica nanocomposites have been shown in the literature to be quite an efficient catalyst for many reactions.¹² To study the effectiveness of Nafion[®] SAC-13 for the Strecker reaction, some of the aldehydes and ketones were subjected to the Strecker reaction using Nafion[®] SAC-13 as the catalyst (Table 2).

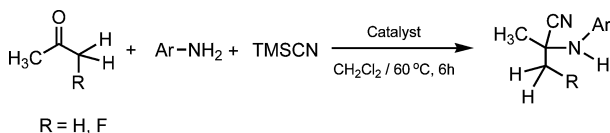
It was observed that both Nafion[®] SAC-13 and Nafion[®]-H catalyzed the reaction giving comparable yields under similar conditions. It has been noticed that the reactions are feasible even with a lower amount of Nafion[®] SAC-13. This is due to the enhancement in bulk acidity by better accessibility of the sulfonic acid groups on the higher surface area of Nafion[®] SAC-13. Therefore Nafion[®] SAC-13 works better than Nafion[®]-H in some cases. The Nafion[®] SAC-13 methodology also does not need further purification of the products in most cases,

Table 2 Nafion[®] SAC-13 catalyzed Strecker reaction of aldehydes/ketones and amines

Entry	Ketone/aldehyde	Amine	Product	Time/h	Yield (%)
1				6	87
2				6	90
3				6	80
4				6	75
5				6	82
6				6	83
7				6	88
8				6	84
9				7	85
10				6	82

thus avoiding further chromatography and product loss during purification. The products were obtained in high yield and purity.

Encouraged by these results and realizing the importance of fluorinated molecules in chemistry,¹⁶ as described earlier, we extended our methodology to fluorinated ketones (Scheme 4). We found that fluoroacetone reacts smoothly with aromatic amines under mild conditions to provide the corresponding fluorinated α -aminonitriles in high yield and purity. Reactions with monofluoroacetone and *p*-toluidine using these catalysts gave comparable results with those obtained in the case of metal triflates and trimethylsilyl triflate.⁹

**Scheme 4** Strecker reaction of acetone and fluoroacetone with various catalysts.

Since Nafion[®]-SAC 13 is a nanocomposite of Nafion[®]-H on silica, we were interested to study the effect of silica alone on this reaction. Silica gels, a key material in organic synthesis (often used for separation and purification of organic compounds, as a drying agent, or as a supporting material for many other organic compounds *etc.*), are acidic and have large pores with a wide range of diameters—typically between 50 and 300 nm. It is an effective mild acid catalyst for many organic synthetic transformations. Drying of the silica gel enhances the acidity and makes silica gel more active. When we performed the Strecker reaction of *p*-toluidine with monofluoroacetone using silica gel, we obtained the desired product in good yield with 95% purity, but the reaction took 16 h for completion (Table 3, entry 4). To further increase the efficiency of the reaction, we decided to use fumed silica instead. Fumed silica^{17,18} is an exceptionally pure form of silicon dioxide particles ranging from 5 to 50 nm with high surface areas. Using fumed silica we were able to slightly increase the yield and purity of the product (Table 3, entry 5). During our further investigation, we found that though silica and fumed silica show catalytic activity, Nafion[®]-H and

Table 3 Strecker reaction of acetone and fluoroacetone with various catalysts

Entry	Catalyst	Ketone	Amine	Product	Time/h	Yield (%) ^a
1	Nafion® SAC-13				6	80
2	Nafion® SAC-13				6	85
3	Nafion®-H				6	86
4	Silica gel				16	80 ^b
5	Fumed silica				16	83
6	Ga(OTf) ₃				6	96 ^c
7	TMSOTf				6	74 ^c

^a Reaction was carried out in 1 mmol scale. Amount of catalysts: 5 mol% of Ga(OTf)₃, trimethylsilyl trifluoromethanesulfonate (TMSOTf) and 200 mg of other catalysts. ^b 95% Pure by ¹H NMR. ^c Reactions carried out at room temperature; see refs 9a,b.

Nafion® SAC-13 gave better results (yield, purity and reaction time—Table 3) and the potential of silica and fumed silica is limited in terms of acidity, catalytic activity and catalyst recovery compared to Nafion®-H and Nafion® SAC-13.

Conclusions

In conclusion, environmentally friendly heterogeneous catalysts such as Nafion®-H (perfluoroalkanesulfonic acid polymer), Nafion® SAC-13, silica gel and fumed silica, are found to be effective catalysts for the direct three component Strecker reaction. Catalytic activity of these catalysts for the Strecker reaction of not only aldehydes but some ketones including fluoroacetone was also demonstrated. Simple and clean reactions, high yields and high purity of the products, and efficient recycling of the catalysts are the salient features of this methodology. Initial studies show that these catalysts are applicable for a wide range of substrates, thus making them versatile catalysts for α -aminonitrile synthesis. The present method clearly manifests the future potential of Nafion®-H (perfluoroalkanesulfonic acid polymer), Nafion® SAC-13, fumed silica and silica gel as catalysts for many multi-component reactions.

Acknowledgements

Support of our work by Loker Hydrocarbon Research Institute is gratefully acknowledged. T. E. T. thanks Ms Shannon Regli and Ms Priscilla Cheney, Troy High School for their helpful

suggestions and Siemens Foundation for Math, Science and Engineering Competition Award.

References

- (a) A. Strecker, *Liebigs. Ann. Chim.*, 1850, **75**, 27; (b) B. Alejandro, C. Najera and J. M. Sansano, *Synthesis*, 2007, 1230; (c) G. A. Olah, T. Mathew, C. Panja, K. Smith and G. K. S. Prakash, *Catal. Lett.*, 2007, **114**, 1; (d) A. Heydari, A. Arefi, S. Khaksar and R. K. Shiroodi, *J. Mol. Catal. A: Chem.*, 2007, **271**, 142.
- (a) S. L. Miller, *Science*, 1953, **117**, 528; (b) J. L. Bada and A. Lazcano, *Science*, 2003, **300**, 745; (c) J. L. Bada, *Earth Planet. Sci. Lett.*, 2004, **226**, 1.
- (a) V. P. Kukhar and V. A. Soloshonok, *Fluorine Containing Amino Acids: Synthesis and Properties*, Wiley, New York, 1995; (b) G. Haufe and S. Kroger, *Amino Acids*, 1996, **11**, 409; (c) V. Tolman, *Amino Acids*, 1996, **11**, 15; (d) N. M. Kelly, A. Sutherland and C. L. Willis, *Nat. Prod. Rep.*, 1997, **14**, 205; (e) A. Sutherland and C. L. Willis, *Nat. Prod. Rep.*, 2000, **17**, 621; (f) R. Dave, B. Badet and P. Meffre, *Amino Acids*, 2003, **24**, 245; (g) X.-L. Qiu, W.-D. Meng and F.-L. Quing, *Tetrahedron*, 2004, **60**, 6711.
- R. Filler, Y. Kobayashi and L. M. Yagupolskii, *Organofluorine Compounds in Medicinal Chemistry and Biomedical Applications*, Elsevier, Amsterdam, 1993.
- A. Relimpio, J. C. Slebe and M. Martinez-Carrion, *Biochem. Biophys. Res. Commun.*, 1975, **63**, 625.
- (a) M. Cairi, J. T. Gerig, S. J. Hammond, J. C. Klinkenborg and R. A. Nieman, *Bull. Magn. Reson.*, 1983, **5**, 157; (b) I. J. Ropson and C. Frieden, *Proc. Natl. Acad. Sci. U. S. A.*, 1992, **89**, 7222; (c) P. Bai, L. Luo and Z.-y. Peng, *Biochemistry*, 2000, **39**, 372; (d) N. C. Yoder and K. Kumar, *Chem. Soc. Rev.*, 2002, **31**, 335; (e) B. Salopek-Sondi, M. D. Vaughan, M. C. Skeels, J. F. Honek and L. A. Luck, *J. Biomol. Struct. Dyn.*, 2003, **21**, 235.
- (a) S. Kobayashi, S. Nagayama and T. Busujima, *Tetrahedron Lett.*, 1996, **37**, 9221; (b) A. Heydari, P. Fatemi and A.-A. Alizadeh, *Tetrahedron Lett.*, 1998, **39**, 3049; (c) J. S. Yadav, B. V. S. Reddy,

- B. Eshwaraiah, M. Sreenivas and P. Vishnumurthy, *New J. Chem.*, 2003, **27**, 462; (d) J. S. Yadav, B. V. S. Reddy, B. Eeshwaraiah and M. Srinivas, *Tetrahedron*, 2004, **60**, 1767; (e) S. K. De and R. A. Gibbs, *Tetrahedron Lett.*, 2004, **45**, 7407.
- 8 (a) J. Mulzer, A. Meier, J. Buschmann and P. Luger, *Synthesis*, 1996, 123; (b) S. Kobayashi, T. Busujima and S. Nagayama, *Chem. Commun.*, 1998, 981; (c) L. Royer, S. K. De and R. A. Gibbs, *Tetrahedron Lett.*, 2005, **46**, 4595; (d) S. K. De, *J. Mol. Catal. A: Chem.*, 2005, **232**, 123.
- 9 (a) G. K. S. Prakash, T. Mathew, C. Panja, S. Alconcel, H. Vaghoo, C. Do and G. A. Olah, *Proc. Natl. Acad. Sci. U. S. A.*, 2007, **104**, 3703; (b) G. K. S. Prakash, C. Panja, C. Do, T. Mathew and G. A. Olah, *Synlett*, 2007, 2395; (c) N. H. Khan, S. Agrawal, R. I. Kureshi, S. H. R. Abdi, S. Singh, E. Suresh and R. V. Jasra, *Tetrahedron Lett.*, 2008, **49**, 640.
- 10 (a) G. Jenner, R. B. Kim, J. C. Salem and K. Matsumoto, *Tetrahedron Lett.*, 2003, **44**, 447; (b) K. Matsumoto, J. C. Kim, H. Iida, H. Hamana, K. Kumamoto, H. Kotsuki and G. Jenner, *Helv. Chim. Acta*, 2005, **88**, 1734.
- 11 (a) G. A. Olah, P. S. Iyer and G. K. S. Prakash, *Synthesis*, 1986, 513, and refs cited therein; (b) G. A. Olah, T. Yamato, P. S. Iyer and G. K. S. Prakash, *J. Org. Chem.*, 1986, **51**, 2826; (c) T. Yamato, C. Hideshima, G. K. S. Prakash and G. A. Olah, *J. Org. Chem.*, 1991, **56**, 2089–2091; (d) G. K. S. Prakash, T. Mathew, S. Krishnaraj, E. R. Martinez and G. A. Olah, *Appl. Catal., A: General*, 1999, **181**, 283; (e) G. A. Olah, T. Mathew, M. Farnia and G. K. S. Prakash, *Synlett*, 1999, 1067; (f) G. A. Olah, T. Mathew and G. K. S. Prakash, *Chem. Commun.*, 2001, 1696; (g) G. K. S. Prakash, T. Mathew, M. Mandal, M. Farnia and G. A. Olah, *Arkivoc*, 2004, 103.
- 12 (a) M. A. Harmer, W. E. Farneth and Q. Sun, *J. Am. Chem. Soc.*, 1996, **118**, 7708; (b) I. Ledneczki and A. Molnár, *Synth. Commun.*, 2004, **34**, 3683; (c) I. Ledneczki, M. Darányi, F. Fülöp and A. Molnár, *Catal. Today*, 2005, **100**, 437.
- 13 (a) G. A. Olah, O. Farooq, S. M. F. Farnia and J. A. Olah, *J. Am. Chem. Soc.*, 1988, **110**, 2560; (b) K. Boumizane, M. H. Herzog-Cance, D. J. Jones, J. L. Pascal, J. Potier and J. Roziere, *Polyhedron*, 1991, **10**, 2757.
- 14 G. A. Olah, G. K. S. Prakash and J. Sommer, *Superacids*, Wiley, New York, 1985.
- 15 (a) P. Tarakeshwar, J. Y. Lee and S. K. Kim, *J. Phys. Chem.*, 1998, **102**, 2253; (b) S.-i. Kawahara, S. Tsuzuki and T. Uchimaru, *Chem.–Eur. J.*, 2005, **11**, 4458, and refs cited therein.
- 16 (a) P. Kirsch, *Modern Fluoroorganic Chemistry*, Wiley-VCH, Weinheim, 2004; (b) R. D. Chambers, *Fluorine in Organic Chemistry*, Blackwell, Oxford, 2004.
- 17 H. Bergna and W. O. Roberts, *Colloidal Silica: Fundamentals and applications*, Taylor & Francis (CRC), Boca Raton, FL, 2006, pp. 499–501 and 575–578.
- 18 J. Fan, S. R. Raghavan, X.-Y. Yu, S. A. Khan, P. S. Fedkiw, J. Hou and G. L. Baker, *Solid State Ionics*, 1998, **111**, 117.

Catalytic application of room temperature ionic liquids: [bmim][MeSO₄] as a recyclable catalyst for synthesis of bis(indolyl)methanes. Ion-fishing by MALDI-TOF-TOF MS and MS/MS studies to probe the proposed mechanistic model of catalysis

Asit K. Chakraborti,* Sudipta Raha Roy, Dinesh Kumar and Pradeep Chopra

Received 6th May 2008, Accepted 22nd July 2008

First published as an Advance Article on the web 15th September 2008

DOI: 10.1039/b807572g

The catalytic application of room temperature ionic liquids (RTILs) has been explored to catalyse the reaction of indole with aldehydes to afford bis(indolyl)methanes. The catalytic efficiency of the RTILs derived from butylmethylimidazolium (bmim) cation is influenced by the structure of the imidazolium moiety and the counter anion following the order: [bmim][MeSO₄] > [bmim][HSO₄] ≈ [bmim][MeSO₃] >> [bmim][BF₄] > [bmim][Br] > [bmim][NTf₂] ≈ [bmim][PF₆] > [bmim][N(CN)₂] ≈ [bmim][ClO₄] ≈ [bmim][HCO₂] > [bmim][N₃] > [bmim][OAc]. Substitution of the C-2 hydrogen in [bmim][MeSO₄] decreased the catalytic efficiency. In the 1-methyl-3-alkylimidazolium methyl sulfates, the best results are obtained with the 3-butyl derivative and the catalytic property was retained with ethyl, n-propyl, and n-pentyl groups at N-3 although to a lesser extent with respect to the 3-butyl analogue. However, much reduction of the catalytic effect is observed with n-hexyl at N-3. The method is simple, environment friendly, compatible with various functional groups such as halogen, alkoxy, nitrile and O-*t*-Boc and gives excellent yields in short times. The catalyst is recyclable upto three consecutive uses. A mechanism has been proposed invoking ambiphilic dual activation role of the IL through the formation of intermediates involving hydrogen bond formation between the oxygen atom of the aldehyde carbonyl (or the transiently formed indolyl methanol in the subsequent step) and the C-2 hydrogen atom of the bmim cation, electrostatic intercation between the quarternary nitrogen atom of the bmim cation with the nitrogen lone pair of electrons of the indole and enforced hydrogen bond formation between the indole N-H hydrogen atom and the anion of the IL. The transient indolyl methanol and intermediate non-covalent clusters were “fished” by MALDI-TOF-TOF MS and MS/MS studies and served as ‘proof-of-concept’ to the mechanistic model.

Introduction

The development of new methodologies¹ for the synthesis of bis(indolyl)methanes is a subject of continuous interest to synthetic organic/medicinal chemists as indole and their derivatives have versatile biological activities² and are widely present in various biologically active natural products.³

However, some of the reported methods have one or more of the following drawbacks: for example, use of expensive reagents and volatile organic solvents, longer reaction times, low yields of products, require complicated reaction assembly and tedious work-up, *etc.* In view of the influence of green chemistry⁴ to maintain greenness in synthetic pathways/processes by prevention of waste, avoiding the use of auxiliary substances (*e.g.* solvents, additional reagents) and minimizing the energy

requirement⁵ presses the need for a convenient and high yielding synthetic method for the timely supply of the designed new chemical entities for biological evaluation.⁶

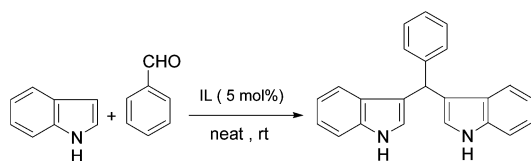
In view of the projected benefits of ILs for organic transformations for sustainable development such as environmental compatibility, reusability, greater selectivity, operational simplicity, non-corrosiveness, and ease of isolation, we were attracted towards the use of ILs.⁷ We observed that ionic liquid has been used as reaction media (2 mL mmol⁻¹ of carbonyl substrate) in the absence⁸ and presence of various Lewis acids⁹ for the reaction of indole with aldehyde/ketone to synthesise bis(indolyl)methanes. Although the low vapour pressure of the RTILs make them safer to use compared to volatile organic solvents, the combustibility of some ILs raises concern over their use in large quantities.¹⁰ The cytotoxicity¹¹ of some of the RTILs also makes a cautionary note for their use as solvents. We noticed that acidic ILs alone or immobilised on silica have been used in catalytic quantities for the synthesis of the targeted compounds.¹² However, these still used organic solvents as the reaction media (8–30 mL mmol⁻¹ of the carbonyl substrate).

Department of Medicinal Chemistry, National Institute of Pharmaceutical Education and Research (NIPER), Sector 67, S. A. S. Nagar, 160 062, Punjab, India.
E-mail: akchakraborti@niper.ac.in

Herein we report the catalytic applications of various RTILs during the reaction of aldehydes with indole under solvent-free conditions for the synthesis of bis(indolyl)methanes.

Results and discussion

To examine the effect of various neutral, acidic and basic ILs derived from the bmim cation,¹³ the reaction of indole with benzaldehyde (Scheme 1) under neat conditions and at rt was considered for a model study.



Scheme 1 The reaction of indole with benzaldehyde catalysed by RTILs.

An initial screening was done to obtain maximum conversion to the product in the shortest period. The progress of the reactions was monitored by TLC taking into consideration the complete consumption of indole. The reaction was completed in 20 min using [bmim][MeSO₄]. Next, the reactions were repeated with different ILs for a 20 min period and [bmim][MeSO₄] was found to be the most effective catalyst affording 92% yield (Table 1). Other ILs such as [bmim][BF₄], [bmim][PF₆] and [bmim][HSO₄]^{8–11} were less effective and gave 60, 38, and 76% yields, respectively. The ILs used for this study (Table 1) were available commercially except [bmim][HCO₂] and [bmim][N₃] that were not reported previously and were prepared for the first time by anion metathesis in aqueous medium instead of organic solvents such as MeCN or DCM used for such purpose in the reported procedures.¹⁴

To optimise the quantities of [bmim][MeSO₄] required for the catalytic effect, the reaction of benzaldehyde (10 mmol) with indole (20 mmol) was carried out in the presence of 1, 5, 10, and 20 mol% [bmim][MeSO₄]. The desired bis(indolyl)methane was formed in 95, 92, 94, and 91% yields after 30, 20, 15, and 10 min, respectively. Thus, the use of a 5 mol% [bmim][MeSO₄] was

Table 1 The catalytic effect of various ILs for synthesis of bis(indolyl)methanes by the reaction of indole with benzaldehyde^a

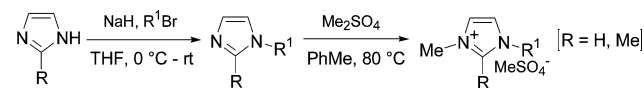
Entry	IL	Yield (%) ^b
1	[bmim][Br]	49
2	[bmim][ClO ₄]	30
3	[bmim][BF ₄]	60
4	[bmim][NTf ₂]	40
5	[bmim][MeSO ₄]	92
6	[bmim][MeSO ₃]	74
7	[bmim][OAc]	20
8	[bmim][HCO ₂]	30
9	[bmim][N(CN) ₂]	32
10	[bmim][PF ₆]	38
11	[bmim][HSO ₄]	76
12	[bmim][N ₃]	25

^a Benzaldehyde (2.5 mmol) was treated with indole (5 mmol, 2 equiv.) in the presence of the IL (5 mol%) at rt for 20 min under neat conditions.

^b Yield of the corresponding bis(indolyl)methane (IR, NMR and APCI-MS) after purification.

considered as the optimal amount keeping in view the feasibility of handling the IL for small scale (1 mmol or less with respect to the carbonyl substrate) reactions.

As the results of Table 1 show the influence of the counter anion of the ILs on the catalytic property, we further planned to elucidate the role of the cationic structure. Thus, various novel ILs derived from 1-methyl-3-alkyl and 1,2-dimethyl-3-butyl imidazolium cations were synthesised (Scheme 2) and used for the reaction of benzaldehyde with indole (Table 2).



Scheme 2 Preparation of novel RTILs.

The lack of formation of any significant amount of the desired product in using 1-methylimidazole (entry 1, Table 2) indicated the specific role of the imidazolium cation in imparting the catalytic property. The length of the alkyl chain of 1-methyl-3-alkyl imidazolium methyl sulfate also had significant influence on the catalytic efficiency of the ILs. The best catalytic activity was observed with 3-n-butyl substituted IL. The corresponding ILs having ethyl, n-propyl and n-pentyl group at N-3 retained the catalytic property but were inferior to the 3-n-butylated analogue. The catalytic property of the IL dropped significantly when N-3 contains an n-hexyl group. However, a decrease in the product yield was observed with [bmim][MeSO₄] having a methyl group substituted at C-2 (entry 7, Table 2) indicating the role of the C-2 hydrogen atom in imparting catalytic efficiency to the IL.

A graphical representation of the formation of bis(indolyl)methane using various ILs having different N-3 alkyl group is provided in Fig. 1.

To establish the generality of the [bmim][MeSO₄] catalysed bis(indolyl)methane formation, various aryl, heteroaryl and aliphatic aldehydes were treated with indole (Scheme 3).

Table 2 The effect of the cationic moiety of the IL on bis(indolyl)methane formation during the reaction of indole with benzaldehyde^a

Entry	Catalyst	Yield (%) ^b
1		Nil
2		75
3		80
4		92
5		70
6		50
7		45

^a Benzaldehyde (2.5 mmol) was treated with indole (5 mmol, 2 equiv.) in the presence of the catalyst (5 mol%) at rt under neat conditions for 20 min.

^b Yield of the corresponding bis(indolyl)methane (IR, NMR and APCI-MS) after purification.

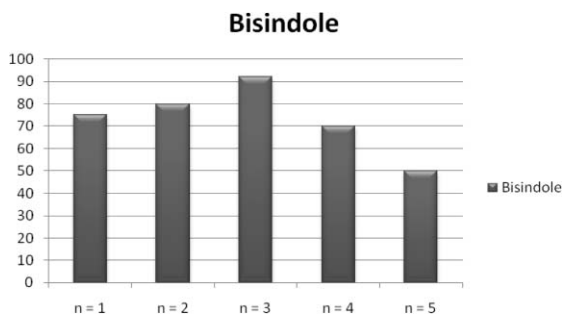
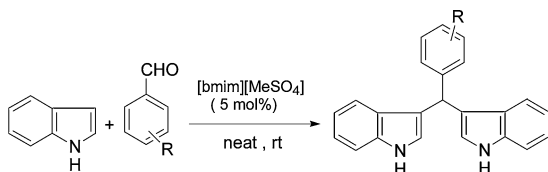


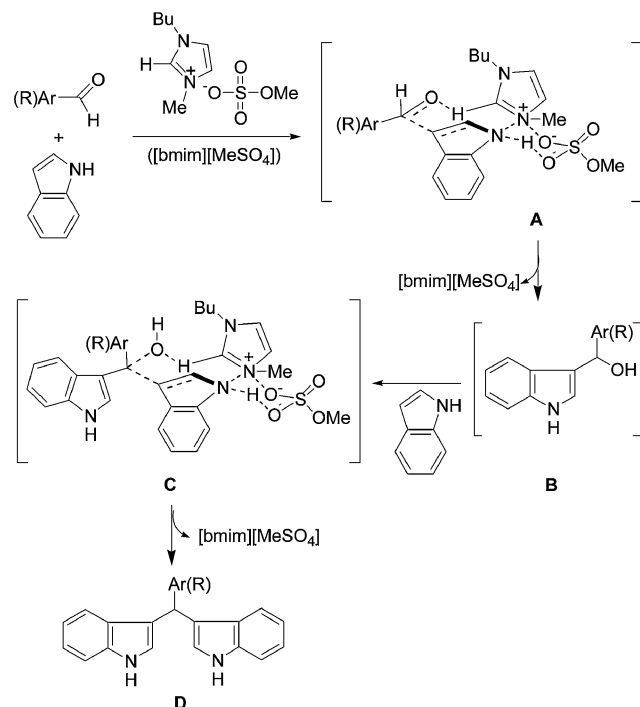
Fig. 1 The importance of the chain length of the 1-alkyl group in 1-alkyl-3-methylimidazolium methyl sulfate on the formation of bis(indolyl)methane.



Scheme 3 The [bmim][MeSO₄] catalysed reaction of indole with various aldehydes.

The results are summarized in Table 3. In all cases, the reaction proceeded smoothly at rt to afford the corresponding bis(indolyl)methanes in excellent yields (85–95%) in very short reaction times (5–40 min). The reaction is compatible with a variety of functional groups such as halogen, alkoxy, nitrile, hydroxy and *O-t*-Boc.

The role of [bmim][MeSO₄] in catalysing the reaction has been envisaged through the mechanistic proposal depicted in Scheme 4. The [bmim][MeSO₄] exhibits an ambiphilic “electrophile–nucleophile” dual activation role¹⁵ through the



Scheme 4 The role of [bmim][MeSO₄] in catalysing the reaction of indole with aldehydes.

Table 3 The [bmim][MeSO₄] catalysed synthesis of bis(indolyl)methanes by the reaction of indole with aryl/heteroaryl/alkyl aldehydes^a

Entry	Aldehyde	Time/min	Yield (%) ^b
1	R = H	20	92
2	R = 4-Me	25	87
3	R = 4-OMe	30	85
4	R = 3-NO ₂	5	95
5	R = 4-Cl	10	90
6	R = 4-CN	10	90
7	R = 4-F	10	92
8	R = 4-OH	15	85
9	R = 4- <i>O-t</i> -Boc	20	92 ^c
10	R ¹ = H; R ² = R ³ = OMe	35	89
11	R ¹ = R ² = R ³ = Me	40	85 ^c
12	R ¹ = H; R ² = OCH ₂ Ph; R ³ = OMe	40	88 ^c
13	R ¹ = H; R ² = OC ₃ H ₇ ; R ³ = OMe	35	86 ^c
14		15	92 ^c
15		20	90
16		10	94
17		10	91
18		15	90
19		15	92

^a The aldehyde (2.5 mmol) was treated with indole (5 mmol, 2 equiv.) in the presence of [bmim][MeSO₄] (5 mol%) at rt under neat conditions. ^b Yield of the corresponding bis(indolyl)methanes (IR, NMR and APCI-MS) obtained after purification. ^c The products are new, were characterised by spectral (IR, ¹H and ¹³C NMR and MS) data and gave satisfactory elemental analyses.

intermediate **A** in which the aldehyde carbonyl undergoes hydrogen bond formation (electrophilic activation) with the C-2 hydrogen atom of the bmim cation due its acidic nature.¹⁶ The quaternary nitrogen atom of the bmim cation undergoes electrostatic interaction with the nitrogen lone pair of the indole and enforces the N–H hydrogen of the indole for hydrogen bond formation with the oxygen atom of the MeSO₄[−] anion (nucleophilic activation) through a six-membered chair-like cyclic structure. In a similar fashion the intermediately formed indolyl methanol **B** undergoes complex formation with another molecule of indole and [bmim][MeSO₄] forming **C** that leads to the product and liberates the IL. The decrease in the product yield in using the C-2 methyl substituted [bmim][MeSO₄] (entry 7, Table 2) provides supports of electrophilic activation of the

aldehyde through hydrogen bond formation with the C-2 hydrogen of [bmim][MeSO₄].

To further demonstrate the involvement of the intermediates A/C, we planned to carry out the [bmim][MeSO₄] (5 mol%) catalysed reaction of benzaldehyde (1 mmol) with indole (2 mmol) in solvents that may interfere with the hydrogen bond formation between the aldehyde carbonyl group and the C-2 hydrogen atom of the bmim cation or destabilise the electrostatic interaction between the quaternary nitrogen atom of the bmim cation and the nitrogen lone pair of electrons of indole. The use of MeCN, EtOH and water afforded the desired bis(indolyl)methane in 62, 41, and 10% yields, respectively, after 20 min at rt.

The lack of appreciable amount of hydrogen bond formation between the aldehyde carbonyl group and the C-2 hydrogen atom of the bmim cation in the hydroxylic solvents EtOH and water that are themselves hydrogen bond donors causes a drastic reduction in the product yield. Similarly the reaction is retarded in MeCN, a hydrogen bond acceptor, due to disruption of the hydrogen-bonded structures A/C. These suggest that the catalytic efficiency of the IL is best exhibited under neat conditions that offer a conducive environment for the hydrogen bond formation between the aldehyde carbonyl oxygen and the C-2 hydrogen atom of the bmim cation. A similar acceleration effect of the imidazolium based ILs has been observed during electron transfer reaction by coordination of the acidic C-2 hydrogen atom of imidazolium ILs with the oxygen radical anions.¹⁷

To seek more convincing support for the proposed mechanistic model (Scheme 3), we adopted the mass spectrometric "ion-fishing" technique due to its rapidly gaining popularity for

mechanistic studies.¹⁸ However, as the presence of a solvent may disrupt the covalent bonded clusters (A and C), we carried out the mass spectrometric experiments using MALDI-TOF-TOF technique since the ESI-MS requires infusion of the analyte dissolved in solvent. Moreover, MALDI-MS involves a soft ionisation mode and the TOF offers added accuracy of detection of ions. The MALDI-TOF-TOF MS (Fig. 2) of an aliquot of sample withdrawn after 5 min during the reaction of benzaldehyde with indole in the presence of [bmim][MeSO₄] as the catalyst revealed the presence of ions at *m/z* 245.719, 273.636, 322.839, 389.989, 494.92, 510.039, 611.254, and 627.241 corresponding to the (B-1) + Na⁺, [bmim][MeSO₄] + Na⁺, D, [bmim]₂[MeSO₄], (A-1) + Na⁺, (A-1) + K⁺, C + Na⁺, and C + K⁺, respectively.

For further structural elucidation, the ions with *m/z* 510.039 (*m*₁) and 627.241 (*m*₂) were subjected to MS/MS study. The MS² spectra (Fig. 3) derived from the ion of *m/z* 510.039 showed ion peaks at *m/z* 510.02, 492.192, 476.644, and 140.307, assigned as the parent ion (*m*₁), *m*₁-H₂O, *m*₁-H₂O-Me, and (bmim + 1) respectively.

In the case of *m*₂, the MS² spectra (Fig. 4) exhibited the parent ion (*m*₂) and the daughter ions with *m/z* 606.967 (*m*₂-H₂O-2H), 588.978 (C), 472.949 (C-Indole), 232.532 (D-C₇H₆), and 139.407 (bmim).

Although it has been conjectured in the literature^{1d,8,19} that the reactions proceed through the intermediate indolyl methanol formed by the initial adduct of one indole moiety with the aldehyde, to the best of our knowledge this is the first experimental evidence in favour of the intermediacy of the indolyl methanol (B).

The influence of the anion in contributing to the catalytic potency towards the IL can be rationalised with this mechanistic

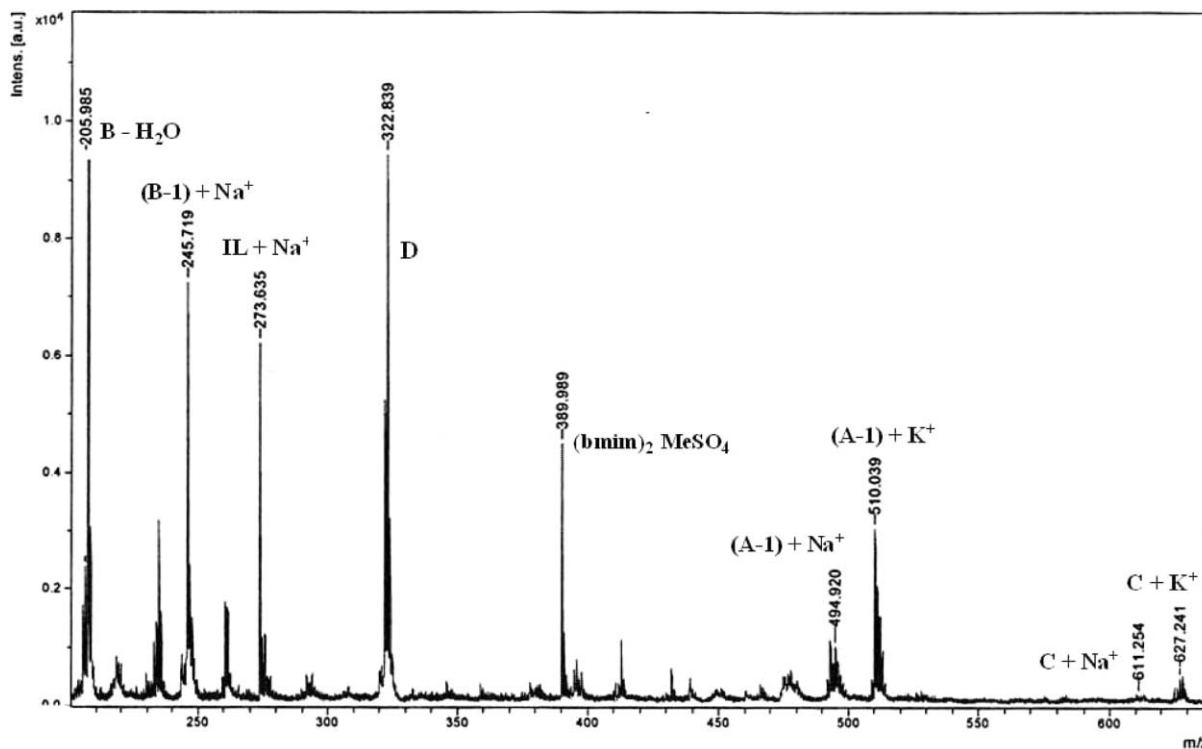
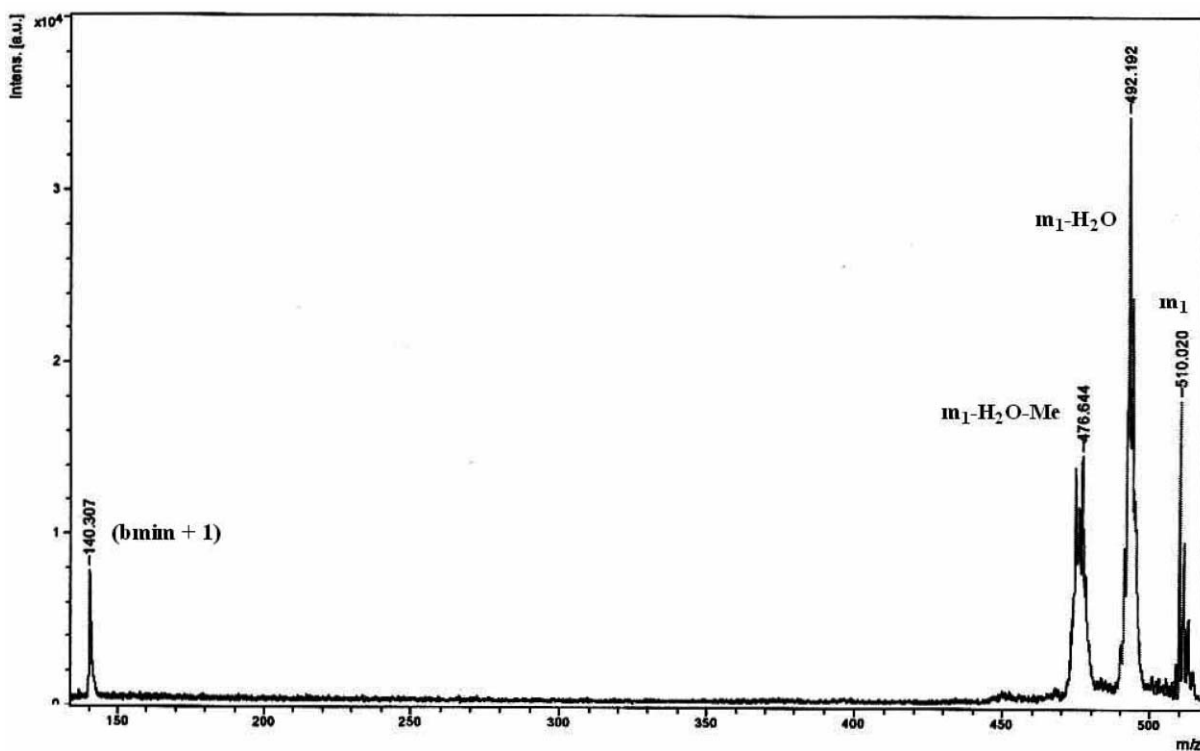
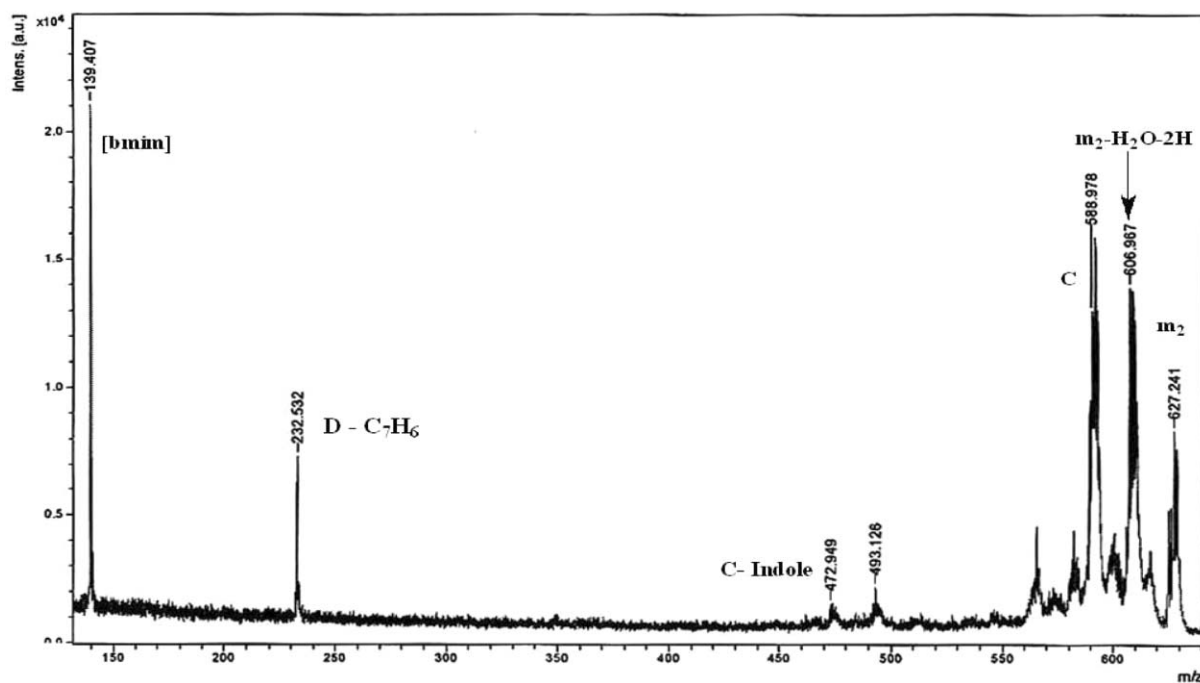


Fig. 2 MALDI-TOF-TOF MS of aliquot of sample withdrawn after 5 min for the reaction of entry 1, Table 3.

Fig. 3 MALDI-TOF-TOF MS² of m_1 .Fig. 4 MALDI-TOF-TOF MS² of m_2 .

proposal. The feasibility of hydrogen bond formation of the N–H hydrogen of the indole with HSO_4^- , MeSO_3^- , and BF_4^- anions through six/five-membered chair/envelop-like cyclic structures **E–G** and **H–J** (Fig. 5) akin to **A** and **C**, respectively, accounts for the catalytic activity of $[\text{bmim}][\text{HSO}_4]$, $[\text{bmim}][\text{MeSO}_3]$, and

$[\text{bmim}][\text{BF}_4]$. In the case of $[\text{bmim}][\text{PF}_6]$, the weak electrostatic interaction of the central phosphorous atom of the PF_6^- anion (due to the lesser charge to size ratio of PF_6^- compared to that of BF_4^-) does not make it feasible to form the intermediate corresponding to **G/J**.

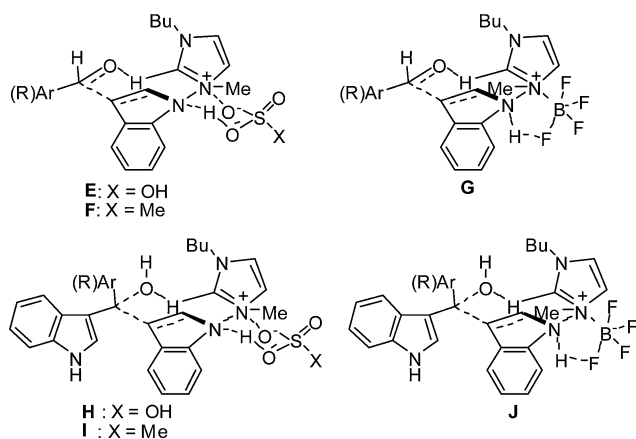


Fig. 5 The role of [bmim][HSO₄], [bmim][MeSO₃] and [bmim][BF₄] in catalysing the reaction of indole with aldehydes.

Conclusions

We have demonstrated herein the catalytic applications of RTILs for the synthesis of bis(indolyl)methanes by the reaction of aromatic/heteroaromatic/alkyl aldehydes with indole. Amongst the various RTILs, [bmim][MeSO₃] was found to be the most effective affording the desired compounds in excellent yields at rt and in short reaction times. The counter anion and the chain length of the N-3 alkyl group of the 1-alkyl-3-methylimidazolium derived ILs was crucial in attributing catalytic efficiency to the IL. A mechanistic proposal invoking ambiphilic dual activation role of the IL has been delineated to rationalise the catalytic behaviour. The “ion-fishing” using MALDI-TOF-TOF MS provided evidence in support of the mechanistic proposal through identification of the respective non-covalent clusters and their structural elucidation with MS/MS technique. This MS data provided for the first time experimental evidence for the long time conjecture of the intermediacy of indolyl methanols in forming the bis(indolyl)methanes during the reaction of aldehydes and indole. The advantages such as (i) the use of commercially available catalyst, (ii) rt and short reaction times, (iii) high yields, (iv) feasibility of large scale operation, (v) catalyst reuse and (vi) with lesser cytotoxic effect of the MeSO₄ anion¹¹ fulfil the requirement of the ‘triple bottom line philosophy’⁷⁵ of green chemistry.

Representative experimental procedure for the synthesis of ILs.

3-Butyl-1,2-dimethyl imidazolium methyl sulfate (Entry 7, Table 2)

2-Methylimidazole (0.205 g, 2.5 mmol) in dry THF (5 mL), was treated with NaH (0.066 g, 2.5 mmol, 1.1 equiv.) under ice cooled conditions followed by n-butylbromide (0.342 g, 2.5 mmol, 1 equiv.). The mixture was stirred magnetically and allowed to attain rt and kept under stirring for 2 h. The mixture was concentrated under reduced pressure to remove the THF, diluted with EtOAc (2 mL), filtered and the residue was washed with EtOAc (2 × 1 mL). The combined EtOAc filtrates were concentrated and treated with freshly distilled Me₂SO₄ (0.315 g, 2.5 mmol, 1.1 equiv.) at 80 °C in PhCH₃ to afford 3-butyl-1,2-dimethyl imidazolium methyl sulfate as a clear viscous liquid (0.462 g, 70%). IR ν_{\max} (neat) = 3480, 2961, 1639, 1466, 1225,

1060, 1011, 746, 669, 580 cm⁻¹; ¹H NMR (300 MHz, DMSO): δ = 0.91 (t, *J* = 7.37 Hz, 3 H), 1.31 (q, 2 H), 1.70 (q, 2 H), 2.60 (s, 3 H), 3.38 (s, 3 H), 3.77 (s, 3 H), 4.13 (t, *J* = 7.2 Hz, 2 H), 7.63 (d, *J* = 1.8 Hz, 2 H), 7.67 (d, *J* = 1.8 Hz, 2 H); ¹³C NMR (75 MHz, DMSO): δ = 9.4, 13.7, 19.2, 31.5, 34.9, 47.6, 53.2, 121.2, 122.2, 144.6.

3-Propyl-1-methyl imidazolium methyl sulfate (Entry 3, Table 2)

Clear viscous liquid; IR ν_{\max} (neat) = 3480, 2961, 1639, 1466, 1225, 1060, 1011, 746, 669, 580 cm⁻¹; ¹H NMR (300 MHz, DMSO): δ = 0.83 (t, 3 H, *J* = 7.2 Hz), 1.80 (q, 2 H), 3.86 (s, 3 H), 4.13 (t, *J* = 7.2 Hz, 3 H), 6.29 (s, 3H), 7.72 (d, *J* = 1.38 Hz, 1 H), 7.78 (d, *J* = 1.38 Hz, 1 H) 9.13 (s, 1 H); ¹³C NMR (75 MHz, DMSO): δ = 10.6, 22.7, 35.9, 50.21, 122.6, 124.8, 137.0

3-Pentyl-1-methyl imidazolium methyl sulfate (Entry 5, Table 2)

Clear viscous liquid; IR ν_{\max} (neat) = 3480, 2961, 1639, 1466, 1225, 1060, 1011, 746, 669, 580 cm⁻¹; ¹H NMR (300 MHz, DMSO): δ = 0.86 (t, *J* = 6.9 Hz, 3 H), 1.26 (m, 4 H), 1.78 (q, 2 H), 3.86 (s, 3 H), 4.16 (t, *J* = 7.2 Hz, 3 H), 5.59 (s, 3H), 7.72 (s, 1 H), 7.79 (s, 1 H) 9.17 (s, 1 H); ¹³C NMR (75 MHz, DMSO): δ = 13.8, 21.5, 27.7, 29.2, 35.7, 48.8, 122.3, 123.3, 136.7.

1-Hexyl-3-methyl imidazolium methyl sulfate (Entry 6, Table 2)

Clear viscous liquid; IR ν_{\max} (neat) = 3480, 2961, 1639, 1466, 1225, 1060, 1011, 746, 669, 580 cm⁻¹; ¹H NMR (300 MHz, DMSO): δ = 0.85 (bs, 3 H), 1.26 (bs, 6 H), 1.78 (bs, 2 H), 3.41 (s, 3 H), 3.38 (s, 3 H), 4.17 (t, *J* = 7.2 Hz, 2 H), 7.72 (s, 1 H), 7.79 (s, 1 H) 9.13 (s, 1 H); ¹³C NMR (75 MHz, DMSO): δ = 13.6, 21.9, 25.6, 29.4, 30.6, 48.8, 53.0, 122.0, 123.4, 135.7.

Representative experimental procedure for anion metathesis (Entry 8, Table 1)

A mixture of [bmin][Br] (0.547 g, 2.5 mmol, 1 equiv.) and distilled water (5 mL) was stirred at rt in the presence of HCOONa (0.255 g, 2.5 mmol, 1.5 equiv.) for 24 h. The aq. mixture was subjected to rotary evaporation at 80 °C under reduced pressure for 45 min. Then MeCN was added, the organic layer was filtered and concentrated under reduced pressure to afford the pure [bmin][HCOO] (0.446 g, 97%). Clear viscous liquid; IR ν_{\max} (neat) = 3423, 2875, 1717, 1572, 1465, 1338, 1169, 825, 754, 623 cm⁻¹; ¹H NMR (300 MHz, DMSO): δ = 0.88 (t, *J* = 7.2 Hz, 3 H), 1.23 (q, 2 H), 1.77 (q, 2 H), 3.88 (s, 3 H), 4.20 (t, *J* = 6.9 Hz, 3 H), 7.78 (s, 1 H), 7.85 (s, 1 H), 8.30 (s, 1 H), 9.34 (s, 1 H); ¹³C NMR (75 MHz, DMSO): δ = 13.5, 19.0, 31.7, 36.5, 48.7, 122.6, 123.9, 136.9, 164.9.

1-Butyl-3-methyl imidazolium azide (Entry 12, Table 1)

Clear viscous liquid; IR ν_{\max} (neat) = 3435, 2962, 2252, 1656, 1574, 1170, 1027, 823, 761, 625 cm⁻¹; ¹H NMR (300 MHz, DMSO): δ = 0.76 (t, *J* = 7.2 Hz, 3 H), 1.11 (q, 2 H), 1.63 (q, 2 H), 3.73 (s, 3 H), 4.05 (t, *J* = 7.2 Hz, 3 H), 7.61 (s, 1 H), 7.68 (s, 1 H), 9.06 (s, 1 H); ¹³C NMR (75 MHz, DMSO): δ = 13.6, 19.1, 31.7, 36.1, 48.8, 122.6, 123.9, 136.9.

Representative experimental procedure for formation of bis(indolyl)methane and recovery of the IL.

3,3'-Bis-indolylphenylmethane (Entry 1, Table 3)

A mixture of benzaldehyde (0.267 g, 2.5 mmol, 1 equiv.) and indole (0.58 g, 5 mmol, 2 equiv.) was stirred at rt in the presence of [bmim][MeSO₄] (5 mol%) for 20 min. After completion of the reaction (TLC) the mixture was diluted with water (1 mL) and EtOAc (5 mL). The organic layer was separated and concentrated under reduced pressure. The crude product on passing through a column of silica gel (60–120 mesh) and elution with EtOAc–petroleum ether (1 : 9) afforded 3,3'-bis(indolyl)phenylmethane (0.74 g, 92%) identical (mp, IR, NMR and MS) with an authentic sample.²⁰ Mp: 125–126 °C. IR ν_{\max} (KBr) = 3416, 1634, 1378, 737 cm⁻¹. ¹H NMR (300 MHz, CDCl₃): δ = 5.89 (s, 1 H), 6.66 (d, J = 1.8 Hz, 2 H), 7.01 (t, J = 7.4 Hz, 2 H), 7.28–7.37 (m, 8 H), 7.91 (brs, 2 H, NH). ¹³C NMR (75 MHz, CDCl₃): δ = 21.5, 114.3, 118.9, 119.4, 123.0, 125.1, 127.1, 130.0, 130.2, 133.7, 134.3, 137. MS (APCI) m/z 323.2 (MH⁺). The aq layer containing the IL was subjected to rotary evaporation at 80 °C under reduced pressure for 20 min to afford the recovered IL which was used/reused for three subsequent fresh batches of reaction of benzaldehyde (2.5 mmol) and indole (5 mmol) to obtain the desired bis(indolyl)methane in 87, 85, and 80% yields, respectively, after usual workup and purification. On a large scale operation, the reaction of benzaldehyde (5.0 g, 47.17 mmol) with indole (11.04 g, 94.34 mmol, 2 equiv.) in the presence of [bmim][MeSO₄] (0.01 g, 1 mol%) for 30 min at rt afforded the desired bis(indolyl)methane (13.9 g, 92%) after usual workup and purification.

3,3'-Bis-indolyl(4-*tert*-butoxyphenyl)methane (Entry 9, Table 3)

Brown needles; mp 115–117 °C; IR ν_{\max} (KBr) = 3413, 1916, 1727, 1397, 1218, 1154, 1037, 772, 687 cm⁻¹; ¹H NMR (300 MHz, CDCl₃): δ = 1.55 (s, 9 H), 5.88 (s, 1 H), 6.62 (s, 2 H), 6.91–7.08 (m, 4 H), 7.13–7.20 (m, 3 H), 7.30–7.38 (m, 5 H), 7.89 (brs, 2 H, NH); Anal. Calcd. For C₂₈H₂₆N₂O₃: C, 76.69; H, 5.98; N, 6.39%. Found: C, 76.67; H, 5.96; N, 6.40%.

3,3'-Bis-indolyl(3,4,5-trimethylphenyl)methane (Entry 11, Table 3)

Solid; mp 197–198 °C; IR ν_{\max} (KBr) = 767, 1005, 1233, 1495, 1625, 2985, 3060, 3440 (NH) cm⁻¹; ¹H NMR (300 MHz, CDCl₃): δ = 3.73 (s, 3 H), 3.84 (s, 3 H), 5.73 (s, 1 H), 6.72 (d, J = 2.4 Hz, 2 H), 6.80 (d, J = 8.2 Hz, 2 H), 6.85 (s, 1 H), 6.92 (d, J = 8.2 Hz, 2 H), 7.05 (t, J = 8.0 Hz, 2 H), 7.33 (t, J = 8.2 Hz, 4 H), 10.45 (brs, 2 H, NH); Anal. Calcd. For C₂₆H₂₄N₂: C, 85.68; H, 6.64; N, 7.69%. Found: C, 85.65; H, 6.69; N, 7.66%.

3,3'-Bis-indolyl(3-methoxy, 4-benzyloxyphenyl)methane (Entry 12, Table 3)

White solid, mp 220–222 °C; IR ν_{\max} (KBr) = 3417, 1508, 1245, 1126, 740 cm⁻¹; ¹H NMR (300 MHz, CDCl₃): δ = 3.77 (s, 3 H), 5.11 (s, 2 H), 5.82 (s, 1 H), 6.65 (s, 2 H), 6.78 (d, J = 8.1 Hz, 2 H), 7.00 (m, 3 H), 7.16 (t, J = 14.8 Hz, 2 H), 7.28–7.44 (m, 8 H), 7.90 (brs, 2 H, NH); ¹³C NMR (75 MHz, CDCl₃): δ = 39.7, 55.9, 71.1, 110.9, 112.7, 113.7, 119.1, 119.9, 120.5, 121.9, 123.5, 127.0, 127.3, 127.7, 128.4, 136.6, 137.3, 137.4, 146.5, 149.4; MS

(APCI) m/z 459.3 (MH⁺); Anal. Calcd. For C₂₃H₁₈N₂: C, 81.20; H, 5.72; N, 6.11%. Found: C, 81.32; H, 5.69; N, 6.13%.

3,3'-Bis-indolyl(3-methoxy,4-isopropyl oxyphenyl)methane (Entry 13, Table 3)

White solid, mp 224–226 °C; IR ν_{\max} (KBr) = 3410, 1402, 1275, 1134, 749 cm⁻¹; ¹H NMR (300 MHz, CDCl₃): δ = 1.34 (d, J = 6.0 Hz, 6 H), 3.72 (s, 3 H), 4.48 (m, 1 H), 5.82 (s, 1 H), 6.56 (s, 2 H), 6.66 (d, J = 1.3 Hz, 2 H), 6.78 (t, J = 17.5 Hz, 2 H), 6.92 (s, 1 H), 7.00 (t, J = 14.7 Hz, 2 H), 7.16 (t, J = 14.5 Hz, 3 H), 7.33–7.41 (m, 4 H), 7.92 (brs, 2 H, NH); ¹³C NMR (75 MHz, CDCl₃): δ = 22.7, 40.3, 56.43, 71.8, 111.5, 113.4, 115.9, 119.7, 120.5, 121.1, 122.4, 127.6, 137.2, 137.5, 146.0, 150.6; MS (APCI) m/z 411.4 (MH⁺). Anal. Calcd. For C₂₃H₁₈N₂: C, 79.00; H, 6.38; N, 6.82%. Found: C, 79.01; H, 6.35; N, 6.80%.

3,3'-Bis-indolyl(4-methyl-2-thiazolyl)methane (Entry 14, Table 3)

Pink solid, mp 155–156 °C; IR ν_{\max} (KBr) = 3406, 1455, 1338, 1094, 740 cm⁻¹; ¹H NMR (300 MHz, CDCl₃): δ = 2.43 (s, 3 H), 6.27 (s, 1 H), 6.73 (s, 1 H), 6.85 (s, 1 H), 7.03 (d, J = 6.75 Hz, 2 H), 7.15 (d, J = 6.75 Hz, 2 H), 7.32 (d, J = 7.32 Hz, 4 H), 7.46 (d, J = 7.2 Hz, 2 H), 8 (brs, 2 H, NH); ¹³C NMR (75 MHz, CDCl₃): δ = 14.2, 38.7, 111.2, 113.4, 117.4, 119.4, 119.6, 122.1, 123.5, 126.6, 136.5, 152.4, 174.5; MS (APCI) m/z 346.3 (MH⁺). Anal. Calcd. For C₂₃H₁₈N₂S: C, 73.01; H, 5.54; N, 12.15; S, 9.28%. Found: C, 73.02; H, 5.52; N, 12.16; S, 9.25%.

Experimental procedure for ion-fishing using MALDI-TOF-TOF

A mixture of benzaldehyde (0.267 g, 2.5 mmol, 1 equiv.) and indole (0.58 g, 5 mmol, 2 equiv.) was stirred magnetically at rt in the presence of [bmim][MeSO₄] (5 mol%). After 5 min, an aliquat portion of the reaction mixture was taken out by capillary and dissolved in DCM. A stock solution (1 μ L) of the matrix [prepared from 2,5-dihydroxybenzoic acid (10 mg), TFA (600 μ L of 0.1% aq. soln) and MeCN (300 μ L)] was added to the solution (1 μ L) of the reaction mixture in DCM and the resultant solution (1 μ L) was added on the MALDI plate. The solvent was evaporated on air drying (10 min) and the spectra were recorded on a Bruker Daltonics® MALDI-TOF-TOF mass spectrometer. Wherever applicable the MS/MS was performed on the chosen parent ion peak.

Acknowledgements

SRR thanks CSIR, New Delhi, India for the award of JRF. Financial support from OPCW, Hague, The Netherlands is also acknowledged.

Notes and references

- (a) Recent examples: S.-Y. Wang and S.-J. Ji, *Synth. Commun.*, 2008, **38**, 1291 and the references cited therein; (b) V. T. Kamble, K. R. Kadama, N. S. Joshia and D. B. Muleya, *Catal. Commun.*, 2007, **8**, 498; (c) H. Firouzabadi, N. Iranpoor and A. A. Jafari, *J. Mol. Catal. A: Chem.*, 2006, **244**, 168; (d) M. L. Deb and P. J. Bhuyan, *Tetrahedron Lett.*, 2006, **47**, 1441; (e) L.-M. Wang, J.-W. Han, H. Tian, J. Sheng, Z.-Y. Fan and X.-P. Tang, *Synlett*, 2005, 337; (f) Z.-H. Zhang, L. Yin

- and Y.-M. Wang, *Synthesis*, 2005, 1949; (g) L.-P. Mo, Z. Chuan and Z.-H. Zhang, *Synth. Commun.*, 2005, **35**, 1997; (h) P. R. Singh, D. U. Singh and S. D. Samant, *Synth. Commun.*, 2005, **35**, 2133; (i) W.-J. Li, X.-F. Lin, J. Wang, G.-L. Li and Y.-G. Wang, *Synth. Commun.*, 2005, **35**, 2765.
- 2 (a) Inhibitors of tumor cells: P. Diana, A. Carbone, P. Baraja, A. Montalbano, A. Martorana, G. Dattolo, O. Gia, L. D. Via and G. Cirrincione, *Bioorg. Med. Chem. Lett.*, 2007, **17**, 2342; (b) Selective COX-2 inhibitors: A. S. Kalgutkar, B. C. Crews, S. W. Rowlinson, A. B. Marnett, K. R. Kozak, R. P. Remmel and L. J. Marnett, *Proc. Natl. Acad. Sci. U. S. A.*, 2000, **97**, 925; (c) PDE-IV inhibitors: C. Hulme, K. Moriarty, B. Miller, R. Mathew, M. Ramanjulu, P. Cox, J. Souness, K. M. Page, J. Uhl, J. Travis, F. Huang, R. Labaudiniere and S. W. Djuric, *Bioorg. Med. Chem. Lett.*, 1998, **8**, 1867; (d) Glycogen synthase kinase-3 inhibitors: H.-C. Zhang, L. V. R. Bonaga, H. Ye, C. K. Derian, B. P. Damiano and B. E. Maryanoff, *Bioorg. Med. Chem. Lett.*, 2007, **17**, 2863.
- 3 (a) R. J. Sundberg, *The Chemistry of Indoles*, Academic Press, New York, 1996; (b) A. Casapullo, G. Bifulco, I. Bruno and R. Riccio, *J. Nat. Prod.*, 2000, **63**, 447; (c) T. R. Garbe, M. Kobayashi, N. Shimizu, N. Takesue, M. Ozawa and H. Yukawa, *J. Nat. Prod.*, 2000, **63**, 596; (d) B. Bao, Q. Sun, X. Yao, J. Hong, C. O. Lee, C. J. Sim, K. S. Im and J. H. Jung, *J. Nat. Prod.*, 2005, **68**, 711.
- 4 K. Alfonso, J. Colberg, P. J. Dunn, T. Fevig, S. Jennings, T. A. Johnson, H. P. Klein, C. Knight, M. A. Nagy, D. A. Perry and M. Stefaniak, *Green Chem.*, 2008, **10**, 31.
- 5 P. Tundo, P. Anastas, D. S. Black, J. Breen, T. Collins, S. Memoli, J. Miyamoto, M. Polyakoff and W. Tumas, *Pure Appl. Chem.*, 2000, **72**, 1207.
- 6 J. Potosky, *Drug Discovery Today*, 2005, **10**, 115.
- 7 M. J. Earle and K. R. Seddon, *Pure Appl. Chem.*, 2000, **72**, 1391.
- 8 J. S. Yadav, B. V. S. Reddy and S. Sunitha, *Adv. Synth. Catal.*, 2003, **345**, 349.
- 9 (a) S.-J. Ji, M.-F. Zhou, D.-G. Gu, S.-Y. Wang and T.-P. Loh, *Synlett*, 2003, 2077; (b) X. Mi, S. Luo, J. He and J.-P. Cheng, *Tetrahedron Lett.*, 2004, **45**, 4567; (c) S.-J. Ji, M.-F. Zhou, D.-G. Gu, Z.-Q. Jiang and T.-P. Loh, *Eur. J. Org. Chem.*, 2004, 1584.
- 10 M. Smiglak, W. M. Reichert, J. D. Holbrey, J. S. Wilkes, L. Sun, J. S. Thrasher, K. Kirichenko, S. Singh, A. R. Katrizky and R. D. Rogers, *Chem. Commun.*, 2006, 2554.
- 11 A. Garcia-Lorenzo, E. Tozo, J. Tojo, M. Teixeira, F. J. Rodriguez-Berrocal, M. P. Gonzalez and V. S. Martinez-Zorzano, *Green Chem.*, 2008, **10**, 508.
- 12 D.-G. Gu, S.-J. Ji, Z.-Q. Jiang, M.-F. Zhou and T.-P. Loh, *Synlett*, 2005, 959; H. Hagiwara, M. Sekifuji, T. Hoshi, K. Qiao and C. Yokoyama, *Synlett*, 2007, 1320.
- 13 D. R. MacFarlane, J. M. Pringle, K. M. Johansson, S. A. Forsyth and M. Forsyth, *Chem. Commun.*, 2006, 1905.
- 14 K. K. Laali and V. J. Gettwert, *J. Org. Chem.*, 2001, **66**, 35; N. L. Lancaster, P. A. Salter, T. Welton and G. B. Young, *J. Org. Chem.*, 2002, **67**, 8855.
- 15 (a) A. Basak (née Nandi), M. K. Nayak, and A. K. Chakraborti, *Tetrahedron Lett.* 1998, **39**, 4883; (b) A. K. Chakraborti, A. Basak (née Nandi), and V. Grover, *J. Org. Chem.* 1999, **64**, 8014; (c) G. L. Khatik, R. Kumar and A. K. Chakraborti, *Org. Lett.*, 2006, **8**, 2433; (d) S. V. Chankeshwara and A. K. Chakraborti, *Org. Lett.*, 2006, **8**, 3259; (e) A. K. Chakraborti, S. Rudrawar, K. B. Jadhav, G. Kaur and S. V. Chankeshwara, *Green Chem.*, 2007, **9**, 1335.
- 16 S. T. Handy and M. Okello, *J. Org. Chem.*, 2005, **70**, 1915.
- 17 D. S. Choi, D. H. kim, U. S. Shin, R. R. Deshmukh, S. Lee and C. E. Song, *Chem. Commun.*, 2007, 3467.
- 18 L. S. Santos, *Eur. J. Org. Chem.*, 2008, 235.
- 19 (a) J.-T. Li, H.-G. Dai, W.-Z. Xu and T.-S. Li, *Ultrason. Sonochem.*, 2006, **13**, 24; (b) S.-J. Ji, S.-Y. Wang, Y. Zhang and T.-P. Loh, *Tetrahedron*, 2004, **60**, 2051; (c) C. J. Magesh, R. N. Nagarajan, M. Karthik and P. T. Perumal, *Appl. Catal., A*, 2004, **266**, 1; (d) B. P. Bandgar and K. A. Shaikh, *Tetrahedron Lett.*, 2003, **44**, 1959; (e) J. S. Yadav, B. V. Subba Reddy, Ch. V. S. R. Murthy, G. M. Kumar and C. Madan, *Synthesis*, 2001, 783; (f) D. Chen, L. Yu and P. G. Wang, *Tetrahedron Lett.*, 1996, **263**, 4467.
- 20 G. Penieres-Carrillo, J. G. Garcia-Estrada, J. L. Gutiérrez-Ramírez and C. Alvarez-Toledano, *Green Chem.*, 2003, **5**, 337.

25 years
of stimulating
progress in all
areas of natural
products research



Join the celebrations...

Natural Product Reports is celebrating 25 years of publishing reviews in key areas including: bioorganic chemistry, chemical biology, chemical ecology and carbohydrates

- Impact factor 7.66*
- High visibility – indexed in MEDLINE
- “Hot off the Press” literature highlights published in each issue

...go online to find out more

* 2007 Thomson Scientific (ISI) Journal Citation Reports®

'I wish the others were as easy to use.'



'ReSource is the best online submission system of any publisher.'

'It leads the way for online submission and refereeing.'



ReSource



A selection of comments received from just a few of the thousands of satisfied RSC authors and referees who have used ReSource to submit and referee manuscripts. The online portal provides a host of services, to help you through every step of the publication process.

authors benefit from a user-friendly electronic submission process, manuscript tracking facilities, online proof collection, free pdf reprints, and can review all aspects of their publishing history

referees can download articles, submit reports, monitor the outcome of reviewed manuscripts, and check and update their personal profile

NEW!! We have added a number of enhancements to ReSource, to improve your publishing experience even further.

New features include:

- the facility for authors to save manuscript submissions at key stages in the process (handy for those juggling a hectic research schedule)
- checklists and support notes (with useful hints, tips and reminders)
- and a fresh new look (so that you can more easily see what you have done and need to do next)

A class-leading submission and refereeing service, top quality high impact journals, all from a not-for-profit society publisher ... is it any wonder that more and more researchers are supporting RSC Publishing? Go online today and find out more.

Registered Charity No. 207890

RSC Publishing

www.rsc.org/resource